Comparative biochemistry of three recently evolved hexachlorocyclohexane dehydrochlorinase variants

A thesis submitted for the degree of Doctor of Philosophy of The Australian National University

Noor Hafizah Mohd Pushiri

30 November 2018

This thesis contains no materials which has been accepted for the award of any other degree or diploma in any university. It contains original work by the author and a collaboration with Dr. Andrew Warden (CSIRO) for Molecular Dynamics work in Chapter 6, where Dr. Warden performed the docking and trajectories and the author performed all the analyses of the trajectories and constructed their discussion herein. To the best of the author's knowledge and belief, it contains no material that has been published or written by another person, except for when due reference is made in the text. The word count for this thesis is 38,457 words.

Noor Hafizah Mohd Pushiri

30 November 2018

Acknowledgement

"Read! In the name of the Lord who have created."

-Al-Quran 96:1-

I have a lot of people to thank for making it possible for me to bring this thesis into completion.

I would like to thank Dr. John Oakeshott for believing in me more than I do and spending countless hours guiding me and editing this thesis to the quality that it is now. I have learned a lot from you, especially during the writing process of this thesis. I would also like to thank Dr. Gunjan Pandey for helping me, especially in the beginning of this project, and for always being there when I needed help. I also thank Dr. Andrew Warden for stepping in and helping me perfecting this thesis. Your willingness to help and input in this thesis are highly appreciated. Not to forget Dr. Hans Peter Kohler, for his professional input on a part of the work in this thesis.

Additionally, this thesis would not have come to completion if it is not for the kindness of my dear friend and her daughters, Marina, Fara and Alysha, who have opened their hearts, home and fridge to me when I really needed it. I can never repay your kindness. To my fellow friends Naqiya, Allina, Mira, Asrina, Jasmin, Rini, and all of my Canberra family, thank you for always supporting me and keeping me sane during my PhD journey. To Lygie, Shahana, Madhura, Sahil, Faisal and Stephen, thank you for being my partners in crime and making countless hours in the lab fun. To Nigel, Michelle, Lyndall and others in the lab, thank you for guiding me and keeping me safe while I worked with dangerous chemicals and equipment in the lab.

Most importantly, I would like to thank my family members – mom, dad, siblings – for always believing in me and supporting me in all areas that I needed during this knowledge-seeking journey. A special thanks to my uncle, Abdul Malik, for stepping in to help me when you really did not need to. This thesis would not have been completed without your help.

Finally, I would like to thank my husband, Mohd Dzulkarnain, for always being by my side and never leaving me alone even when the situation seemed very tough. Thank you for always loving

me, believing in me, proud of me, and being my strength when I was weak. Your contribution and support in this work is immeasurable.

I dedicate this thesis to my two sons, Daiyan and Daris. I hope that this thesis serves as an inspiration and a reminder for you to never stop learning, always strive to be your very best, and never give up. I did it, boys.

Abstract

The synthetic compound hexachlorocyclohexane (HCH) was widely used as a pesticide for several decades from the 1940s onwards but concerns about detrimental off-target effects have led to progressive reductions in its use in most countries since the 1970s. Even so, its persistence in the environment has meant it remains a concern and bioremediation options are therefore being explored to rehabilitate HCH-contaminated environments. Part of the research towards bioremediation solutions has involved studies of the bacterial enzymes responsible for the biodegradation of HCH, one of the key enzymes being the HCH-dehydrochlorinase LinA. Previous work has suggested LinA can catalyse two successive eliminations of *trans*-diaxial H-Cl pairs from various HCH isomers.

This thesis compares the biochemistry of three different types of LinA, namely the LinA-type1 $LinA2_{B90A}$, the LinA-type2 $LinA1_{B90A}$ and the novel LinA-type3 $LinA_{LL02}$. $LinA_{LL02}$ was found to differ from $LinA1_{B90A}$ and $LinA2_{B90A}$ in several respects, but particularly in its preference to degrade the δ-HCH isomer over the γ-HCH isomer in the first elimination reaction and its ability to produce all three trichlorobenzene isomers (TCBs) as eventual dead-end products following the second elimination reaction. Valines at position 44 and 64 of $LinA_{LL02}$ were hypothesised as having roles in these unique characteristics and this hypothesis was supported to a degree by empirical analysis of synthetic mutants at these positions.

Additionally, differences were found between the three LinA enzymes in their degradation of the (+)-α-HCH versus (-)-α-HCH enantiomers, and greater preferences were observed in assays of whole *Escherichia coli* cells expressing the enzymes than in assays with purified enzymes. The variants also differed in their enantiopreferences in the second elimination reactions, specifically among the β-, γ-, and δ-pentachlorocyclohexenes (PCCHs) which are respectively produced from α-, γ-, and δ-HCH degradation in the first elimination reactions.

While most of my data are consistent with the accepted view that LinA works by eliminating *trans*-diaxial H-Cl pairs, I found it necessary to invoke *syn*- and *anti*-1,4-elimination of H-Cl pairs to account for the activities seen with δ- and β-PCCH, respectively. A possible role for LinA in the previously proposed spontaneous production of TCBs from the proximal product of PCCH degradation, tetrachlorocyclohexadiene (TCDN), was also discussed.

Molecular dynamics trajectories were performed for the three enzymes with α-, γ-, and δ-HCH, and their corresponding PCCHs, but it was found that the percentage of time which substrates spent in productive poses in the active sites of the enzymes were not correlated to the enzymes' activity on the substrates.

Table of Contents

List of Figures

List of Tables

List of Abbreviations

APVMA	Australian Pesticides and Veterinary Medicines Authority
CHQ	Chlorohydroquinone
CoA	Coenzyme A
DCHQ	Dichlorohydroquinone
DCP	Dichlorophenol
DDOL	Dichlorocyclohexadiene
DDT	Dichlorodiphenyltrichloroethane
DNOL	Trichlorocyclohexadiene
ECD	Electron capture detector
FAISD Handbook	First Aid Instructions, Safety Directions, Warning Statements and General Safety Precautions for Agricultural and Veterinary Chemicals
GC	Gas chromatography
GMO	Genetically Modified Organism
GSH	Glutathione
HCH	Hexachlorocyclohexane
HID	Histidine with hydrogen on the delta nitrogen
HIE	Histidine with hydrogen on the epsilon nitrogen
HMSA	Hydroxymuconic semialdehyde
HQ	Hydroquinone
MA	Malylacetate
MD	Molecular dynamics
NMR	Nuclear magnetic resonance
PCCH	Pentachlorocyclohexene
PCHL	Pentachlorocyclohexanol
PCNB	Pentachloronitrobenzene
PLP	Pyridoxal-5’-phosphate
POP	Persistent organic pollutant
SDS-PAGE	Sodium dodecyl sulfate-polyacrylamide gel electrophoresis
TCA	Tricarboxylic acid
TCB	Trichlorobenzene
TCDN	Tetrachlorocyclohexadiene
TCOL	Tetrachlorocyclohexene
TriCDL	Trichlorocyclohexenediol

CHAPTER 1:

Introduction and literature review

1.1 Introduction

The modern industrial era has seen a proliferation of synthetic compounds with a wide variety of medical, agricultural and other industrial and domestic uses. The dispersal of these compounds through the environment, together with waste products from their synthesis and breakdown products from their decay, has created a mix of novel toxicity challenges and nutrient source opportunities for microorganisms in the environment.

Understanding how bacterial enzymes evolve to deal with recently developed synthetic xenobiotics like pesticides is proving to be a very useful way of exploring the evolution of new functions at a molecular level (Liu and Suflita, 1993; Pearce et al., 2015). Some much-studied examples of this evolution are the emergence of the enzymes OpdA, an organophosphate degrading enzyme originating from *Agrobacterium radiobacter*, and AtzA, an atrazine chlorohydrolase originating from *Pseudomonas sp*. strain ADP (De Souza et al., 1996; Horne et al., 2002). Both these enzymes emerged as highly effective catalysts less than 50 years after their respective substrates were introduced to the environment (Mandelbaum et al., 2008; Soltaninejad and Shadnia, 2014).

However, the targets for many of these bacterial degradation systems, including the organophosphates and atrazine, are fairly simple molecules whose degradation requires relatively short catabolic pathways. Many other, much more complex and recalcitrant synthetic molecules have now been introduced into the environment and the pathways, and some of the individual enzymes within them, required for their degradation may be more difficult evolutionary challenges.

This thesis concerns one such molecule, hexachlorocyclohexane (HCH), which the *lin*/Lin gene/enzyme systems in various aerobic bacteria are in the process of evolving to degrade. The isomeric complexity and recalcitrance to biodegradation of both HCH and several of its degradation products make this a particularly challenging system to study. However considerable progress has been made over the last decade (Bajaj et al., 2017; Tabata et al.,

2016b). As might be expected, it is already clear that the pathway evolving is much more complex than those for the precedent model systems above. This thesis seeks to resolve some of the complexity around a key Lin enzyme and its role in the isomer-specific degradation of HCH and the first set of its degradation products.

1.2 Hexachlorocyclohexane: background information

HCH was first synthesised in 1825 but its commercial use as an organochlorine insecticide for agricultural and public health purposes did not begin until more than a century later, in the 1940s (Bourne, 1945; Faraday, 1825; Hartley, 1881; Tanaka, 2015; Taylor, 1945). HCH is a six carbon ring with a hydrogen atom and a chlorine atom attached to each carbon. The positions of the hydrogen and the chlorine atoms on the ring determine the isomer of each HCH molecule. Thirteen isomers of HCH are known but four of them (α-, β-, γ-, and δ-HCH) are particularly stable (Zdravkovski, 2004) (Figure 1). The vapour pressure for these four HCH isomers ranges from $(4.2 \pm 0.3) \times 10^{-5}$ Pa for β-HCH to $(1.6 \pm 0.9) \times 10^{-2}$ pa for α-HCH at 20~25 ^{o}C (Willett et al., 1998), which makes them more volatile than the pesticide dichlorodiphenyltrichloroethane (DDT) that has a vapour pressure value of 2.5×10^{-5} Pa at 25 ^{o}C (Kidd and James, 1991). Of these four, only γ-HCH has significant insecticidal activity (Taylor, 1945). Another one of the four, α-HCH, has two enantiomeric forms (optical isomers) (Buser and Müeller, 1995).

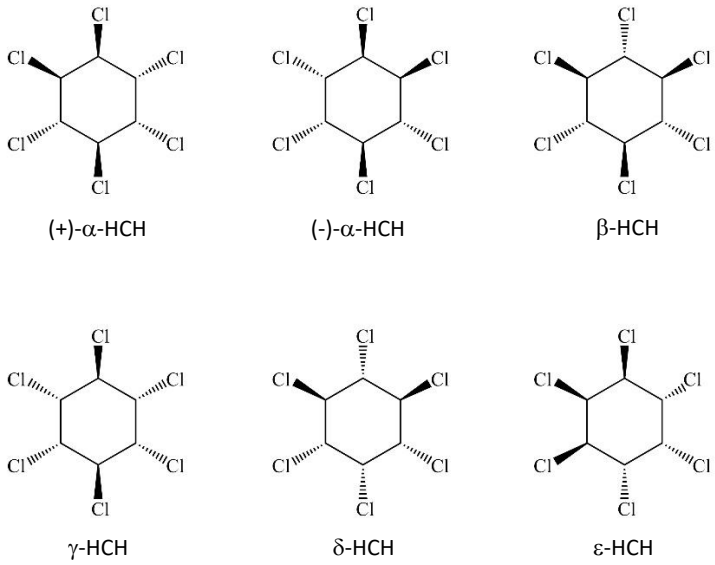

Figure 1 *The five major HCH isomers in technical HCH formulations, including the two enantiomers of α-HCH. Hydrogen atoms are not shown.*

Although only γ-HCH has insecticidal activity, it is not the only isomer found in some commercial HCH-based insecticides. These insecticides come in two types of formulation, namely technical HCH and lindane. Technical HCH consists of many HCH isomers, mainly α-, β-, γ-, δ-, and ε-HCH. In 1946, Ramsey and Patterson (1946) reported that the technical HCH used at that time contained 65-70% α-HCH, 5% β-HCH, 10-12% γ-HCH, 6% δ-HCH, and 4% ε-HCH. They also reported the existence of heptachlorocyclohexane and octachlorocyclohexane in the formulation (Ramsey and Patterson, 1946; Tanaka, 2015). On the other hand, lindane, which was named after the scientist who discovered γ-HCH in 1912, consists almost entirely of γ-HCH, (Li, 1999; Tanaka, 2015; van der Linden, 1912). Unfortunately γ-HCH cannot be produced without producing many other HCH isomers as well, so those other isomers need to be separated by recrystallization (Campbell, 1951) (Patent No. US2573676A) and disposed of before it is formulated into lindane; otherwise it is sold as technical HCH (Vijgen et al., 2006; Weber et al., 2008).

All HCH isomers were classified as 'reasonably anticipated to be human carcinogens' by the United States of America in 2016 (National Toxicology Program, 2016b). They have also been

found to have other toxic properties (Li, 1999; Willett et al., 1998). Data from accidental poisonings and occupational exposures to HCH have shown that it can cause tremors, ataxia, convulsions, stimulated respiration, and even death (Willett et al., 1998). Studies on its effects on animals have found that it can also cause renal, liver and reproductive problems, as well as disrupt the function of the central nervous system (Willett et al., 1998).

Studies on the global usage of HCH and its consequences in the environment have found that HCH exists not only in places where it has been directly applied, but also in less likely places such as human breast milk, the Arctic air and seawater (Li, 1999; Willett et al., 1998). The persistent and volatile nature of HCH has allowed it to be transferred in several ways, including via the food chain and the air. Transfer via the food chain is believed to have concentrated the level of HCH in organisms higher up in the chain (Li, 1999). Also, the more volatile nature of α- and γ-HCH is believed to be the cause of their transfer to the Arctic air and seawater (Glotfelty et al., 1984; Gregor and Gummer, 1989; Li, 1999; Willett et al., 1998). In fact, HCH has been found to be the most abundant organic compound in the Arctic atmosphere and seawater (Bidleman et al., 1995; Hargrave et al., 1988; Iwata et al., 1993). Samples of air and surface seawater taken between October 2007 and January 2008 also showed the presence of HCH in the southern oceans and atmosphere (Luek et al., 2017).

Due to its persistence and detrimental effects on human health, the usage of both forms of HCH has been severely limited since the 1970s (Voldner and Li, 1995). In 2009, the Stockholm Convention included α-, β- and γ-HCH in its list of Persistent Organic Pollutants (POPs), and recommended banning further production and restricting its use to second line treatments for head lice and scabies (The new POPs under the Stockholm Convention, 2017). Currently, most countries have completely banned its usage and many others have strictly limited its usage to a few specific purposes (Li, 1999; National Toxicology Program, 2016b) (Figure 2). Li (1999) reported that Australia banned HCH usage in 1994 but Immig (2010) subsequently reported that lindane was still being used in pineapple plantations in Australia, but had been nominated for

review by the Australian Pesticides and Veterinary Medicines Authority (APVMA). Currently, lindane is still used in a few agricultural formulations in Australia (FAISD Handbook, 2018).

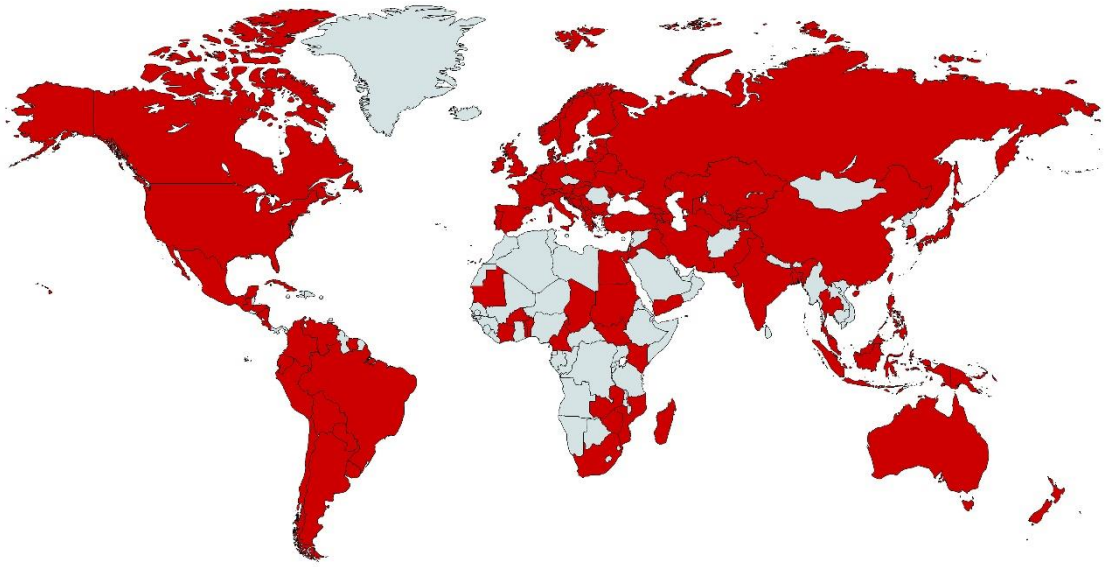

Figure 2 *World map highlighting in red countries that have banned or severely restricted the usage of HCH. Adapted from Li (1999).*

Despite the bans and restrictions, the persistent nature of HCH means it still exists in the environment, as outlined above. Efforts to recycle HCH waste dumps by thermal recycling have proven unsuccessful as the process results in the unintentional production of some other POPs (Jürgens and Roth, 1989; Vijgen et al., 2011; Weber et al., 2008). Relying on spontaneous degradation is also inadequate, given that HCH waste is still abundant and widespread even after decades of declining production and usage (Vijgen et al., 2011).

The half-lives of HCHs vary greatly according to the isomer and the environment but can be quite long. Atmospheric HCH is estimated to have a half-life of three to four years in locations with very low atmospheric hydroxyl radical concentration (Cortes and Hites, 2000), whereas its aquatic half-life is much shorter: 3-30 days in rivers, 30-300 days in lakes and >300 days in groundwater (Zoeteman et al., 1980). It is believed that biodegradation is the major degradation pathway for aquatic HCH (Sharom et al., 1980). One study of agricultural soils obtained quite short estimates of half-lives; 54-56 days for α-HCH, 100-184 days for β-HCH, 62-107 days for γ-

HCH and 23-34 days for δ-HCH (Singh et al., 1991). However, the results of another study implied much longer half-lives; it found that γ-HCH concentration only decreased from 95 ppb to below 10 ppb dry weight in loamy sand (1-2% organic matter) and from 426 ppb to 168 ppb dry weight in 'muck' soil (27-56% organic matter) over an 18 year time frame (Szeto and Price, 1991). As with aquatic HCH, HCH degradation in sediment and soil is also believed to be predominantly caused by biodegradation (Lal et al., 2010). Many HCH-degrading bacteria have been successfully isolated from soil (Lal et al., 2010) and some fungal degradation of HCH has also been discovered (Kaur et al., 2016).

1.3 HCH-degrading bacteria

Two of the bacterial strains first isolated for their HCH-degrading ability were a *Bacillus* sp. isolated in 1967 from Ontario, Canada (Yule et al., 1967) and a *Clostridium* sp. isolated in 1969 from an unnamed location (MacRae et al., 1969). These strains degraded γ-HCH aerobically and anaerobically, respectively (MacRae et al., 1969; Yule et al., 1967). It was initially believed that anaerobic degradation is the major process by which bacteria degrade HCH, but it is apparent now that aerobic degradation is more common (Lal et al., 2010). Several species of aerobic HCH-degrading bacteria have now been isolated around the world, including *Pseudomonas*, *Rhodanobacter*, *Pandoraea*, *Chromohalobacter* and, most frequently, *Sphingomonas* species (Bajaj et al., 2017; Kumar et al., 2005; Lal et al., 2010; Nagata et al., 2007; Nalin et al., 1999; Okeke et al., 2002). The three most intensively studied are *Sphingobium japonicum* UT26 from lindane-contaminated land in Japan, *Sphingobium indicum* B90A from Indian sugarcane rhizosphere soil contaminated with technical HCH, and *Sphingobium francense* Sp+ from soil contaminated with technical HCH in France (Cérémonie et al., 2006; Lal et al., 2010; Sahu et al., 1990; Senoo and Wada, 1989).

There are two main pathways by which bacteria are known to degrade HCH aerobically. Each pathway is isomer-specific. In the first step, one pathway degrades α-, γ-, and δ-HCH via a dehydrochlorination reaction, converting them into β-, γ-, and δ-pentachlorocyclohexene

(PCCH) respectively, and the other pathway degrades β- and δ-HCH via a hydrolytic dechlorination reaction, converting them into β- and δ-pentachlorocyclohexanol (PCHL) respectively (Lal et al., 2010).

α-HCH degradation has been extensively studied in *S. indicum* B90A, where it was found to be converted first into β-PCCH via a dehydrochlorination reaction catalysed by a dehydrochlorinase enzyme, LinA (Kumari et al., 2002; Suar et al., 2005). The pathway by which β-PCCH is further metabolized has not been established empirically but is believed to follow the degradation pathway of γ-HCH described below. This belief is based on the formation of the same dead-end product, 1,2,4-trichlorobenzene (1,2,4-TCB), as was formed in the degradation of γ-HCH by *S. japonicum* UT26 (Lal et al., 2010) (Figure 3).

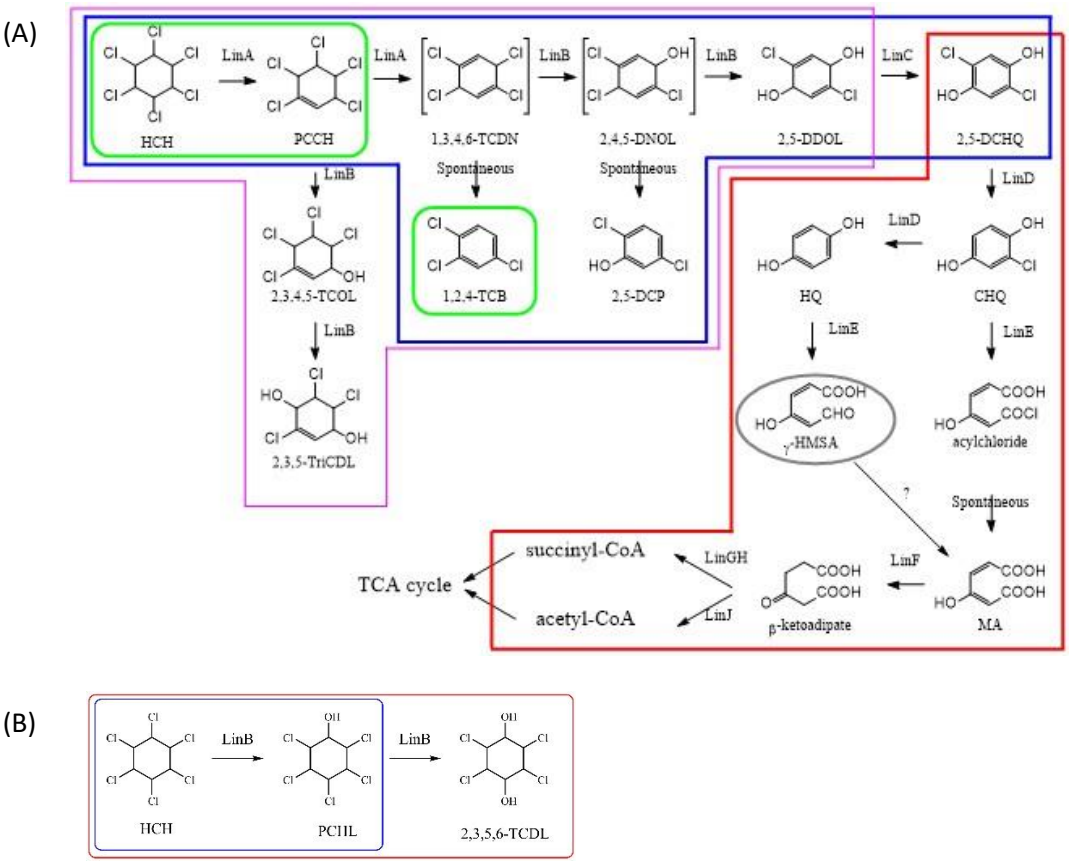

Figure 3 *The two main pathways of aerobic biodegradation of HCH by bacteria. (A) The dehydrochlorination pathway – This pathway is divided into two main stages, the upstream pathway (outlined in blue) and the downstream pathway (outlined in red), as observed in the γ-HCH degradation by S. japonicum UT26. The green-rounded boxes highlight the metabolites observed during α-HCH degradation by S. indicum B90A, and the magenta box highlights all but one (2,3,4,5-TCOL) of the metabolites observed during δ-HCH degradation by Sphingobium sp. BHC-A. 2,3,4,5-TCOL was observed in δ-HCH degradation by S. indicum B90A. These observations suggest that both α- and δ-HCH degradation by bacteria also follow the dehydrochlorination pathway. This pathway is initiated by a dehydrochlorination reaction catalysed by dehydrochlorinase encoded by linA, and produces two final products (succinyl-CoA and acetyl-CoA) that are used in the TCA cycle. 1,2,4-TCB and 2,5-DCP are dead-end products. Fates of γ-HMSA and 2,3,5-TriDCL are unknown. Compounds in brackets have not been observed empirically. Most CHQ is transformed into the putative acylchloride rather than HQ. (B) The hydrolytic dechlorination pathway – this pathway is initiated by a hydrolytic dechlorination reaction catalysed by LinB. It is observed in both β- and δ-HCH degradation by S. indicum B90A, S. japonicum UT26, S. francense Sp+, and Sphingobium sp. BHC-A. While both β- and δ-HCH undergo two hydrolytic dechlorination reactions to produce 2,3,5,6-TCDL in S. indicum B90A, as highlighted in the red-rounded box, their degradation by S. japonicum UT26 and S. francense Sp+ was observed to stop after only one round of hydrolytic dechlorination, as highlighted in the blue-rounded box. The fate of 2,3,5,6-TCDL is unknown but it was observed to disappear in Sphingobium sp. BHC-A. The enzymes involved in the reactions are written next to the arrows. Full names of the compounds are written in the text.*

β-HCH degradation has been studied in most detail in *S. japonicum* UT26, *S. indicum* B90A, and *S. francense* Sp+. In these strains it was found to be converted into β-pentachlorocyclohexanol (β-PCHL) via a hydrolytic dechlorination catalysed by the haloalkane dehalogenase, LinB (Lal et al., 2010; Nagata et al., 2005; Raina et al., 2007; Sharma et al., 2006). While β-PCHL was observed to be the end-product in *S. japonicum* UT26 and *S. francense* Sp+, it was found to be converted

further into 2,3,4,6-tetrachlorocyclohexanediol (2,3,4,6-TCDL) by a variant of the same enzyme in *S. indicum* B90A. However, the fate of this latter metabolite is unknown (Lal et al., 2010; Raina et al., 2007; Sharma et al., 2006) (Figure 3).

The most studied HCH-degradation pathway is that for γ-HCH degradation in *S. japonicum* UT26. In the upstream part of this pathway, γ-HCH undergoes two consecutive dehydrochlorination reactions catalysed by LinA, converting it first into γ-PCCH, and then into a hypothetical and unstable metabolite 1,3,4,6-tetrachloro-1,4-cyclohexadiene (1,3,4,6-TCDN) (Nagasawa et al., 1993). The two catabolic routes proposed for the 1,3,4,6-TCDN are (i) transformation into the dead-end product 1,2,4-trichlorobenzene (1,2,4-TCB) via a spontaneous reaction (Lal et al., 2010; Nagasawa et al., 1993b) or (ii) metabolic transformation into yet another putative metabolite, 2,4,5-trichloro-2,5-cyclohexadiene-1-ol (2,4,5-DNOL), via a hydrolytic dechlorination reaction catalysed by LinB (Lal et al., 2010; Wu et al., 2007). 2,4,5-DNOL could also spontaneously transform into another dead-end product, 2,5-dichlorophenol (2,5-DCP), or undergo another hydrolytic dechlorination reaction also catalysed by LinB, forming 2,5-dichloro-2,5-cyclohexadiene-1,4-diol (2,5-DDOL) (Lal et al., 2010; Nagasawa et al., 1993b; Nagata et al., 1993c). 2,5-DDOL then undergoes a dehydrogenation reaction catalysed by the LinC dehydrogenase, forming 2,5-dichlorohydroquinone (2,5-DCHQ) as the final metabolite in the upstream part of the pathway (Lal et al., 2010; Nagata et al., 1994) (Figure 3).

The downstream part of the pathway for γ-HCH degradation by *S. japonicum* UT26 starts with chlorohydroquinone (CHQ) formation from a reductive dechlorination reaction of 2,5-DCHQ, catalysed by a reductive dechlorinase enzyme, LinD (Miyauchi et al., 1998). The majority of CHQ is cleaved by a ring-cleaving oxygenase enzyme, LinE, into a hypothetical acylchloride metabolite which is spontaneously converted into the empirically observed malylacetate (MA). However, some CHQ is also converted into hydroquinone (HQ) by a reductive dechlorination catalysed by LinD. The HQ is then cleaved into γ-hydroxymuconic semialdehyde (γ-HMSA) by LinE, but the fate of the γ-HMSA is unclear (Miyauchi et al., 1998). However, the product of the major route,

MA, is known to be transformed into β-ketoadipate by the malylacetate reductase LinF, and then into succinyl coenzyme A (succinyl-CoA) and acetyl-CoA, which will be metabolized in the TCA cycle. The formation of succinyl-CoA and acetyl-CoA is catalysed by acyl-CoA transferase and thiolase enzymes, called LinGH and LinJ, respectively (Endo et al., 2005; Lal et al., 2010; Nagata et al., 2007) (Figure 3).

δ-HCH has been shown to be degraded via both the dehydrochlorination and hydrolytic dechlorination pathways. The hydrolytic pathway follows the β-HCH degradation route in *S. japonicum* UT26, *S. indicum* B90A, and *S. francense* Sp+. This includes hydrolytic dechlorination catalysed by LinB to form δ-PCHL, which is a dead-end product in *S. japonicum* UT26 and *S. francense* Sp+ but is further degraded in *S. indicum* B90A, forming 2,3,4,6-TCDL via another hydrolytic dechlorination by LinB (Lal et al., 2010; Nagata et al., 2007; Raina et al., 2007; Sharma et al., 2006; Wu et al., 2007). 2,3,4,6-TCDL was also observed to form during δ-HCH degradation in *Sphingobium sp.* BHC-A. However, while the fate of 2,3,4,6-TCDL is unknown in *S. indicum* B90A, it was observed to disappear in *Sphingobium sp.* BHC-A after prolonged incubation (Sharma et al., 2006; Wu et al., 2007) (Figure 3).

There are two routes within the dehydrochlorination pathway by which δ-HCH may be degraded. The first route is observed in *Sphingobium sp.* BHC-A and is similar to the γ-HCH degradation pathway. This includes two successive dehydrochlorination reactions of δ-HCH catalysed by LinA, forming δ-PCCH and the putative metabolite 1,3,4,6-TCDN; the formation of the dead-end product 1,2,4-TCB following a spontaneous reaction of 1,3,4,6-TCDN; two successive hydrolytic dechlorination reactions of 1,3,4,6-TCDN by LinB, forming the putative metabolite 2,4,5-DNOL and 2,5-DDOL; and the formation of another dead-end product 2,5-DCP following a spontaneous reaction of 2,4,5-DNOL (Wu et al., 2007). However, while 2,5-DDOL was observed to be converted further during γ-HCH degradation by *Sphingobium sp.* BHC-A, this was not observed in δ-HCH degradation by the same strain. This may be because of the different enantiomeric configuration of 2,5-DDOL formed from δ-HCH (Wu et al., 2007) (Figure 3).

In the second route of the dehydrochlorination pathway for δ-HCH, as demonstrated in *S. indicum* B90A, δ-PCCH undergoes two successive hydrolytic dechlorination reactions catalysed by LinB to first form 2,3,4,5-tetrachloro-5-cyclohexene-1-ol (2,3,4,5-TCOL) and then 2,3,5-trichloro-5-cyclohexene-1,4-diol (2,3,5-TriCDL) (Raina et al., 2007). While the formation of 2,3,4,5-TCOL was not detected in *Sphingobium* sp. BHC-A, the formation of 2,3,5-TriCDL was observed, and it was suggested that 2,3,4,5-TCOL or 2,4,5,6-TCOL might also have formed in *Sphingobium* sp. BHC-A, catalysed by LinB (Wu et al., 2007) (Figure 3). Nevertheless, to the best of my knowledge, this observation was not seen in α-, β- or γ-HCH degradation by *S. indicum* B90A, *S. japonicum* UT26, and *S. francense* Sp+. While the fate of 2,3,4-TriCDL has not been mentioned for *S. indicum* B90A (Raina et al., 2007), it was observed to be degraded further with prolonged incubation in *Sphingobium* sp. BHC-A (Wu et al., 2007).

1.4 The lin genes

Despite degrading HCH via several different routes, all HCH-degrading bacteria so far characterised use the products of essentially the same set of *lin* genes for the aerobic degradation of HCH. These genes were first identified and characterized in *S. japonicum* UT26, and very similar genes have also been found in other HCH degraders (Dogra et al., 2004; Kumari et al., 2002; Lal et al., 2010; Singh et al., 2007). Seventeen *lin* genes have been identified in *S. japonicum* UT26 (Lal et al., 2010). Table 1 lists the Lin proteins corresponding to the *lin* genes and the bacteria known to carry them.

The *lin* genes, especially those involved in the upstream pathway, have been found to be organized both chromosomally and on plasmids in different HCH degrading bacterial strains (Lal et al., 2006; Nagata et al., 2011; Tabata et al., 2011; Tabata et al., 2013). In *S. japonicum* UT26, the *lin* genes involved in the upstream pathway are found in a region on the chromosome associated with the insertion sequence IS6*100* (Lal et al., 2006; Nagata et al., 2011). IS6*100* is a member of the IS6 family, which can mobilise genes between two directly repeated IS6 elements (Mahillon and Chandler, 1998). This association of some *lin* genes with the IS6*100* elements

suggests horizontal transfers of the genes have taken place (Lal et al., 2006; Nagata et al., 2011). Evidence for the horizontal transfer of some of the *lin* genes can also be seen in *Sphingomonas sp*. MM-1, where all of the upstream *lin* genes are found on plasmids (Tabata et al., 2013; Tabata et al., 2011). Some strains have also been observed to be missing some of the *lin* genes, suggesting they are at early stages in the acquisition of the HCH degrading pathway (Dogra et al., 2004; Kohli et al., 2013; Singh et al., 2013; Pearce, 2015). All these lines of evidence suggest that the HCH-degrading pathways have been developed and acquired by HCH degraders after the introduction of HCH to the environment, and that horizontal transfer plays a role in this pathway acquisition (Pearce, 2015). While there is also information on the other *lin*/Lin gene/enzyme systems, I will only elaborate on *linA*/LinA for the purpose of this thesis.

Table 1 *Proteins encoded by the lin genes in HCH-degrading bacteria*

Proteins	Total amino acids	Function	Strains and accession number on NCBI	References
LinA	154-156	Dehydrochlorinase	*Sphingobium indicum* B90A (AAR05959), Sphingobium *japonicum* UT26 (AAC60443), *Rhodanobacter lindaniclasticus* (AAT00794), *Sphingomonas* sp DS3-1 (CAI43922), *Sphingomonas* sp. Alpha4-2 (CAI43921), *Sphingomonas* sp. Alpha1-2 (CAI43920), *Sphingomonas* sp. Gamma16-1 (CAI43919), *Sphingomonas* sp. Gamma12-7 (CAI43918), *Sphingomonas* sp. Gamma1-7 (CAI43917), *Sphingomonas* sp. DS2 (CAI43915), *Sphingomonas* sp. MM-1 (AGH51793), *Sphingobium* sp. TKS (AMK26746), *Sphingobium* sp. MI1205 (AMK20791), *Sphingomonas* sp. NM05 (ABG77566)	Böltner et al., 2005; Dogra et al., 2004; Manickam et al., 2008; Nagata et al., 1993; Tabata et al., 2016a; Tabata et al., 2016c; Tabata et al., 2013; Thomas et al., 1996
LinB	296	Haloalkane dehalogenase	*Sphingobium indicum* B90A (AAR05978), *Sphingobium sp*. MI1205 (BAF56673), *Sphingomonas sp*. NM05 (ABG77567), *Sphingobium japonicum* UT26 (BAI96793), *Sphingobium sp*. SS04-5 (BAF80345), *Sphingobium sp*. SS04-4 (BAF80342), *Sphingobium sp*. SS04-3 (BAF80339), *Sphingobium sp*. SS04-2 (BAF80336), *Sphingobium sp*. SS04-1 (BAF80333)	Dogra et al., 2004; Ito et al., 2007; Manickam et al., 2008; Nagata et al., 2010; Yamamoto et al., 2009
LinC	250	2,5-dichloro-2,5-cyclohexadiene-1,4-diol dehydrogenase	*Sphingobium indicum* B90A (AAR05964), *Sphingomonas sp*. MM-1 (BAI82456), *Sphingobium japonicum* UT26S (BAI95393), *Sphingobium francense* (AAZ14097), *Pseudomonas aeruginosa* ITRC-5 (ABP93367), *Sphingomonas sp*.	Dogra et al., 2004; Lal et al., 2006; Manickam et al., 2008; Nagata et al., 2010; Singh et al., 2007; Tabata et al.,

			NM05 (ABG77568), *Sphingobium sp*. MI1205 (AMK20834)	2011; Tabata et al., 2016c
LinD	346	Reductive dechlorinase	*Sphingobium japonicum* (BAA14011), *Pseudomonas aeruginosa* ITRC-5 (ABP93365), *Sphingobium indicum* B90A (AAQ96756), *Sphingomonas sp*. MM-1 (AGH52022), *Sphingobium sp*. TKS (AMK26908), *Sphingobium sp*. MI1205 (AMK20961)	Dogra et al., 2004; Miyauchi, et al., 1998; Singh et al., 2007; Tabata et al., 2013; Tabata et al., 2016a; Tabata et al., 2016c
LinE	321	Ring cleavage dioxygenase	*Sphingobium indicum* B90A (AAQ96752), *Sphingobium japonicum* (BAA76672), *Sphingomonas sp*. NM05 (ABG77570), *Sphingomonas sp*. MM-1 (YP_003537102), *Sphingobium sp*. TKS (AMK26904), *Sphingobium sp*. MI1205 (AMK20347)	Dogra et al., 2004; Manickam et al., 2008; Miyauchi et al., 1999; Tabata et al., 2011; Tabata et al., 2016a; Tabata, et al., 2016c
LinR	303	Transcriptional regulator	*Sphingobium indicum* B90A (AAQ96751), *Sphingobium japonicum* UT26 (BAA36280), *Pseudomonas aeruginosa* ITRC-5 (ABP93363), *Sphingomonas sp*. MM-1 (YP_003537101), *Sphingobium sp*. MI1205 (AMK20956)	Dogra et al., 2004; Miyauchi et al., 2002; Singh et al., 2007; Tabata et al., 2011; Tabata et al., 2016b
LinF	352	Maleylacetate reductase	*Sphingobium japonicum* UT26 (BAD66863), *Pseudomonas aeruginosa* ITRC-5 (ABP93368), *Sphingomonas sp*. MM-1 (AGH51637), *Sphingobium sp*. MI1205 (AMK20338)	Endo et al., 2005; Singh et al., 2007; Tabata et al., 2013; Tabata et al., 2016c
LinEb	320	2,6-dichloro-p-hydroquinone 1,2-dioxygenase	*Sphingobium japonicum* UT26S (BAI98848), *Sphingobium sp*. MI1205 (AMK20336)	Nagata et al., 2010; Tabata et al., 2016c
LinG	156	Acyl-CoA transferase	(not found in NCBI database)	
LinH	212	3-oxoadipate CoA-succinyltransferase	*Sphingobium japonicum* UT26S (BAI98885), *Sphingomonas sp*. MM-1 (AGH51674), *Sphingobium sp*. MI1205 (AMK20299)	Nagata et al., 2010; Tabata et al., 2013; Tabata et al., 2016c
LinI	267	IcIR-family transcriptional regulator	*Sphingobium japonicum* UT26S (BAI98883), *Sphingomonas sp*. MM-1 (AGH51672)	Nagata et al., 2010; Tabata et al., 2013
LinJ	403	Acetyl-CoA acetyltransferase	*Sphingobium japonicum* UT26S (BAI98882), *Sphingomonas sp*. MM-1 (AGH51671)	Nagata et al., 2010; Tabata et al., 2013
LinK	316	Putative ABC transporter system	*Sphingobium japonicum* UT26 (BAF51698)	Endo et al., 2007
LinL	282	ABC-type transport system ATPase component	*Sphingobium japonicum* UT26S (BAI94856)	Nagata et al., 2010
LinM	320	ABC-type transport system periplasmic protein	*Sphingobium japonicum* UT26S (BAI94857), *Sphingobium* sp. TKS (AMK21006)	Nagata et al., 2010; Tabata et al., 2016a
LinN	202	ABC-type transport system auxiliary component	*Sphingobium japonicum* UT26S (BAI94858)	Nagata et al., 2010
LinX	250	2,5-dichloro-2,5-cyclohexadiene-1,4-diol dehydrogenase	*Sphingobium japonicum* UT26S (BAI96692), *Sphingobium indicum* B90 (AAN64237), *Sphingomonas sp*., MM-1 (AGH51791), *Sphingobium sp*. TKS	Kumari et al., 2002; Nagata et al., 2010; Tabata et al., 2013; Tabata et al., 2016a; Tabata, et al., 2016c

	(AMK26744), *Sphingobium sp*. MI1205 (AMK20793)

1.4.1 LinA - HCH dehydrochlorinase

The *linA* gene encodes a dehydrochlorinase with a very narrow substrate range (only α-, γ-, δ-, ε-HCH and their respective PCCH isomers, and heptachlorocyclohexane) (Bala et al., 2012; Nagata et al., 1993a; Nagata et al., 1993b). The expression of *linA* is found to be constitutive in *S. japonicum* UT26 and *S. indicum* B90A but inducible in *Rhodanobacter lindaniclasticus* (Lal et al., 2010; Nalin et al., 1999). Notably LinA is a co-factor-independent dehydrochlorinase, unlike the sequence-unrelated DDT dehydrochlorinase from the housefly, *Musca domestica*, and a 3-chloro-D-alanine dehydrochlorinase from *P. putida*, which need glutathione (GSH) and pyridoxal 5'-phosphate (PLP), respectively (Nagata et al., 1999).

LinA has never been reported from bacteria other than those associated with HCH contaminated sites, nor have activities on any other substrates beside HCH been reported for LinA. These facts suggest that it has evolved to recognise HCH as its specific physiological substrate (Lal et al., 2010).

LinA has no known close relatives, although it shows low sequence similarity (less than 10%) to a functionally diverse group of proteins that share an α+β barrel fold tertiary structure (Nagata et al., 2001; Okai et al., 2010; Trantírek et al., 2001). The best characterised of this group of proteins are a scytalone dehydratase, a nuclear transport factor 2, a 3-oxo-Δ-steroid isomerase and LinA (Macwan et al., 2012; Nagata et al., 2001; Trantírek et al., 2001). The common fold in these enzymes comprises a central six-stranded β-sheet with the strand order 2-1-6-5-4-3 (Macwan et al., 2012; Nagata et al., 2001; Okai et al., 2010).

Mutagenesis analysis of LinA has indicated that its D25, H73 and R129 residues are important for its catalytic activity (Nagata et al., 2001). This supports the suggestion that H73 and D25 form a catalytic dyad, similar to the function proposed for H85 and D31 of scytalone dehydratase (Nagata et al., 2001; Trantírek et al., 2001). It is suggested that the H73-D25 catalytic dyad works

by abstracting a proton from the substrate, causing a chloride ion to be released (Brittain et al., 2011; Manna et al., 2015; Okai et al., 2010). While the position of R129 in the active site seems to be too far away to interact directly with the substrate, it is suggested that R129 may be important for the stabilization of the spatial locations of F113 and K20, both of which have been found to affect LinA activity when mutated (Okai et al., 2010) (Figure 4).

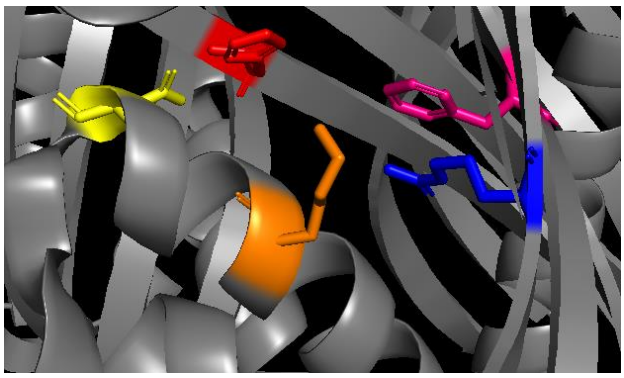

Figure 4 *$LinA_{UT26}$ active site, highlighting key residues: D25 (yellow), H73 (red), R129 (blue), F113 (magenta), and K20 (orange). It is suggested that D25 and H73 form a catalytic dyad that absorbs a proton from substrate and removes a chlorine from the substrate in the process. R129 is suggested to stabilise the spatial locations of F113 and K20, which have been found to affect LinA activity when mutated (Okai et al., 2010).*

Earlier, SDS-polyacrylamide gel electrophoresis (SDS-PAGE) analysis (Imai et al., 1991) suggested LinA is a monomeric 16.5 kDa protein. A more recent crystallographic study reveals it to be a homotrimer, with each protomer forming a cone-shaped α+β barrel fold (Okai et al., 2010).

While most HCH-degrading strains carry only one copy of *linA*, some strains carry two non-identical copies, as seen in *S. indicum* B90A and *Pseudomonas aeruginosa* ITRC-5 (Dogra et al., 2004; Kumari et al., 2002; Lal et al., 2010; Singh et al., 2007). Several other variants have been found in other strains with only single copies of *linA* (Dogra et al., 2004; Tabata et al., 2016b). Two grouping systems have been suggested for categorising the LinA variants; four groups were suggested by Lal and colleagues (2010) (Figure 5), and two groups by Macwan and colleagues (2011) (Figure 6).

1.4.1.1 Categorisation of LinA

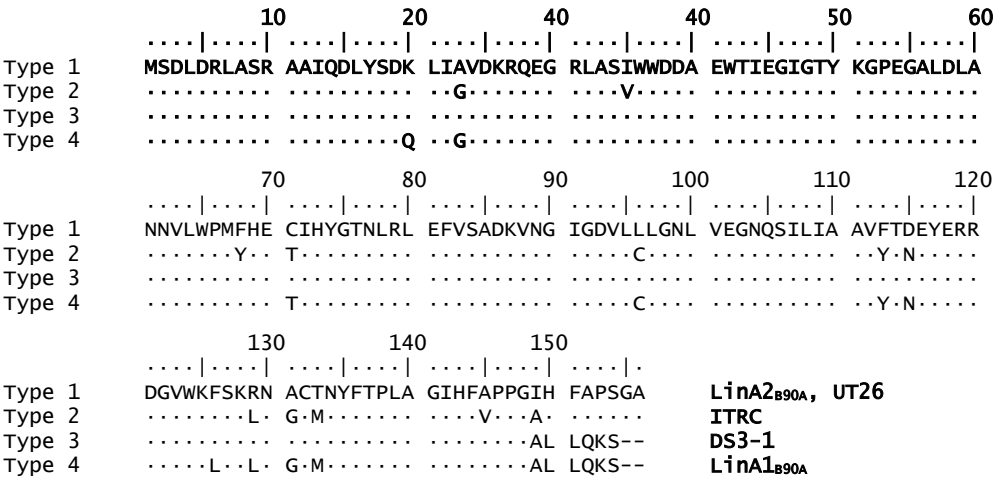

Figure 5 *Alignment of some of LinA variants based on amino acid sequences. Four identified groups are shown, as suggested by* Lal and colleagues, 2010*.*

In the four-group system, the first group was found to be the largest, consisting at that time of ten sequences, including LinA2 of *S. indicum* B90A. While most of the LinAs in this group share the same sequences, some differences were identified in positions 110, 111, 151, 152, and 154. On the other hand, the second group consisted of only one member, LinAa of *P. aeruginosa*. This sequence differed by about twelve residues from the first group: four of these differences cluster around the catalytic dyad H73-D25, and the other five cluster around (and include) R129. The remaining differences are at positions 96, 145, and 149. As noted above, the modification of R129 affects substrate binding and catalysis, purportedly by destabilising the binding site structure. Interestingly, sequences in the third and the fourth group were found to be more similar to the first and the second group, respectively. The main difference between the first group and the third group, and the second group and the fourth group, is located close to the C-terminus; both the third group and the fourth group have an insertion of a five-residue motif from the transposon IS6*100*. The usual IHFAPSGA in the C-terminal of the first and second groups is replaced with ALLQKS in the third and fourth groups. Examples of members of the third and fourth groups are LinA of *Sphingomonad* sp. DS3-1 and LinA1 of *S. indicum* B90A, respectively (Lal et al., 2010).

Since there are minimal differences between the first group and the third group, and the second group and the fourth group, these groups have been merged and named as LinA-type1 and LinA-type2, respectively, in the two group system. Members of these groups that carry the remnants of IS6*100* are considered to be minor variants within their respective groups (Figure 6). Regardless of the C-terminal sequence, both LinA-type1 and LinA-type2 have been observed to degrade α- and γ-HCH faster than δ-HCH in *in vitro* assays, with LinA-type1 having higher activity than LinA-type2 for all three HCH isomers (Sharma et al., 2011). It has also been observed that LinA1 (LinA-type2) and LinA2 (LinA-type1) of *S. indicum* B90A show opposite enantioselective preferences for (+)-α-HCH and (-)-α-HCH *in vivo* (Suar et al., 2005).

```
                    10         20         40         40         50         60
                ....|....| ....|....| ....|....| ....|....| ....|....| ....|....|
Type 1          MSDLDRLASR AAIQDLYSDK LIAVDKRQEG RLASIWWDDA EWTIEGIGTY KGPEGALDLA
Type 1-minor    .......... .......... .......... .......... .......... ..........
Type 2          .......... .......... ..G....... ....V..... .......... ..........
Type 2-minor    .......... .........Q ..G....... .......... .......... ..........

                     70         80         90        100        110        120
                ....|....| ....|....| ....|....| ....|....| ....|....| ....|....|
Type 1          NNVLWPMFHE CIHYGTNLRL EFVSADKVNG IGDVLLLGNL VEGNQSILIA AVFTDEYERR
Type 1-minor    .......... .......... .......... .......... .......... ..........
Type 2          .......Y.. T......... .......... .....C.... .......... ..Y.N.....
Type 2-minor    .......... T......... .......... .....C.... .......... ..Y.N.....

                    130        140        150
                ....|....| ....|....| ....|....| ....|.
Type 1          DGVWKFSKRN ACTNYFTPLA GIHFAPPGIH FAPSGA     LinA2B90A, UT26
Type 1-minor    .......... .......... .........L LQKS--     DS3-1
Type 2          ........L. G.M....... ....V...A. ......     ITRC
Type 2-minor    .....L..L. G.M....... ........AL LQKS--     LinA1B90A
```

Figure 6 *Alignment of some of LinA variants based on their amino acids sequences. Two types of LinA, LinA-type1 and LinA-type2, are shown, as suggested by* Macwan and colleagues, 2011*. Examples of the minor variants of LinA-type1 and LinA-type2 are also included.*

Recently, a new type of LinA, LinA-type3, was discovered from *Novosphingobium barchaimii* LL02, isolated from a lindane production site in the Czech Republic (Pearce, 2015). $LinA_{LL02}$ was found to differ from LinA-type2 by eleven amino acids and from LinA-type1 by eighteen amino acids. In addition, $LinA_{LL02}$ has a truncated C-terminus, believed to be a consequence of excision of the IS6*100* element. This truncation has left the C-terminus of $LinA_{LL02}$ with only alanine instead of the known ALLQKS or IHFAPSGA motifs (Figure 7) (Pearce, 2015). Preliminary studies on $LinA_{LL02}$ have shown that while it can also degrade α-, γ- and δ-HCH, its degradation pattern

differs from those of LinA-type1 and LinA-type2, mainly due to its ability to degrade δ-HCH faster than α- and γ-HCH (Pearce, 2015). This finding was corroborated by a recent study of another LinA-type3 that was purified from a soil sample in India (Shrivastava et al., 2015). Interestingly also, while all type 1 and type 2 LinA variants characterised to date accumulate a single TCB (1,2,4-TCB) as a dead-end product *in vitro* (Lal et al., 2010), the newly characterized LinA-type3 variants accumulate all three TCBs (1,2,3-TCB, 1,3,5-TCB, and 1,2,4-TCB) (Pearce et al., 2015; Shrivastava et al., 2015).

One of the reasons proposed for these latter differences is that LinA-type3 has valine residues at position 44 and 64 whereas LinA-type1 and LinA-type2 both bear bulkier isoleucine and leucine residues at these positions, respectively; it is estimated that their replacement with valine residues would increase the volume of the active site by 22.3% (Pearce, 2015). This might allow for better positioning of δ-HCH but too much movement of γ-HCH, causing it to spend less time in the correct orientation for the reaction with the latter substrate to occur (Pearce, 2015).

```
                    10         20         30         40         50         60
                ....|....| ....|....| ....|....| ....|....| ....|....| ....|....|
Type1           MSDLDRLASR AAIQDLYSDK LIAVDKRQEG RLASIWWDDA EWTIEGIGTY KGPEGALDLA
Type1-minor     .......... .......... .......... .......... .......... ..........
Type2           .......... .......... ..G....... ....V..... .......... ..........
Type2-minor     .......... .........Q ..G....... .......... .......... ..........
Type3           .......... .........Q ..G....... .......... ...V...... .........V

                    70         80         90        100        110        120
                ....|....| ....|....| ....|....| ....|....| ....|....| ....|....|
Type1           NNVLWPMFHE CIHYGTNLRL EFVSADKVNG IGDVLLLGNL VEGNQSILIA AVFTDEYERR
Type1-minor     .......... .......... .......... .......... .......... ..........
Type2           .......Y.. T......... .......... .....C.... .......... ..Y.N.....
Type2-minor     .......... T......... .......... .....C.... .......... ..Y.N.....
Type3           ...V..RW.D F......... .......... .....C.... .......... ..Y.S.....

                   130        140        150
                ....|....| ....|....| ....|....| ....|.
Type1           DGVWKFSKRN ACTNYFTPLA GIHFAPPGIH FAPSGA     LinA2B90A, UT26
Type1-minor     .......... .......... .........L LQKS--     DS3-1
Type2           ........L. G.M....... ....V...A. ......     ITRC
Type2-minor     .....L..L. G.M....... ........AL LQKS--     LinA1B90A
Type3           ........L. GRM....... ....V..--- -----..    LL02
```

Figure 7 *Alignment of some of LinA variants based on their amino acid sequences. Three types of LinA, including the recently discovered LinA-type3, are shown.*

1.4.1.2 LinA mechanism

Nagasawa et al. (1993b) proposed a reaction mechanism by which γ-HCH is degraded by LinA, based on their observation of *S. japonicum* UT26 (LinA-type1) activity on γ-HCH. They concluded that the first two steps of the degradation happened by removing *trans*-diaxial H-Cl pairs (see Figure 8 for illustration of what constitutes a *trans*-diaxial H-Cl pair) from γ-HCH and γ-PCCH, yielding the putative 1,3,4,6-TCDN that could spontaneously degrade into 1,2,4-TCB. They concluded this by observing only 1,2,4-TCB in their assay, and not the 1,2,3- or 1,3,5-TCB which could have formed from attacks on other H-Cl pairs. Nagasawa et al. (1993b) also discovered γ-PCCH acts as a competitor for γ-HCH dehydrochlorination by LinA, which is at least consistent with the idea that similar mechanisms are involved in the two steps (Figure 8).

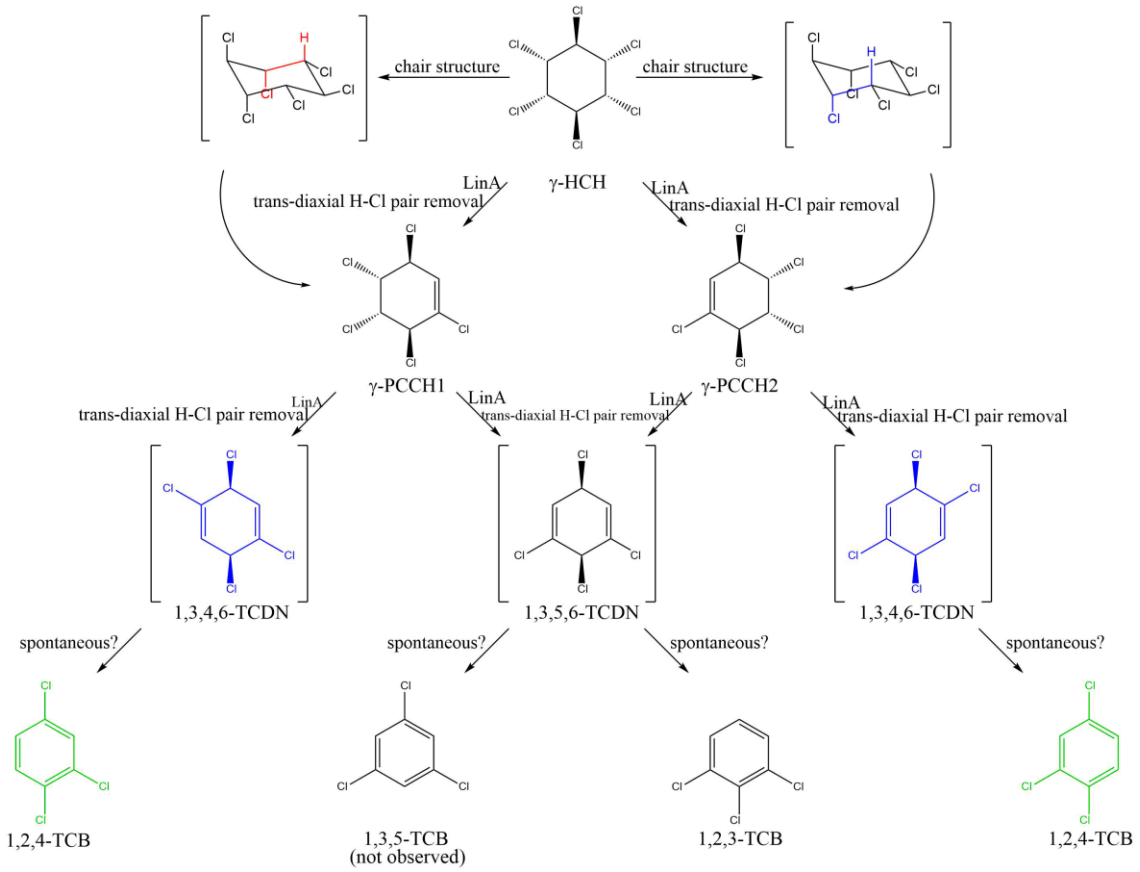

Figure 8 *γ-HCH transformation pathway by LinA$_{UT26}$ as observed by Nagasawa et al. (1993b) and Trantírek et al. (2001), with the addition of a possible route to producing 1,3,5-TCB (not observed). Both studies suggested the removal of trans-diaxial H-Cl pairs from γ-HCH and γ-PCCH, producing TCDN (TCDN molecules have not been observed empirically). Nagasawa et al. (1993b) suggested that TCDN would spontaneously transform into TCB due to its unstable diene-type structure, supported by their observation of only 1,2,4-TCB in their assay, which brings to their conclusion of γ-HCH goes through only the 1,3,4,6-TCDN route and not 1,3,5,6-TCDN. However, Trantírek et al. (2001) challenged this idea after observing 1,2,3-TCB formation in addition to 1,2,4-TCB in their assay; particularly when the pathway from γ-PCCH to 1,2,3-TCB would involve 1,3,5,6-TCDN formation, which could also transform spontaneously into 1,3,5-TCB (Orloff and Kolka, 1954). Additionally, Trantírek et al. (2001) believes γ-PCCH1 and γ-PCCH2 get transformed into 1,3,5,6-TCDN and 1,3,4,6-TCDN, and 1,2,3-TCB and 1,2,4-TCB, respectively (see text below). The chair structure for γ-HCH highlighting the trans-diaxial H-Cl pairs that can be removed by LinA are included. Trans-diaxial H-Cl pairs on γ-HCH that can be removed to produce γ-PCCH1 and γ-PCCH2 are highlighted in red and blue, respectively. Only H of the trans-diaxial pairs on γ-HCH are shown.*

Notwithstanding the findings of Nagasawa et al. (1993b), another study of γ-HCH degradation, in this case by purified LinA$_{UT26}$, found that it also produced 1,2,3-TCB, in addition to 1,2,4-TCB (Trantírek et al., 2001), but only in assays using chemically synthesized γ-PCCH consisting of similar amounts of both γ-PCCH1 and γ-PCCH2 enantiomers as substrate. Like Nagasawa et al. (1993b), they found it was not produced in assays using γ-HCH as substrate, which was found to only be transformed into γ-PCCH2 (Trantírek et al., 2001). γ-PCCH1 and γ-PCCH2 result from the removal of either one or other of the two *trans*-diaxial H-Cl pairs on γ-HCH by LinA. Hence,

Trantírek et al. (2001) concluded that $LinA_{UT26}$ transforms γ-PCCH1 and γ-PCCH2 into 1,3,5,6-TCDN and 1,3,4,6-TCDN, and eventually 1,2,3-TCB and 1,2,4-TCB, respectively. Interestingly, while it is generally accepted that TCDN is spontaneously transformed into TCB due to its unstable diene-type structure (Lal et al., 2010; Nagasawa et al., 1993a; Nagasawa et al., 1993b), Trantírek and colleagues (2001) did not observe any 1,3,5-TCB in their assay, although theoretically, 1,3,5,6-TCDN can be transformed into both 1,2,3- and 1,3,5-TCB (Figure 8) (Orloff and Kolka, 1954). Thus there remain significant questions on the mechanism by which TCDN transforms into TCB.

Intriguingly, a study of the activities of the type 2 and type 1 enzymes $LinA1_{B90A}$ and $LinA2_{B90A}$ respectively, on δ-HCH found that both enzymes can degrade both the δ-PCCH enantiomers produced from δ-HCH dehydrochlorination. Neither of the latter carry any *trans*-diaxial H-Cl pairs, suggesting LinA can also catalyse *syn*-1,4-elimination (Geueke et al., 2013) (Figure 9), supporting a similar elimination mechanism observed on a hexachlorocylohexene isomer by the same enzymes (Bala et al., 2012). However, Geueke et al. (2013) also postulated that $LinA1_{B90A}$ and $LinA2_{B90A}$ are able to discriminate which *syn*-H-Cl pair to remove from δ-PCCH as they found that only 1,2,4- and 1,2,3-TCB were produced from the degradation, and not 1,3,5-TCB. While 1,2,3- and 1,3,5-TCB are postulated to originate from the same 1,3,5,6-TCDN during γ-HCH degradation (Nagasawa et al., 1993b; Trantírek et al., 2001), they are thought to originate from 1,2,5,6-TCDN and 1,3,5,6-TCDN, respectively, during δ-HCH degradation, suggesting that only 1,2,5,6-TCDN (which can also spontaneously degrade into 1,2,4-TCB) was formed during δ-HCH degradation by $LinA1_{B90A}$ and $LinA2_{B90A}$ (Geueke et al., 2013) (Figure 9).

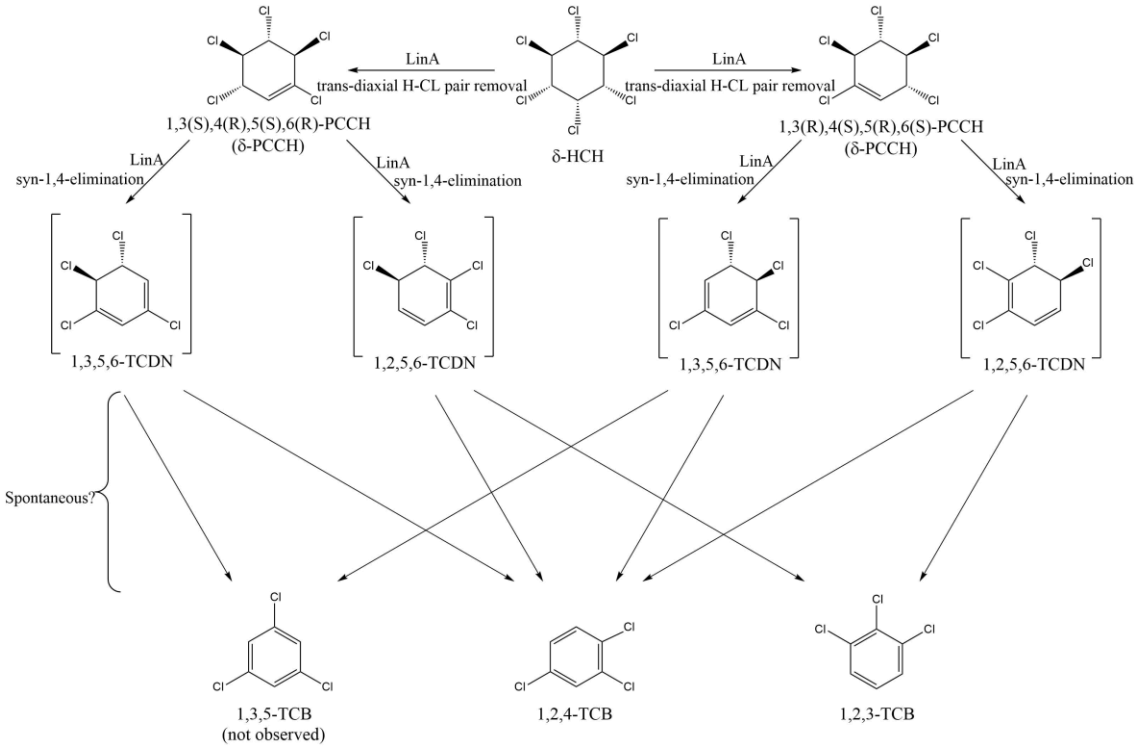

Figure 9 *δ-HCH transformation pathway by LinA1$_{B90A}$ and LinA2$_{B90A}$ as observed by Geueke et al. (2013). Possible routes to producing 1,3,5-TCB from δ-HCH are also included, although the study did not observe 1,3,5-TCB formation. TCDN molecules have not been observed empirically. Geueke et al. (2013) suggested LinA1$_{B90A}$ and LinA2$_{B90A}$ are able to initiate syn-1,4-elimination of H-Cl pairs from both δ-PCCH enantiomers, since both enantiomers lack trans-diaxial H-Cl pairs, but were able to be transformed by both enzymes into (eventually) 1,2,3- and 1,2,4-TCB. Geueke et al. (2013) also suggested that the pathway does not go through 1,3,5,6-TCDN due to the lack of 1,3,5-TCB formation (Orloff and Kolka, 1954). They further suggested that LinA1$_{B90A}$ and LinA2$_{B90A}$ discriminate which syn-1,4 H-Cl pairs on δ-PCCH enantiomers to remove, based on the lack of 1,3,5-TCB formation (Geueke et al., 2013). TCB formation from TCDN is believed to be spontaneous, although Trantírek et al. (2001) study on γ-HCH degradation by LinA$_{UT26}$ challenges this understanding (see Figure 8).*

Additionally, LinA has also been shown to degrade (+)-α-HCH and (-)-α-HCH into β-PCCH1 and β-PCCH2, respectively, and eventually 1,2,4-TCB (Shrivastava et al., 2015; Suar et al., 2005). Neither 1,2,3-TCB nor 1,3,5-TCB was observed in these studies (Shrivastava et al., 2015; Suar et al., 2005). As noted above, there is evidence that some forms of LinA catalyse *trans*-diaxial H-Cl removal from α-, γ-, and δ-HCH and γ-PCCH (Nagasawa et al., 1993b; Trantírek et al., 2001), and possibly a *syn*-1,4-elimination of an H-Cl pair from δ-PCCH and a hexachlorocyclohexene isomer (Bala et al., 2012; Geueke et al., 2013), but neither of these two H-Cl pair configurations exists in β-PCCH. Given also the evidence presented earlier (Section 1.4.1.1) that LinA1$_{B90A}$ and LinA2$_{B90A}$ prefer to degrade (+)-α-HCH and (-)-α-HCH, respectively (Suar et al., 2005), it seems

that different LinA types have different enantiopreferences for both the first and second steps in HCH degradation (Figure 10).

(A)

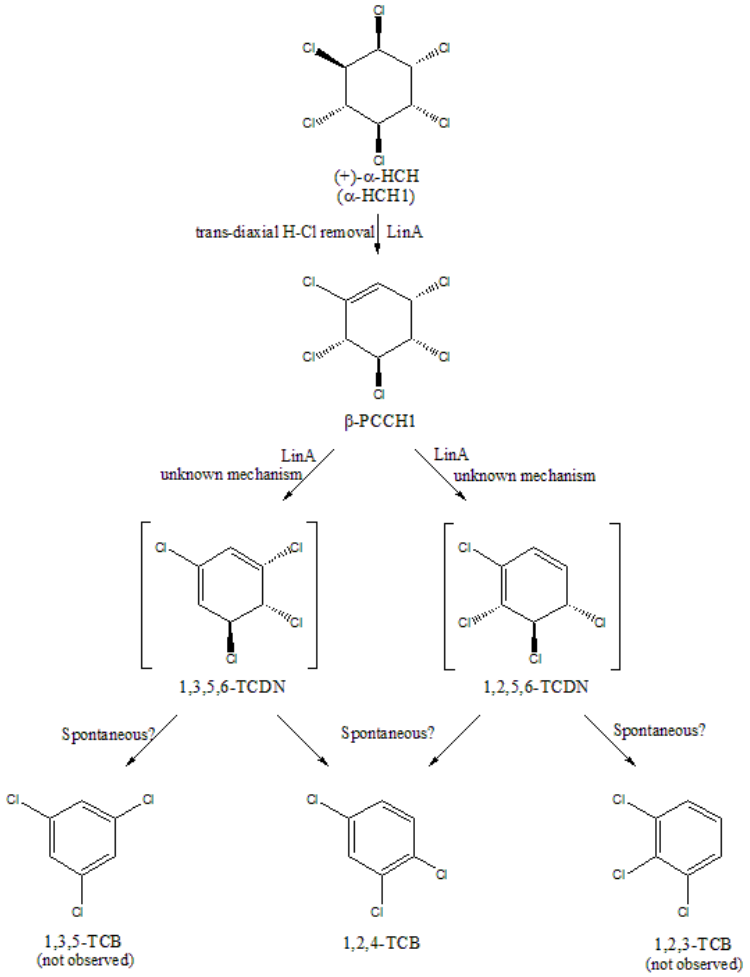

(B)

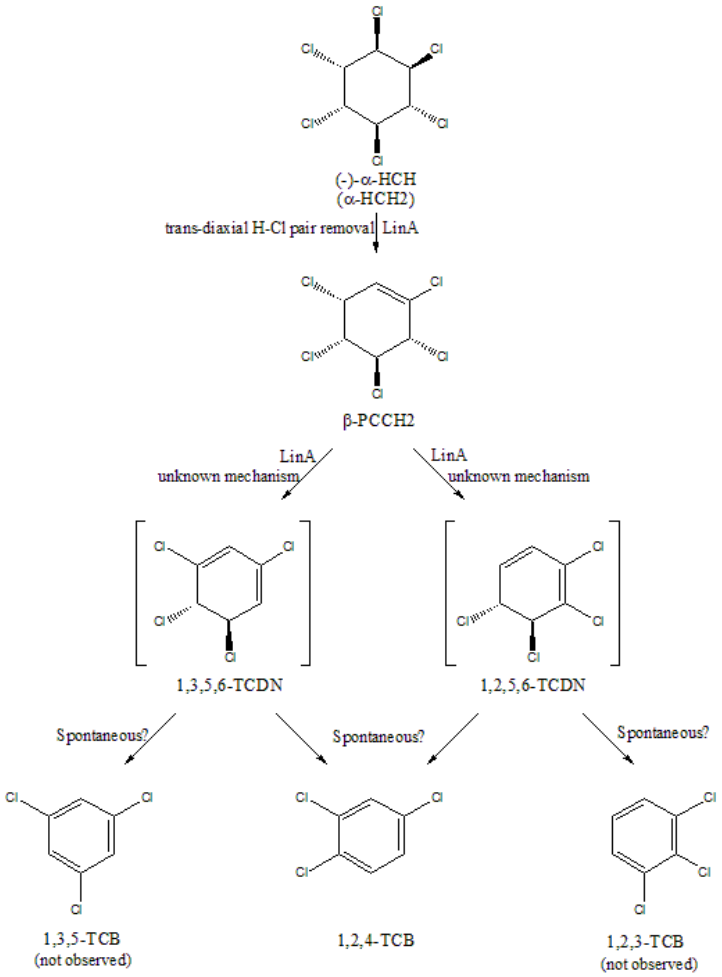

Figure 10 *(+)-α-HCH (A) and (-)-α-HCH (B) transformation pathways by LinA1$_{B90A}$ and LinA2$_{B90A}$, as observed by Suar et al. (2005). The possible pathways to producing 1,2,3- and 1,3,5-TCB from (+)-α-HCH and (-)-α-HCH are also included, although not observed. TCDN molecules have not been observed empirically. It is believed that LinA works by eliminating trans-diaxial H-Cl pairs from substrate, which is fitted for the transformation of (+)-α-HCH and (-)-α-HCH into β-PCCH1 and β-PCCH2, respectively (Nagasawa et al., 1993b; Trantírek et al., 2001). However, the mechanism by which these enzymes transform β-PCCH1 and β-PCCH2 into TCDN is unknown. The 1,3,5,6- and 1,2,5,6-TCDN in the figures are possible TCDN molecules that could transform into the observed 1,2,4-TCB. Additionally, these TCDN molecules can also be transformed into 1,3,5- and 1,2,3-TCB, respectively (see Chapter 5), although these were not observed in the study (Suar et al., 2005). (+)-α-HCH and (-)-α-HCH are also referred to as α-HCH1 and α-HCH2, respectively, in this thesis, as discussed in Section 5.2.1.*

Overall, there are two major outstanding issues surrounding the LinA mechanism. The first concerns the ways LinA eliminates H-Cl pairs from substrates, either by removing the *trans*-diaxial H-Cl pairs as suggested by Nagasawa et al. (1993b) for a type 1 enzyme acting on γ-HCH and γ-PCCHs, by *syn*-1,4-elimination as suggested by Bala et al. (2012) and Geueke et al. (2013) for type 1 and type 2 enzymes acting on δ-PCCHs and a hexachlorocyclohexene isomer, or by an unknown mechanism as observed by Suar et al. (2005) for type 1 and type 2 enzymes acting on

β-PCCHs. The second issue surrounds the enzymes' enantiopreferences as exemplified in both the initial α-HCH substrate preferences of $LinA1_{B90A}$ and $LinA2_{B90A}$ (Suar et al., 2005), and in the production of downstream metabolites during γ-HCH degradation by $LinA_{UT26}$ (Trantírek et al., 2001). Specifically, the enantiopreferences of all three types of LinA on transformation of its various substrates and production of its various metabolites have not been fully studied in detail.

1.5 This work

The research described in the following chapters has two foci, characterisation of the activities of the new type 3 form of LinA and further resolution of the mechanism(s) of action of LinAs of all three types on HCHs and PCCHs. Specifically, it aims to determine the activities of the type 3 enzyme $LinA_{LL02}$ against α-, γ-, and δ-HCH in *in vitro* enzymatic assays and to compare them to the corresponding activities of the LinA-type2 and LinA-type1 enzymes LinA1 and LinA2, respectively, from S. *indicum* B90A. In addition to their activities on α-, γ-, and δ-HCH, the activities of the three enzymes on γ- and δ-PCCH are also compared. Subsequently, the mechanisms of the LinAs' activities on these substrates are investigated by molecular dynamics (MD). The project is divided into five main parts, as described below.

(i) A comparison of the degradation of γ-HCH and γ-PCCH by $LinA_{LL02}$, $LinA1_{B90A}$, and $LinA2_{B90A}$ (Chapter 2).

(ii) A comparison of the degradation of δ-HCH and δ-PCCH by $LinA_{LL02}$, $LinA1_{B90A}$, and $LinA2_{B90A}$ (Chapter 3).

(iii) A comparison of mutants of $LinA_{LL02}$ and $LinA1_{B90A}$ at positions 44 and 64 with the wild-type enzymes for their activities on γ- and δ-HCH, and γ- and δ-PCCH (Chapter 4).

(iv) Testing the enantiopreference of $LinA_{LL02}$ for α-HCH and comparing it to those of $LinA1_{B90A}$ and $LinA2_{B90A}$ (Chapter 5).

(v) MD simulation of $LinA1_{B90A}$, $LinA2_{B90A}$ and $LinA_{LL02}$ with α-, γ-, δ-HCH and their corresponding PCCH isomers to investigate the correlation between the enzymes' activity and proximity of substrates to H73 (Chapter 6).

My assays are primarily based on estimates of specificity constants, because the solubility of all the above substrates in the assay condition is too low to estimate K_m (National Toxicology Program, 2016a). Most of the data presented are obtained using the HCHs as the primary substrates, with the specificity constants for the degradation of both those and their PCCH products being estimated from the same reaction tubes using the Copasi 4.15 software (Hoops et al., 2006). Assays were also carried out using the various PCCHs as the primary substrates but refractory mass balance problems for key compounds in some of these latter assays restricted my use of them (see Figure 15, Section 2.3 *Results* below). Even where used, I have generally just presented progress curves for key compounds, with specificity constants only occasionally presented from these assays.

MD simulations were run for 100 ns for each enzyme-substrate pair, providing enough data for a statistically meaningful analysis. The analysis was done by examining the percentages of time the ligands are in productive poses and relating those percentages to the efficiency statistics obtained from the enzyme assays. The interaction between the substrates and other residues in the active sites was also considered.

My study provides evidence of novel LinA mechanisms in addition to the known dehydrochlorination on diaxial H-Cl pairs on its substrates. Novel quantitative information on $LinA_{LL02}$, $LinA1_{B90A}$, and $LinA2_{B90A}$ degradation activities, including their enantiopreferences where relevant, on α-, γ-, and δ-HCH and γ- and δ-PCCH are also obtained. It also yields new insights into the role of residues at position 44 and 64 in LinA's degradation activities. To the best of my knowledge, my study is also the first to report extensive simulations of LinA enzymes' interactions with their substrates. The significance of my findings for an understanding of the LinA mechanism and the evolution of the Lin pathway is described in Chapter 7.

CHAPTER 2:

γ-HCH degradation kinetics by wild type $LinA1_{B90A}$, $LinA2_{B90A}$ and $LinA_{LL02}$ enzymes

2.1 Introduction

As detailed in Chapter 1, LinA-type3 is a new type of LinA that has not been thoroughly characterised. Hence, I decided to test $LinA_{LL02}$ activities on α-, γ- and δ-HCH. In this chapter, I report the kinetic characterization of the first two dehydrochlorination steps in the degradation of γ-HCH by a LinA-type3 ($LinA_{LL02}$), LinA-type1 ($LinA2_{B90A}$), and LinA-type2 variant ($LinA1_{B90A}$).

2.2 Materials and methods

2.2.1 γ-PCCH synthesis

A published protocol (Trantírek et al., 2001) was followed for the synthesis of γ-PCCH for use as a standard in the gas chromatography (GC) below, and as a substrate in some assays. 1 g of γ-HCH (Sigma-Aldrich, Castle Hill, NSW) was dissolved in 100 mL acetonitrile before the addition of 50 mL of 0.1 M NaOH into the mixture. The mixture was then heated for 20 min at 40 ^{o}C. The resulting γ-PCCH was extracted twice with 150 mL of hexane. The hexane fractions were combined and reduced in volume to approximately 1.5 ml before purification using a silica column with 20% dichloromethane in hexane as the eluent. The solvent was then evaporated under a stream of nitrogen gas. The crude product was a colourless liquid weighing 3.5 mg which resisted further evaporation even under a prolonged nitrogen gas stream. The crude yield was thus 0.35%. 1.5 mg of γ-PCCH was then dissolved in 1 mL of dimethyl sulfoxide (DMSO) to create a stock solution for use in the experiments below.

The purity of the synthesised γ-PCCH was determined by GC using a 1:200 dilution of the dissolved product in hexane (1 µL injection volume, capillary column (30 m, 320 µm, 0.25 µm), Astec® Chiraldex® B-DP column (Sigma-Aldrich, Castle Hill, NSW), electron capture detector (ECD)). The chromatogram (Figure 11) indicated that the synthesised γ-PCCH was >90% pure; proton NMR subsequently carried out by Dr Andrew Warden (CSIRO Land and Water) estimated the purity at >97% (data not shown). The γ-PCCH stock was kept at room temperature until needed.

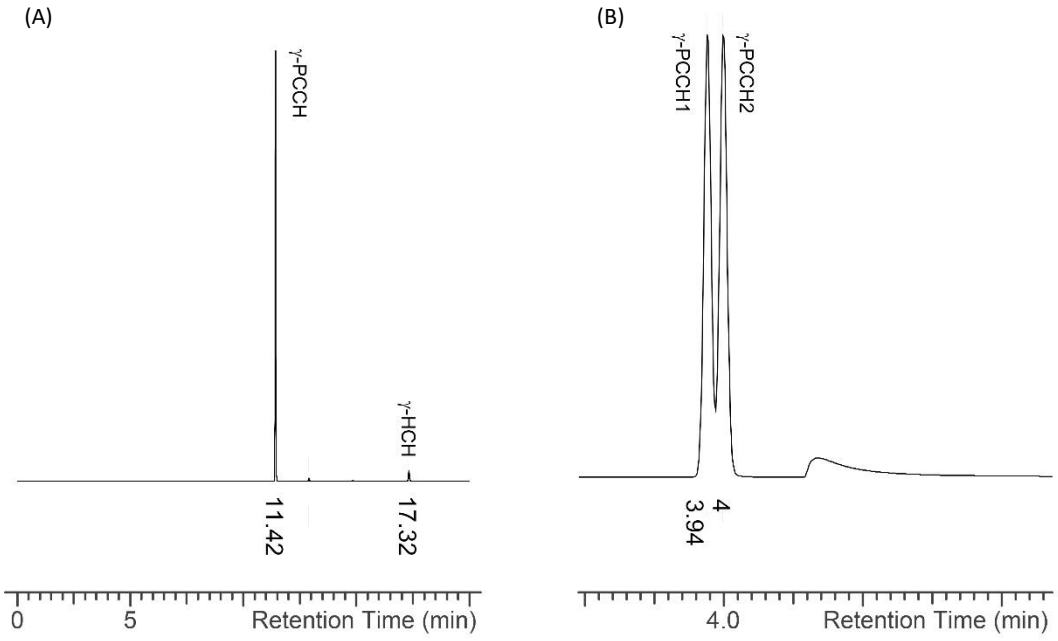

Figure 11 *Chromatograms showing the synthesised γ-PCCH when ran through (A) a (non-chiral) capillary column and (B) an Astec® Chiraldex® B-DP chiral column. The peaks in (A) demonstrate the purity of the synthesised γ-PCCH to be >90%, while the peaks in (B) demonstrate resolution of the two enantiomers of γ-PCCH, γ-PCCH1 and γ-PCCH2, with retention times of 3.94 and 4.00 min, respectively.*

The chromatography above also successfully separated the two enantiomers of γ-PCCH expected (Figure 12), hereafter designated γ-PCCH1 and γ-PCCH2, at a ratio of 49:51 and retention times of 3.94 and 4.00 min respectively (Figure 11B). Trantírek et al. (2001) had used 2D-NMR to resolve these enantiomers and they went on to show that their 1,3(*R*),4(*S*),5(*S*),6(*R*)-PCCH was degraded more rapidly than 1,3(*S*),4(*R*),5(*R*),6(*S*)-PCCH by $LinA_{UT26}$, which is identical in amino acid sequence to the $LinA2_{B90A}$ used here (Suar et al., 2005). To determine which of 1,3(*R*),4(*S*),5(*S*),6(*R*)-PCCH and 1,3(*S*),4(*R*),5(*R*),6(*S*)-PCCH corresponded to γ-PCCH1 and γ-PCCH2, I assayed the degradation of my γ-PCCH preparation with $LinA2_{B90A}$ as per the methods below (Figure 13). I had problems recovering the relatively very high starting concentrations of the γ-PCCHs in these assays (I cover this in more detail in later sections) but the GC progress curves from 50 minutes onwards clearly show that more γ-PCCH2 than γ-PCCH1 was degraded. I observed two TCBs to accumulate from the subsequent degradation of the PCCHs with 1,2,4-TCB more abundant than 1,2,3-TCB (see Appendix A). This is consistent with Trantírek et al.

(2001) who also found LinA2$_{B90A}$ produces mostly 1,2,4-TCB and some 1,2,3-TCB from the degradation of his PCCHs. Since the two enantiomers were in roughly equimolar amounts in my preparation (which is reasonable for a chemical synthesis: Trantírek et al., 2001), I conclude that my γ-PCCH1 and γ-PCCH2 most likely correspond to 1,3(*S*),4(*R*),5(*R*),6(*S*)-PCCH and 1,3(*R*),4(*S*),5(*S*),6(*R*)-PCCH, respectively (Figure 12).

Figure 12 *Expected γ-PCCH enantiomers from γ-HCH degradation*

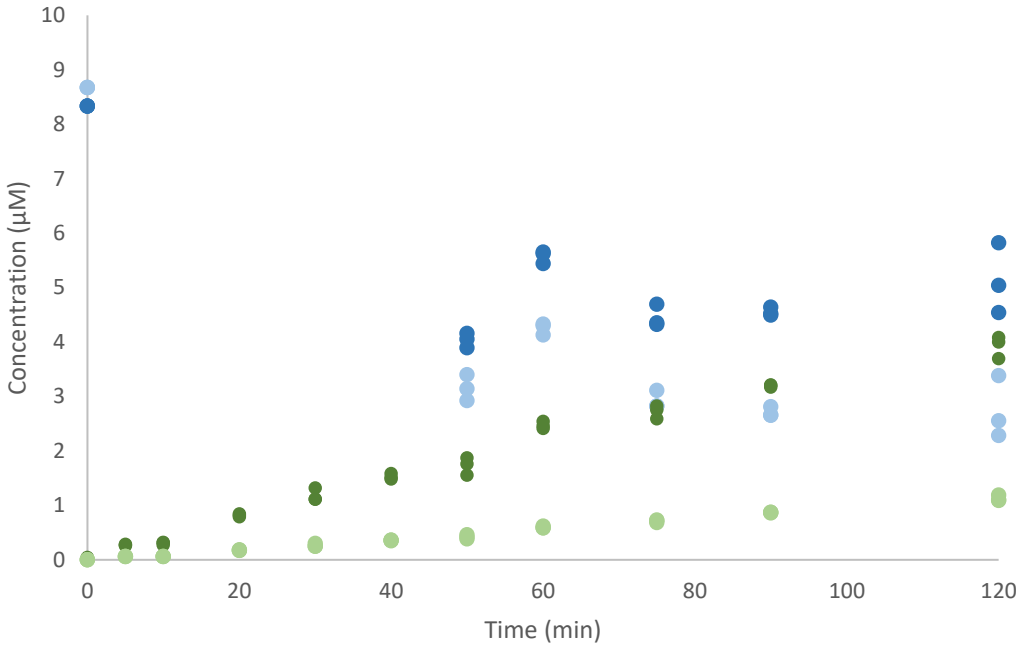

Figure 13 *Production of 1,2,4-TCB (●) and 1,2,3-TCB (●) from a total of 17 μM of my synthesised γ-PCCH1 (●) and γ-PCCH2 (●) by 0.01 μg/mL LinA2$_{B90A}$. The data for both γ-PCCHs from 0 to 50 minutes have been excluded because there were problems recovering and measuring the high starting concentrations of γ-PCCH in these assays – see Section 2.2.4 below. The initial γ-PCCH1 and γ-PCCH2 concentrations shown are those calculated from the volume of stock solution added (see section 2.2.1). Note that γ-PCCH2 concentration is significantly lower than γ-PCCH1 concentration at the end of the assay.*

2.2.2 Gene sequences and enzyme purifications

His6-tagged and codon optimized *linA1*$_{B90A}$ (GenBank accession number AAN64239) and *linA*$_{LL02}$ (GenBank accession number KMS50456) in pDEST14 and codon optimized *linA2*$_{B90A}$ (GenBank

accession number AAN64240) in pDEST17 were used for expression in *Escherichia coli* BL21*(DE3). pDEST 14 and pDEST17 were sourced from Invitrogen (Mulgrave, VIC). Overnight seed cultures of this strain containing $linA1_{B90A}$, $linA2_{B90A}$, or $linA_{LL02}$ in the respective expression vector were prepared by using the corresponding glycerol stock to inoculate two 10 mL Luria Broth (LB) cultures containing 100 µg/mL ampicillin and incubating them at 37 °C with shaking at 200 rpm. Each 10 mL culture was then used to inoculate 1 L LB media containing 100 µg/mL ampicillin. The latter cultures were incubated overnight at 28 °C with shaking at 200 rpm to express the proteins. It was not necessary to induce the cultures with IPTG, due to the high basal expression characteristic of *E. coli* strain BL21*(DE3) (data not shown).

After the overnight incubation, the cells were pelleted by centrifugation at 4,000 g for 15 min at 4 °C. The cell pellet was then resuspended in 40 mL of binding buffer (0.02 M sodium phosphate, 0.5 M NaCl, 0.02 M imidazole, pH 7.4) and put through three rounds of sonication (alternating 0.5 s active and 1 s rest periods for a total of 45 s of active periods for each round) to break open the cells. The preparation was then centrifuged at ~33,000 g for 40 min at 4 °C and the supernatant passed through a 0.45 µm filter to remove impurities.

The His6-tagged enzyme was purified by applying the supernatant to a 250 µL gravity flow Ni-NTA agarose column (ThermoFisher Scientific, Scoresby, Vic) that had been washed with 10 mL of Milli-Q H_2O and treated with 10 mL of the binding buffer. The column was then washed with 10 mL of the binding buffer to remove any unbound enzymes. The enzyme was eluted with 3 mL of elution buffer (0.02 M sodium phosphate, 0.5 M NaCl, 0.5 M imidazole, pH 7.4) and transferred into two 3 mL 3.5 MWCO Slide-A-Lyzer® dialysis cassettes (ThermoFisher Scientific) before being left to dialyse overnight in 2 L of storage buffer (0.02 M sodium phosphate, 0.5 M NaCl, pH 7.4) at 4 °C with slow stirring. A small sample of the dialyzed enzyme was then checked for purity by running it through a pre-cast 4-12% Bis-Tris SDS-PAGE gel (ThermoFisher Scientific) and staining it with Coomassie Blue (Figure 14). The enzyme was kept at 4 °C if it was to be used

within five days or otherwise stored at -80 °C for future use. No loss of activity was detected when the enzymes were kept in these conditions (data not shown).

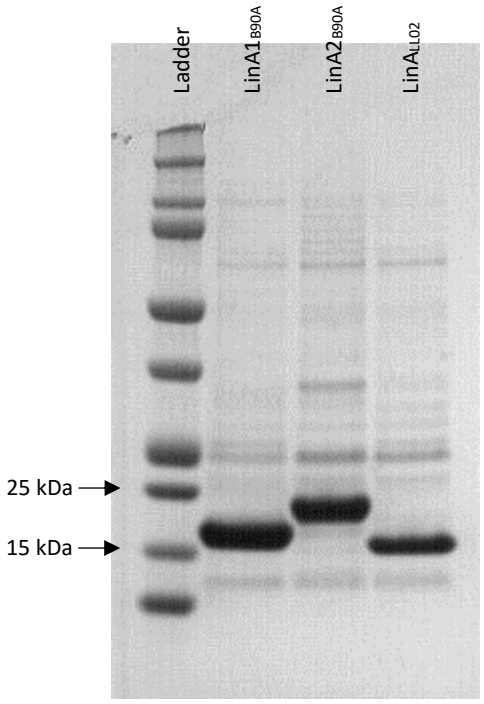

Figure 14 *SDS-PAGE gel of partially, but substantially, purified LinA1$_{B90A}$, LinA2$_{B90A}$, and LinA$_{LL02}$ stained with Coomassie Blue. The difference in mass is due to the difference in sequences between the enzymes, especially in the C-terminal, as discussed in Section 1.4.1.1.*

2.2.3 Degradation assays with γ-HCH as substrate

Triplicate γ-HCH degradation assays were set up at room temperature in individual 1.5 mL amber glass screw-cap vials for each enzyme and time point. 250 µL of working buffer (50 mM potassium phosphate, 10% glycerol, pH 7.5) containing 34 µM γ-HCH was added to each vial. The preparation was then sonicated for 2 min to ensure that the substrate was completely dissolved before the addition of 250 µL of working buffer containing twice the final concentration of the enzyme, which was 10 µg/mL for LinA1$_{B90A}$ and LinA$_{LL02}$, and 0.1 µg/mL for LinA2$_{B90A}$. The final concentrations of the enzymes were selected so as to allow each enzyme to degrade γ-HCH at a conveniently measurable rate, which I found in pilot experiments to be approximately 100% γ-HCH degradation in one hour (data not shown), although the experimental assays were left for 2 h, to observe for additional activity that may take place during this additional hour (e.g. metabolites degradation and production). Each vial was then sealed immediately with a septa cap to prevent any loss of possible volatile metabolites. At each

time point, the reaction was stopped by the injection of 400 µL of ethyl acetate through the septa cap. Then, 100 µL of 56 µM pentachloronitrobenzene (PCNB, >94% pure, Sigma-Aldrich, Castle Hill, NSW) in ethyl acetate was injected into each vial to a final concentration of 11 µM PCNB to act as an internal standard. The septa caps were replaced with new ones before the vials were shaken vigorously for a second by hand, and let rest for at least 8 h to separate the ethyl acetate layer from the aqueous layer. Each sample was then analysed on a GC fitted with an Astec® Chiraldex B-DP column (Sigma-Aldrich) and an electron capture detector (GC-ECD). The injection volume was 1 µL, the split ratio was 30:1, and the temperature was 150 ^{o}C for 30 min.

The concentrations of HCH, PCCHs, and TCBs were calculated from the areas under the curves from the GC-ECD chromatograms using standard curves prepared from the synthesized γ-PCCH and commercially available γ-HCH and TCBs (all from Sigma-Aldrich). Chromatogram showing the retention times for 1,2,3-, 1,2,4- and 1,3,5-TCB are provided in Appendix A. Graphs of the kinetics of γ-HCH degradation for each enzyme in the final experiments were then constructed using Copasi 4.15 (Hoops et al., 2006). Mass action (irreversible) was set as the rate law. The graphs and kinetics were calculated by applying the experimental data to the parameter estimation function, using the evolutionary programming method. The graphs were chosen based on the lines which best fitted the experimental data. The enzyme efficiency (k_{cat}/K_m) value of each reaction was calculated using the *k* value (the rate constant) given by the program divided by the concentration of the enzyme (Fersht, 1999).

2.2.4 Degradation assays with γ-PCCH as substrate

As noted in Section 2.2.1 above, γ-PCCH degradation assays were also carried out. The intention was to use these assays for two purposes: firstly, assays with $LinA2_{B90A}$ were carried out in order to identify the two γ-PCCH enantiomers and, secondly, assays were carried out with all three enzymes to provide independent estimates of the specificity constants for the second

dehydrochlorination step. These assays used 17 µM of the synthesised γ-PCCH but otherwise followed the same methods described above for γ-HCH degradation.

These assays worked sufficiently well for my first purpose, identifying the two γ-PCCH enantiomers, but mass balance problems frustrated my attempts to get usable kinetic data for the second purpose. These problems seemed mainly to be due to less than stoichiometric recovery and measurement of the 17 µM γ-PCCH initially provided to the assay mix. I tried several modifications to the assay conditions (including varying the initial substrate and enzyme concentrations and assay duration) but none of them improved the assay sufficiently to satisfy mass balance criteria and enable meaningful estimates of specificity constants.

2.3 Results

10 µg/mL of $LinA1_{B90A}$ and $LinA_{LL02}$, and 0.1 µg/mL of $LinA2_{B90A}$ were incubated with 17 µL of γ-HCH at room temperature for 2 h and the concentrations of γ-HCH and its metabolites were measured over time by GC-ECD (Figure 15). All three enzymes were observed to degrade γ-HCH, with $LinA2_{B90A}$ degrading it completely in less than 2 h and $LinA1_{B90A}$ and $LinA_{LL02}$ degrading more than 90% of it in 2 h. γ-HCH degradation by all three enzymes produced both γ-PCCH1 and γ-PCCH2, with the γ-PCCH2 level higher than that of γ-PCCH1 in all assays. However, γ-PCCH1 and γ-PCCH2 levels were both lower in the $LinA1_{B90A}$ assay than the others. The great majority of both γ-PCCHs was converted to TCB by all three enzymes, predominantly 1,2,4-TCB in the case of $LinA2_{B90A}$ and $LinA1_{B90A}$ but a mix of 1,2,4-TCB, 1,2,3-TCB and 1,3,5-TCB, with the 1,2,3-TCB slightly more abundant, in the case of $LinA_{LL02}$ (Figure 15). There was no evidence for further degradation of the TCBs in any of the assays, at least within the two hour time frames of the assays.

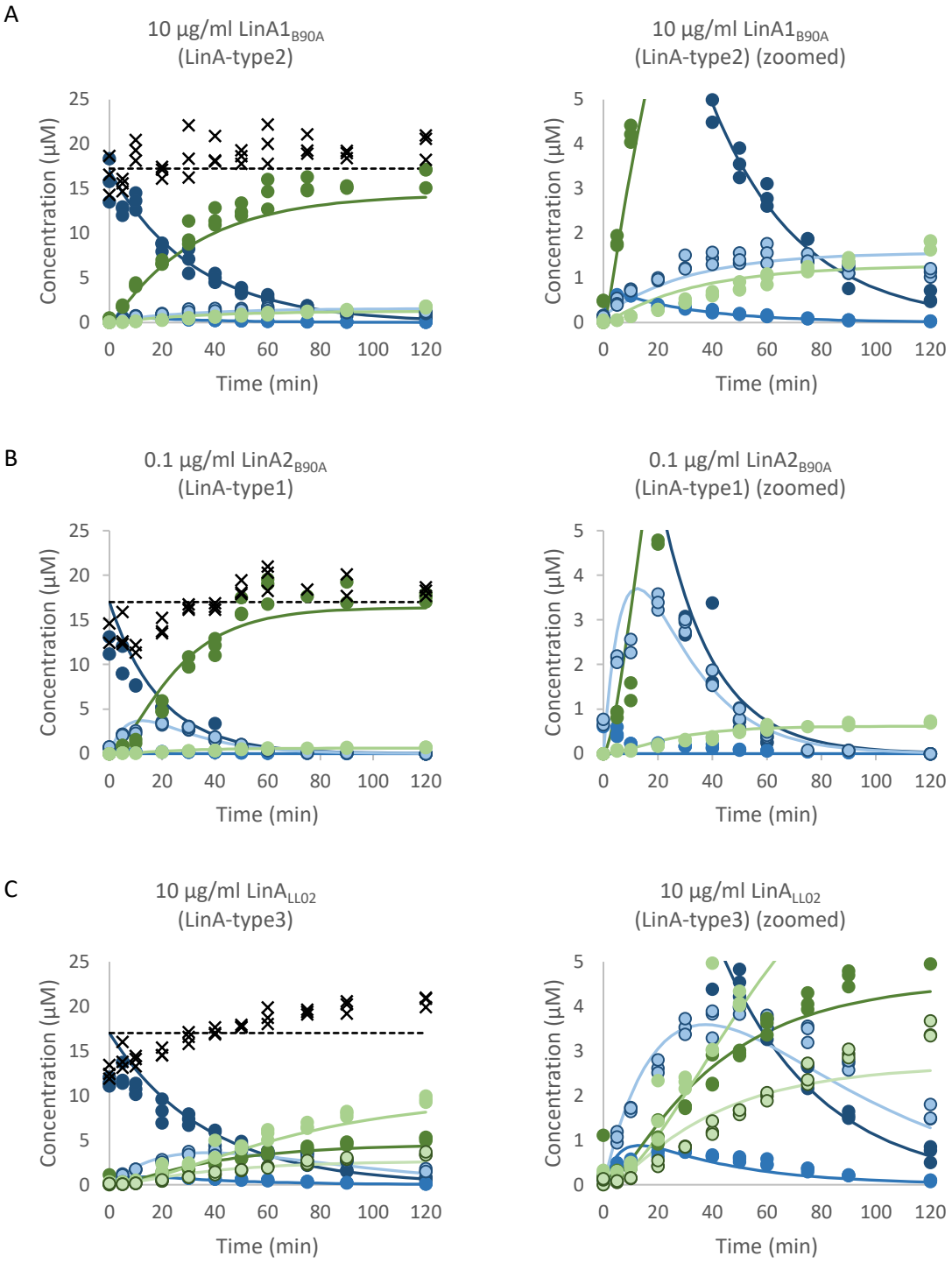

Figure 15 *Graphs showing the concentrations of γ-HCH and its metabolites over time (min) in γ-HCH degradation assays by (A) 10 µg/mL LinA1$_{B90A}$, (B) 0.1 µg/mL LinA2$_{B90A}$, and (C) 10 µg/mL LinA$_{LL02}$. The compounds are as follows: γ-HCH (●), γ-PCCH1 (●), γ-PCCH2 (○), 1,2,4-TCB (●), 1,2,3-TCB (●), and 1,3,5-TCB (○). Also shown in the graphs are the best fit lines deduced by Copasi. Total measured mass is marked with (x) and the total mass assumed by Copasi is drawn with dotted line (---). Zoomed version of the graphs are provided on the right to provide better resolution for some less abundant metabolites. LinA2$_{B90A}$ completely degraded γ-HCH faster than LinA1$_{B90A}$ and LinA$_{LL02}$, despite being 100 times less concentrated than the other two enzymes.*

In line with these progress curves and the relative concentrations of the enzymes used, the enzyme efficiency (k_{cat}/K_m) values calculated (Table 2) show that LinA2$_{B90A}$ is the most efficient of the three enzymes in degrading γ-HCH, with no clear preference between conversion into γ-PCCH2 or γ-PCCH1. There is little difference between the other two enzymes although LinA1$_{B90A}$ shows less efficient conversion to γ-PCCH2.

The statistics also show LinA2$_{B90A}$ to be the most efficient enzyme in converting both γ-PCCH1 and γ-PCCH2 to 1,2,4- and 1,2,3-TCB, although its efficiency converting γ-PCCH1 is 2-3 logs higher than it is for γ-PCCH2. LinA1$_{B90A}$ is slightly more efficient than LinA$_{LL02}$ in converting γ-PCCH1 to 1,2,3- and 1,2,4-TCB whereas there is a clear difference between the two enzymes in the opposite direction for the conversion of γ-PCCH2 into these TCBs. Like LinA2$_{B90A}$, LinA1$_{B90A}$ is more efficient in transforming γ-PCCH1 than γ-PCCH2 but the difference is smaller and not consistent for LinA$_{LL02}$. LinA2$_{B90A}$ also transforms both γ-PCCH1 and γ-PCCH2 into 1,2,4-TCB more efficiently than it does into 1,2,3-TCB, but LinA1$_{B90A}$ and LinA$_{LL02}$ only do so for γ-PCCH1; the efficiencies of LinA1$_{B90A}$ for γ-PCCH2 are generally too low for confident discrimination while LinA$_{LL02}$ shows the reverse preference. LinA$_{LL02}$ transforms γ-PCCH1 more efficiently than γ-PCCH2 into 1,3,5-TCB and its rate for the former is intermediate between its rate for the other two TCBs (Table 2).

Table 2 *k_{cat}/K_m values (min^{-1} μM^{-1}) and their standard errors (SEs) (min^{-1} μM^{-1}) for reactions involved in γ-HCH and γ-PCCH degradation by LinA1$_{B90A}$, LinA2$_{B90A}$, and LinA$_{LL02}$. Levels that are not detected are denominated with a dash symbol (-). Number of independent replicate is 3.*

Reactions	LinA1$_{B90A}$ (LinA-type2)	SE LinA1$_{B90A}$	LinA2$_{B90A}$ (LinA-type1)	SE LinA2$_{B90A}$	LinA$_{LL02}$ (LinA-type3)	SE LinA$_{LL02}$
γ-HCH -> γ-PCCH1	3.2E-03	*5.2E-04*	3.7E-01	*4.2E-03*	1.5E-03	*4.3E-04*
γ-HCH -> γ-PCCH2	2.9E-04	*9.7E-05*	4.1E-01	*2.5E-03*	1.9E-03	*4.9E-04*
γ-PCCH1 -> 1,2,4-TCB	6.6E-02	*1.1E-02*	5.0E+02	*1.2E+02*	1.2E-02	*7.2E-03*
γ-PCCH1 -> 1,2,3-TCB	5.8E-03	*1.8E-03*	3.1E+01	*7.3E+00*	1.6E-03	*9.8E-03*
γ-PCCH1 -> 1,3,5-TCB	-		-		7.1E-03	*4.8E-03*
γ-PCCH2 -> 1,2,4-TCB	<1.0E-04	*7.4E-04*	8.0E-01	*7.1E-03*	1.0E-04	*1.3E-03*
γ-PCCH2 -> 1,2,3-TCB	<1.0E-04	*4.6E-04*	5.2E-03	*8.4E-04*	3.1E-03	*1.8E-03*
γ-PCCH2 -> 1,3,5-TCB	-		-		<1.0E-04	*8.6E-04*

The problems with stoichiometric recovery of the initially high γ-PCCH concentrations outlined in Section 2.2.4 prevented meaningful analysis of the γ-PCCH-based assay data. It is simply noted here that they confirm the results from the γ-HCH-based assays to the extent that they show 1,2,4-TCB and 1,2,3-TCB accumulating in the assays with $LinA1_{B90A}$ and $LinA2_{B90A}$ (with 1,2,4-TCB in excess in both cases) and both these (in similar amounts) and 1,3,5-TCB (lesser quantities) in the $LinA_{LL02}$ assays (Figure 16).

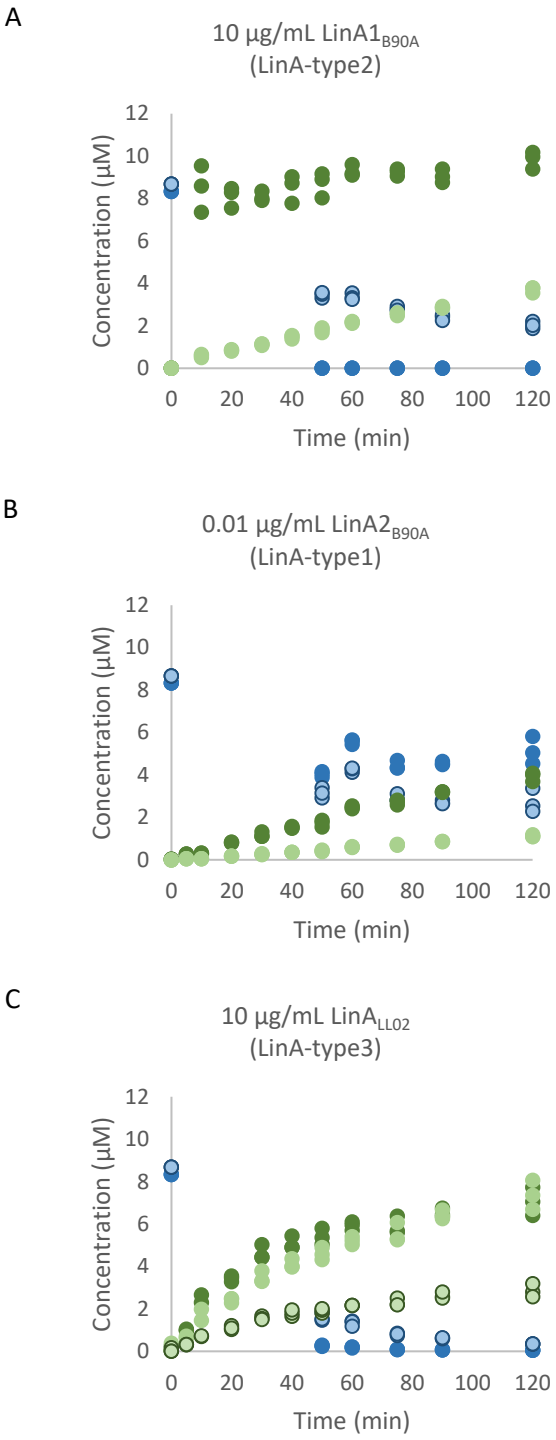

Figure 16 *Graphs showing the formation of TCB isomers in γ-PCCH degradation assays by (A) 10 µg/mL LinA1$_{B90A}$, (B) 0.01 µg/mL LinA2$_{B90A}$, and (C) 10 µg/mL LinA$_{LL02}$ over time. All assays produced 1,2,3-TCB (●) and 1,2,4-TCB (●), but only the LinA$_{LL02}$ assay produced 1,3,5-TCB (○), supporting my observations on γ-HCH degradation assays by the same enzymes. Also note that 1,2,4- and 1,2,3-TCB were produced in approximately the same amounts in the LinA$_{LL02}$ γ-PCCH assay, but not the LinA$_{LL02}$ γ-HCH assay (Figure 15), most probably due to the different ratios of γ-PCCH1 and γ-PCCH2 available as substrates in these assays. Also shown on the graphs are the measured concentrations of γ-PCCH1 (●) and γ-PCCH2 (○), excluding the data from 0 to 50 minutes due to the mass balance issues outlined earlier. Thus the γ-PCCH1 and γ-PCCH2 concentrations shown at 0 minutes are those calculated from the volume of stock solution added (see section 2.2.1). Kinetic analysis of these assays were not done due to the mass balance issues. The data shown for LinA2B90A are the same as those in Figure 13.*

2.4 Discussion

2.4.1 γ–HCH transformations

This study has shown that the LinA-type1 enzyme, $LinA2_{B90A}$, degrades γ-HCH at least two orders of magnitude more efficiently than does the LinA-type2 enzyme $LinA1_{B90A}$ and the LinA-type3 $LinA_{LL02}$. The difference between $LinA2_{B90A}$ and $LinA1_{B90A}$ is in qualitative agreement with Sharma et al. (2011), who found that the turnover number (min^{-1}) for γ-HCH degradation is almost 10 times higher for $LinA2_{B90A}$ than for $LinA1_{B90A}$. Sharma et al. (2011) did not study $LinA_{LL02}$, but did include four other LinA-type1 enzymes and one other LinA-type2 in their assays, finding that the difference between the two LinA-types was consistent across all those enzymes. It therefore seems likely that this difference may be a generally discriminating feature of the two enzyme types.

While my study did not find clear differences in enantiopreferences in terms of the conversion of γ-HCH into γ-PCCH1 or γ-PCCH2 for either the type1 $LinA2_{B90A}$ or the type3 $LinA_{LL02}$, it did find that the type2 enzyme $LinA1_{B90A}$ converted γ-HCH preferentially into γ-PCCH1. The only previous study investigating this preference, by Trantírek et al. (2001), only used the type1 enzyme $LinA_{UT26}$ and they found it only converts γ-HCH into 1,3(*R*),4(*S*),5(*S*),6(*R*)-PCCH, presumptively γ-PCCH2. I cannot fully explain the difference between the two studies but I note that HP Kohler (EAWAG, Switzerland, pers. comm.) has produced a schema which shows how the γ-PCCH produced depends on which of two spontaneously interconverting conformers of γ-HCH is used to generate the γ-PCCH, as explained in Figure 17. (This schema also impacts on downstream TCB production, as explained in Section 2.4.2 below.) It may be that this process is influenced both by the enzyme variant and the assay conditions. The enzyme variant could be important if the interconversion between conformers occurs in the active site and is affected by the amino acid differences between variants in the active site (Pearce, 2015) (see Chapter 6). The assay conditions could also be important given that there will be competition not just between enantiomers and conformers but between the reactants for the first and (generally faster; see

below) second dehydrochlorination steps; Trantírek et al. (2001) used much more enzyme (45 cf. 0.1 µg/mL) and much longer incubation times (24 cf. 2 hr) than my methods.

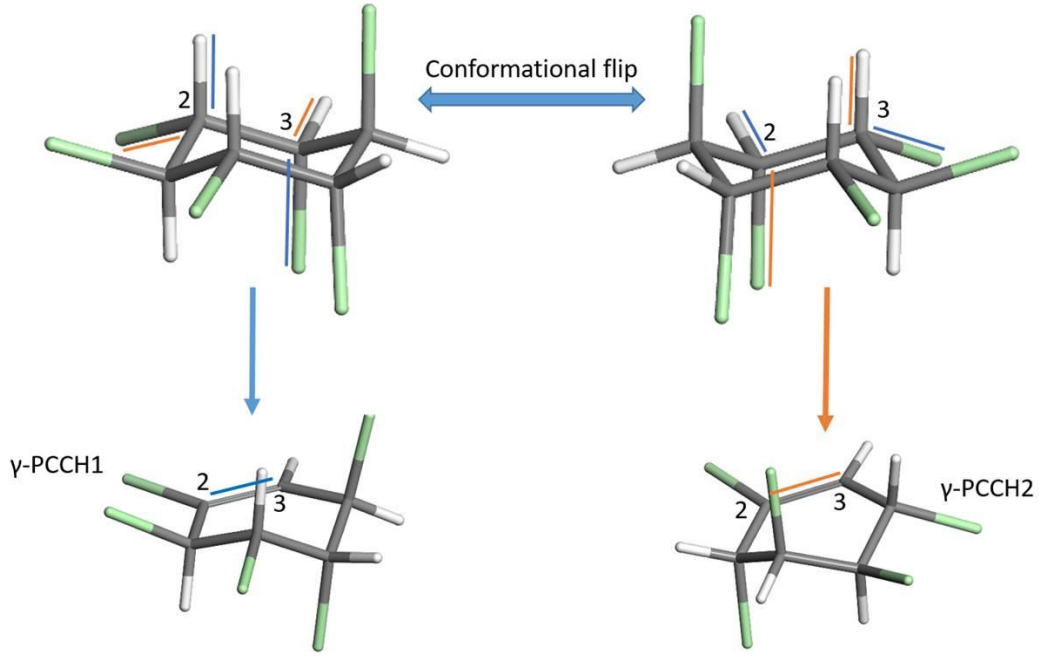

Figure 17 *Depiction of the trans-diaxial pairs on γ-HCH giving rise to the two PCCH enantiomers. The coloured lines indicate the H-Cl pairs eliminated in the dehydrochlorination step. The conformation flip from left to right above, swaps between the susceptible pairs (from the blue to the orange in this case). The numbers indicate the ring carbon atoms hosting the H-Cl pairs. Notably, the conformationally flipped γ-HCH is actually identical to its partner when rotated 180 degree around a vertical axis. A computational investigation employing docking of the substrate into the active site of LinA would shed more light on the enantiopreference of the enzyme, and whether there is sufficient steric allowance for the conformational transition to occur in the active site, or whether γ-HCH can enter the active site in two different and productive orientations (See Chapter 6).*

2.4.2 γ-PCCH transformations

The current study has found $LinA2_{B90A}$, and by and large the other enzymes as well, degrade γ-PCCH more efficiently than they do γ-HCH. This explains the relatively low level, and in some cases quite transient, appearance of the γ-PCCHs in the progress curves. This study also finds that $LinA1_{B90A}$ and $LinA2_{B90A}$ have a strong enantiopreference for γ-PCCH1 over γ-PCCH2 as a substrate, regardless of the type of TCB produced. However, $LinA_{LL02}$ only does so in the case of 1,2,4-TCB and 1,3,5-TCB production; $LinA_{LL02}$ shows no clear preference between γ-PCCH1 and γ-PCCH2 as substrates in the case of 1,2,3-TCB production.

Enantiopreference differences between the enzymes are also evident in two aspects of the TCB production data from the γ-PCCHs, firstly the preference between 1,2,4- and 1,2,3-TCB and secondly in respect of 1,3,5-TCB. Regarding the first, $LinA2_{B90A}$ shows a strong enantiopreference in the production of 1,2,4-TCB over 1,2,3-TCB, whichever γ-PCCH is used as a substrate. $LinA1_{B90A}$ and $LinA_{LL02}$ also show a preference for 1,2,4-TCB as a product but only from γ-PCCH1; $LinA_{LL02}$ preference was for 1,2,3-TCB from γ-PCCH2, while the relevant efficiency statistics for $LinA1_{B90A}$ for γ-PCCH2 were too low to determine its TCB preference. Regarding the second, $LinA_{LL02}$ was found to be unique in producing 1,3,5-TCB, which it does from γ-PCCH1, at a rate intermediate between those for the two other TCB isomers. The efficiency statistic for 1,3,5-TCB production from γ-PCCH2 for $LinA_{LL02}$ is negligible.

The complication in interpreting these two sets of differences in TCB production is that the conversion of the γ-PCCHs into TCBs is believed to be a two-step process via TCDN intermediates, the first step being LinA-catalysed and the second spontaneous (Figure 3). Nagasawa et al. (1993) initially proposed that 1,3,4,6-TCDN is produced from γ-PCCH, and that gets spontaneously degraded into 1,2,4-TCB. While they did consider γ-PCCH enantiomer and conformer differences and other TCBs that could be produced, they believed that only 1,3,4,6-TCDN was produced from γ-PCCH because they only observed 1,2,4-TCB and not 1,2,3- or 1,3,5-TCB production in their γ-HCH degradation assays with *S.japonicum* UT26 (formerly known as *Pseudomonas paucimobilis* UT26). Trantírek et al. (2001) also recognised that different TCBs might be derived from different TCDNs but they went further by suggesting that the different TCDNs would be produced from different γ-PCCHs, specifically that 1,2,3- and 1,2,4-TCB are produced from the degradation of 1,3(*S*),4(*R*),5(*R*),6(*S*)-PCCH (likely γ-PCCH1) and 1,3(*R*),4(*S*),5(*S*),6(*R*)-PCCH (likely γ-PCCH2), respectively, based on their observations on $LinA_{UT26}$. Most recently, Shrivastava and colleagues (2015) suggested that 1,3,5-TCB formation is due to the metabolism of 1,3(*R*),4(*S*),5(*S*),6(*R*)-PCCH (γ-PCCH2) and not 1,3(*S*),4(*R*),5(*R*),6(*S*)-PCCH (γ-PCCH1), based on their analysis of γ-PCCH degradation by a LinA-type3 originating from

a metagenome. While accepting the proposition that the TCBs ultimately produced depend in part on the TCDNs produced by the previous LinA-catalysed step, the results presented here are at odds with the idea underlying both Trantírek et al. (2001) and Shrivastava et al. (2015), that different TCDNs are necessarily produced by different γ-PCCHs; my efficiency statistics show that 1,2,4-, 1,2,3- and 1,3,5-TCB can all be produced from both γ-PCCH enantiomers, depending on the enzyme.

Specifically, I interpret my data as indicating that all three enzymes share the same quantitative preference for producing 1,3,4,6-TCDN and thence 1,2,4-TCB, as opposed to the 1,3,5,6-TCDN isomer generating 1,2,3-TCB, from γ-PCCH1 degradation (see Figure 18). However, only $LinA2_{B90A}$ clearly maintains this preference during γ-PCCH2 degradation; $LinA1_{B90A}$ has too little activity with γ-PCCH2 to tell, while $LinA_{LL02}$ instead produces more of the 1,3,5,6-TCDN isomer that can give rise to 1,2,3-TCB when degrading this substrate. In addition, $LinA_{LL02}$ can apparently influence the 'spontaneous' degradation of 1,3,5,6-TCDN in such a way that some 1,3,5-TCB is also produced (1,3,5,6-TCDN being the only TCDN capable of producing 1,3,5-TCB; Figure 18) when either γ-PCCH is degraded. This might happen for example if the conversion of TCDN to TCB actually occurs whilst the TCDN is still in the active site of the enzyme.

The issues surrounding TCDN conversions into TCB will be discussed more in Chapter 7. Meanwhile, the MD trajectories discussed in Chapter 6 will shed light on the mechanisms by which LinA enzymes remove H-Cl pairs from γ-HCH, γ-PCCH1 and γ-PCCH2. However I conclude this Chapter by noting that, in line with previous data for LinA enzymes (Imai et al., 1991; Kumari et al., 2002; Nagata, et al., 2007; Shrivastava et al., 2015; Suar et al., 2005), I found no evidence for further breakdown of any of the TCBs in any of the assays. This concurs with the widely held view that TCBs are major dead-end products of γ-HCH degradation by the *lin*/Lin pathway (Imai et al., 1991; Lal et al., 2010; Nagata et al., 1999; Trantírek et al., 2001). Interestingly, biodegradations of 1,2,3-, 1,2,4-, and 1,3,5-TCB by various bacteria and fungi have been reported previously (Bosma et al., 1988; Marco-Urrea et al., 2009; Marinucci and Bartha, 1979;

van der Meer et al., 1991) but none of these TCB degraders were also known to be HCH degraders. It appears that HCH degrading strains have not yet incorporated the genes necessary to further degrade the TCBs.

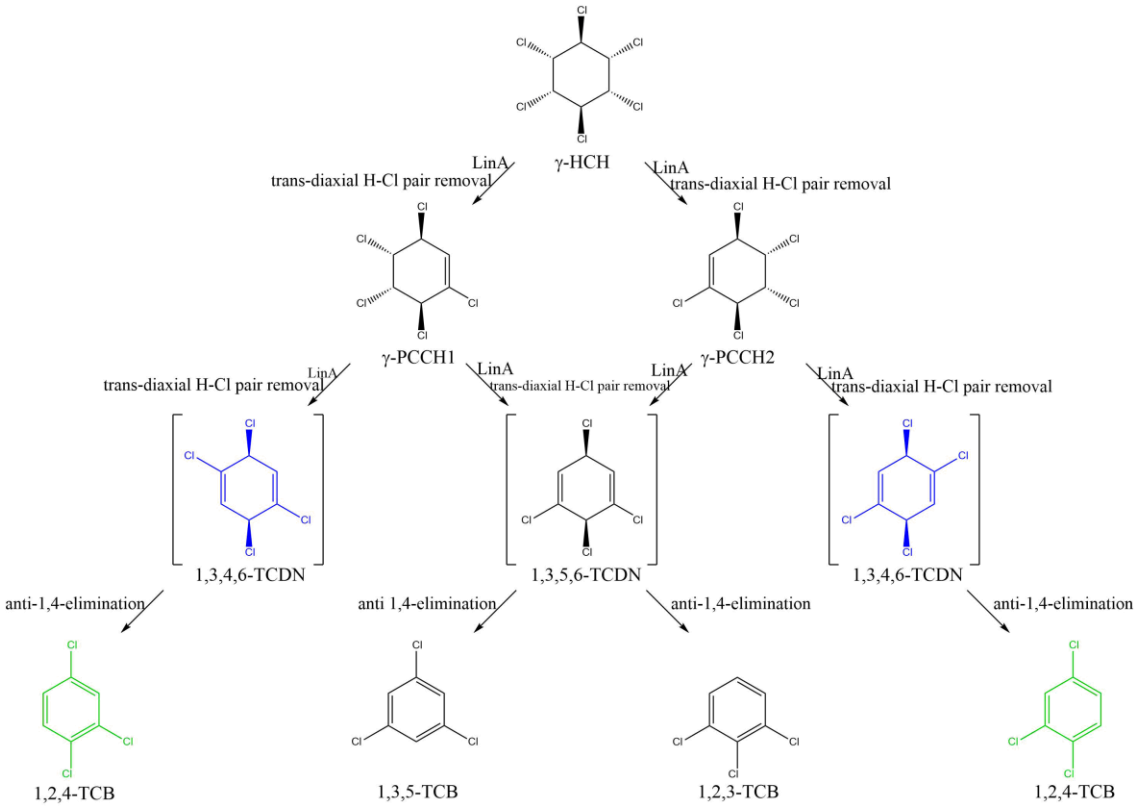

Figure 18 *Proposed degradation pathways for γ-HCH. In the first step, one trans-diaxial HCl pair is removed from γ-HCH molecules by LinA, resulting in γ-PCCH1 or γ-PCCH2. Then another trans-diaxial HCl pair is removed from the γ-PCCH molecules, again by LinA, resulting in their corresponding TCDN isomers. Note that each γ-PCCH enantiomer can exist in two conformations, allowing LinA to remove either of the two different trans-diaxial HCl pairs, thus forming two TCDN isomers. A spontaneous reaction removes an HCl pair from the TCDN molecules, possibly via an anti-1,4-elimination reaction, resulting in either 1,2,4-, 1,2,3-, or 1,3,5-TCB. Note that both γ-PCCH1 and γ-PCCH2 can be transformed into all three TCB isomers. The two molecules in blue and the two molecules in green are 1,3,4,6-TCDN and 1,2,4-TCB, respectively. (Adapted from Nagasawa et al., (1993) and Dr. Hans Peter Kohler (Personal Communication, 21 August 2017)). Chapter 7 will consider further the TCDN/TCB issue, plus the sequence/structure bases for the different enantiopreferences of the three enzymes, once the data on their degradation of other HCH isomers have been presented in Chapter 3, 4 and 5.*

CHAPTER 3:

δ-HCH degradation kinetics for wild type $LinA1_{B90A}$, $LinA2_{B90A}$, and $LinA_{LL02}$ enzymes

3.1 Introduction

In a similar vein to Chapter 2, this chapter reports the kinetic characterization of the first two dehydrochlorination steps in the degradation of δ-HCH by the LinA-type3 enzyme $LinA_{LL02}$, the LinA-type1 enzyme $LinA2_{B90A}$, and the LinA-type2 enzyme $LinA1_{B90A}$.

3.2 Materials and methods

3.2.1 δ-PCCH synthesis

The methods for the synthesis and purification of δ-PCCH were as per those for γ-PCCH in Section 2.2.1 except that δ-HCH was used as the starting material. The yield after purification was calculated to be approximately 20% and the purity to be >90% (Figure 19). As with γ-PCCH, there were two enantiomers of δ-PCCH, which I have named δ-PCCH1 and δ-PCCH2 on the basis of their elution order on the GC Astec® Chiraldex® B-DP column (Sigma-Aldrich, Castle Hill, NSW) (retention times 8.3 min and 8.8 min, respectively). In this case, there was no prior information to determine which of these two correspond to 1,3(*S*),4(*R*),5(*S*),6(*R*)-PCCH or 1,3(*R*),4(*S*),5(*R*),6(*S*)-PCCH (Figure 20).

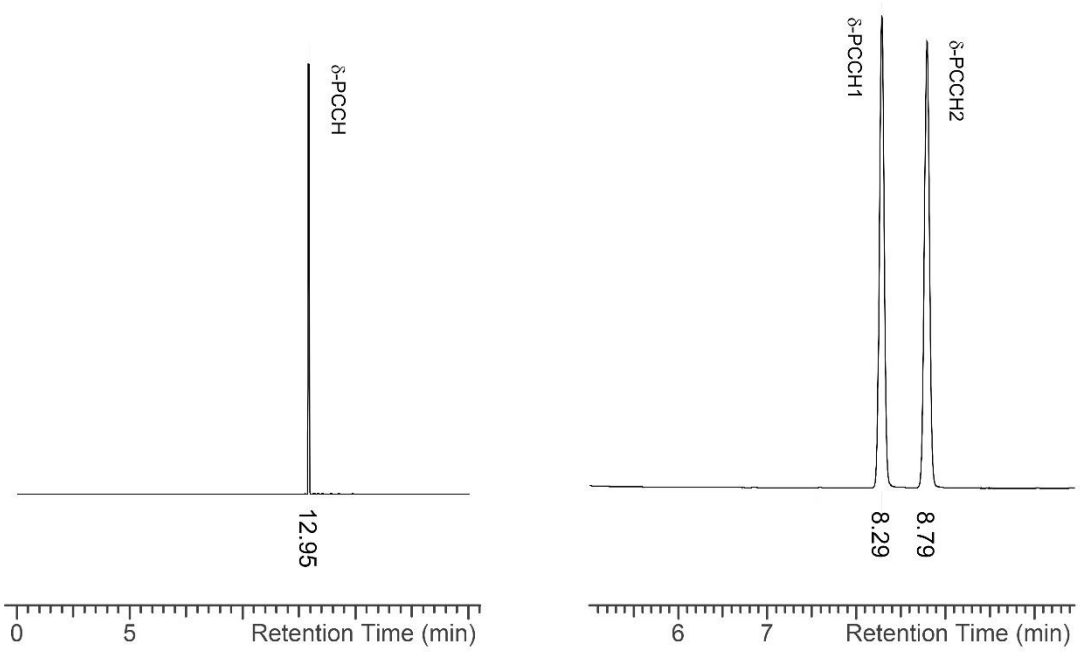

Figure 19 *Gas chromatograph showing separation of the synthesised δ-PCCH enantiomers, designated as δ-PCCH1 and δ-PCCH2 with retention times of 8.3 and 8.8 min, respectively.*

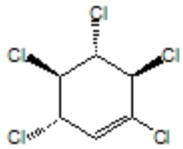

1,3(S),4(R),5(S),6(R)-PCCH

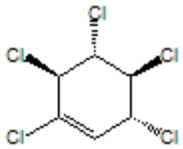

1,3(R),4(S),5(R),6(S)-PCCH

Figure 20 *Expected δ-PCCH enantiomers from δ-HCH degradation.*

3.2.2 Enzyme expression and purification

$LinA1_{B90A}$, $LinA2_{B90A}$ and $LinA_{LL02}$ were expressed and purified following the methods in Section 2.2.2.

3.2.3 Degradation assays

δ-HCH and δ-PCCH degradation assays were carried out as per the γ-HCH and γ-PCCH assays described in Sections 2.2.3 and 2.2.4, respectively. Once again, the starting concentrations of each enzyme were adjusted on the basis of pilot experiments to best suit the calculation of specificity constants by Copasi 4.15 (Hoops et al., 2006). As with the γ-PCCH assays in Chapter 2, problems with stoichiometric recoveries of the relatively high initial concentrations of the δ–PCCHs meant that the data from these assays could not be used for kinetic calculations.

3.3 Results

10 µg/ml of $LinA1_{B90A}$ and $LinA2_{B90A}$, and 0.1 µg/ml of $LinA_{LL02}$ were incubated with 17 µM of δ-HCH at room temperature for 2 h and concentrations of δ-HCH and its metabolites were measured over time using GC-ECD (Figure 21). $LinA1_{B90A}$ showed minimal degradation of δ-HCH but $LinA2_{B90A}$ degraded it completely within 75 min and $LinA_{LL02}$ degraded approximately 90% of it within 2 h (even though only $1/100^{th}$ as much of the latter enzyme was used). Much higher levels of δ-PCCH2 than δ-PCCH1 were seen in both the $LinA2_{B90A}$ and $LinA_{LL02}$ assays, but the δ-PCCH2 level declined over time in the $LinA2_{B90A}$ assays whereas it continued to accumulate in the $LinA_{LL02}$ assays. On the other hand, δ-PCCH1 level was less than 1 µM in both assays throughout the two hour period, so any degradation of it was undetectable. Consistent with

these observations of the δ-PCCHs, TCBs were only clearly detectable in the LinA2$_{B90A}$ assays, where 1,2,4-TCB was found to be most abundant, followed by 1,2,3-TCB and with no detectable 1,3,5-TCB. No evidence of TCB degradation by LinA2$_{B90A}$ was detected within the two hour timeframe of the assay.

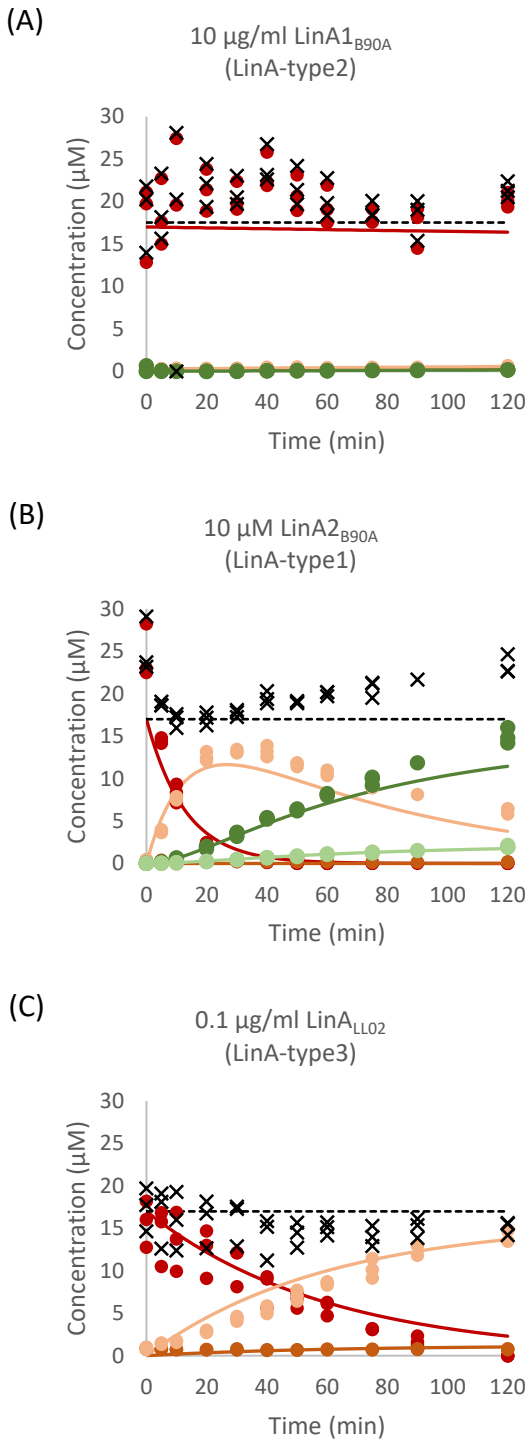

Figure 21 *Graphs showing the concentration (µM) of δ-HCH and its metabolites over time (min) in δ-HCH degradation assays by (A) 10 µg/ml LinA1$_{B90A}$, (B) 10 µg/ml LinA2$_{B90A}$, and (C) 0.1 µg/ml LinA$_{LL02}$. The compounds are as follows: δ-HCH (●), δ-PCCH1 (●), δ-PCCH2 (●), 1,2,4-TCB (●), and 1,2,3-TCB (●). Also shown in the graphs are the best fit lines assumed by Copasi. LinA2$_{LL02}$ degraded δ-HCH the fastest despite being 100 times less concentrated than the other two enzymes. Notably, it is also the only enzyme that did not produce any TCB isomers upon degrading δ-HCH. Total measured mass is marked with (x) and the total mass deduced by Copasi is drawn with dotted line (---).*

In line with the degradation curves and the relative concentrations of the enzymes used, the enzyme efficiency (k_{cat}/K_m) values calculated (Table 3) show that $LinA_{LL02}$ is the most efficient of the three in degrading δ-HCH, followed by $LinA2_{B90A}$, with $LinA1_{B90A}$ showing negligible activity. Both the active enzymes show a clear preference for converting the δ-HCH into δ-PCCH2 rather than δ-PCCH1. $LinA2_{B90A}$ is the most efficient enzyme in degrading both δ-PCCHs, while $LinA_{LL02}$ has no detectable activity with either δ-PCCH. $LinA2_{B90A}$ shows a clear preference for converting δ-PCCH2 into 1,2,4-TCB with the efficiency values for this conversion is 1 log higher than the conversion into 1,2,3-TCB, but such preference was not observed for δ-PCCH1 degradation. The statistics also suggest that $LinA1_{B90A}$ converts some δ-PCCH1 and δ-PCCH2 into 1,2,4-TCB, albeit the values in both cases are low.

Table 3 *k_{cat}/K_m values (min^{-1} μM^{-1}) and their standard errors (SEs) (min^{-1} μM^{-1}) for reactions involved in δ-HCH degradations by $LinA1_{B90A}$, $LinA2_{B90A}$, and $LinA_{LL02}$. Levels that are not detected are denominated with a dash symbol (-). Number of independent replicate is 3.*

Reactions	$LinA1_{B90A}$ (LinA-type2)	SE $LinA1_{B90A}$	$LinA2_{B90A}$ (LinA-type1)	SE $LinA2_{B90A}$	$LinA_{LL02}$ (LinA-type3)	SE $LinA_{LL02}$
δ-HCH → δ-PCCH1	<1.0E-04	*8.1E-05*	<1.0E-04	*3.8E-03*	1.5E-02	*4.1E-05*
δ-HCH → δ-PCCH2	<1.0E-04	*8.1E-05*	9.8E-03	*1.1E-02*	1.9E-01	*5.2E-04*
δ-PCCH1 → 1,2,4-TCB	4.5E-04	*4.1E-03*	3.1E+04	*4.5E+12*	-	
δ-PCCH1 → 1,2,3-TCB	-		3.4E+04	*4.9E+10*	-	
δ-PCCH2 → 1,2,4-TCB	<1.0E-04	*3.5E-03*	1.5E-03	*1.3E-03*	-	
δ-PCCH2 → 1,2,3-TCB	-		2.4E-04	*1.8E-04*	-	

Figure 22 shows the progress curves for the concentrations of the δ-PCCHs in my δ-PCCH-based assays. As noted, the initial concentrations measured were significantly less than the combined 17 μM added, stymying the reliable calculation of specificity constants and therefore also comparisons with the corresponding specificity constants from the δ-HCH degradation assays. Nevertheless, the results from these assays are in qualitative agreement with those of the δ-HCH-based assays above in most respects. Once again, the δ-PCCH-based assays show a preference by $LinA2_{B90A}$ for 1,2,4-TCB over 1,2,3-TCB production. The other two enzymes in the δ-HCH-based assays show little to no δ-PCCH degradation activity but it is now clear both can degrade δ-PCCH, albeit considerably more slowly than $LinA2_{B90A}$. As with $LinA2_{B90A}$, they produce

very predominantly 1,2,4-TCB, with very little 1,2,3-TCB. The δ-PCCH-based assays now show $LinA_{LL02}$ can produce minor amount of 1,3,5-TCB, although that had not been evident in the δ-HCH-based assays. Perhaps the most notable difference from the δ-PCCH-based assays is that they show enantiopreference for $LinA2_{B90A}$ to degrade d-PCCH2 whereas the δ-HCH-based assays above showed this enzyme prefers δ-PCCH1. This discrepancy is discussed further in Section 3.4.2 below.

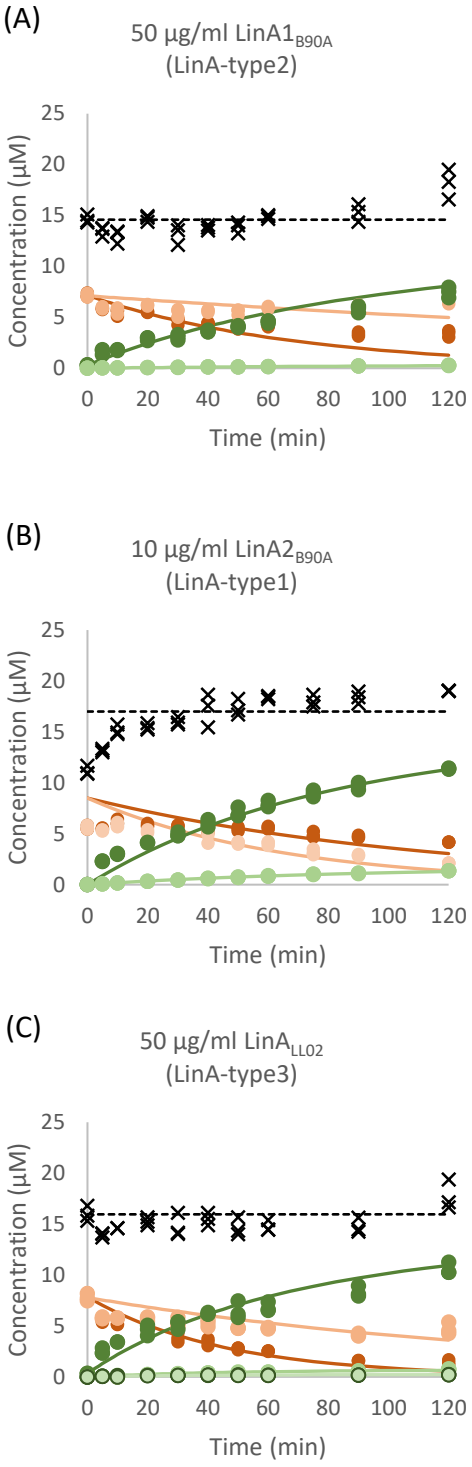

Figure 22 *Graphs show the concentrations (µM) of δ-PCCH1, δ-PCCH2, 1,2,4-TCB, 1,2,3-TCB, and 1,3,5-TCB over time (min) in δ-PCCH degradation assays by (A) 50 µg/ml LinA1$_{B90A}$, (B) 10 µg/ml LinA2$_{B90A}$, and (C) 50 µg/ml LinA$_{LL02}$. The compounds are as follows: δ-PCCH1 (●), δ-PCCH2 (●), 1,2,4-TCB (●), 1,2,3-TCB (●), and 1,3,5-TCB (○). Also shown in the graphs are the best fit lines deduced by Copasi. Note that LinA1$_{B90A}$ and LinA$_{LL02}$ show enantiopreference towards degrading δ-PCCH1 than δ-PCCH2, but LinA2$_{B90A}$ show opposite enantiopreference, where it prefers to degrade δ-PCCH2 than δ-PCCH1. All three assays produced 1,2,4-TCB as the major TCB isomer, and 1,2,3-TCB in trace amount. No TCB degradation were detected in any of the assays. Total measured mass is marked with (x) and the total mass deduced by Copasi is drawn with dotted line (---).*

3.4 Discussion

3.4.1 δ-HCH transformations

This study shows that the LinA-type3 enzyme $LinA_{LL02}$ is at least 2 logs more efficient in degrading δ-HCH than the LinA-type1 enzyme $LinA2_{B90A}$, while the efficiency values for the LinA-type2 enzyme $LinA1_{B90A}$ are effectively negligible. These observations are in agreement with previous studies, where $LinA2_{B90A}$ was observed to degrade δ-HCH two logs more rapidly than $LinA1_{B90A}$ (Geueke et al., 2013) and a LinA-type3 from a metagenome was observed to have a greater δ-HCH degradation activity than LinA-type1 and LinA-type2 enzymes (Shrivastava et al., 2015).

Thus, whereas Shrivastava et al. (2015) and my work both found type1 and type2 enzymes are more efficient than type3 in degrading γ-HCH, my results and Shrivastava et al. (2015) showed that LinA-type3 is more efficient in degrading δ-HCH. Notably, the efficiency statistics for conversion of δ-HCH into δ-PCCH2 by $LinA_{LL02}$ are comparable to the efficiency statistics for conversions of γ-HCH into γ-PCCH1 and γ-PCCH2 by $LinA2_{B90A}$ (1.9E-01 vs 3.7E-01 and 4.1E-01, respectively).

It is not clear why LinA-type3 has such high activity on δ-HCH but, as noted in Section 1.4.1.1, Pearce (2015) proposed that residues 44 and 64 in the active site were crucial to the difference in the δ-HCH and γ-HCH degradation activities of the three types of LinA. As outlined in that Section, $LinA1_{B90A}$ has bulkier isoleucine and leucine residues at these positions respectively, whereas $LinA_{LL02}$ has smaller valine residues, the latter resulting in a larger active site. Following Macwan et al. (2012) and Manna et al. (2015), it is now understood that the hydrogen atom in an axial H-Cl pair in the substrate molecule needs to be close enough to the catalytic H73 in the active site for dechlorination at this pair to be achieved. On the basis of his *in silico* docking studies, Pearce (2015) proposed that the $LinA_{LL02}$ active site is effectively too big to ensure appropriate orientation of a γ-HCH substrate and conversely the $LinA1_{B90A}$ active site will be too small to ensure appropriate configuration of a δ-HCH substrate. This hypothesis will be tested in Chapter 4 below.

Notwithstanding their very different efficiencies in degrading δ-HCH, I found that both $LinA2_{B90A}$ and $LinA_{LL02}$ show a strong enantiopreference for transforming δ-HCH into δ-PCCH2 rather than δ-PCCH1. This observation is in agreement with the results of Shrivastava et al. (2015), who observed >95% δ-PCCH2 production in their LinA-type1 and LinA-type3 δ-HCH degradation assays. However previous studies on this enantiopreference have produced contradictory results for type2 enzymes such as $LinA1_{B90A}$; Geueke et al. (2013) also found $LinA1_{B90A}$ prefers producing δ-PCCH2 but Shrivastava et al. (2015) found their LinA-type2 produced slightly more δ-PCCH1 than δ-PCCH2. I cannot fully explain these discrepancies, but perhaps the difference between assay conditions may be relevant for causing the difference between these studies. It is described further below.

3.4.2 δ-PCCH transformations

Based on the δ-HCH assays, I found $LinA2_{B90A}$ degrades δ-PCCH1 significantly (up to at least 8 logs) more efficiently than it degrades δ-HCH, but it degrades δ-PCCH2 less efficiently than it degrades δ-HCH. $LinA1_{B90A}$ is also more efficient, with δ-PCCH1 at least, than it is with δ-HCH. By contrast, $LinA_{LL02}$ shows barely detectable activity with either δ-PCCH enantiomer, despite being the most efficient of the three enzymes in transforming δ-HCH. These observations on the relative δ-PCCH and δ-HCH activities of the three enzyme types concur in qualitative terms with Shrivastava et al. (2015), at least for LinA-type3. They also agree with Geueke et al. (2013) with respect to $LinA1_{B90A}$ but only with respect to δ-PCCH2 for $LinA2_{B90A}$ (that study not including a type3 enzyme). Below, some possible reasons for both this discrepancy and another one on δ-PCCH1/δ-PCCH2 enantiopreferences, which also concerns $LinA2_{B90A}$ are considered.

In my δ-HCH-based assays, both $LinA1_{B90A}$ and $LinA2_{B90A}$ show an enantiopreference in transforming δ-PCCH1 rather than δ-PCCH2. In the case of $LinA2_{B90A}$, this preference is large, with a difference of up to eight logs in specificity constants between the two transformations. While the corresponding values for $LinA1_{B90A}$ are much lower, they still show the same preference. This enantiopreference is shown by $LinA2_{B90A}$ regardless of which TCB isomers were

produced and it is also true for LinA1$_{B90A}$ for the one TCB, 1,2,4-TCB, it produces. The preference for δ-PCCH1 agrees with the findings of Geueke et al. (2013) and Shrivastava et al. (2015) for LinA1$_{B90A}$ but not LinA2$_{B90A}$; both those studies found LinA2$_{B90A}$ prefers δ-PCCH2 as do my δ-PCCH–based assays. The negligible levels of δ-PCCH degradation I saw for LinA$_{LL02}$ precluded determination of any enantiopreference but Shrivastava et al. (2015) saw sufficient activity under their assay conditions to report that their LinA-type3 prefers δ-PCCH1 transformation over δ-PCCH2, i.e. similar to the preference they saw for LinA-type1.

It is informative to note that the results of my δ-HCH-based assays on the enantiopreference of LinA2$_{B90A}$ for δ-PCCH1 disagree with those from the δ-PCCH-based assays of both myself, Geueke et al. (2013) and Shrivastava et al. (2015). The amounts of δ-PCCH available as substrate in my δ-HCH-based assays would have been at most in the low micromolar range and δ-HCH would also have been present as a potential competitor, whereas in the δ-PCCH-based assays the starting substrate concentrations would approach mM amounts. Shrivastava et al. (2015) only reported their results in the form of GC traces and did not report several key aspects of their methods (e.g. starting substrate concentrations, buffer conditions, pH). However, Geueke et al. (2013) more fully described their methods, which involved starting concentrations of 0.4 mM of a racemic mix of δ-PCCH1 and δ-PCCH2, and presented their results in terms of quantitative kinetic estimates. It remains unclear how Geueke et al. (2013) solubilised their substrate without impacting the activity of the enzyme, given that I found even relatively low concentrations of organic solvents compromised enzyme activity and still left me with problems of less-than-stoichiometric recovery of substrate. Nevertheless, the differing rates of production of the two δ-PCCHs in my δ-HCH-based assays will mean their relative (and absolute) amounts will be very different from the approximately equimolar starting amounts in the δ-PCCH-based assays of Geueke et al. (2013) and myself. I cannot decompose my specificity constants into their k_{cat} and K_m components and therefore cannot infer the relative binding affinities of the different enzymes for the various competing substrates in my assays. However, it seems very possible

that the binding of LinA to the δ-PCCHs in the two sorts of assays will have been impacted by the very different δ-PCCH concentrations and the presence of potentially competing δ-HCH in the δ-HCH-based assays.

Another interesting aspect of my $LinA2_{B90A}$ results in this chapter is that both δ-PCCH1 and δ-PCCH2 are eventually transformed into both 1,2,3- and 1,2,4-TCB. As discussed in Chapter 2, Trantírek et al. (2001) and Shrivastava et al. (2015) suggested that LinA transforms different γ-PCCH enantiomers into different TCDN isomers and the latter are then spontaneously converted into different TCB isomers. However, the specificity constants I reported in Chapter 2 suggest that both γ-PCCH enantiomers can be transformed into all three TCB isomers. My results for δ-PCCH transformation thus complement my findings in Chapter 2, confirming that the transformation of both PCCH enantiomers into the different TCBs applies to both γ- and δ-PCCH. This notion is also supported to some degree by Geueke et al. (2013) who proposed that both δ-PCCH enantiomers are degraded into one TCDN isomer (1,2,5,6-TCDN), but this is then further degraded into both 1,2,4- and 1,2,3-TCB. This issue is further considered in Chapter 6 and 7.

My δ-HCH-based assays show that $LinA1_{B90A}$ and $LinA2_{B90A}$ have a clear enantiopreference for 1,2,4-TCB production, regardless of which δ-PCCH enantiomer is degraded, and only those with the type1 enzyme $LinA2_{B90A}$ show the production of both 1,2,3- and 1,2,4-TCB. Similarly, the δ-PCCH-based assays, which are more sensitive to the production of TCBs (owing to the much higher concentrations of δ-PCCHs used), imply that $LinA1_{B90A}$ also produces small amounts of 1,2,3-TCB and that $LinA_{LL02}$ produces some of both, again with 1,2,4-TCB in excess. No 1,3,5-TCB was evident in any assays with $LinA1_{B90A}$ and $LinA2_{B90A}$. Our data are in good agreement with the work on type1 and type2 enzymes by Geueke et al. (2013) and on all three enzyme types by Shrivastava et al. (2015); both those studies report greatest TCB production with type1 and a strong preference for 1,2,4-TCB over 1,2,3-TCB production by all enzymes studied, and again no 1,3,5-TCB reported in any assays for these two types of enzymes.

CHAPTER 4:

δ-HCH degradation kinetics by mutants enzymes of $LinA1_{B90A}$ (I44V) and $LinA_{LL02}$ (V44I and V64L)

4.1 Introduction

As a continuation from Chapter 2 and 3, this chapter investigates the effects of mutations at residues 44 and 64 of the LinA-type3 enzyme $LinA_{LL02}$ and the LinA-type2 enzyme $LinA1_{B90A}$ on their ability to catalyse the first two dehydrochlorination steps in the degradation of γ- and δ-HCH. Specifically, the chapter tests the hypothesis of Pearce (2015) that the substitutions of I44 and L64 in LinA-type2 (and LinA-type1) with V44 and V64 in LinA-type3 allow for more efficient degradation of δ-HCH but to the detriment of their degradation of γ-HCH. This chapter also tests whether similar differences carried through to the second dehydrochlorination step, involving the degradation of δ- and γ-PCCH. However, my analysis of this latter step was limited to HCH-based assays; given the issues with the PCCH-based assays noted above, it was not felt worthwhile to attempt precise dissection of the effects of the mutants with these assays.

4.2 Materials and methods

4.2.1 γ- and δ-PCCH synthesis

The methods for the synthesis of γ- and δ-PCCH standards are as detailed in Sections 2.2.1 and 3.2.1 respectively.

4.2.2 Mutagenesis

Mutagenesis of $LinA1_{B90A}$ and $LinA_{LL02}$ were performed using the QuikChange™ (Stratagene, La Jolla, CA, USA) site-directed mutagenesis protocol. Primers for replacing valines with isoleucine and leucine at positions 44 and 64 of $LinA_{LL02}$, respectively, and isoleucine and leucine with valines at the same positions of $LinA1_{B90A}$, respectively, were designed based on codon-optimized wildtype sequences of both genes in pDEST14. Table 4 lists the primer sequences. The mutagenesis was done using a Phusion® High-Fidelity PCR kit (New England Biolabs) with $LinA1_{B90A}$ and $LinA_{LL02}$ in pDEST14 as templates. The identity of the mutated genes was verified using 1% agarose gel electrophoresis and sequencing (Micromon). The vectors were transformed into *E. coli* Top10 competent cells for long term storage at -80 °C.

Table 4 *Mutagenesis primer sequences used for creating $LinA1_{B90A}$ and $LinA_{LL02}$ mutants*

Template	Mutation	Primer sequences	Tm (°C)
$linA1_{B90A}$_pDEST14	I44V	Fwd: CCGATTCCCTCAACGGTCCACTCTGC Rev: GCAGAGTGGACCGTTGAGGGAATCGG	65
$linA1_{B90A}$_pDEST14	L64V	Fwd: AATAACGTAGTGTGGCCAATGTATCAC Rev: CATTGGCCACACTACGTTATTGG	57
$linA_{LL02}$_pDEST14	V44I	Fwd: TGCCGATTCCCTCAATGGTCCACTCTGCATC Rev: GATGCAGAGTGGACCATTGAGGGAATCGGCA	66
$linA_{LL02}$_pDEST14	V64L	Fwd: AATAACGTACTCTGGCCAAGGTGGCAC Rev: CCTTGGCCAGAGTACGTTATTGACCAAATC	62

4.2.3 Enzyme expression and purification

The four mutant enzymes were expressed and purified following the methods in Section 2.2.2.

4.2.4 Degradation assay

γ- and δ-HCH degradation assays were carried out as per the methods described in Sections 2.2.3 and 3.2.3 respectively. Once again, the starting concentration of each enzyme was adjusted on the basis of pilot experiments to best suit the calculation of specificity constants by Copasi 4.15 (Hoops et al., 2006).

Unfortunately, some technical issues with the GC system occurred while processing the $LinA1_{B90A}$ L64V samples, causing data loss for half of the samples and unreliable readings on the rest. Due to these difficulties, data for $LinA1_{B90A}$ L64V is omitted from this thesis.

4.3 Results

The mutagenesis of pDEST14 $LinA1_{B90A}$ and pDEST14 $LinA_{LL02}$ was successful, producing the desired expression vectors for $LinA1_{B90A}$ I44V, $LinA1_{B90A}$ L64V, $LinA_{LL02}$ V44I and $LinA_{LL02}$ V64L, as verified by sequencing (data not shown). I then successfully expressed and purified $LinA1_{B90A}$ I44V, $LinA_{LL02}$ V44I and $LinA_{LL02}$ V64L to at least 90% purity (Appendix F). I was only able to purify $LinA1_{B90A}$ L64V to 40% purity (Appendix F) but as noted in section 4.2.4 above, problems with the assays of this mutant meant the data for it were not used anyway.

4.3.1 δ-HCH and δ-PCCH transformations

Like the parental $LinA1_{B90A}$ enzyme, $LinA1_{B90A}$ I44V showed minimal δ-HCH degradation activity. Conversely, the two $LinA_{LL02}$ mutants both showed considerable δ-HCH degradation activity, as

had their parental $LinA_{LL02}$ enzyme (noting that much less starting enzyme concentration had been used in the parental enzyme assays). $LinA_{LL02}$ V44I was found to be the most efficient mutant enzyme to degrade δ-HCH, followed by $LinA_{LL02}$ V64L, with complete degradation in 25 and 60 min, respectively. $LinA1_{B90A}$ I44V degraded less than 20% of the δ-HCH within the two hour assay. δ-PCCH2 was much more abundant than δ-PCCH1 in all the assays and reached relatively high levels in the assays of both $LinA_{LL02}$ mutants, as it had done in the assays of the parental $LinA_{LL02}$ enzyme. 1,2,4-TCB was the only TCB isomer detected among all assays and no further degradation of it was detected (Figure 23).

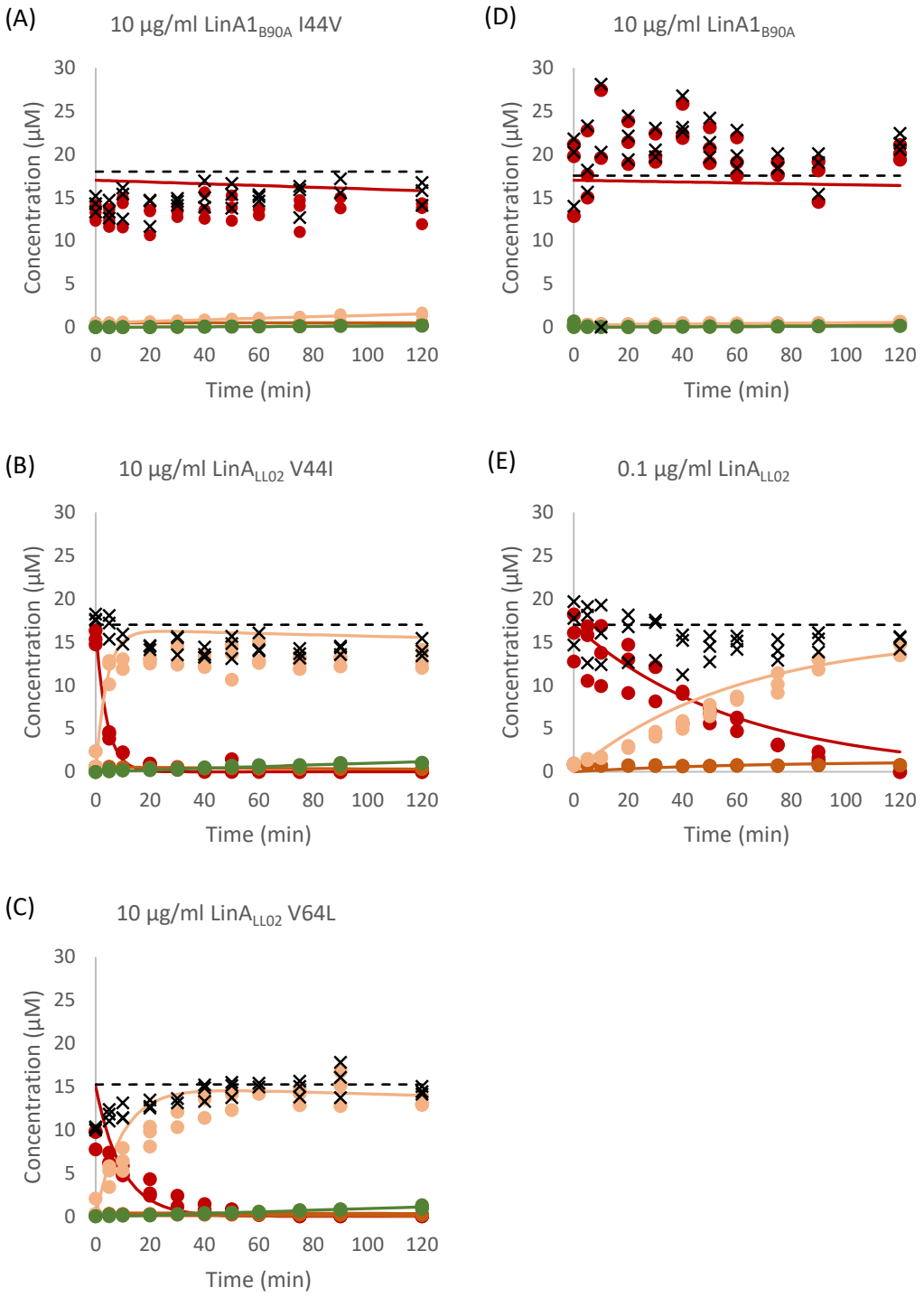

Figure 23 *Graphs showing the concentration (µM) of δ-HCH and its metabolites over time (min) in δ-HCH degradation assays by (A) 10 µg/ml LinA1$_{B90A}$ I44V, (B) 10 µg/ml LinA$_{LL02}$ V44I, and (C) 10 µg/ml LinA$_{LL02}$ V64L. The compounds are as follows: δ-HCH (●), δ-PCCH1 (●), δ-PCCH2 (●), and 1,2,4-TCB (●).Total measured mass is marked with (x) and the total mass assumed by Copasi is drawn with dotted line (---). LinA$_{LL02}$ V44I degraded δ-HCH the fastest while LinA1$_{B90A}$ I44V barely degraded it. All three enzymes produce only 1,2,4-TCB as a dead-end product. Progress curves for δ-HCH degradation assays by (D) 10 ug/ml LinA1$_{B90A}$ and (E) 0.1 mg/ml LinA$_{LL02}$ are also included. Note that mutation from isoleucine to valine at position 44 of LinA1$_{B90A}$ does not hugely affect the enzyme's activity on δ-HCH. However, due to the different enzyme concentrations used for LinA$_{LL02}$ assay and its mutants' assays, similar direct comparison based on these graphs is unfeasible. A detailed comparison between the activities of the wildtype and mutant enzymes can be found in Section 4.4.1 and 4.4.*

In line with the degradation curves of the mutant enzymes, the enzyme efficiency (k_{cat}/K_m) values calculated from the δ-HCH-based assays (Table 5) show that all three mutant enzymes give very low values for the conversion of δ-HCH to δ-PCCH1, as does the parental LinA1$_{B90A}$ enzyme, with the LinA$_{LL02}$ parent having values about two orders of magnitude higher. LinA1$_{B90A}$ I44V, like its LinA1$_{B90A}$ parent, also shows very low δ-HCH to δ-PCCH2 activity. On the other hand, LinA$_{LL02}$ V44I and LinA$_{LL02}$ V64L both give higher values for this conversion, much higher than that for LinA1$_{B90A}$ but still about an order of magnitude less than the value for LinA$_{LL02}$.

The efficiency values for the conversions of either δ-PCCH1 or δ-PCCH2 into 1,2,4-TCB are low but measurable for all three mutants. While the values are low, however, both the LinA$_{LL02}$ V44I and LinA$_{LL02}$ V64L mutants show some preference for converting δ-PCCH1 rather than δ-PCCH2 into 1,2,4-TCB, in contrast to the non-existent transformations by their LinA$_{LL02}$ parent. On the other hand, LinA1$_{B90A}$ I44V showed no obvious preference for converting δ-PCCH1 or δ-PCCH2 to TCB, whereas the LinA1$_{B90A}$ parent had some preference for converting δ-PCCH1 (Table 5).

Table 5 *k_{cat}/K_m values (min^{-1} μM^{-1}) and their standard errors (SEs) (min^{-1} μM^{-1}) for δ-HCH degradation reactions by LinA1$_{B90A}$ I44V, LinA$_{LL02}$ V44I, and LinA$_{LL02}$ V64L. The values for LinA1$_{B90A}$ and LinA$_{LL02}$ were also included for comparison. Detailed explanation and comparison between the mutant and wildtype enzymes can be found in Section 4.4.1 and 4.4.2. Levels that are not detected are denominated with a dash symbol (-). Number of independent replicate is 3.*

Reactions	LinA1$_{B90A}$	LinA$_{LL02}$	LinA1$_{B90A}$ I44V	SE LinA1$_{B90A}$ I44V	LinA$_{LL02}$ V44I	SE LinA$_{LL02}$ V44I	LinA$_{LL02}$ V64L	SE LinA$_{LL02}$ V64L
δ-HCH -> δ-PCCH1	<1.0E-04	1.5E-02	<1.0E-04	*9.8E-06*	<1.0E-04	*2.0E-04*	<1.0E-04	*9.1E-05*
δ-HCH -> δ-PCCH2	<1.0E-04	1.9E-01	<1.0E-04	*1.3E-05*	2.5E-02	*7.2E-03*	1.2E-02	*3.3E-03*
δ-PCCH1 -> 1,2,4-TCB	4.5E-04	-	1.1E-04	*2.4E-04*	5.2E-04	*4.6E-04*	3.1E-04	*8.6E-04*
δ-PCCH2 -> 1,2,4-TCB	<1.0E-04	-	1.2E-04	*1.3E-04*	<1.0E-04	*1.6E-05*	<1.0E-04	*2.2E-05*

4.3.2 γ-HCH and γ-PCCH degradations

The activities of the LinA1$_{B90A}$ I44V and LinA$_{LL02}$ V64L mutants on γ-HCH were generally lower than those of their respective parents. However, the activity of LinA$_{LL02}$ V44I on γ-HCH was similar to that of its parent. LinA$_{LL02}$ V44I degraded approximately 98% of the γ-HCH by the end of the assay, LinA$_{LL02}$ V64L approximately 85% and LinA1$_{B90A}$ I44V only approximately 70%. γ-HCH degradation by all three mutant enzymes produced both γ-PCCH1 and γ-PCCH2, albeit more of

the latter for the all of them, particularly $LinA_{LL02}$ V44I. Both parents had also produced more γ-PCCH2 and γ-PCCH1. Both 1,2,3- and 1,2,4-TCB were produced by all three mutants, with 1,2,4-TCB being more abundant in the $LinA1_{B90A}$ I44V and $LinA_{LL02}$ V64L assays, and 1,2,3-TCB more abundant in the $LinA_{LL02}$ V44I assay. No 1,3,5-TCB was produced by any of the mutants, although it had been evident in low amounts in the $LinA_{LL02}$ parent assays. No degradation of any TCB isomer was detected in any of the assays (Figure 24).

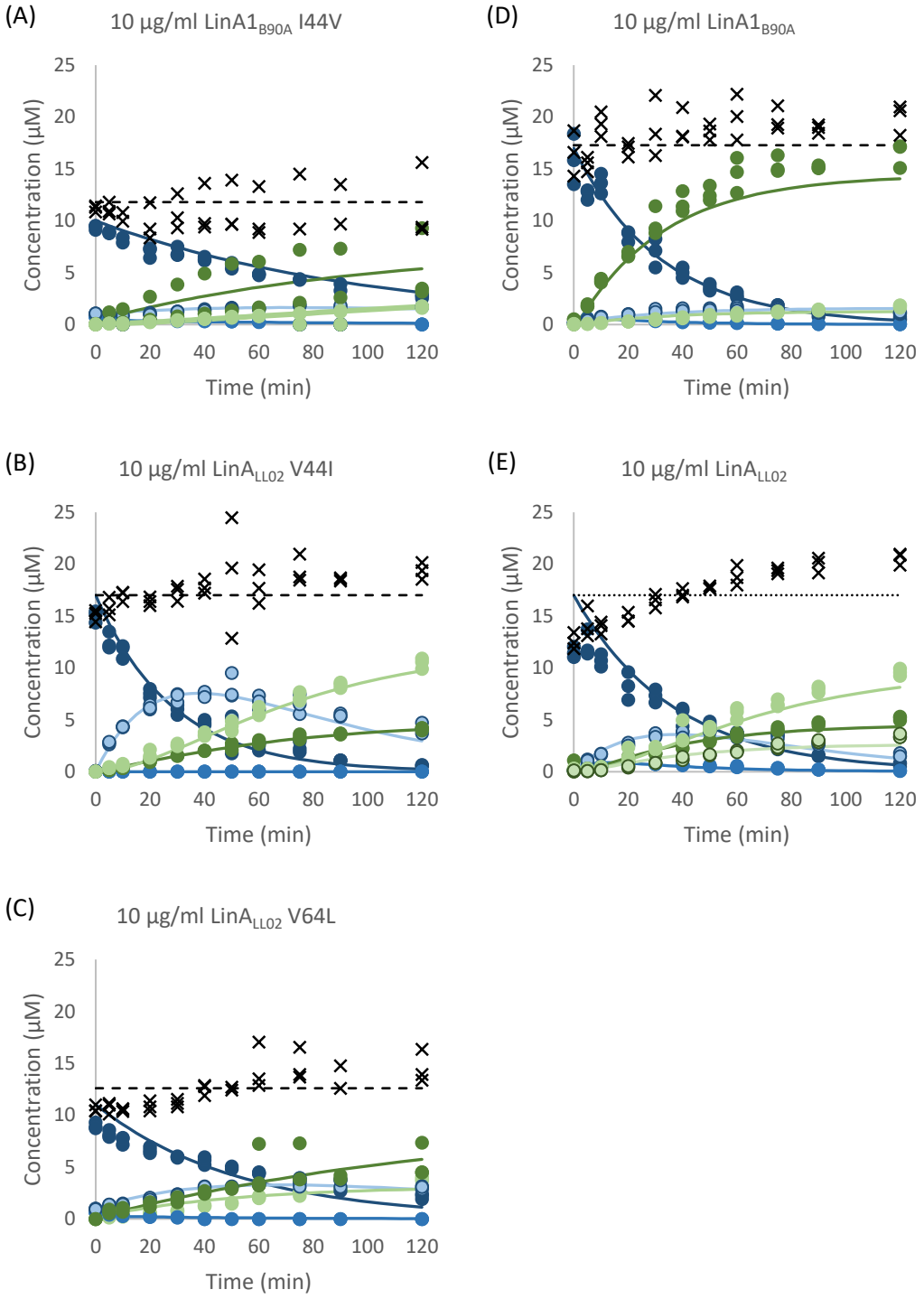

Figure 24 *Graphs showing the concentration (µM) of γ-HCH and its metabolites over time (min) in γ-HCH-based assays by (A) 10 µg/ml LinA1$_{B90A}$ I44V, (B) 10 µg/ml LinA2$_{LL02}$ V44I, and (C) 10 µg/ml LinA$_{LL02}$ V64L. The compounds are as follows: γ-HCH (●), γ-PCCH1 (●), γ-PCCH2 (○), 1,2,4-TCB (●), 1,2,3-TCB (●), and 1,3,5-TCB (○).Total measured mass is marked with (x) and the total mass assumed by Copasi is drawn with dotted line (---). Of the three, LinA$_{LL02}$ V44I is the most efficient at degrading γ-HCH, followed by LinA$_{LL02}$ V44L and LinA$_{B90A}$ I44V. The progress curves for γ-HCH degradation assays by (D) 10 µg/ml LinA1$_{B90A}$ and (E) 10 µg/ml LinA$_{LL02}$ were also included for comparison. Notice that the I44V mutation of LinA1$_{B90A}$ slows down the enzyme's activity on γ-HCH. On the other hand, while the V44I mutation of LinA$_{LL02}$ does not significantly affect the enzyme's activity on γ-HCH, it removes the enzyme's ability to produce 1,3,5-TCB as one of its dead-end products, and increases the retention of γ-PCCH2. The V64L mutation of LinA$_{LL02}$ also removes the enzyme's ability to produce 1,3,5-TCB, in addition to flipping the major TCB isomer from 1,2,3-TCB to 1,2,4-TCB. This mutation also negatively affects the rate at which this enzyme degrades γ-HCH. Detailed comparison between the mutant and wildtype enzymes can be found in sections 4.4.3 and 4.4.*

The two parental enzymes had both yielded similarly low k_{cat}/K_m values for the conversion of γ-HCH to γ-PCCH1 and the three mutants were also low, all within a magnitude of their respective parent and of each other (Table 6). The same was true of the data for the conversion of γ-HCH to γ-PCCH2. There was also little difference between the values of each enzyme for the conversion to the two γ-PCCHs; the largest difference, just over a magnitude higher efficiency of γ-PCCH2 over γ-PCCH1 production for $LinA_{LL02}$ V44I, was not mirrored by either parent and may well have been within the margin of error.

The conversion efficiency of γ-PCCH1 to its preferred TCB isomer, 1,2,4-TCB was higher than the efficiency of its production for the $LinA1_{B90A}$ parent but the values for production and conversion of γ-PCCH2 by this parent were all too low to reliably discriminate between them. For the $LinA_{LL02}$ parent the conversion efficiency of γ-PCCH1 to its preferred TCB isomer, again 1,2,4-TCB, was again higher than the corresponding production efficiency while the conversion efficiency of γ-PCCH2 to its preferred TCB isomer, in this case 1,2,3-TCB, was essentially the same as its production efficiency. Two of the mutants showed only minor differences in the profile of efficiency values of their respective parents but $LinA_{LL02}$ V44I produced a major change (Table 6).

Specifically, conversion efficiencies for the $LinA1_{B90A}$ I44V mutant were generally similar to those of its parent, with relatively minor differences among minor reactions, such that the value for 1,2,3-TCB production by this mutant was somewhat lower from γ-PCCH1 and somewhat higher from γ-PCCH2. The conversion efficiencies for the $LinA_{LL02}$ V64L mutant were also generally similar to those of its parent although in this case the conversion of γ-PCCH1 to 1,2,3-TCB was about a magnitude higher, and now similar to its values for the conversion of γ-PCCH1 to 1,2,4-TCB. However, the efficiency statistic for the $LinA_{LL02}$ V44I mutant for the conversion of γ-PCCH1 to 1,2,4-TCB, i.e. the favoured second step reaction of both parents, was now over six logs higher. In respect of minor activities, this mutant had little effect on 1,2,3-TCB production from

either γ-PCCH, although it slightly reduced the value from γ-PCCH1, and it eliminated any detectable production of 1,3,5-TCB from either γ-PCCHs.

Table 6 *k_{cat}/K_m values (min^{-1} μM^{-1}) and their standard errors (SEs) (min^{-1} μM^{-1}) for γ-HCH degradation reactions by $LinA1_{B90A}$ I44V, $LinA_{LL02}$ V44I, and $LinA_{LL02}$ V64L. The values for $LinA1_{B90A}$ and $LinA_{LL02}$ were also included for comparison. Detailed explanation and comparison between the mutant and wildtype enzymes can be found in Section 4.4.3 and 4.4.4. Levels that are not detected are denominated with a dash symbol (-). Number of independent replicate is 3.*

Reactions	$LinA1_{B90A}$	$LinA_{LL02}$	$LinA1_{B90A}$ I44V	SE $LinA1_{B90A}$ I44V	$LinA_{LL02}$ V44I	SE $LinA_{LL02}$ V44I	$LinA_{LL02}$ V64L	SE $LinA_{LL02}$ V64L
γ-HCH -> γ-PCCH1	3.2E-03	1.5E-03	7.4E-04	*4.8E-04*	2.9E-04	*1.9E-04*	1.1E-03	*5.4E-04*
γ-HCH -> γ-PCCH2	2.9E-04	1.9E-03	3.5E-04	*4.1E-04*	3.2E-03	*3.7E-04*	9.9E-04	*4.7E-04*
γ-PCCH1 -> 1,2,4-TCB	6.6E-02	1.2E-02	2.0E-02	*1.1E-02*	8.9E+04	*4.0E+07*	2.3E-02	*1.8E-02*
γ-PCCH1 -> 1,2,3-TCB	5.8E-03	1.6E-03	<1.0E-04	*4.4E-03*	<1.0E-04	*6.7E+03*	2.2E-02	*1.2E-02*
γ-PCCH1 -> 1,3,5-TCB	-	7.1E-03	-		-		-	
γ-PCCH2 -> 1,2,4-TCB	<1.0E-04	1.0E-04	<1.0E-04	*1.9E-03*	4.1E-04	*2.2E-04*	9.1E-04	*9.4E-04*
γ-PCCH2 -> 1,2,3-TCB	<1.0E-04	3.1E-03	1.1E-03	*9.4E-04*	1.5E-03	*2.4E-04*	<1.0E-04	*6.3E-04*
γ-PCCH2 -> 1,3,5-TCB	-	<1.0E-04	-		-		-	

4.4 Discussion

4.4.1 δ-HCH and δ-PCCH transformation

This study shows that both the V44I and V64L mutations in $LinA_{LL02}$ decrease the enzyme's activity to degrade δ-HCH, although the effect of both mutants is much bigger for the transformation to δ-PCCH1 than δ-PCCH2. Given that wildtype $LinA_{LL02}$ already preferred the transformation to δ-PCCH2, these mutations effectively enhance this enantiopreference further. This suggests that the larger isoleucine and leucine residues at positions 44 and 64, respectively, not only negatively affect δ-HCH positioning in the LinA active site but also affect the positioning in such a way that it encourages the removal of the *trans*-diaxial H-Cl pair that gives rise to δ-PCCH2 but not the pair that gives rise to δ-PCCH1 (Figure 9).

The negative effects of these two mutations on the transformations to both δ-PCCHs support the hypothesis proposed by Pearce (2015) that the valine residues at position 44 and 64 of $LinA_{LL02}$ help to increase the size of the active site and hence allow enough room for δ-HCH to

assume a productive pose for reaction with the catalytic residues. However, I also note that both mutant enzymes still give higher efficiency statistics for this reaction than $LinA1_{B90A}$, implying that other residues also contribute to the differences between the two parent enzymes in this reaction.

To further test the hypothesis of Pearce (2015), the I44V mutant of $LinA1_{B90A}$ was also tested with δ-HCH. However, this mutant generated very low efficiency statistics for the transformations to both δ-PCCH1 and δ-PCCH2 and they could not be confidently distinguished from the parental values. This reinforces my conclusion above that other residues also contribute to the differences between the two parent enzymes in this reaction.

Unfortunately, there is little specific guidance in the literature as to what those other residues at play might be, apart from the sequence comparisons and structural and modelling work of Sharma et al. (2011) and Shrivastava et al. (2017). As noted in Chapter 1, the only other mutagenesis study investigating the effects of LinA active site residues on HCH or PCCH preferences was the recent work of Shrivastava et al. (2017) who found the amino acids at residues 20, 96, 131 and 133 of LinA-Type1 and LinA-type2 enzymes affected their enantiopreference for (-)-α-HCH and (+)-α-HCH, respectively. They did not include other substrates in their experiments. However, the four residues they did study are the same between the two LinA parent enzymes for my mutagenesis, therefore they are not candidates to contribute to the differences between them in δ-HCH transformation which are not explained by residues 44 and 64. The other sequence differences between $LinA1_{B90A}$ and $LinA_{LL02}$ are at residues 64, 67, 68, 70, 71, 115, 126, 132, 145 and in the C-terminal sequences. Of these, 64, 67, 70, 71, 115, and 132 are situated in the vicinity of the active site and might therefore be prime candidates for further mutagenesis analysis.

Both the V44I or V64L mutants of $LinA_{LL02}$ had low but measurable abilities to convert δ-PCCH1 and δ-PCCH2 into 1,2,4-TCB, whereas the parent $LinA_{LL02}$ enzyme had no detectable ability to catalyse either of these transformations. While the values are all low, both mutations also show

some enantiopreference for δ-PCCH1 rather than δ-PCCH2 transformation. Intriguingly, the efficiency statistics for both mutants now closely resemble the corresponding values for parent LinA1$_{B90A}$, which in isolation might suggest that either mutation may be sufficient to explain the difference between the two parent enzymes. However, the I44V mutation in LinA1$_{B90A}$ yielded low but measureable efficiency statistics for both δ-PCCH to 1,2,4-TCB transformations, with no apparent enantiopreference between them. Thus, in a LinA1$_{B90A}$ background, this change is not sufficient to explain the difference between the two parent enzymes. I conclude that the two mutations are important to the differences between the two parent enzymes in their ability to catalyse the second reaction in the degradation of δ-HCH, but, as with the first reaction, and at least for the difference at residue 44, differences at another residue or residues must also be at play.

4.4.2 γ-HCH and γ-PCCH transformation

Unlike the situation for δ-HCH, there were no major differences between LinA1$_{B90A}$ and LinA$_{LL02}$ in the k_{cat}/K_m values for the transformations of γ-HCH to the corresponding PCCHs. Very similar values were also obtained for the three mutants. Therefore all that can be concluded from the mutant data is (a) that none of the mutations tested at residues 44 or 64 had large effects on catalytic efficiency in the absence of the corresponding mutations at the other site and (b) that the genetic background (i.e. the other amino acid differences between the two parent enzymes) did not affect the role of the mutant residues in the catalysis of γ-HCH either.

I also note that Pearce (2015) had predicted that the substitutions of valines for isoleucine and leucine, respectively, at residues 44 and 64 in LinA$_{LL02}$ compared to LinA1$_{B90A}$ would enhance the catalytic efficiency of δ-HCH but to the detriment of γ-HCH. I therefore also reiterate my observation in Chapter 2 that the γ-HCH data for the parental strains does not support his hypothesis.

There was also little difference between the two parent enzymes in their k_{cat}/K_m values for the transformations of the two γ-PCCHs into 1,2,4- and 1,2,3-TCB. In this case however, all three

mutants differed significantly from both parents. By far the largest effect was due to the V44I mutation in $LinA_{LL02}$ which increased k_{cat}/K_m for the transformation of γ-PCCH1 to 1,2,4-TCB by six orders of magnitude. It also had a much smaller, negative effect on the catalytic efficiency of the conversion of γ-PCCH1 transformation into 1,2,3-TCB. The V64L mutation in $LinA_{LL02}$ had a minor positive effect on the efficiency of the production of 1,2,3-TCB from γ-PCCH1 and a minor negative effect on its production from γ-PCCH2. Conversely, the I44V mutation in $LinA1_{B90A}$ had a minor negative effect on the efficiency of the production of 1,2,3-TCB from γ-PCCH1 and a minor positive one on its production from γ-PCCH2.

Thus, the net effect of all three mutations was to significantly alter and in some cases significantly magnify the γ-PCCH to TCB enantiopreferences evident in the two parental enzymes. It is difficult to rationalise some of the changes in structural or mechanistic terms, particularly given that this reaction is actually believed to proceed in two steps via TCDN intermediates and the evidence in Chapters 2 and 3 suggesting the second step can occur in the active site of the enzyme and be influenced by sequence differences there. However, it appears that in some way the V64L mutation in the $LinA_{LL02}$ background may enhance the positioning of γ-PCCH1 for a productive pose that removes the *trans*-diaxial H-Cl pair to produce 1,3,5,6-TCDN and thence 1,2,3-TCB, and likewise it enhances γ-PCCH2 positioning for a productive pose that removes the *trans*-diaxial H-Cl pair to produce 1,2,4,6-TCDN and thence 1,2,4-TCB (see Chapter 1). My evidence that these effects of a leucine at residue 64 depend on the background sequence of the enzymes, including but not limited to residue 44, indicates that these γ-PCCH to TCB enantiopreferences depend on additional residues in the active site. Section 4.1.1 above enumerated residues in the vicinity of the active site which differ between the two parental sequences. These are prime candidates to exert some of these effects.

It is also notable that the mutants I made had such significant effects on γ-PCCH to TCB enantiopreferences when they had had so little influence on γ-HCH to γ-PCCH enantiopreferences. Molecular dynamic (MD) simulations might resolve this paradox. MD

simulations are presented in Chapter 6 below but those presented do not in fact elucidate this particular issue.

Another notable aspect of the γ-PCCH to TCB transformations is the failure to detect 1,3,5-TCB in any of the mutant assays although it had been observed in the corresponding $LinA_{LL02}$ assays. This result suggests both V44 and V64 are important to the production of 1,3,5-TCB by $LinA_{LL02}$. Further, in the case of V44, where V44 could be analysed in a $LinA1_{B90A}$ background, it is clear that V44 is not sufficient alone to bring about the formation of 1,3,5-TCB, albeit it does increase 1,2,3-TCB formation from γ-PCCH2. As shown in Chapter 1, 1,2,3- and 1,3,5-TCB are both produced from 1,3,5,6-TCDN (Orloff and Kolka, 1954), which means 1,3,5-TCB production is also expected where 1,2,3-TCB is formed. In this respect it is unfortunate that I did not carry out γ-PCCH-based assays on the mutants, given that the yields of all TCBs were greater in these assays than the corresponding γ-HCH-based assays (presumptively because of the greater amounts of γ-PCCH available as substrate; see Section 2.4.2). Issues around the production of the different TCDNs and their transformation to TCBs will be discussed further in subsequent Chapters.

CHAPTER 5:

α-HCH degradation by wild type $LinA1_{B90A}$, $LinA2_{B90A}$, and $LinA_{LL02}$ enzymes

5.1 Introduction

As mentioned in Chapter 1, Suar et al. (2005) have previously reported strong enantiopreference differences between the type 2 and type 1 enzymes $LinA1_{B90A}$ and $LinA2_{B90A}$, respectively, in whole *E. coli* BL21 cell assays of (+)-α-HCH or (-)-α-HCH degradation. They found $LinA1_{B90A}$ prefers to degrade (+)-α-HCH and $LinA2_{B90A}$ prefers to degrade (-)-α-HCH. That study also found the enzymes to preferentially produce two β-PCCH enantiomers, 1,3(*S*),4(*S*),5(*R*),6(*R*)-PCCH and 1,3(*R*),4(*R*),5(*S*),6(*S*)-PCCH, respectively, from their (+)-α-HCH and (-)-α-HCH degradations (Figure 25). Subsequently, and after I commenced my project, Shrivastava et al. (2017, 2015) confirmed these patterns in purified enzyme assays and extended them to a type 3 enzyme, for which they found a very slight enantiopreference for the (+)-α-HCH to 1,3(*S*),4(*S*),5(*R*),6(*R*)-PCCH transformation.

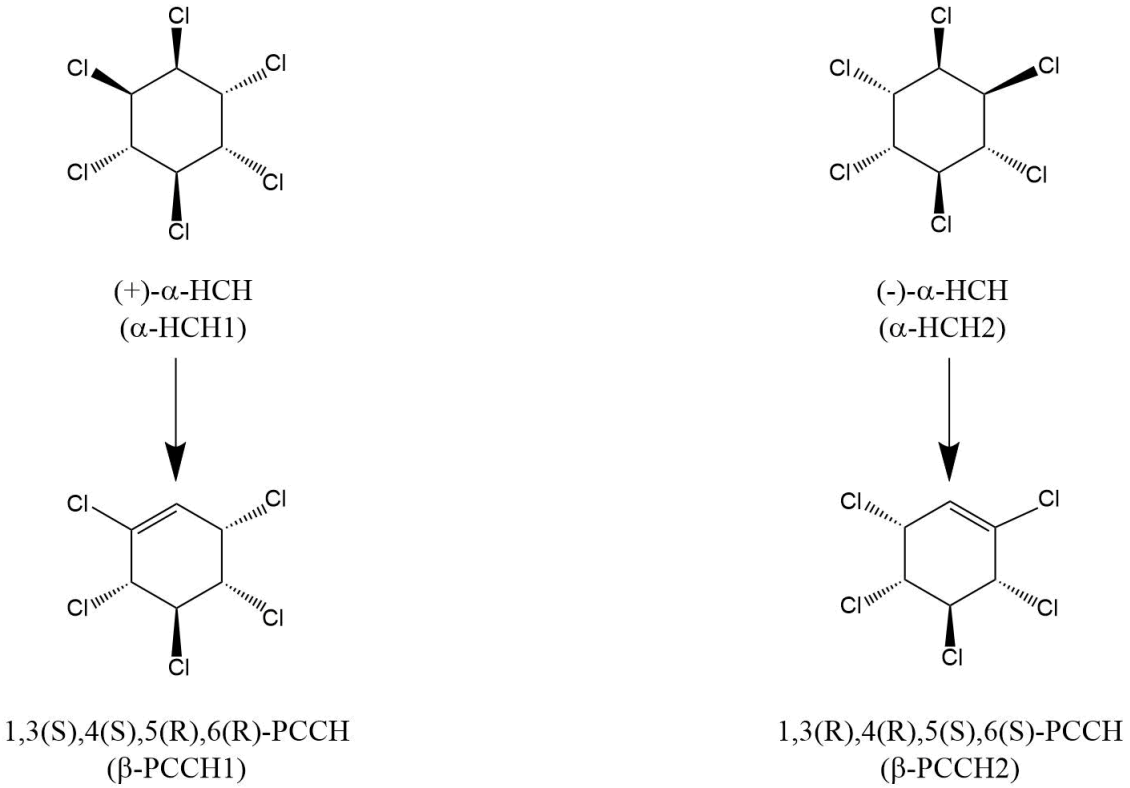

Figure 25 *Expected β-PCCH molecules from α-HCH degradation. (Suar et al., 2005) found that the LinA-type2 $LinA1_{B90A}$ and the LinA-type1 $LinA2_{B90A}$ prefers to degrade (+)-α-HCH and (-)-α-HCH, respectively.*

This Chapter describes my whole cell and purified enzyme assay on all three enzymes, and uses the Copasi software again to obtain catalytic efficiency statistics from the purified enzyme assays. This enables me to more rigorously assess the proposed enantiopreferences between the two α-HCH to β-PCCH transformations and to explore and characterise the various second step transformations of the two β-PCCHs to three different TCBs. The purified enzyme assays are also repeated in the presence of *E. coli* extracts in an effort to understand to what extent cellular material might be influencing the various reactions. This was done because it emerged that my results with purified enzymes differed in some respects from the earlier work with whole cells. I therefore wanted to test whether this was because there was some effect of cellular material that modified the enantiopreferences of the enzymes.

5.2 Materials and methods

5.2.1 Whole cell assays

E. coli strain BL21*(DE3) containing the His6-tagged and codon optimized $linA1_{B90A}$ and $linA_{LL02}$ in pDEST14 and $linA2_{B90A}$ in pDEST17 were used in these assays.

The assays were prepared by first inoculating 5 ml aliquots of LB media containing 100 μg/ml ampicillin with *E. coli* strain BL21*(DE3) containing one of the three expression constructs above, and incubating the cultures overnight at 37 °C with shaking at 200 rpm. Then 3.8 ml aliquots of LB containing 100 μg/ml ampicillin and 17 μM α-HCH were inoculated with 200 μl of one of the overnight cultures. Triplicate cultures were set up for each of the three expression constructs. A 500 μl sample of each freshly inoculated culture was immediately taken for analysis and the cultures then left to incubate at 37 °C with shaking at 200 rpm for 24 hr. Further 500 μl samples were taken for analysis at 1, 3, 5, 7, and 24 h.

Each 500 μl sample taken for analysis was immediately injected into a vial with a septa cap already filled with 400 μl ethyl acetate. 100 μl of 56 μM PCNB in ethyl acetate was then also injected into the mixture, to a final concentration of 11 μM PCNB, to act as an internal standard.

The mixture was vigorously shaken by hand before letting it rest for roughly 8 h to separate the ethyl acetate layer from the aqueous layer. 400 μl of the ethyl acetate layer was then transferred into an Eppendorf tube and centrifuged for 5 min at ~18,000 g to further separate the aqueous layer from the ethyl acetate layer. 200 μl of the ethyl acetate layer from the centrifuged mixture was transferred to a new vial before being analysed in a GC unit fitted with an Astec® Chiraldex B-DP column (Sigma-Aldrich) and an electron capture detector as described in Section 2.2.3 in Chapter 2.

The commercially available α-HCH used in this study is a mixture of both enantiomers and my GC methods indeed detected two, which I denoted α-HCH1 and α-HCH2 (with retention times of 12.09 and 12.79, respectively). I then inferred their correspondence to (+)-α-HCH and (-)-α-HCH from the α-HCH enantiomer preferences of $LinA1_{B90A}$ and $LinA2_{B90A}$ published by Suar et al. (2005). Those authors found $LinA1_{B90A}$ and $LinA2_{B90A}$ preferentially degraded (+)-α-HCH and (-)-α-HCH, respectively, and, as Section 5.2.4 below shows, I found they preferentially degraded α-HCH1 and α-HCH2, respectively. So I expect that α-HCH1 and α-HCH2 correspond to (+)-α-HCH and (-)-α-HCH, respectively. α-HCH1 and α-HCH2 concentrations in my assays were calculated as per the methods described for γ-HCH in Section 2.2.3 using GraphPad Prism version 5.02 for Windows (GraphPad Software).

5.2.2 Purified enzyme assays without cell lysate

$LinA1_{B90A}$, $LinA2_{B90A}$, and $LinA_{LL02}$ for these assays were expressed and purified following the methods in Section 2.2.2 and the assays were carried out as per Section 2.2.3 except that α-HCH was used as substrate. As in Section 2.2.3, the starting concentration of substrate was adjusted on the basis of pilot experiments to best suit the calculation of specificity constants by the Copasi 4.15 software (Hoops et al., 2006); in this case 17 μM α-HCH was used for each enzyme. The enzyme concentration was 10 μg/ml for each enzyme. α-HCH1 and α-HCH2 concentrations were monitored as per Section 5.2.1 above and TCB concentrations as per previous Chapter 2, 3, and

4. The concentrations of the two β-PCCHs formed from the initial dehydrochlorination reaction were estimated as per Section 5.2.4 below.

5.2.3 Purified enzyme assays with cell lysate

These assays were conducted as per those in Section 5.2.2 above except that cell lysate from *E. coli* strain BL21*(DE3) without any expression plasmid was also added. The lysate was prepared by inoculating 55.5 ml LB with the cells and incubating overnight at 37 °C with shaking at 200 rpm. The cells were then pelleted by centrifugation at ~1,000 g for 15 min at 4 °C, resuspended in 21 ml of working buffer (50 mM potassium phosphate, 10% glycerol, pH 7.5) and subjected to three rounds of sonication (alternating 0.5 s active and 1 s rest periods for a total of 45 s of active periods for each round). The preparation was then centrifuged at ~33,000 g for 40 min at 4 °C and the supernatant filtered through a 0.45 μm filter to remove impurities. The filtrate was divided into three aliquots which were each brought to a final volume of 7 ml with working buffer. These preparations were kept at 4 °C until ready to use, always within five days. All of the 7 ml lysate was used in each assay.

5.2.4 Identification of β-PCCH enantiomers and estimation of their concentrations

As noted, previous work (Suar et al., 2005) has shown that the LinA1 and LinA2 enzymes degrade the two α-HCHs into two β-PCCH enantiomers, 1,3(*S*),4(*S*),5(*R*),6(*R*)-PCCH and 1,3(*R*),4(*R*),5(*S*),6(*S*)-PCCH (Figure 25). My assays also generated two enantiomers, which I named β-PCCH1 and β-PCCH2 based on their elution times on GC chromatograms (9.1 min and 9.9 min, respectively) (Figure 26). My attempts to synthesise 1,3(*S*),4(*S*),5(*R*),6(*R*)-PCCH and 1,3(*R*),4(*R*),5(*S*),6(*S*)-PCCH were unsuccessful (see Appendix B), but I was able to confidently infer the respective identities of β-PCCH1 and β-PCCH2 from the findings of Suar et al. (2005) that $LinA1_{B90A}$ and $LinA2_{B90A}$ degrade (+)-α-HCH and (-)-α-HCH into 1,3(*S*),4(*S*),5(*R*),6(*R*)-PCCH and 1,3(*R*),4(*R*),5(*S*),6(*S*)-PCCH, respectively. My whole cell α-HCH degradation assays showed $LinA1_{B90A}$ or $LinA2_{B90A}$ preferentially, albeit not exclusively, produced β-PCCH1 and β-PCCH2,

respectively (Figure 26). So I conclude that my β-PCCH1 and β-PCCH2 most likely to correspond to 1,3(*S*),4(*S*),5(*R*),6(*R*)-PCCH and 1,3(*R*),4(*R*),5(*S*),6(*S*)-PCCH, respectively.

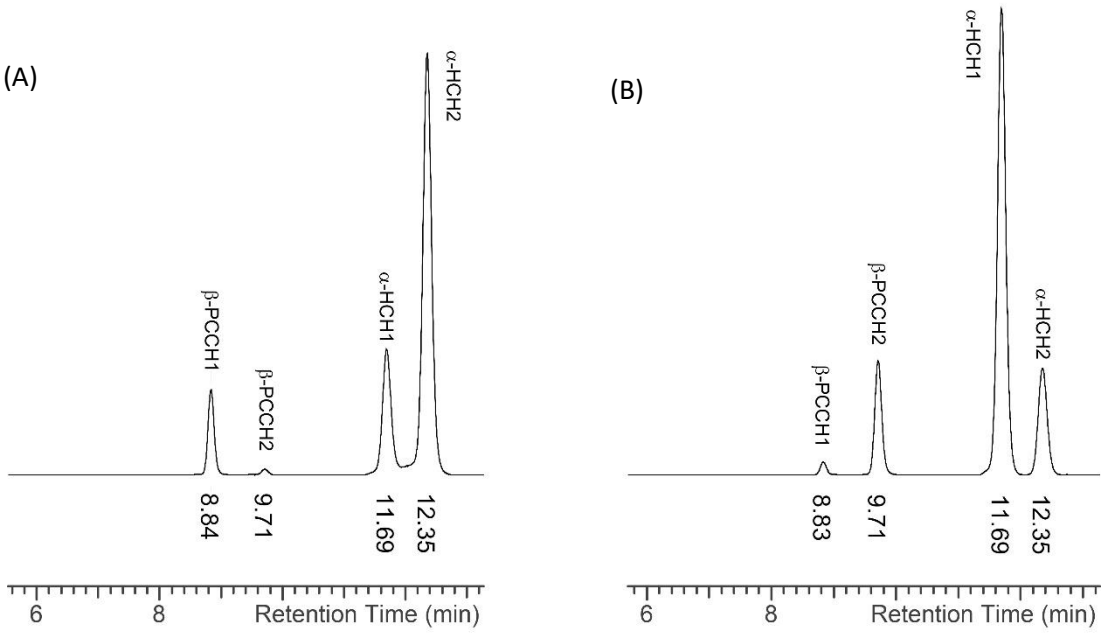

Figure 26 *Chromatograms showing the retention times for α-HCH1, α-HCH2, β-PCCH1, and β-PCCH2. (A) and (B) are derived from LinA1$_{B90A}$ and LinA2$_{B90A}$ whole cell assay, respectively, measured at 1 h into the assays. Notice the β-PCCH1 formation and α-HCH1 degradation in (A), and β-PCCH2 formation and α-HCH2 degradation in (B).*

In the absence of standards for β-PCCH1 and β-PCCH2, my first pass estimations of their concentrations were simply based on the standard curves of the synthesised γ-PCCHs and δ-PCCHs in Chapters 2 and 3. As Table 7 shows, the slopes for the two γ-PCCH enantiomers were essentially indistinguishable from one another (~0.048 μMpA^{-1}min^{-1}), as were those of the two δ-PCCH enantiomers (~0.060 μMpA^{-1}min^{-1}), and the two pairs of slopes were about 20% different from one another. I therefore initially tried using each of the two values and their average in the calculations for the α-HCH degradation data for purified LinA2$_{B90A}$ enzyme in Section 5.3.2 below, finding that all of them give similar good mass balance results. Therefore, I chose the averages, 0.0534 and 0.0531 μMpA^{-1}min^{-1} for β-PCCH1 and β-PCCH2, respectively, as the slopes to use for estimating their concentrations (Appendix C). Values using those slopes are therefore shown throughout Section 5.3 below. However, the β-PCCH was converted to TCB

relatively rapidly in all assays and broadly similar kinetic estimates were also obtained using the other two slopes (Appendix D).

Table 7 *Observed β-, γ-, and δ-PCCH retention times on chromatograms and the observed slopes of the standard curves for γ- and δ-PCCH and the average slopes used below for the β-PCCH.*

PCCH isomer/enantiomer	Retention times (min)	Slope ($\mu MpA^{-1}min^{-1}$)
γ-PCCH1	3.9	0.0484
γ-PCCH2	4.0	0.0477
δ-PCCH1	8.3	0.0596
δ-PCCH2	8.8	0.0600
β-PCCH1	9.1	0.0534
β-PCCH2	9.9	0.0531

5.3 Results

5.3.1 Whole cell assays

E. coli BL21*(DE3) cultures expressing either $LinA1_{B90A}$, $LinA2_{B90A}$, or $LinA_{LL02}$ were incubated with a starting concentration of 17 μM α-HCH at room temperature for 24 h and the concentration of α-HCH measured over time by GC-ECD (Figure 27). $LinA1_{B90A}$ cultures completely degraded α-HCH1 and α-HCH2 in 7 and 24 h, respectively, while $LinA2_{B90A}$ cultures showed the opposite enantiopreference, with complete degradation of α-HCH2 and α-HCH1 in 7 and 24 h, respectively. $LinA_{LL02}$ took 24 h to fully degrade both isomers, with a very slight preference for α-HCH1 degradation evident in the early time points. Both β-PCCH1 and β-PCCH2 were themselves degraded over the 24 h in all three sets of assays. Nevertheless, more β-PCCH1 than β-PCCH2 was produced by $LinA1_{B90A}$ and to a much lesser extent $LinA_{LL02}$, and more β-PCCH2 than β-PCCH1 was produced by $LinA2_{B90A}$. TCB's were not monitored in these assays. Otherwise, these results are in qualitative agreement with the whole cell assays of Suar et al. (2005) and the purified enzyme assays of Shrivastava et al. (2017, 2015).

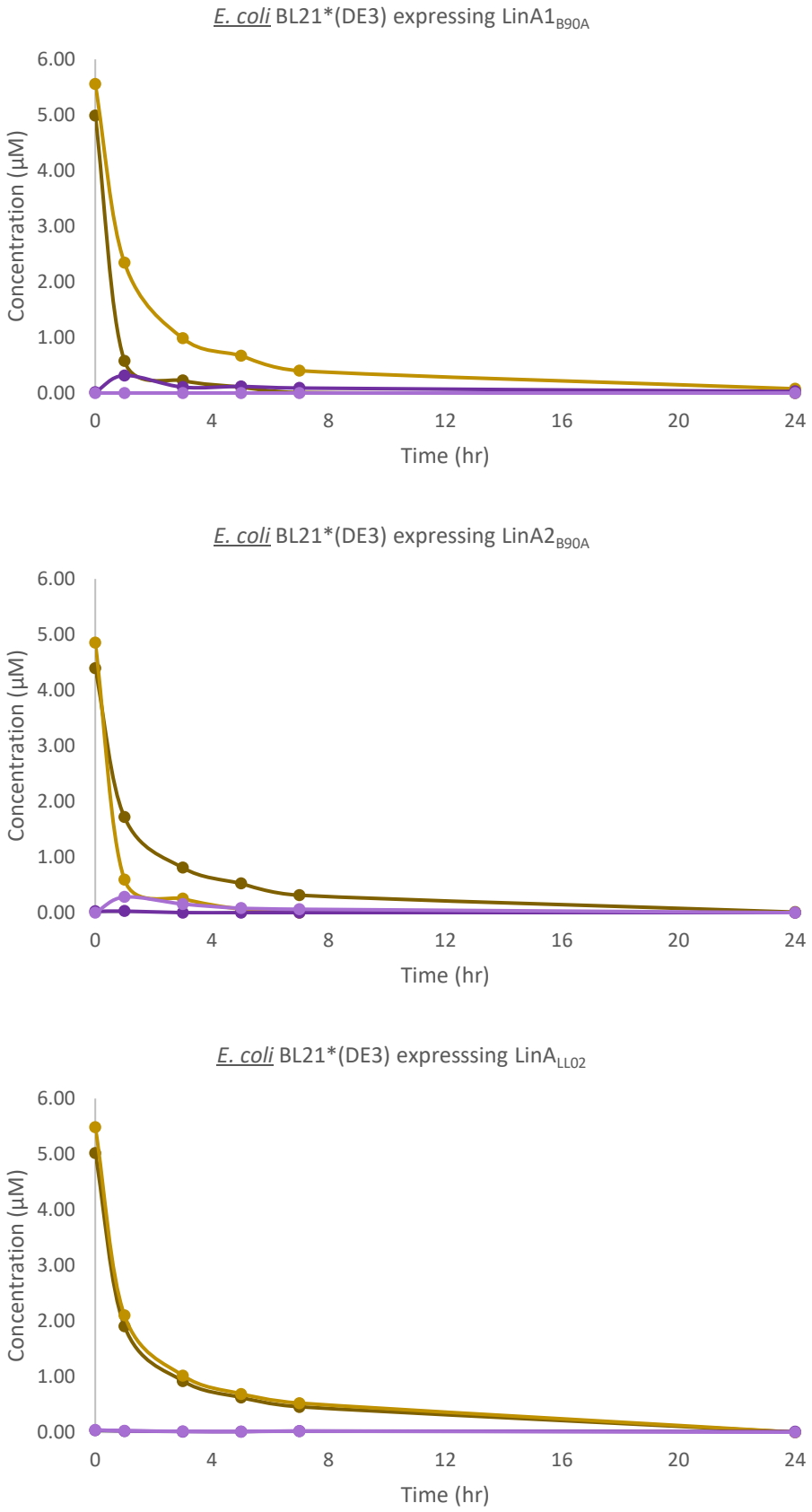

Figure 27 *Graphs showing the concentrations (µM) of α-HCH1 (●) and α-HCH2 (●) over time (min) in α-HCH degradation assays by E. coli BL21*(DE3) whole cells expressing (a) LinA1$_{B90A}$, (B) LinA2$_{B90A}$, and (C) LinA$_{LL02}$. Concentrations of β-PCCH1 (●) and β-PCCH2 (●) were estimated using the slopes discussed in Section 5.2.4. TCB concentrations were not measured. LinA1$_{B90A}$ and LinA2$_{B90A}$ show enantiopreferences for α-HCH1 and α-HCH2, respectively, while LinA$_{LL02}$ show no clear preference for either enantiomer.*

5.3.2 Purified enzyme assays

Triplicates reactions of 10 μg/ml of each of the three purified enzymes with 17 μM α-HCH were allowed to proceed at room temperature for 2 h (Figure 28). All enzymes were observed to degrade both α-HCH1 and α-HCH2, with $LinA2_{B90A}$ being the most efficient, followed by $LinA_{LL02}$ and then $LinA1_{B90A}$ (k_{cat}/K_m values of 8.6E-03 $min^{-1}\mu M^{-1}$ c.f. 3.4E-03 $min^{-1}\mu M^{-1}$ and 1.0E-03 $min^{-1}\mu M^{-1}$, and 1.2E-02 $min^{-1}\mu M^{-1}$ c.f. 2.9E-03 $min^{-1}\mu M^{-1}$ and 1.0E-03 $min^{-1}\mu M^{-1}$ for α-HCH1 and α-HCH2 degradations, by $LinA2_{B90A}$, $LinA_{LL02}$ and $LinA1_{B90A}$, respectively) (Table 8). All three enzymes produced small amounts of β-PCCH1 and β-PCCH2 with $LinA1_{B90A}$ clearly producing more than the other two enzymes (Figure 28). By far the major TCB isomer detected in these assays was 1,2,4-TCB, which accumulated steadily, with no clear evidence of further degradation, in all the assays. Trace amounts of 1,2,3-TCB and 1,3,5-TCB also accumulated in the $LinA2_{B90A}$ and $LinA_{LL02}$ assays (Figure 28).

The data in Figure 28 show no major α-HCH to β-PCCH enantiopreferences for any of the enzymes but such differences as are seen are broadly consistent in direction with those seen in my whole cell assays and the earlier assays of Suar et al. (2005) and Shrivastava et al. (2017, 2015). The preferences show most clearly in the early time points of the β-PCCH data, when the differences are much greater in proportion to absolute amounts than are the corresponding α-HCH differences and before most of the β-PCCH is lost via the relatively rapid second step transformations into TCBs. It is clear from these early time point β-PCCH data that $LinA1_{B90A}$ and $LinA_{LL02}$ produce more β-PCCH1 than β-PCCH2 while the reverse is true for $LinA2_{B90A}$.

It is important to note here that Shrivastava et al. (2017, 2015) did not report their assays as time courses and only presented their relevant data as chromatography traces at an unreported but (based on the small amounts of HCH then degraded) presumptively early time point. My data on enantiopreferences are thus reasonably comparable and consistent with theirs.

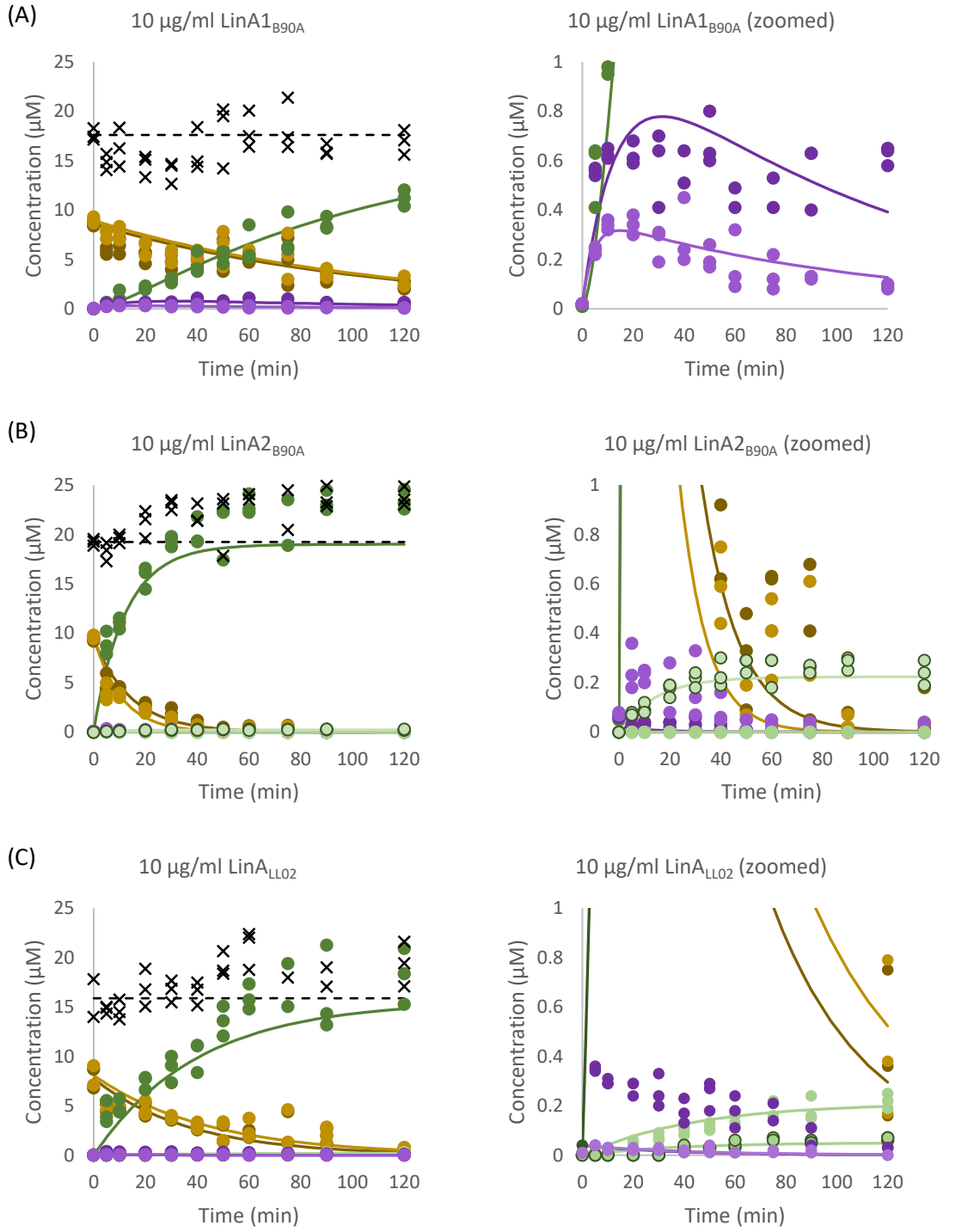

Figure 28 *Graphs showing the concentrations (µM) of α-HCH1, α-HCH2 and their metabolites over time (min) in α-HCH degradation assays by (A) 10 µg/ml LinA1$_{B90A}$, (B) 10 µg/ml LinA2$_{B90A}$, and (C) 10 µg/ml LinA$_{LL02}$. The results for each enzyme are shown on two graphs, the ones on the left showing all the data and the ones on the right just showing concentrations in the range 0 to 1 µM. The compounds are as follows: α-HCH1 (●), α-HCH2 (●), β-PCCH1 (●), β-PCCH2 (●), 1,2,4-TCB (●), 1,2,3-TCB (●), and 1,3,5-TCB (○). Also shown in the graphs are the best fit lines assumed by Copasi. Total measured mass is marked with (x) and the total mass assumed by Copasi is drawn with a dotted line (---). All three enzymes degraded most, if not all, of the α-HCH1 and α-HCH2 within the two hour period, producing β-PCCH1 and β-PCCH2, which are then transformed into TCB. The only TCB detected in the LinA1$_{B90A}$ assays was 1,2,4-TCB but trace amounts of the other two TCBs were evident in the other assays.*

The k_{cat}/K_m calculations from the above progress curves are given in Table 8. Given the issues in estimating β-PCCH amounts explained in Section 5.2.4 above, only values of at least 1.0E-03 are quantified and even then they are interpreted cautiously. However, the following three sets of observations are all borne out by the progress curves and hold true using the other assumptions about β-PCCH quantification tested (Appendix D).

First, the k_{cat}/K_m calculations find no major enantiopreferences for any of the enzymes in the first reaction. Very small differences in the respective directions expected from the earlier work are found for $LinA2_{B90A}$ and $LinA_{LL02}$, and no difference is found for $LinA1_{B90A}$. Thus the differences in the relative amounts of the two β-PCCH isomers early in the reactions seen by both myself and Shrivastava et al. (2017, 2015) do not carry through to differences in my catalytic efficiency statistics.

Second, the calculations show all enzymes degrade the β-PCCHs more efficiently than the α-HCHs. For $LinA2_{B90A}$ in particular, the differences between the values for the first step and the preferred reactions in the second step, for β-PCCH1 and β-PCCH2 to 1,2,4-TCB, are over two and six orders of magnitude, respectively. These second step values for $LinA2_{B90A}$ are actually the highest of any obtained in this experiment; about one and five orders of magnitude higher than the corresponding values for $LinA_{LL02}$ and about three and six orders of magnitude higher than those for $LinA1_{B90A}$. While all the k_{cat}/K_m estimates for the first reaction are orders of magnitude smaller than those for most enzymes with their natural substrates (Bar-Even et al., 2011), the estimate for $LinA2_{B90A}$ for the β-PCCH1 transformation to 1,2,4-TCB is about average for enzymes with their natural substrates and that for its transformation of β-PCCH1 to 1,2,4-TCB is considerably higher than that average.

Third, and following on from the second, there are some very large differences between the enzymes in the catalytic efficiency values for different reactions in the second step. In particular, (a) for 1,2,4-TCB production, $LinA1_{B90A}$ and $LinA2_{B90A}$ strongly prefer to use β-PCCH2 as substrate while $LinA_{LL02}$ shows little preference, (b) for 1,2,3-TCB production, $LinA_{LL02}$ strongly prefers β-

PCCH2 as substrate while LinA1$_{B90A}$ and LinA2$_{B90A}$ have little or no activity for either β-PCCH, and (c) for 1,3,5-TCB production, LinA2$_{B90A}$ and LinA$_{LL02}$ strongly prefer β-PCCH1 as substrate while LinA$_{LL02}$ has no activity for either β-PCCH. Thus, while there may be little evidence from the k_{cat}/K_m statistics for major enantiopreference differences between the enzymes in the first reaction, there certainly is for the second reaction.

Table 8 *k_{cat}/K_m values ($min^{-1}\mu M^{-1}$) and their standard errors (SEs) ($min^{-1}\ \mu M^{-1}$) for α-HCH degradation reactions by LinA1$_{B90A}$, LinA2$_{B90A}$, and LinA$_{LL02}$ in assays without cell lysate. Levels that are not detected are denominated with a dash symbol (-). Number of independent replicate is 3.*

Reactions	LinA1$_{B90A}$	SE LinA1$_{B90A}$	LinA2$_{B90A}$	SE LinA2$_{B90A}$	LinA$_{LL02}$	SE LinA$_{LL02}$
α-HCH1 → β-PCCH1	1.0E-03	*2.6E-04*	8.6E-03	*4.3E-03*	3.4E-03	*1.6E-03*
α-HCH2 → β-PCCH2	1.0E-03	*2.7E-04*	1.2E-02	*6.4E-03*	2.9E-03	*1.1E-03*
β-PCCH1 → 1,2,4-TCB	8.5E-03	*2.1E-03*	3.9E+00	*5.9E+00*	6.7E-01	*2.3E+00*
β-PCCH1 → 1,2,3-TCB	-		<1.0E-03	*1.1E-04*	<1.0E-03	*1.4E-01*
β-PCCH1 → 1,3,5-TCB	-		9.5E-02	*1.5E-01*	4.4E-03	*4.4E-02*
β-PCCH2 → 1,2,4-TCB	2.5E-02	*6.3E-03*	2.1E+04	*6.7E+08*	5.8E-01	*2.4E-01*
β-PCCH2 → 1,2,3-TCB	-		<1.0E-03	*5.4E-01*	1.6E-02	*1.3E-01*
β-PCCH2 → 1,3,5-TCB	-		<1.0E-03	*2.2E+02*	<1.0E-03	*3.8E-02*

5.3.3 Purified enzyme assays with E. coli cell lysate

I then repeated the purified enzyme assays in the presence of *E. coli* BL21*(DE3) cell lysate in order to test to what extent cellular material might be influencing the various reactions. The progress curves for the assays in the presence of the lysate (Figure 29) were found to be qualitatively similar to those in its absence.

Again there was no major difference in the degradation fates for the two α-HCHs for any of the enzymes, but β-PCCH1 was again more prevalent than β-PCCH2 in the LinA1$_{B90A}$ and LinA$_{LL02}$ assays and β-PCCH2 again more prevalent than β-PCCH1 in the LinA2$_{B90A}$ assays. And again these differences were most evident in the early stages of the assays before the β-PCCHs were further transformed to TCBs. In this respect these data bear out the enantiopreferences observed in the earlier whole cell and purified enzyme minus lysate assays by Suar et al. (2005), Shrivastava et al. (2017, 2015) and myself.

1,2,4-TCB was again the dominant end product in all assays, but now there were traces of the other two TCBs with all three enzymes, whereas only 1,2,4-TCB has been detectable in the purified $LinA1_{B90A}$ assay in the absence of the lysate.

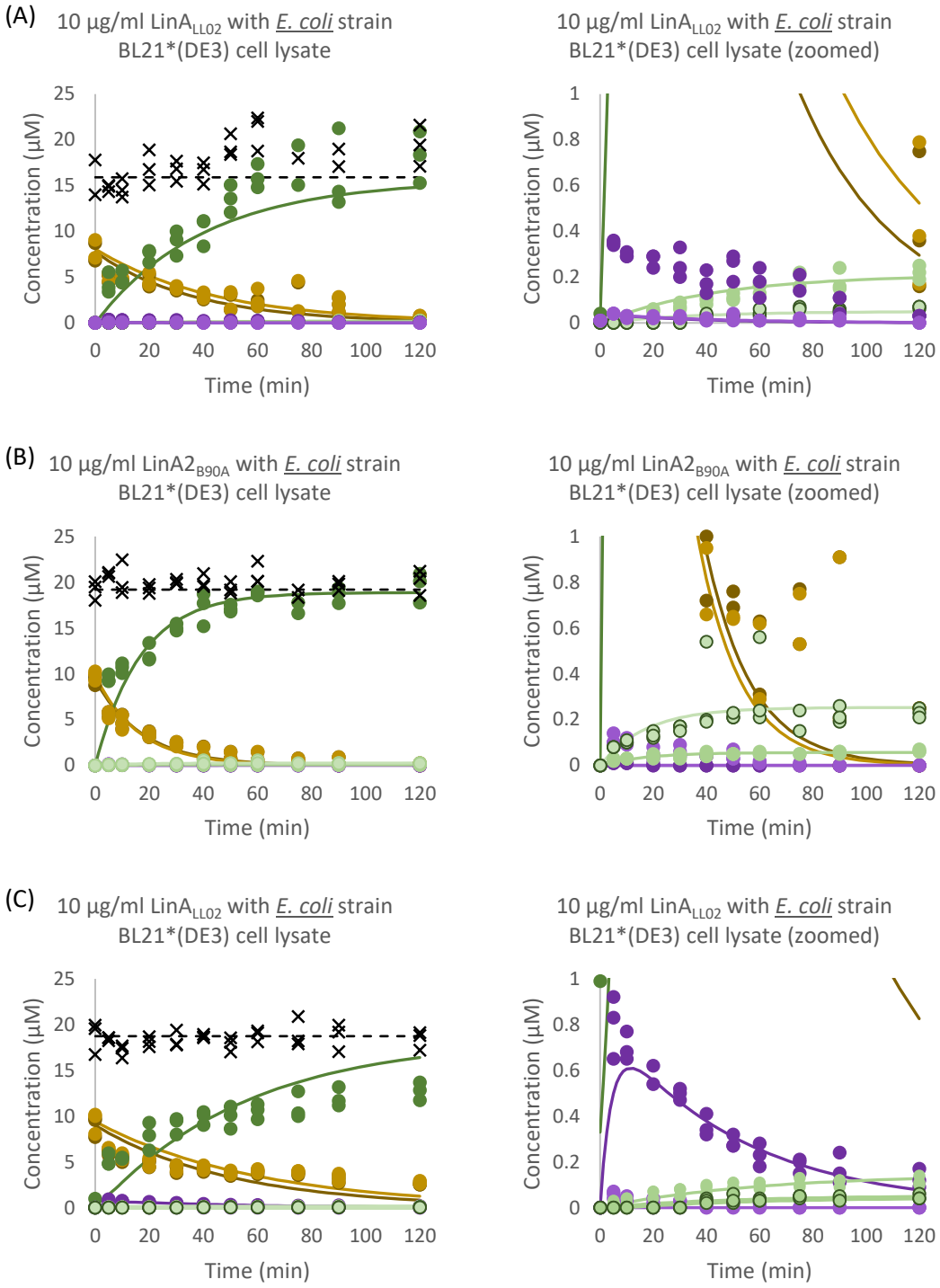

Figure 29 *Graphs showing the concentrations (µM) of α-HCH1, α-HCH2, and their metabolites over time (min) in α-HCH degradation assays by (A) 10 µg/ml LinA1$_{B90A}$, (B) 10 µg/ml LinA2$_{B90A}$, and (C) 10 µg/ml LinA$_{LL02}$. All of these assays had the addition of E. coli BL21*(DE3) cell lysate, as opposed to only purified enzyme in Figure 27. The results for each enzyme are shown on two graphs, the ones on the left showing all the data and the ones on the right just showing concentrations in the range 0 to 1 µM. The compounds are as follows: α-HCH1 (●), α-HCH2 (●), β-PCCH1 (●), β-PCCH2 (●), 1,2,4-TCB (●), 1,2,3-TCB (●) and 1,3,5-TCB (○). Also shown in the graphs are the best fit lines assumed by Copasi. Total measured mass is marked with (x) and the total mass assumed by Copasi is drawn with a dotted line (---). All three enzymes degraded most, if not all, of the α-HCH1 and α-HCH2 within the two hour period, producing β-PCCH1 and β-PCCH2, which are then transformed into TCB as the dead-end product. All three assays produced 1,2,3-, 1,3,5- and 1,2,4-TCB, with 1,2,4-TCB being the major TCB isomer.*

The k_{cat}/K_m values for the above reactions are presented in Table 9. The same cautions apply to their interpretation as for the assays without added lysates but, with one major exception, the general pattern of the results is similar to those assays.

The values for the first reaction are all within a log of those seen in the minus lysate assays and confirm the absence of any major enantiopreference as represented by k_{cat}/K_m between the α-HCH1 to β-PCCH1 and α-HCH2 to β-PCCH2 transformations by either enzyme. Interestingly, however, such differences as do occur are remarkably similar to those seen in the minus lysate assays; again $LinA1_{B90A}$ shows no difference between the two transformations, $LinA2_{B90A}$ shows a slight α-HCH1 to β-PCCH1 preference, and $LinA_{LL02}$ a slight α-HCH2 to β-PCCH2 preference.

The k_{cat}/K_m values for the preferred transformations for the second reaction generally exceed those for α-HCH degradation, as they had done for the minus lysate assays. However there is a major difference from the minus lysate assays in that many of the values for the second step are significantly higher than those from the minus lysate assays; some of the very low values (<1.0E-03) remain low, but most of the higher values are now higher again. This is clearly the case for the transformations of β-PCCH1 into all three TCBs in the $LinA2_{B90A}$ assays and for the β-PCCH2 transformation into 1,2,4-TCB for all three enzymes.

Some of the lower k_{cat}/K_m values for the second step also increased sufficiently to clarify the enantiopreferences among the second step reactions. In respect of 1,2,4-TCB production, all three enzymes now show a preference for β-PCCH2 as substrate, whereas only $LinA1_{B90A}$ and $LinA2_{B90A}$ did so without added lysate. In respect of 1,2,3-TCB production, $LinA1_{B90A}$ and $LinA_{LL02}$ now show a strong preference for β-PCCH2 and $LinA2_{B90A}$ for β-PCCH1, with the minus-lysate values concurring for $LinA_{LL02}$ but having been too low to discriminate for the other two enzymes. In respect of 1,3,5-TCB production, $LinA2_{B90A}$ shows a clear preference for β-PCCH1, with the other enzymes yielding values too low to discriminate, whereas the values for all three enzymes were too low to discriminate in the minus-lysate assays.

Table 9 *k_{cat}/K_m values (min^{-1} μM^{-1}) and their standard errors (SEs) (min^{-1} μM^{-1}) for α-HCH degradation reactions by $LinA1_{B90A}$, $LinA2_{B90A}$, and $LinA_{LL02}$ in assays with cell lysate. Number of independent replicate is 3. The corresponding values from the minus lysate assays from Table 8 are shown in parentheses for comparison.*

Reactions	$LinA1_{B90A}$	SE $LinA1_{B90A}$	$LinA2_{B90A}$	SE $LinA2_{B90A}$	$LinA_{LL02}$	SE $LinA_{LL02}$
α-HCH1 -> β-PCCH1	2.9E-03 (1.0E-03)	*1.1E-03*	7.2E-03 (8.6E-03)	*7.0E-03*	2.5E-03 (3.4E-03)	*9.3E-04*
α-HCH2 -> β-PCCH2	2.9E-03 (1.0E-03)	*1.5E-03*	7.8E-03 (1.2E-02)	*1.0E-02*	2.1E-03 (2.9E-03)	*9.5E-04*
β-PCCH1 -> 1,2,4-TCB	4.1E-03 (8.5E-03)	*1.5E-03*	4.6E+02 (3.9E+00)	*2.2E+04*	2.9E-02 (6.7E-01)	*1.2E-02*
β-PCCH1 -> 1,2,3-TCB	<1.0E-03	*4.2E-05*	2.8E+00 (<1.0E-03)	*1.5E+02*	<1.0E-03 (<1.0E-03)	*3.2E-03*
β-PCCH1 -> 1,3,5-TCB	<1.0E-03	*4.3E-05*	1.3E+01 (9.5E-02)	*6.1E+02*	<1.0E-03 (4.4E-02)	*1.2E-03*
β-PCCH2 -> 1,2,4-TCB	1.6E+04 (2.5E-02)	*4.5E+09*	1.2E+05 (2.1E+04)	*3.1E+08*	3.7E+01 (5.8E-01)	*8.4E+02*
β-PCCH2 -> 1,2,3-TCB	1.2E-03	*3.5E+02*	<1.0E-03 (<1.0E-03)	*1.4E+04*	5.6E-01 (1.6E-02)	*1.4E+01*
β-PCCH2 -> 1,3,5-TCB	<1.0E-03	*1.1E+02*	<1.0E-03 (<1.0E-03)	*6.8E-01*	<1.0E-03 (<1.0E-03)	*1.5E+00*

5.4 Discussion

5.4.1 α-HCH to β-PCCH transformation

The results from my whole cell assays show that the LinA-type2 enzyme $LinA1_{B90A}$ clearly prefers the (+)-α-HCH (also referred to as α-HCH1 herein) to β-PCCH1 transformation, unlike the LinA-type1 enzyme $LinA2_{B90A}$ which clearly shows the opposite enantiopreference, while the LinA-type3 enzyme $LinA_{LL02}$ shows a slight preference for the (+)-α-HCH/α-HCH1 to β-PCCH1 transformation. The findings for $LinA1_{B90A}$ and $LinA2_{B90A}$ are in qualitative agreement with the whole cell study by Suar et al. (2005), who did not study $LinA_{LL02}$.

The same enantiopreferences could also be seen in the relative β-PCCH1 and β-PCCH2 amounts early in the progress curves from my purified enzyme assays, both with and without the addition of *E. coli* BL21*(DE3) cell lysate. These differences also broadly concur with the single time point purified enzyme assay results of Shrivastava et al. (2015). However, the k_{cat}/K_m values from my purified enzyme assays showed much smaller enantiopreference differences; the preferences of $LinA2_{B90A}$ and $LinA_{LL02}$ were still in the same directions, but the preference of $LinA1_{B90A}$ was essentially non-existent in both the with and without lysate assays.

Several factors could explain the differences between the enantiopreferences evident in the k_{cat}/K_m values from the purified enzyme assays and those from the early stage β-PCCH amounts from these assays and the whole cell assays. One factor which may well be important concerns the relative importance of k_{cat} versus K_m differences between the enzymes in the different assays and measurements from those assays. However, without being able to deconvolute our catalytic efficiency statistics into separate k_{cat} and K_m estimates, we cannot assess the contribution of this factor. Another factor relevant to the whole cell versus purified enzyme assays is the very different operating environments for the enzymes in these two forms of assay. Substrate transport across the cell membrane may be limiting in the case of the whole cell assays and indeed those reactions proceeded much more slowly than the purified enzyme ones. pH and solvent conditions will also be very different between the intracellular environments relevant to the whole cell assays and the extracellular ones relevant to the purified enzyme assays, and these differences could easily have large effects on the kinetics of the reaction. Finally I note that even the comparison between the purified enzyme assays of Shrivastava et al. (2017, 2015) and myself is problematic at some level because they used vastly higher substrate concentrations than I did in my purified enzyme assays and did not report many other key aspects of their assay conditions (see also Section 3.4.2 above).

Interestingly, Shrivastava et al. (2017) found that the enantiopreference differences they saw between $LinA1_{B90A}$ and $LinA2_{B90A}$ were at least partly due to differences in residues at positions 20, 96, 131 and 133 in those proteins. When they mutated K20, L96, A131 and T133 of $LinA2_{B90A}$ to the Q20, C96, G131 and M133 found in $LinA1_{B90A}$, the enantiopreference of the mutant was reversed from (-)-α-HCH to (+)-α-HCH.

5.4.2 The β-PCCH to TCB transformation

The previous whole cell and purified enzyme assays of Suar et al. (2005) and Shrivastava et al. (2017, 2015) only reported the production of 1,2,4-TCB from the degradation of β-PCCH1 and β-PCCH2 by $LinA1_{B90A}$, $LinA2_{B90A}$ and $LinA_{LL02}$. My purified enzyme assays without added lysate

concur with these findings to the extent that I find 1,2,4-TCB to be the major TCB produced in all reactions. However, I also found traces of 1,2,3- and 1,3,5-TCB in the assays with two of the enzymes, $LinA2_{B90A}$ and $LinA_{LL02}$ assays. Suar et al. (2005) speculated that TCBs other than 1,2,4-TCB might have been produced but lost due to their high volatility in their assays, because their assays were done in open vials. Shrivastava et al. (2017, 2015) did not describe their assay conditions in sufficient detail for me to assess whether this could have also been the case in their work.

My purified enzyme assays with added cell lysate showed all three enzymes produced traces of 1,2,3- and 1,3,5-TCB. Given that they were not apparent in the corresponding minus lysate $LinA1_{B90A}$ assays, it is however possible that their appearance in the $LinA1_{B90A}$ assays with added lysate was due to some other activity in the added cell lysate. This possibility is discussed further below.

The k_{cat}/K_m estimates from the assays without added lysate are always higher for the transformations of the β-PCCHs to the favoured TCBs than are the corresponding transformations of the α-HCHs to the β-PCCHs. Unlike the estimates for the first reaction however, those for the second step show large enantiopreference differences. In particular, $LinA2_{B90A}$ strongly prefers to transform β-PCCH2 to 1,2,4-TCB whereas the other two enzymes each transform both β-PCCHs to 1,2,4-TCB with similar (much less than an order of magnitude difference) efficiencies.

Intriguingly, the k_{cat}/K_m estimates from the assays with added lysate were generally higher for the second step than they had been for this step in the assays without added lysate, although the estimates for the first step were essentially the same in the two forms of the assay. On its face, this suggests that some other factor(s) in the lysate was also contributing to the second step reaction, as was also suggested above from the appearance of the minor TCBs in the $LinA1_{B90A}$ assays with added lysate. On the other hand, the higher rates in the added lysate assays were generally positively correlated with the rates in the minus lysate assays across the three

enzymes and six different β-PCCH to TCB transformations (Figure 30). Such a correlation would not be expected if the lysate factor(s) was acting independently of the LinA enzyme. Rather it suggests that the factor(s) was in some way facilitating LinA in the second, but not the first, reaction. It would also suggest that the traces of 1,2,3- and 1,3,5-TCB seen in the minus lysate $LinA1_{B90A}$ assays above were due in part to the enzyme.

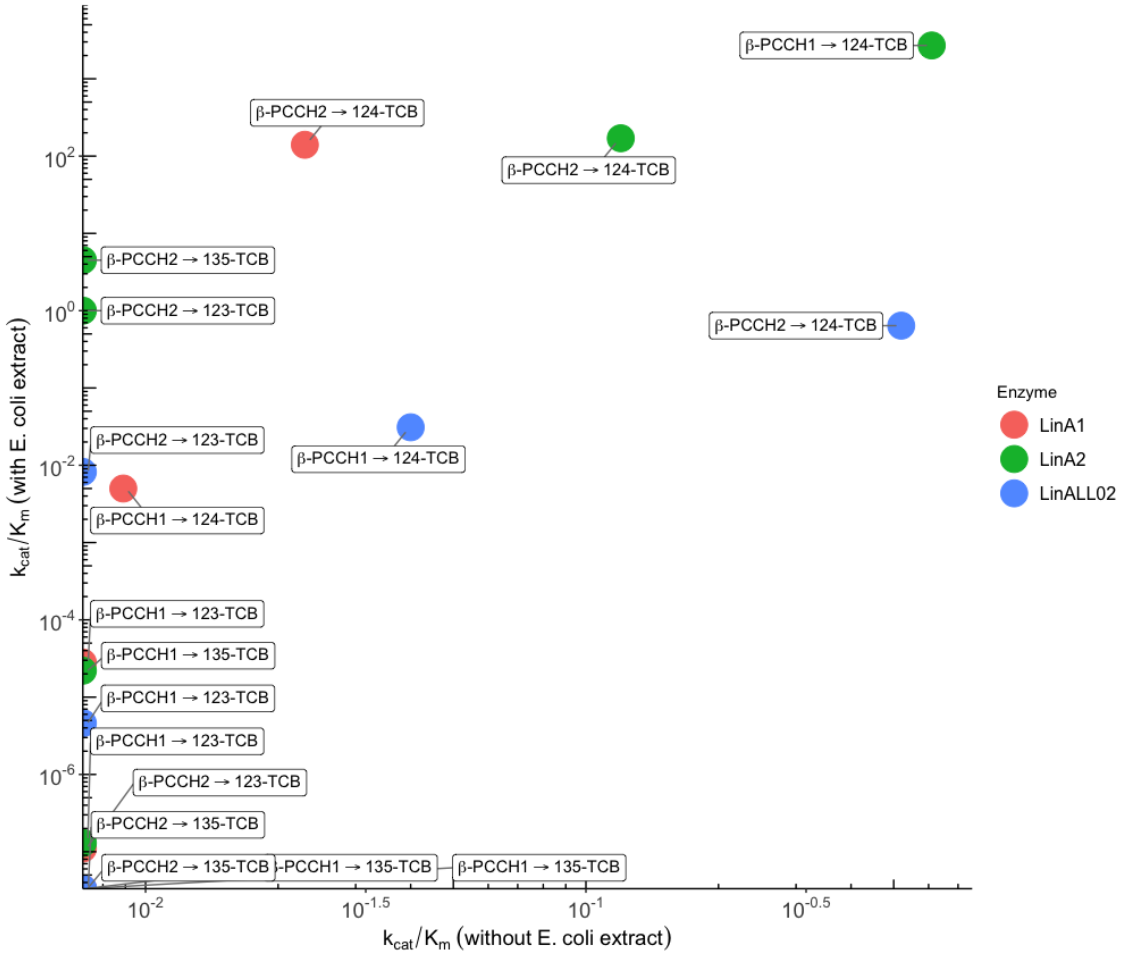

Figure 30 *Graph showing positive correlation of k_{cat}/K_m for β-PCCHs transformation into the different TCB isomers between purified LinA assays with and without cell lysate. Note that the data for activity reactions with E. coli extract are given as actual estimates in this figure rather than simply shown as $<10^{-3}$ as per previous tables. This is because the log_{10} scale used enables worthwhile separation of points in the range below 10^{-3} min^{-1} μM^{-1}.*

One important consideration for the interpretation of the β-PCCH to TCB transformations is that it is generally accepted to be a two-step process. This involves first a LinA catalysed transformation of the β-PCCHs to the corresponding TCDN isomers, followed by the spontaneous degradation of the TCDNs to TCBs (Lal et al., 2010; Nagasawa et al., 1993b, 1993a;

and see also Section 1.4.1.2). As noted in earlier chapters, the available evidence suggests that LinA generally transforms HCHs to PCCHs by removing a *trans*-diaxial H-Cl pair and it is assumed that the transformation of most PCCHs to TCDNs involves the same mechanism. In cases such as δ-PCCH and a hexachlorocyclohexene isomer which lack *trans*-diaxial H-Cl pairs, a *syn*-1,4-elimination reaction is believed to occur (Bala et al., 2012; Geueke et al., 2013). However, β-PCCH does not carry any H-Cl pair that allows for either of these reactions to happen (Figure 31).

I propose that LinA converts β-PCCH1 and β-PCCH2 to the corresponding TCDN isomers via an *anti*-1,4-elimination reaction. Each of these TCDN isomers could spontaneously transform into 1,2,4-TCB and either 1,2,3- or 1,3,5-TCB (Figure 31). Bickelhaupt (2001) proposed that an *anti*-1,4-elimination reaction could be induced by a strong base, such as OH^-. The catalytic dyad D25-H73 in the LinA active site could extract a hydrogen from the C3 of β-PCCH, resulting in the removal of chlorine from C6, or vice versa. This could explain my observation of 1,2,3- and 1,3,5-TCB in the α-HCH degradation assays by purified LinA, particularly in the case where cell lysate is added to more closely resemble the conditions of the whole cell assays. In fact, it could explain my observation that most of the β-PCCH to TCB transformations were facilitated by the presence of the cell lysates. Perhaps some strong base is present in the cell lysate that may have helped to facilitate the reaction. It is unclear what provides the strong base in the absence of added cell lysate, although some carry-over of cell contents could be expected in the purification of the enzymes. At the least, my proposition seems worthy of testing in future work to better understand the mechanisms of action of LinA on variously configured H-Cl pairs. Additionally, I note that some uncertainty in the interpretation of the TCDN to TCB transformation also arises in the case of the purified $LinA1_{B90A}$ assays, where 1,2,3- and 1,3,5-TCB were not observed in the assay without cell lysate, but were observed in the assay with cell lysate (see Section 5.3.2 and 5.3.3), although the various TCDN isomers that transform into 1,2,4-TCB can also transform into either 1,2,3- or 1,3,5-TCB (Figure 31). The various elimination mechanisms underpinning the PCCH to TCDN and TCDN to TCB transformations are discussed further in Chapter 7 below.

(A)

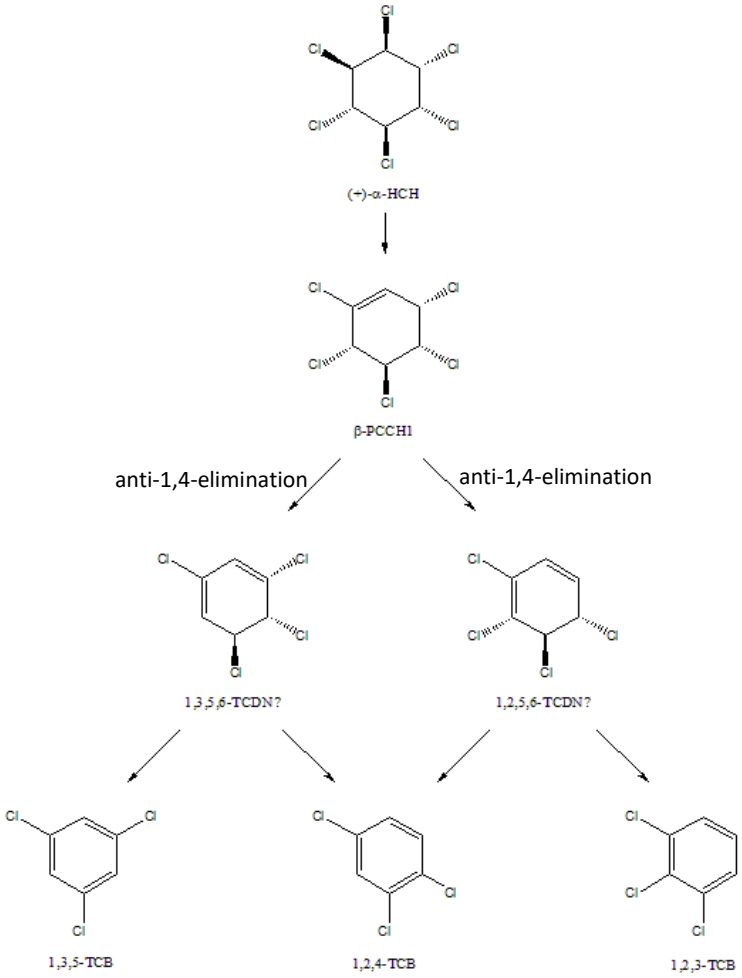
(+)-α-HCH
β-PCCH1
anti-1,4-elimination
anti-1,4-elimination
1,3,5,6-TCDN?
1,2,5,6-TCDN?
1,3,5-TCB
1,2,4-TCB
1,2,3-TCB

(B)

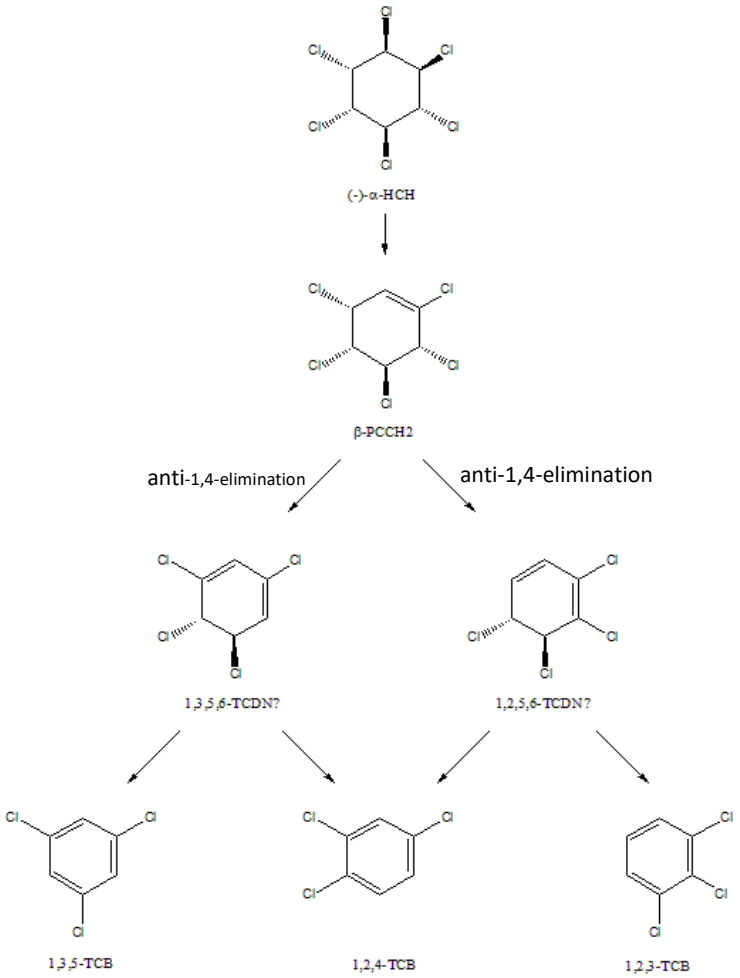

Figure 31 *Proposed degradation pathways for (A) (+)-α-HCH and (B) (-)-α-HCH. In the first step, axial H-Cl pair is removed from α-HCH molecules, resulting in their corresponding β-PCCH enantiomers. Then another H-Cl pair is removed from β-PCCH molecules by an anti-1,4-elimination step, resulting in their corresponding TCDN enantiomers. Finally, a spontaneous reaction removes another H-Cl pair from the TCDN molecules, resulting in 1,2,4-TCB and either 1,2,3- or 1,3,5-TCB. Note that each TCDN molecule can be transformed into two possible TCB isomers.*

CHAPTER 6:
Molecular dynamics

6.1 Introduction

Molecular dynamics (MD) simulations were performed on all three Lin enzymes with each of the eight HCH isomers and each of the six PCCH isomers discussed in this thesis. Each simulation was run for 100 ns, providing sufficient sampling to obtain statistically meaningful positional distributions for the ligands, along with various distance parameters for productive orientations of the ligands. The following sections outline the MD results for the δ-, γ-, and α-HCH and δ-, γ-, β-PCCH isomers and discuss productive poses, positional variability of the ligands within the active sites, and distances to catalytic residues (primarily H73) over the course of the trajectories. Also covered is the effect of different protonation states of H73.

Altogether, 48 MD simulations were performed for a total of 4.8 μs simulation time.

6.2 Methodology

PDB ID: 5KVB was used as the initial structure for $LinA_{LL02}$ and PDB ID: 3A76 was used for $LinA2_{B90A}$. The starting structure for $LinA1_{B90A}$ was constructed via homology model building using the Phyre2 server (Kelley et al., 2015) in 'intensive' mode. The crystallographic trimer was used in the cases of $LinA_{LL02}$ and $LinA2_{B90A}$ with the respective ligands being docked into just one of the monomers. The trimer of the $LinA1_{B90A}$ was constructed from the Phyre2 monomer model using $LinA_{LL02}$ as a template in Chimera (Pettersen et al., 2004). Overlapping atoms from symmetry artefacts (L7 in $LinA1_{B90A}$) were resolved by choosing alternative rotamers from the Dynameomics library (Scouras and Daggett, 2011) in Chimera. Ligands were constructed manually in Materials Studio 2017 (Dassault Systèmes BIOVIA, 2017) and subjected to geometry optimisation using density functional theory through the DMol3 module ('fine' default parameters, DNP basis set [equivalent to 6-31G**]) to obtain reasonable starting geometries.

Docking of the ligands was performed using Autodock Vina (Trott and Olson, 2010) through the Chimera python scripting interface, with the search space restricted to the vicinity of the known active site. The highest scoring pose in each case was used as the starting co-ordinates for MD simulations. The ligands were parameterised using the Antechamber module of AMBER18 (Case

et al., 2018) employing the GAFF2 forcefield and Mulliken charges. The enzymes were treated with the ff14SB forcefield. Each system was solvated in a truncated octahedral TIP3P periodic water box with a minimum analyte-to-boundary distance of 12 Å, and were charge neutralised with Na^+ ions (from frcmod.ionsjc_tip3p). Close contacts were relaxed with a minimisation routine (maximum 25,000 steps steepest descent, 25,000 steps conjugate gradient) while restraining protein backbone atoms. Production runs were then performed for 100 ns for each system at 298 K using the GPU-enabled pmemd.cuda code on CSIRO's Bracewell GPU cluster. A distance cut-off of 12 Å was employed and long range interactions were treated using the particle mesh Ewald method (Darden et al., 1993). Trajectories were centred and waters were removed prior to analysis using AMBER18's cpptraj module.

Trajectory analyses were performed using either VMD (Humphrey et al., 1996) or Chimera. Given the dynamic nature of the ligand orientation across all of the simulations, we chose a 4 Å H(ligand)…N(H73) (hereon referred to as the 'H…N' distance for brevity) cut-off distance criterion for whether the ligand was in a productive pose or not. Deeper analyses examining various distance minima are also discussed. The additional criterion of the H being part of a *trans*-diaxial pair is discussed separately in the Results and Discussion section below.

6.3 Results and Discussion

6.3.1 γ-HCH, γ-PCCH1 and γ-PCCH2

γ-HCH, γ-PCCH1, and γ-PCCH2 contain *trans* and diaxial H-Cl pairs (Manna and Dybala-Defratyka, 2013), making the displacement of H-Cl from these substrates predictable. As mentioned in Chapter 1, $LinA_{UT26}$ removes *trans*-diaxial H-Cl pairs from γ-HCH and γ-PCCHs via dehydrochlorination reactions (Nagasawa et al., 1993b). The N(H73) acts as a base and extracts the hydrogen from the *trans*-diaxial H-Cl pair, causing the removal of the *trans* chlorine atom from the adjacent carbon via an E2 mechanism (Brittain et al., 2011; Manna and Dybala-Defratyka, 2013). This removal of a *trans* and diaxial H-Cl pair has been shown to require a much lower activation energy than the removal of a *cis* and equatorial H-Cl pair (Cristol et al., 1951).

Figure 32 highlights the *trans*-diaxial H-Cl pairs on γ-HCH, γ-PCCH1, and γ-PCCH2 that can be removed by LinA. The removal of H-Cl pairs highlighted in blue and red from γ-HCH will result in the formation of γ-PCCH1 (1,3(*S*),4(*R*),5(*R*),6(*S*)-pentachlorocyclohex-1-ene) and γ-PCCH2 (1,3(*R*),4(*S*),5(*S*),6(*R*)-pentachlorocyclohex-1-ene), respectively. The removal of H-Cl pairs highlighted in magenta and aqua will result in the formation of 1,3,4,6-TCDN and 1,3,5,6-TCDN, respectively. 1,3,4,6-TCDN can later transform into 1,2,4-TCB, while 1,3,5,6-TCDN transforms into 1,2,3- and 1,3,5-TCB (Figure 8).

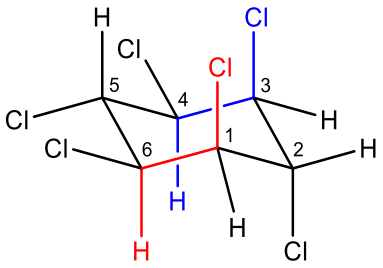

1(R),2(r),3(S),4(R),5(r),6(S)-1,2,3,4,5,6-hexachlorocyclohexane (γ-HCH)

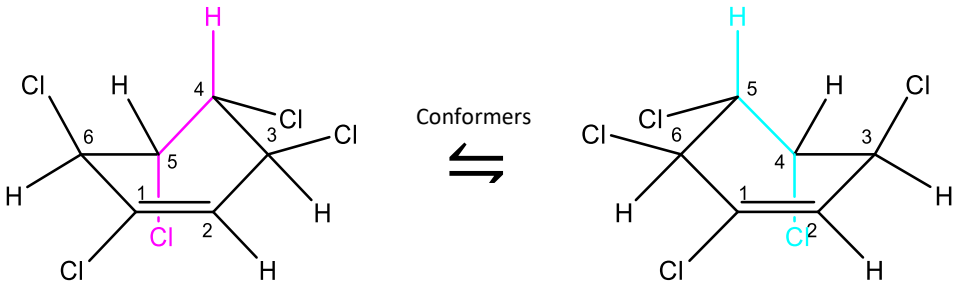

1,3(*S*),4(*R*),5(*R*),6(*S*)-pentachlorocyclohex-1-ene (γ-PCCH1)

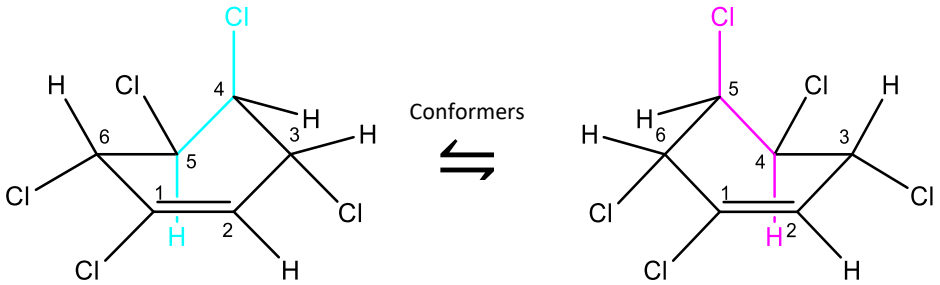

1,3(*R*),4(*S*),5(*S*),6(*R*)-pentachlorocyclohex-1-ene (γ-PCCH2)

Figure 32 *Trans-diaxial H-Cl pairs on γ-HCH, γ-PCCH1, and γ-PCCH2 that can be removed by LinA. Removal of blue and red H-Cl pairs from γ-HCH will result in the formation of γ-PCCH1 and γ-PCCH2, respectively. Removal of H-Cl pairs in magenta and aqua from either of the γ-PCCH enantiomers will result in the formation of 1,3,4,6-TCDN and 1,3,5,6-TCDN, respectively.*

As mentioned in Section 6.1, productive poses are considered to be those where the H…N distance between the ligand and H73 is equal to or closer than 4 Å. The H's highlighted in Figure 32 above are chosen as the leaving H due to their *trans*-diaxial position with Cl on the adjacent C. Table 10 shows the total percentage of time the substrates (γ-HCH, γ-PCCH1, and γ-PCCH2) were in productive poses in the active sites of $LinA1_{B90A}$, $LinA2_{B90A}$, and $LinA_{LL02}$ over the course of the 100 ns trajectories. Both HID and HIE protonation states for the catalytic histidine (protonation at δ- or ε- nitrogen, respectively) were considered in the MD simulations. Based on the values, HID appears to allow for a better positioning of the substrates in the active sites of the enzymes, with only γ-PCCH1 failing to be in a productive pose for the duration of the simulation in $LinA_{LL02}$. However, HIE of H73 in $LinA1_{B90A}$ and $LinA_{LL02}$ allows for better positioning of γ-PCCH1, while in $LinA2_{B90A}$ it allows for better positioning of γ-PCCH2 than HID. Furthermore, in this state, γ-PCCH2 was not able to position itself in a productive pose in $LinA1_{B90A}$ or $LinA_{LL02}$ for the duration of the simulation.

Table 10 *Total percentage* of time γ-HCH, γ-PCCH1, and γ-PCCH2 spent in productive poses in the active site of $LinA1_{B90A}$, $LinA2_{B90A}$, and $LinA_{LL02}$ for the duration of MD simulation (100 ns). HID and HIE refer to the nitrogen (δ- or ε-nitrogen, respectively) on H73 that is protonated.*

Enzyme	**HID**			**HIE**		
	γ-HCH	**γ-PCCH1**	**γ-PCCH2**	**γ-HCH**	**γ-PCCH1**	**γ-PCCH2**
$LinA1_{B90A}$	28.0%	1.0%	17.8%	26.0%	6.8%	0.0%
$LinA2_{B90A}$	48.8%	2.3%	1.3%	0.3%	0.8%	2.3%
$LinA_{LL02}$	43.5%	0.0%	1.3%	5.3%	9.5%	0.0%

*in cases where there are two possible leaving H atom, the numbers shown are the sum of two percentages of time the substrates spent in productive poses, one for each leaving H atom.

While it is tempting to hypothesise that the time spent in productive poses will be correlated with reaction efficiencies, a comparison between the specificity constants, k_{cat}/K_m (Table 2), and the percentage of time spent in productive poses (Table 10) does not support this hypothesis (Figure 33).This result suggests that the positioning of the substrates in the active site alone is not the definitive factor in predicting that a reaction will occur.

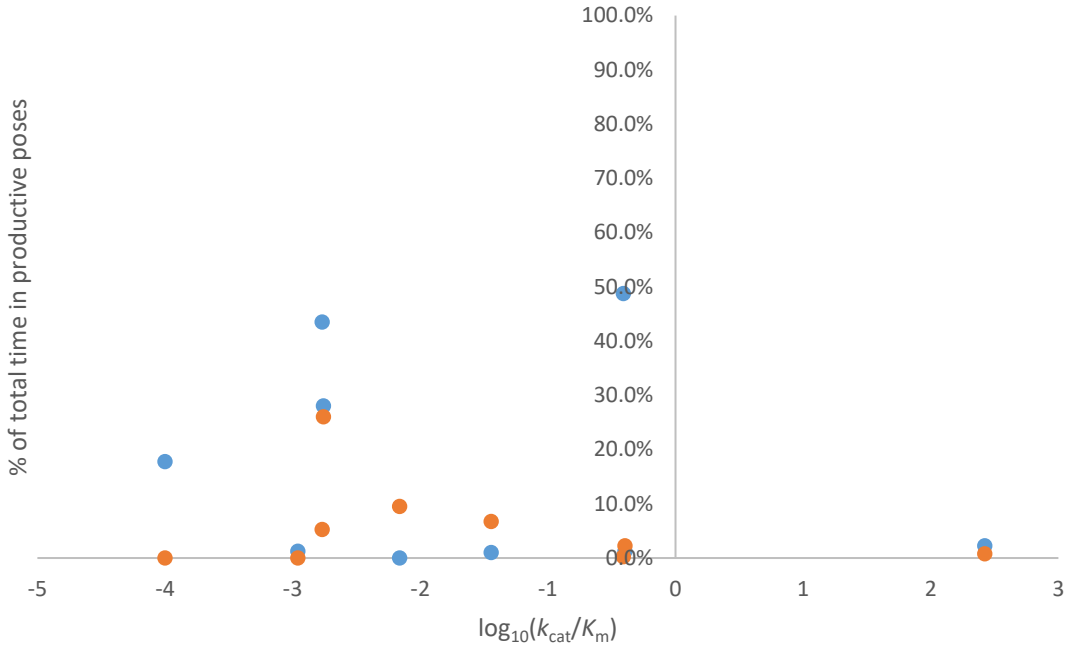

Figure 33 *Graph showing the lack of correlation between percentages of total time spent in productive poses and k_{cat}/K_m values for γ-HCH and γ-PCCHs transformations. Blue and orange dots correspond to the HID and HIE protonation state of H73, respectively. In cases where substrates can have two or more productive poses, individual percentages of time for each pose were calculated and summed to give the percentage of total time in productive poses.*

As a part of a catalytic dyad, H73 needs to be in proximity to D25 to allow for proton transfer. This process is important to transform H73 into an anion, which in turn will act as a base in the E2 reaction that takes place on the substrates. A similar reaction has been shown for scytalone dehydratase, whose D31 and H85 also act as a catalytic dyad similar to the function of D25 and H73 of LinA (Nagata et al., 2001). The mechanism by which the D25-H73 catalytic dyad works has been studied in detail by Brittain et al. (2011) using quantum chemical calculations. In that study, three possible mechanisms have been considered; (i) deprotonation of neutral H73 by D25 to form an anionic intermediate before abstracting a proton from the substrate, (ii) simultaneous deprotonation of H73 by D25 and abstraction of a proton from the substrate, and (iii) abstraction of a proton from the substrate by H73, forming a cationic intermediate, before transfer of a proton to D25 (Figure 34). Energy calculations favour mechanism (i), which was 20 kJ mol^{-1} lower in activation energy than (ii) and (iii).

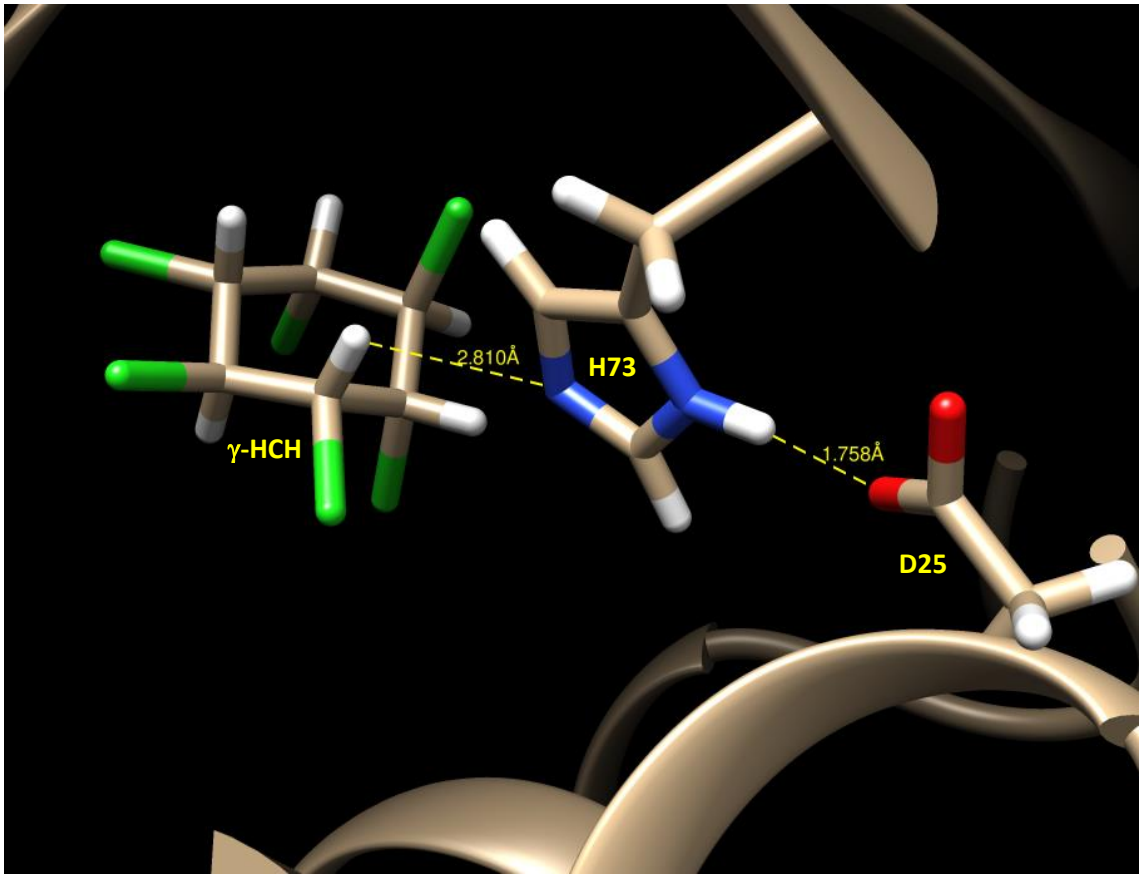

Figure 34 *The above figure models the active site of LinA1$_{B90A}$ when interacting with γ-HCH. H73, D25, and γ-HCH are as labelled. In this particular position, the distance between the (O)D25 and (H)H73 is 1.758 Å, and between N(H73) and trans-diaxial H(HCH) is 2.810 Å. This position was taken from a representative frame from the MD trajectories.*

In addition to the time spent in productive poses by the substrates, the mechanism by which LinA works may be another important piece of information to consider when predicting if a reaction would occur. Assuming that H73 needs to be deprotonated by D25 before abstracting a proton from the substrate (following Brittain et al., 2011), D25 needs to be in the proximity of H73 to allow for the transfer at least immediately preceding, if not during, the productive pose of the substrate. In this case, a minimum distance between D25 and H73, and the time when this occurs, need to be considered.

Another docking study using LinA$_{UT26}$ has been performed previously to study the LinA elimination mechanism (Manna and Dybala-Defratyka, 2013). That study predicted the best model of docked HCH isomers in the LinA$_{UT26}$ active site based on the lowest energy calculation. It also took into consideration the distances between the chlorine of the *trans*-diaxial H-Cl pair

and W42, and between the chlorine and R129, based on the proposition that these residues might be important in the enzyme mechanism (Manna and Dybala-Defratyka, 2013; Nagata et al., 2001). The study found that the best docked position for γ-HCH in $LinA_{UT26}$ has the distances of 2.12 Å, 3.95 Å, and 6.01 Å between H…N(H73), Cl…H(W42), and Cl…H(R129), respectively (Manna and Dybala-Defratyka, 2013).

While both Manna and Dybala-Defratyka (2013) and my studies look at H…N distances between the substrates and H73 to understand the LinA mechanism, our approaches are quite different (MD vs static docking). MD allows the substrates and the enzymes to move freely for the duration of the trajectories (100 ns), allowing the calculation of the percentage of time the substrates spent in productive poses. On the other hand, the study by Manna and Dybala-Defratyka (2013) looked at the best substrate positions in $LinA_{UT26}$ active site based on single docked poses, which resulted in only one H…N distance for each substrate. Another difference is while I considered both HID and HIE protonation states for H73 in my study, it was not mentioned in Manna and Dybala-Defratyka (2013) study, although they used the best protonation state for $LinA_{UT26}$ predicted by PROPKA 3.1 (Olsson et al., 2011). Nevertheless, we observed that γ-HCH spends less than 48.8% and 0.3% of time being in a productive pose in the active site of HID and HIE protonated H73 $LinA2_{B90A}$, respectively, regardless of the protonation state for H73 used by Manna and Dybala-Defratyka (2013) (Table 10).

6.3.2 δ-HCH, δ-PCCH1 and δ-PCCH2

As mentioned in Chapter 1, there is some ambiguity around which H-Cl pairs are viable for elimination by the LinA enzymes. It was initially proposed (Nagasawa et al., 1993b) that only *trans* and diaxial pairs were able to be displaced from HCH and PCCH to produce PCCH and TCDN, respectively. However there is empirical evidence from two studies by Bala et al. (2012) and Geueke et al. (2013), that cross-ring *syn*-oriented pairs can also be viable leaving groups.

In one of these studies, Geueke et al. (2013) observed δ-PCCH enantiomers and subsequently 1,2,3- and 1,2,4-TCB being produced from δ-HCH dehydrochlorination by $LinA1_{B90A}$ and $LinA2_{B90A}$.

Given the absence of a *trans* and diaxial H-Cl pair on either of the δ-PCCH enantiomers, and notwithstanding that the TCDN intermediate has never been observed, they suggested that the catalytic dyad D25-H73 of LinA is able to mediate a *syn*-1,4-elimination by abstracting a proton and subsequently the removal of chlorine from the opposite side of the ring (Geueke et al., 2013).

Bala et al. (2012) also postulated a *syn*-1,4-elimination of an H-Cl pair to explain the TCB products they observed during the degradation of a 1,2,3(*S*),4(*R*),5(*R*),6(*S*)-hexachlorocyclohexene isomer by $LinA1_{B90A}$ and $LinA2_{B90A}$, albeit, as per Geueke et al. (2013), the presumptive pentachlorocyclohexadiene intermediate was not actually observed.

Figure 35 highlights the various H-Cl pairs on δ-HCH, δ-PCCH1 and δ-PCCH2 that can be eliminated by LinA. Removal of the *trans*-diaxial H-Cl pairs highlighted in red and blue on δ-HCH results in the formation of δ-PCCH1 (1,3(*S*),4(*R*),5(*S*),6(*R*)-pentachlorocyclohex-1-ene) and δ-PCCH2 (1,3(*R*),4(*S*),5(*R*),6(*S*)-pentachlorocyclohex-1-ene), respectively. Removal of the cross-ring *syn*-oriented H-Cl pairs highlighted in green and blue on δ-PCCH1 and δ-PCCH2 would then result in the formation of 1,2,5,6- and 1,3,5,6-TCDN, respectively. While both TCDN isomers can transform into 1,2,4-TCB, in contrast to what is observed in the case for the γ-PCCHs (Figure 8), apparently only 1,2,5,6-TCDN transforms into 1,2,3-TCB and 1,3,5,6-TCDN into 1,3,5-TCB (Figure 9).

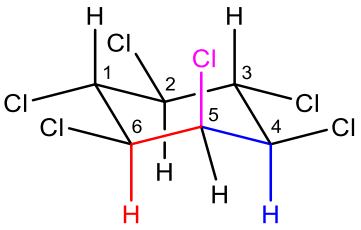

1(*R*),2(*r*),3(*S*),4(*R*),5(*s*),6(*S*)-hexachlorocyclohexane (δ-HCH)

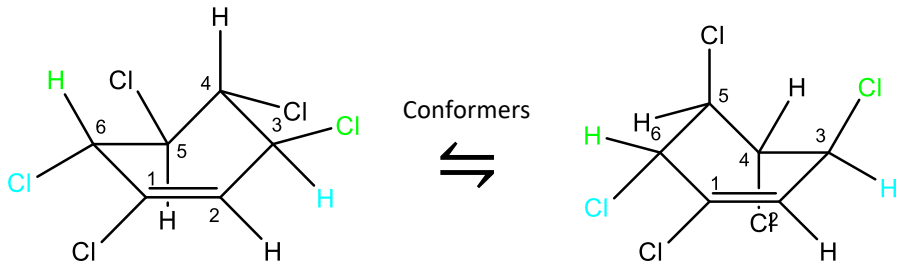

1,3(*S*),4(*R*),5(*S*),6(*R*)-pentachlorocyclohex-1-ene (δ-PCCH1)

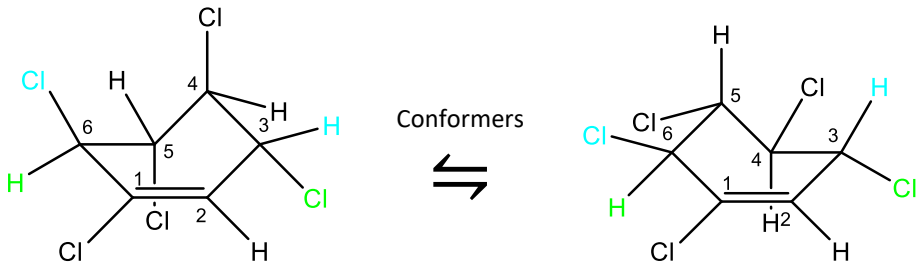

1,3(*R*),4(*S*),5(*R*),6(*S*)-pentachlorocyclohex-1-ene (δ-PCCH2)

Figure 35 *Trans-diaxial H-Cl pairs on δ-HCH and cross-ring syn-oriented H-Cl pairs on δ-PCCH1 and δ-PCCH2 that are proposed to be removed by LinA. Both the red and blue hydrogens on δ-HCH can be paired with the chlorine highlighted in magenta. Removal of blue and red hydrogen (and the magenta chlorine) from δ-HCH will result in the formation of δ-PCCH1 and δ-PCCH2, respectively. Removal of H-Cl pairs in green and aqua from either of the δ-PCCH enantiomers will result in the formation of 1,2,5,6- and 1,3,5,6-TCDN, respectively.*

The *syn*-1,4-elimination suggested by Bala et al. (2012) and Geueke et al. (2013) was also supported by a previous study that investigated 1,2- and 1,4-elimination from 3-chlorocyclohexene (Gronert and Kass, 1997). This *ab initio* study investigated the likelihood of a 1,2- or 1,4-elimination reaction happening if 3-chlorocyclohexene was treated with a base. They found that 3-chlorocyclohexene is more likely to undergo a 1,4-elimination than a 1,2-elimination when it is treated with a base. They also found a slight preference towards *anti*-1,4-

elimination than *syn*-1,4-elimination; however, the opposite preference is shown when the leaving Cl is in equatorial position. A review by Bickelhaupt (2001) also shows that 1,4-elimination is highly favoured when the molecule is treated by a strong base, such as NH_2^- or OH^-. This finding is applicable to our present study, where the anionic N(H73) acts as a base that mediates LinA dehydrochlorination reaction.

The studies by Gronert and Kass (1997) and Bickelhaupt (2001) fit nicely with our study on δ-PCCH and LinA. In addition to N(H73) acting as a base that mediates LinA dehydrochlorination reaction, which is comparable to the study by Bickelhaupt (2001), both possible leaving Cl atoms on each δ-PCCH1 and δ-PCCH2 are in equatorial positions and *anti*- to each other. These *anti*- and equatorial Cl atoms allow for the leaving H atoms to be in a *syn*- position to the leaving Cl atoms (Figure 36), hence allowing for a *syn*-1,4-elimination to occur, perfectly following the preference discussed by Gronert and Kass (1997).

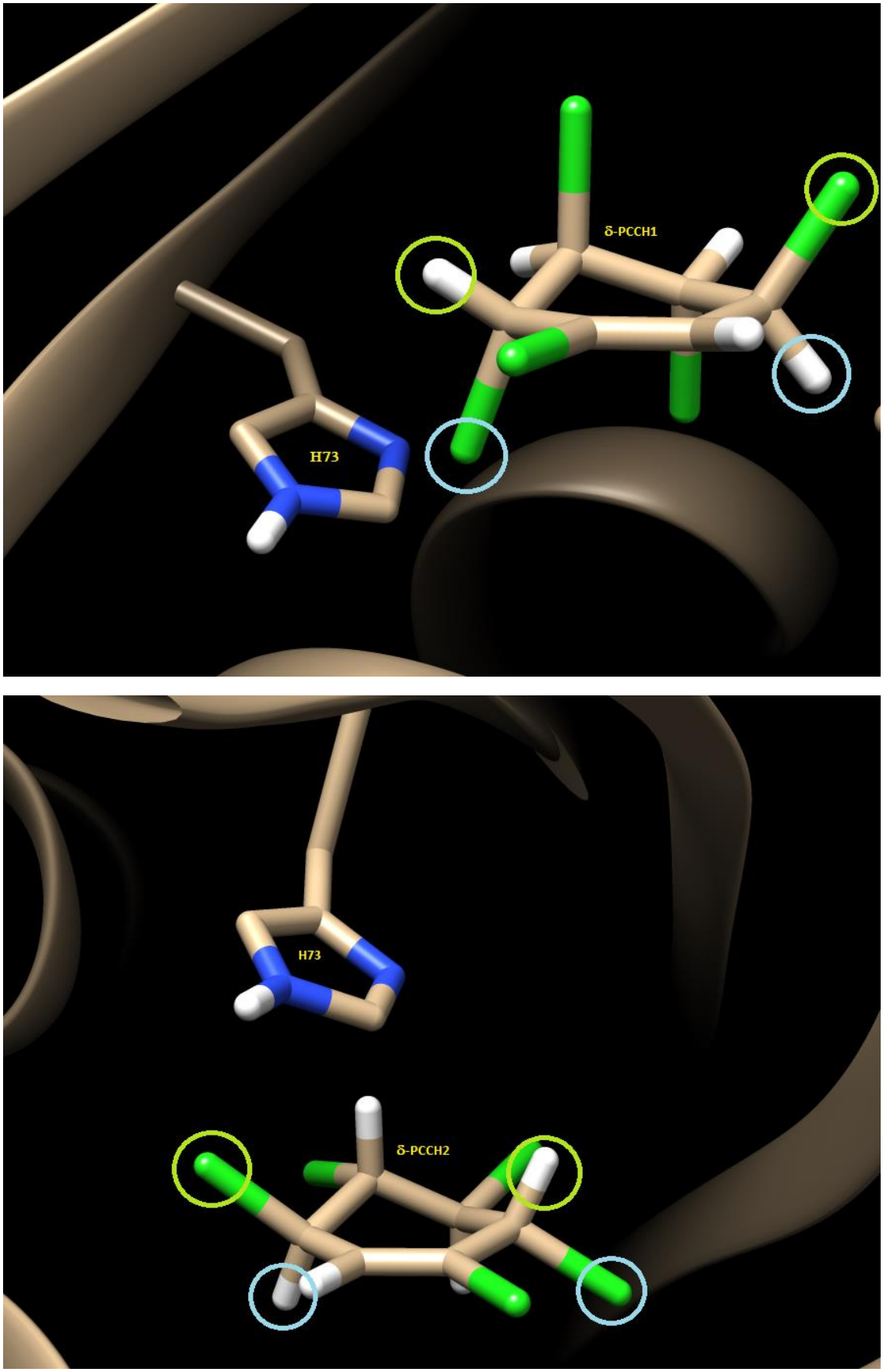

Figure 36 *Figures model δ-PCCH1 (top) and δ-PCCH2 (bottom) in LinA1$_{B90A}$ (HIE) active site taken from representative frames from the MD trajectories. Note that both possible leaving Cl are equatorial and anti- to each other, allowing for a syn-1,4,-elimination to occur. Removal of H-Cl pairs indicated by green or aqua rings from either of the δ-PCCH enantiomers will result in the formation of 1,2,5,6- and 1,3,5,6-TCDN, respectively.*

The H…N distances between δ-HCH, δ-PCCH1, and δ-PCCH2 and H73 for the duration of the MD trajectories were analysed. The highlighted H atoms in Figure 35 above were selected as the leaving H's due to their positions on the molecules (part of a *trans*-diaxial H-Cl pair or cross-ring to a leaving Cl atom). Table 11 shows the total percentage of time these substrates were in productive poses in LinA1$_{B90A}$, LinA2$_{B90A}$, and LinA$_{LL02}$. Similar to the result for γ- isomers, the percentage of time these substrates spent in productive poses in the active sites of the enzymes seems not to be associated with catalytic efficiency. Thus the specificity constants (k_{cat}/K_m) for the reactions (Table 3) show no correlation with the percentage of time the substrates are in productive poses (Table 11) (Figure 37).

Table 11 *Total percentages* of time δ-HCH, δ-PCCH1, and δ-PCCH2 spent in productive poses in the active site of LinA1$_{B90A}$, LinA2$_{B90A}$, and LinA$_{LL02}$ for the duration of MD simulation (100 ns). HID and HIE refer to the nitrogen (δ- or ε-nitrogen, respectively) on H73 that is protonated.*

Enzyme	**HID**			**HIE**		
	δ-HCH	**δ-PCCH1**	**δ-PCCH2**	**δ-HCH**	**δ-PCCH1**	**δ-PCCH2**
LinA1$_{B90A}$	N/A	41.5%	32.8%	0.0%	18.5%	20.8%
LinA2$_{B90A}$	0.0%	12.8%	10.8%	0.0%	9.5%	0.0%
LinA$_{LL02}$	161.8%	48.5%	63.3%	42.8%	20.8%	64.5%

*numbers shown are the sum of two percentages of time the substrates spent in productive poses, one for each leaving H atom.

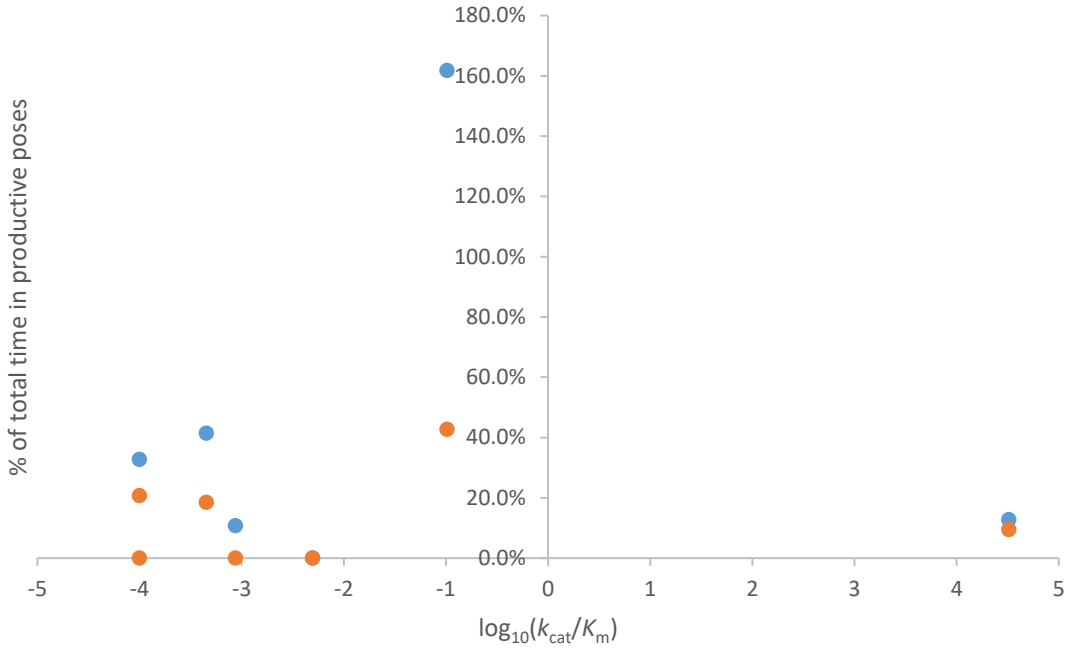

Figure 37 *Graph showing the lack of correlation between percentages of total time spent in productive poses and k_{cat}/K_m values for δ-HCH and δ-PCCHs transformations. Blue and orange dots correspond to the HID and HIE protonation states of H73, respectively. In cases where substrates can have two or more productive poses, individual percentages of time for each pose was calculated and added to give the percentage of total time in productive poses.*

Based on the values from Table 11, it is obvious that, overall, HID of H73 in $LinA1_{B90A}$, $LinA2_{B90A}$ and $LinA_{LL02}$ allows for better positioning of the substrates in the active sites. All but δ-HCH in $LinA1_{B90A}$ and $LinA2_{B90A}$, and δ-PCCH2 in $LinA_{LL02}$ spent more time being in productive poses in the active sites with HID protonated H73 than HIE. However, HID of H73 does not improve the positioning of δ-HCH in the active sites of $LinA1_{B90}$ and $LinA2_{B90A}$ when compared to HIE of H73. In fact, HID of H73 decreases the time spent in productive pose for δ-PCCH2 in $LinA_{LL02}$, although by only 1.2%. This observation on HID being the overall better protonation state of H73 than HIE for the correct positioning of δ- isomers (except for some substrates in certain enzymes as mentioned earlier) is consistent with our observations for the γ- isomers (Table 10).

However, while it is clear that we cannot predict the catalytic efficiency solely based on the H…N distance between the substrate and H73 (Figure 37), the fact that δ-HCH failed to position itself in a productive pose in $LinA1_{B90A}$ and $LinA2_{B90A}$ for the duration of the MD trajectories regardless of the protonation state of H73 (Table 11) might explain the large difference in activities on δ-

HCH between these enzymes and $LinA_{LL02}$. As discussed in Chapters 1 and 4, the larger I44 and L64 in $LinA1_{B90A}$ and $LinA2_{B90A}$ compared to V44 and V64 in $LinA_{LL02}$ may be interfering with the correct positioning of δ-HCH in the active sites. A closer look into the enzymes' active sites during the MD trajectories highlights these interferences, with δ-HCH seemingly unable to position itself to allow any H's of the two *trans*-diaxial H-Cl pairs to project towards H73 in $LinA1_{B90A}$ and $LinA2_{B90A}$, regardless of the protonated state of H73. In contrast, δ-HCH in the $LinA_{LL02}$ active site positions itself with both H's from the two available *trans*-diaxial H-Cl pairs facing N(H73) (regardless of HID or HIE protonation states) allowing more optimal H…N distances (Figure 38). However, from this current study, it is unclear if the ineffective positioning of δ-HCH in $LinA1_{B90A}$ and $LinA2_{B90A}$ active sites is due to the more restrictive size of the active sites due to the larger I44 and L64 residues. A more detailed study that looks into the residues along the path which the substrates take to get into the active site would be needed to investigate this issue further. Discussions on future works are mentioned in Chapter 7.

(A)

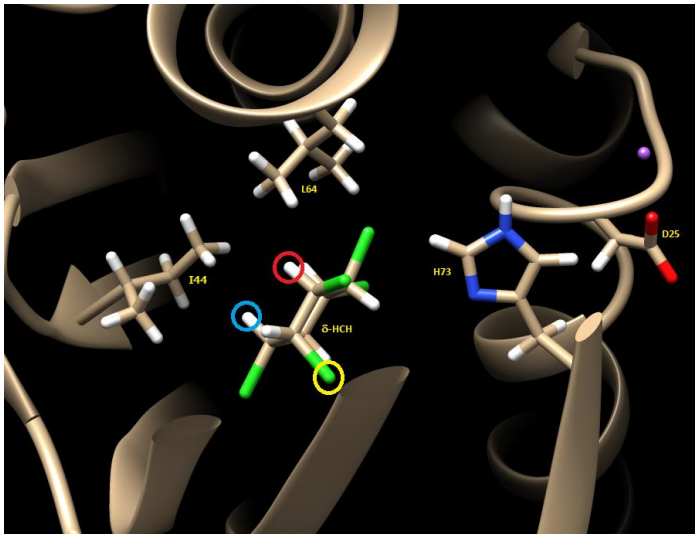

(B)

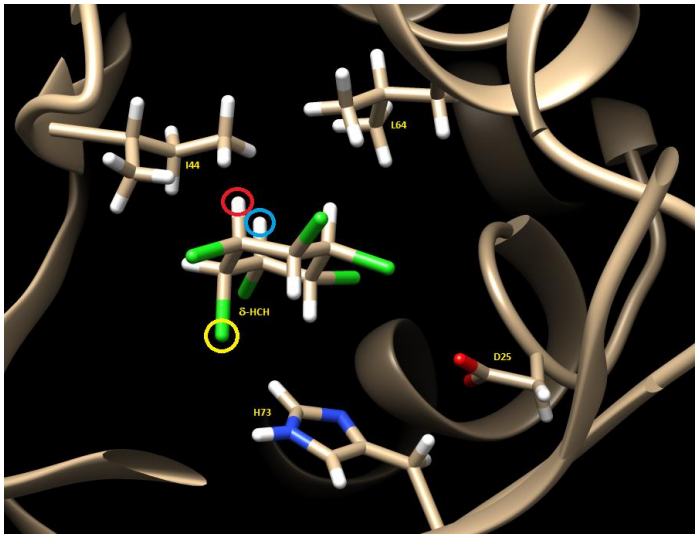

(C)

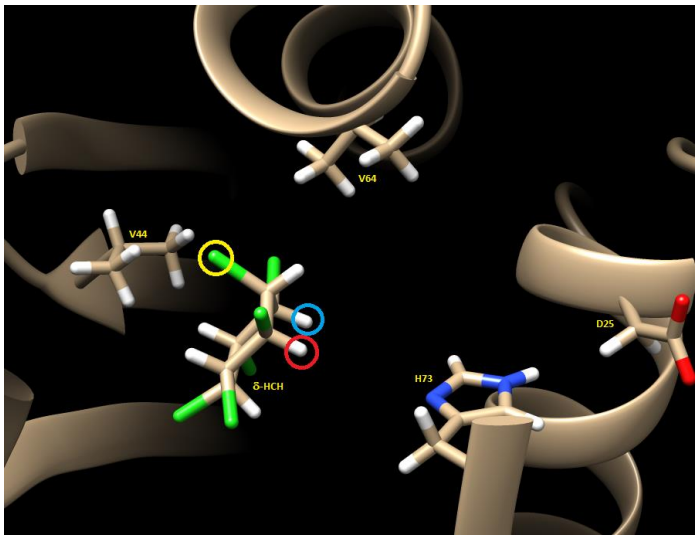

Figure 38 *The figures above model the positioning of δ-HCH in HIE of (A) LinA1$_{B90A}$, (B) LinA2$_{B90A}$ and (C) LinA$_{LL02}$. The possible leaving trans-diaxial H-Cl pairs are circled. Both hydrogens (circled in blue and red) can be paired with the chlorine (circled in yellow). Removals of the hydrogen circled in blue and red will result in δ-PCCH1 and δ-PCCH2, respectively.*

6.3.3 (+)-α-HCH, (-)-α-HCH, β-PCCH1 and β-PCCH2

Similar to γ- and δ-HCH, α-HCH1 and α-HCH2 also have two *trans*-diaxial H-Cl pairs that can be removed via dehydrochlorination by LinA. However, while the removal of either of the H-Cl pairs on γ- and δ-HCH results in one PCCH enantiomer, the removal of either of the *trans*-diaxial H-Cl pairs from both α-HCH isomers results in only one β-PCCH enantiomer. This is due to the structure of α-HCH itself, which remains the same when flipped horizontally at 180°, causing both *trans*-diaxial H-Cl pairs on each α-HCH molecule to be similar to one another (Figure 39). Hence, the removal of either *trans*-diaxial H-Cl pairs on α-HCH1 and α-HCH2 (blue and red H-Cl pairs) will result in 1,3(*S*),4(*S*),5(*R*),6(*S*)-pentachlorocyclohex-1-ene (β-PCCH1) and 1,3(*R*),4(*R*),5(*S*),6(*R*)-pentachlorocyclohex-1-ene (β-PCCH2), respectively (Figure 39).

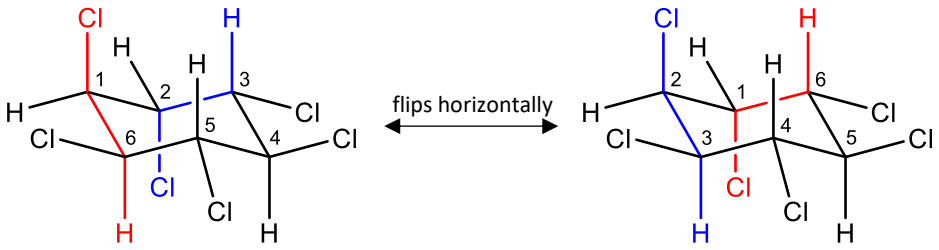

1(*R*),2(*R*),3(*S*),4(*S*),5(*S*),6(*S*)-hexachlorocyclohexane ((+)-α-HCH or α-HCH1)

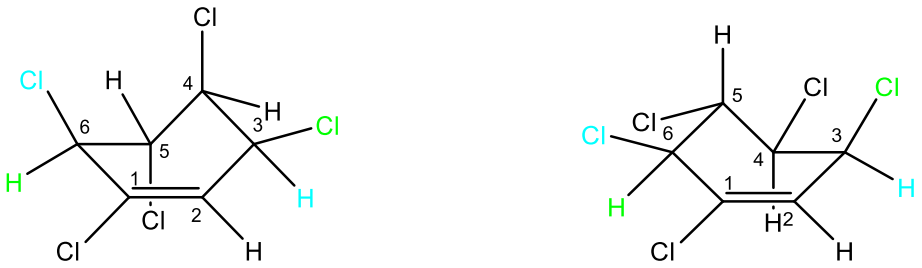

1,3(*S*),4(*S*),5(*R*),6(*S*)-pentachlorocyclohex-1-ene (β-PCCH1)

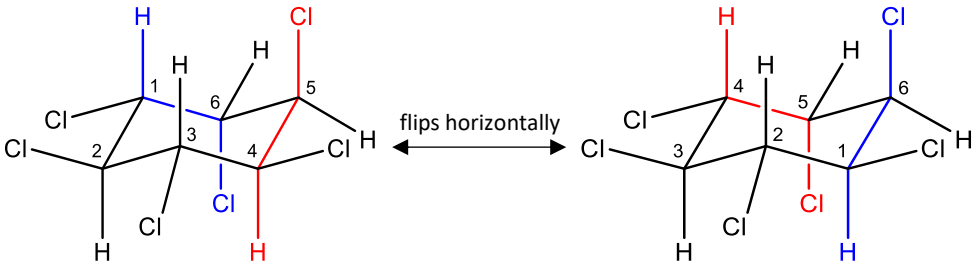

1(*R*),2(*R*),3(*R*),4(*R*),5(*S*),6(*S*)-hexachlorocyclohexane ((-)-α-HCH or α-HCH2)

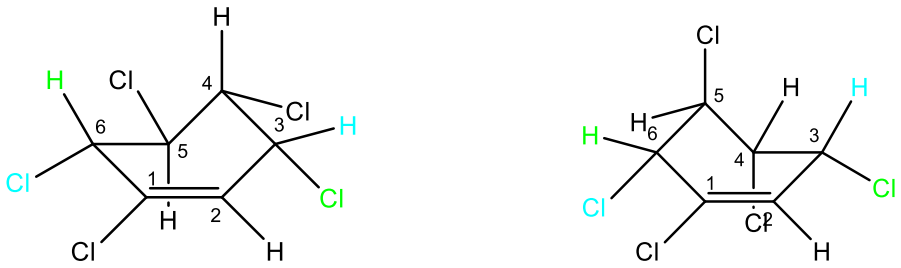

1,3(*R*),4(*R*),5(*S*),6(*R*)-pentachlorocyclohex-1-ene (β-PCCH2)

Figure 39 *The figure above highlights the trans-diaxial H-Cl pairs on α-HCH1 and α-HCH2, and anti-cross-ring H-Cl pairs on β-PCCH1 and β-PCCH2 that are the possible leaving groups in LinA dehydrochlorination reaction. The removal of trans-diaxial blue and red H-Cl pairs from α-HCH1 results in the formation of β-PCCH1, while the removal of the pairs from α-HCH2 results in β-PCCH2. The removal of green and blue cross-ring H-Cl pairs from either β-PCCHs results in the formation of 1,2,5,6-TCDN and 1,3,5,6-TCDN, respectively.*

Nonetheless, unlike γ-PCCH1 and γ-PCCH2, but similar to δ-PCCH1 and δ-PCCH2, β-PCCH1 and β-PCCH2 do not have any *trans*-diaxial H-Cl pairs that would otherwise be a perfect leaving group for a LinA dehydrochlorination reaction. To the best of my knowledge, no previous studies have investigated the mechanism by which LinA removes an H-Cl pair from β-PCCH1 and β-PCCH2. Here, I propose that $LinA1_{B90A}$, $LinA2_{B90A}$ and $LinA_{LL02}$ remove H-Cl pairs from β-PCCH1 and β-PCCH2 via an anti-1,4-elimination.

As discussed in Section 6.3.2, Gronert and Kass (1997) found that 3-chlorocyclohexene is more likely to undergo a 1,4-elimination than 1,2-elimination when treated with a base. They also found that a *syn*-1,4-elimination is slightly preferred than an *anti*-1,4-elimination when the leaving Cl is in equatorial position; otherwise the opposite preference applies. Additionally, Bickelhaupt (2001) found that a 1,4-elimination is much preferred when the molecule is treated with a strong base such as NH_2^-.

Since N(H73) acts as a base that mediates the E2 reaction in LinA, and both possible leaving Cl's on both β-PCCH1 and β-PCCH2 are in equatorial positions, a *syn*-1,4-elimination is expected (Figure 40). However, both the equatorial Cl's on each β-PCCH enantiomer are *syn* to each other, making a *syn*-1,4-elimination impossible and an *anti*-1,4-elimination more desirable. Given that the preference towards a *syn*-1,4-elimination is only marginal when the leaving Cl is in equatorial position, an *anti*-1,4-elimination is not an impossible route. In this case, we would expect β-PCCH1 and β-PCCH2 to undergo an *anti*-1,4-elimination when reacting with N(H73) of $LinA1_{B90A}$, $LinA2_{B90A}$ and $LinA_{LL02}$. Removal of the cross-ring *anti*-oriented H-Cl pairs highlighted in green and blue on β-PCCH1 and β-PCCH2 would then result in the formation of 1,2,5,6- and 1,3,5,6-TCDN, respectively. Similar to δ- isomers, both TCDN isomers that resulted from β-PCCH1 and β-PCCH2 degradation can transform into 1,2,4-TCB, but only 1,2,5,6-TCDN transforms into 1,2,3-TCB and only 1,3,5,6-TCDN transforms into 1,3,5-TCB.

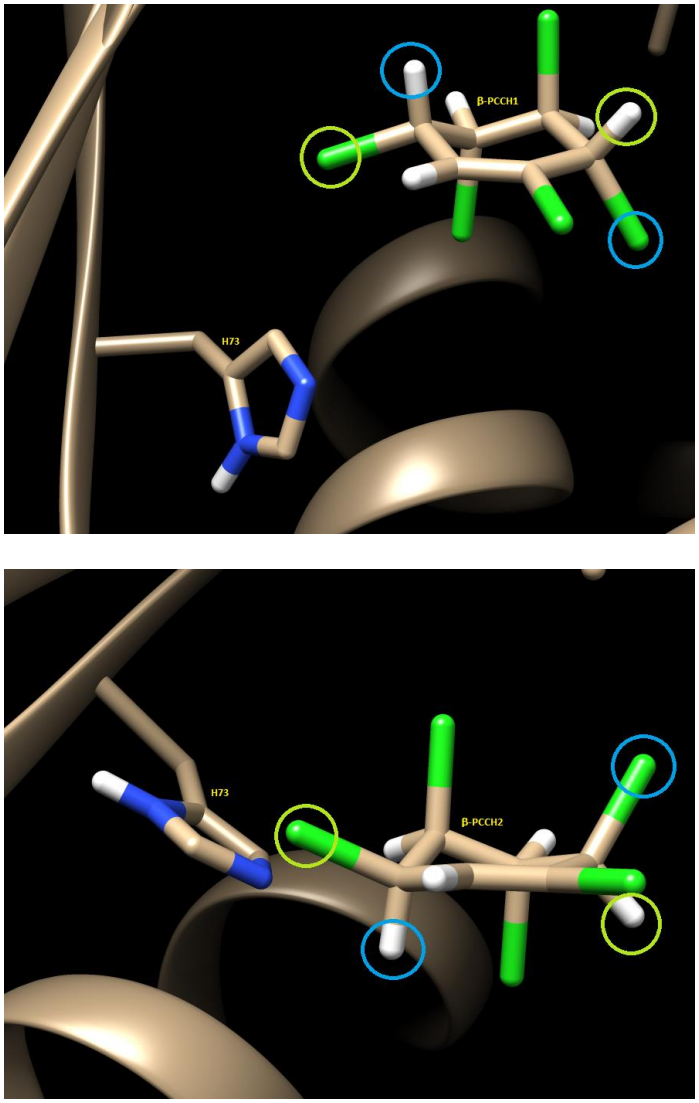

Figure 40 *Figures model β-PCCH1 (top) and β-PCCH2 (bottom) in LinA1$_{B90A}$ (HID) active site taken from representative frames from the MD trajectories. Note that both possible leaving Cl are equatorial and syn- to each other, allowing for a anti-1,4,-elimination to occur. Removal of H-Cl pairs indicated by green and blue rings from either of the δ-PCCH enantiomers will result in the formation of 1,2,5,6- and 1,3,5,6-TCDN, respectively.*

The H…N distances between α-HCH1, α-HCH2, β-PCCH1 and β-PCCH2, and LinA1$_{B90A}$, LinA2$_{B90A}$ and LinA$_{LL02}$ were analysed. Table 12 lists the percentage of time the substrates spent in productive poses in each enzyme. As with the studies on γ- and δ- isomers in Section 6.3.1 and 6.3.2, the HID and HIE protonation state of H73 of the enzymes were considered. Interestingly, based on the percentages, the overall better protonation state for substrates' positioning in the enzymes is not as clear as for the γ- and δ- isomers. While HID of H73 of all three enzymes is overall a better accommodator for most γ- and δ- isomers in all three enzymes, the same cannot be said for α-HCHs and β-PCCHs. Instead, HIE of H73 of LinA1$_{B90A}$ is observed to be better at

allowing α-HCH1, α-HCH2 and β-PCCH2 to be in productive poses, but HID is preferred for β-PCCH1 positioning. HID of H73 of $LinA2_{B90A}$ on the other hand is preferred for the correct positioning of α-HCH2, β-PCCH1 and β-PCCH2, but HIE is preferred for α-HCH1 positioning. $LinA_{LL02}$ is the only enzyme that prefer one protonation state (HIE) for the correct positioning of α-HCH1, α-HCH2, β-PCCH1 and β-PCCH2.

Table 12 *Percentages of time α-HCH1, α-HCH2, β-PCCH1 and β-PCCH2 spent in productive poses in $LinA1_{B90A}$, $LinA2_{B90A}$ and $LinA_{LL02}$ for the duration of MD trajectories (100 ns). HID and HIE refer to the nitrogen (δ- or ε- nitrogen, respectively) on H73 that is protonated.*

Enzyme	HID				HIE			
	α-HCH1	α-HCH2	β-PCCH1	β-PCCH2	α-HCH1	α-HCH2	β-PCCH1	β-PCCH2
$LinA1_{B90A}$	32.5%	19.3%	0.5%	46.8%	82.8%	45.3%	3.0%	26.0%
$LinA2_{B90A}$	0.3%	4.8%	2.5%	5.0%	5.8%	0.3%	0.0%	0.3%
$LinA_{LL02}$	66.3%	62.8%	3.3%	27.0%	78.5%	88.8%	29.5%	56.8%

Interestingly, while we have established that the percentage of time substrates spent in productive poses in the active sites is not directly correlated to the k_{cat}/K_m of the enzymes (Figure 41), the percentages in Table 12 reflect the enantiopreference that we observed for $LinA1_{B90A}$, $LinA2_{B90A}$ and $LinA_{LL02}$ on α-HCH1, α-HCH2, β-PCCH1 and β-PCCH2 (Figure 28 and Table 8), if we only consider the HID form of H73, following the preferred protonation state observed for γ- and δ- isomers as discussed in Section 6.3.1 and 6.3.2. Based on our discussion in Chapter 5, we learned that $LinA1_{B90A}$ and $LinA2_{B90A}$ prefer to degrade α-HCH1 and α-HCH2 respectively, while $LinA_{LL02}$ shows a very slight preference towards α-HCH1. All three enzymes also prefer to degrade β-PCCH2 than β-PCCH1 albeit to different degrees (Table 8). These observations fit nicely with the percentages for HID (Table 12), with all three enzymes showing a higher percentage for β-PCCH2 than β-PCCH1, $LinA1_{B90A}$ showing a much higher percentage for α-HCH1 than α-HCH2, $LinA2_{B90A}$ showing a higher percentage for α-HCH2 than α-HCH1, and $LinA_{LL02}$ showing a slightly higher percentage for α-HCH1 than α-HCH2. However, when we compare the percentages (HID) for γ- and δ- isomers (Table 10 and Table 11) with the enzymes' enantiopreference in Section 2.4.2 and 3.4.2, no apparent correlation is found. Perhaps, as with the lack of correlation between the times spent in productive poses with the occurrence of

activity, there are other aspects that may contribute to the enzymes' enantiopreference, such as the distance between (O)D25 and (H)H73 as discussed in Section 6.3.1.

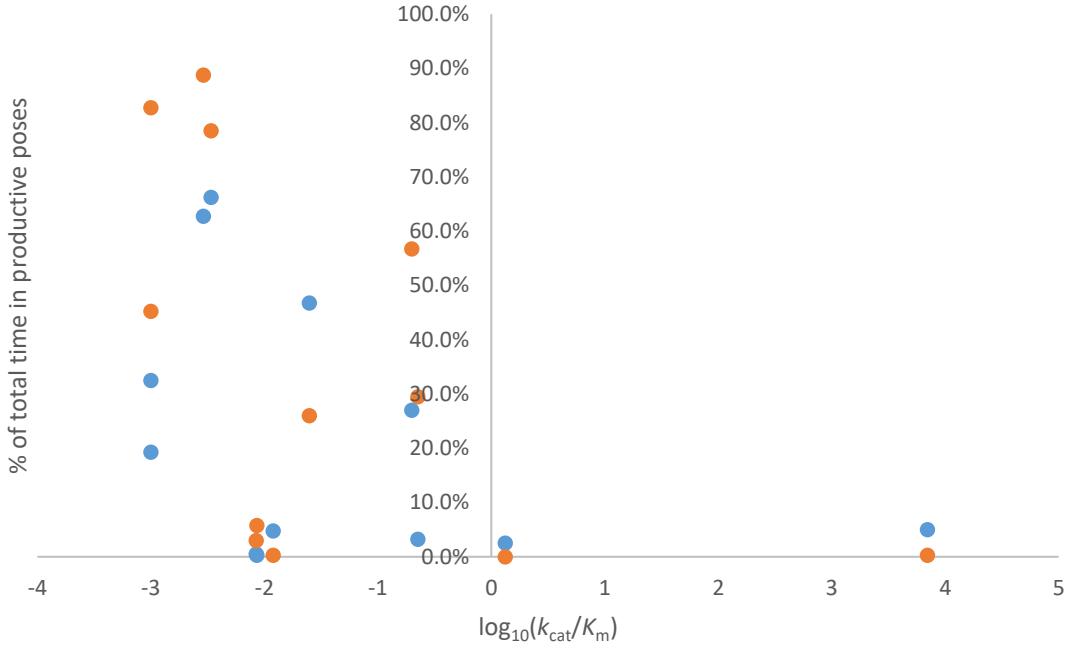

Figure 41 *Graph showing the lack of correlation between percentages of total time spent in productive poses and k_{cat}/K_m values for α-HCHs and β-PCCHs transformations. Blue and orange dots correspond to the HID and HIE protonation states of H73, respectively. In cases where substrates can have two or more productive poses, individual percentages of time for each pose was calculated and added to give the percentage of total time in productive poses.*

I end this Chapter by highlighting that while MD trajectories can be used as a tool to investigate substrates positioning in enzymes' active sites, using it only to look at the times substrates spent in productive poses is not enough to predict catalytic activity. Other aspects that may play a role in a reaction, such as the interaction between the catalytic residues (in this case between D25 and H73) also need to be studied before making a prediction. In addition to the residues affecting the size of the active site, residues that are involved along the route from the periphery of the enzyme towards the active site should also be considered when investigating the positioning of substrates in active sites.

CHAPTER 7:
General discussion

The results of the comparative biochemistry presented in this thesis provide new insights into the catalytic mechanism of LinA and the way it is evolving and adapting to its new function as a hexachlorocyclohexane dehydrochlorinase. In particular they reveal the differing biochemical properties of the recently discovered LinA-type3 $LinA_{LL02}$.

7.1 LinA mechanisms

Prior to this work, it was commonly accepted that LinA degrades a range of HCH and PCCH isomers by displacing a *trans*-diaxial H-Cl pair from the substrate via an E2 mechanism. This idea originated with Nagasawa et al. (1993b) who found that the LinA-type1 $LinA_{UT26}$ has activity against γ-HCH and γ-PCCH, both of which have at least one *trans*-diaxial H-Cl pair, and that γ-PCCH is a specific competitive inhibitor of the dehydrochlorination of γ-HCH. Since then, other studies on various LinA types (Bala et al., 2012; Geueke et al., 2013; Shrivastava et al., 2015; Suar et al., 2005; Trantírek et al., 2001), including this work, have supported this proposition with data for other substrates with *trans*-diaxial H-Cl pairs, such as α- and δ-HCH. It was also supported by the fact that the enzyme had negligible activity against β-HCH, which has no *trans*-diaxial H-Cl pairs (Lal et al., 2010; Nagasawa et al., 1993b; Nagata et al., 1993c; Zdravkovski, 2004).

Subsequently however, it was proposed that the enzyme can also mediate a *syn*-1,4-elimination reaction. This was based on $LinA1_{B90A}$ and $LinA2_{B90A}$ having activity against both δ-PCCH enantiomers and a hexachlorocyclohexene isomer, all of which lack *trans*-diaxial H-Cl pairs (Bala et al., 2012; Geueke et al., 2013). Since then, Shrivastava et al. (2015) and myself have corroborated this proposition via our observations that LinA-type1, LinA-type2 and LinA-type3 enzymes all have activity on δ-PCCH enantiomers.

Additionally, I propose herein that LinA can also mediate an *anti*-1,4-elimination reaction. This is based on Shrivastava et al. (2015) and my observation that LinA-type2 $LinA1_{B90A}$, LinA-type1 $LinA2_{B90A}$ and LinA-type3 $LinA_{LL02}$ can all degrade both β-PCCH1 and β-PCCH2 into various TCB isomers as dead-end products. Examination of the structures of β-PCCH1 and β-PCCH2 reveals

that they have neither *trans*-diaxial nor *syn*-1,4 H-Cl pairs that could allow LinA to mediate either of the previously proposed mechanisms.

Another aspect of LinA HCH degradation activity that I suggest is informative in respect of its functions and mechanisms is the formation of the dead-end product, TCB. It was earlier believed that TCB is formed spontaneously from the intermediate metabolite TCDN. Specifically Nagasawa et al. (1993b) suggested that the unstable nature of TCDN due to its diene-type structure would mean that it would spontaneously transform into TCB. However, Trantírek et al. (2001) and myself have both observed a lack of 1,3,5-TCB formation in assays where its formation should have happened if it was simply a spontaneous reaction. Interestingly, Orloff and Kolka (1954) had long ago investigated the possibility of non-enzymatic dehydrohalogenation of HCH and shown that TCDN could be transformed into TCB when it reacts with a base. Intriguingly, the catalytic dyad D25-H73 in the LinA active site works by acting as a base to extract a proton from LinA substrates (Brittain et al., 2011), raising the possibility of a similar role in the transformation of TCDN to TCB. These observations by Orloff and Kolka (1954), Trantírek et al. (2001) and myself suggest further studies are now warranted on the mechanism by which TCDN is transformed into TCB during the degradation of HCHs by LinA.

7.2 Evolution of new functions

As mentioned in Chapter 1, LinA has no known close relative with other proteins, including other dehydrochlorinases. It shows less than 10% sequence similarity to a functionally diverse group of proteins that share an $\alpha+\beta$ barrel fold tertiary structure (Nagata et al., 2001; Okai et al., 2010; Trantírek et al., 2001). It is also co-factor independent, unlike other dehydrochlorinases such as DDT dehydrochlorinase and a 3-chloro-D-alanine dehydrochlorinase that need glutathione and pyridoxal 5'-phosphate, respectively.

Given its very low sequence similarity with other proteins, the origin of LinA remains a mystery. However, its association with IS6*100* elements in *Sphingobium* species suggests it could have been acquired from bacteria outside this genus (Lal et al., 2006; Mahillon and Chandler, 1998;

Nagata et al., 2011; Pearce et al., 2015). The detailed sequence analyses of Pearce (2015) could not resolve any clear ancestral versus derived relationship between the LinA-type1 and LinA-type2 enzymes. However, one relationship that the analysis of Pearce (2015) did clearly show was that the LinA-type3 enzyme $LinA_{LL02}$ arose via recombination between the other two forms, with subsequent mutation then generating further divergence.

Bar-Even et al. (2011) studied the global trends of several thousand enzymes and ranked them based on their catalytic efficiency, k_{cat}/K_m. They found that moderately efficient enzymes exhibit a k_{cat}/K_m of approximately 10^5 $s^{-1}M^{-1}$ against their natural substrates, which translates to 10^1 $min^{-1}\mu M^{-1}$. Kinetic calculations in this study summarised in Table 13 below have shown that the LinA-type2 $LinA1_{B90A}$ and the LinA-type3 $LinA_{LL02}$ fall slightly below this average value, in the range of 10^{-2} $min^{-1}\mu M^{-1}$ to 10^{-1} $min^{-1}\mu M^{-1}$, respectively, on their most active substrates. However, the LinA-type1 $LinA2_{B90A}$ has higher k_{cat}/K_m values, in the range of 10^4 $min^{-1}\mu M^{-1}$, on its most active substrates, thus putting it above the moderately average enzymes. Assuming that positive selection is needed for an enzyme to achieve a high maximal efficiency on its preferred substrate, and given the relative recency of selection for HCH activity and the isomeric complexity of HCH, it seems reasonable to suggest that divergent positive selection has driven the divergent sequences and substrate preferences of the three LinA types.

The sequence analysis of Pearce (2015) indeed provided strong evidence in support of this idea; specifically he found no synonymous site substitutions between type1 and type2 enzymes, despite a total of twelve non-synonymous site differences between them. (My sequence alignment in Appendix E does in fact find one synonymous change, in the IS6*100*-associated 3' region). It seems reasonable now to extend his argument to the LinA-type3 enzyme $LinA_{LL02}$; it also shows no synonymous site differences (Appendix E), despite its non-synonymous site sequence divergence, and it also has clearly distinct substrate preferences.

Given the biochemical divergence between the three enzymes, and the sequence-based evidence that it was at least in part driven by divergent positive selection, questions obviously

arise as to whether there are further biochemical innovations that remain to be achieved in the LinA system, and whether there is any evidence that they are now emerging.

Table 13 summarises the catalytic efficiency values of the LinA-type1 $LinA2_{B90A}$, LinA-type2 $LinA1_{B90A}$ and LinA-type3 $LinA_{LL02}$ on α-, γ- and δ-HCH and their corresponding PCCHs derived from this work. In respect of the first step in the pathway, $LinA1_{B90A}$ gives the lowest values overall, with $LinA2_{B90A}$ yielding significantly higher values for the transformations of γ-HCH to the two γ-PCCHs in particular, and $LinA_{LL02}$ yielding moderately higher values for the transformations of δ-HCH into the two δ-PCCHs. Notably the highest values are therefore obtained with the lindane substrate γ-HCH but the lowest values are obtained for the major component (65-70%) of technical HCH, namely α-HCH. The statistics for the second step in the pathway suggest that this step is generally not limiting for any of the enzymes. As noted, TCB subsequently accumulates in all these reactions, and whole organism assays suggest it does *in vivo* as well (Lal et al., 2010).

Given all the above, I make the following observations in respect of possible drivers of ongoing selection on LinA by HCH contamination in the environment. Firstly, one major qualification is that we do not know how any of the catalytic efficiency values break down into component affinity and turnover statistics, nor do we know which of the latter two parameters are limiting for the host bacteria in the field. Secondly, while none of the efficiency statistics are high in absolute terms, the first step in the pathway in particular is quite energetically demanding (Manna and Dybala-Defratyka, 2013), and only so much improvement on the highest values tabulated may be possible. Thirdly, at least for β-HCH or δ-HCH, the LinB enzyme is also able to initiate a degradation pathway, and most of the bacteria so far found to have LinA also have LinB (Böltner et al., 2005; Pearce et al., 2015). Fourthly, there is an obvious deficit in catalytic efficiency for one HCH isomer, α-HCH, which will have been one of the two most abundant HCHs released into the environment. Fifthly, there are no data as yet for LinA on β-HCH and β-HCH may be one of the most stable HCH isomers in the environment (Zdravkovski, 2004).

Notwithstanding the caveats in the first three of these observations, I suggest there may still be ongoing selection for additional LinA variants by environmental HCH, with α-HCH possibly a particularly strong driver.

Parenthetically, because it is not directly related to selection on LinA, I also note there is no record of TCB being further transformed in whole cell or *in vivo* assays of HCH degradation by LinA-containing bacteria. This is despite the facts that all of the carbon in HCH will still be unavailable as a nutrient source if the TCB is not metabolised further and that other bacteria are known to be able to mineralise TCBs (Bosma et al., 1988; Marinucci and Bartha, 1979; van der Meer et al., 1991). There would seem to be strong selection pressure for the transfer of that capability to LinA-containing bacteria exposed to HCH.

Table 13 *Table listing the efficiency statistics ($min^{-1}\mu M^{-1}$) of the three LinA enzymes tested in this study. Yellow highlights the moderate-range activities among the enzymes, red highlights the low-range activities and green highlights the high-range activities.*

	α-HCH1 → β-PCCH1	α-HCH2 → β-PCCH2	γ-HCH -> γ-PCCH1	γ-HCH -> γ-PCCH2	δ-HCH → δ-PCCH1	δ-HCH → δ-PCCH2
$LinA1_{B90A}$	1.00E-03	1.00E-03	3.20E-03	2.90E-04	<1.0E-04	<1.0E-04
$LinA2_{B90A}$	8.60E-03	1.20E-02	3.70E-01	4.10E-01	<1.0E-04	9.80E-03
$LinA_{LL02}$	3.40E-03	2.90E-03	1.50E-03	1.90E-03	1.50E-02	1.90E-01

	β-PCCH1 → 1,2,4-TCB	β-PCCH1 → 1,2,3-TCB	β-PCCH1 → 1,3,5-TCB	β-PCCH2 → 1,2,4-TCB	β-PCCH2 → 1,2,3-TCB	β-PCCH2 → 1,3,5-TCB
$LinA1_{B90A}$	8.50E-03			2.50E-02		
$LinA2_{B90A}$	3.90E+00	<1.0E-03	9.50E-02	2.10E+04	<1.0E-03	<1.0E-03
$LinA_{LL02}$	6.70E-01	<1.0E-03	4.40E-03	5.80E-01	1.60E-02	<1.0E-03

	γ-PCCH1 -> 1,2,4-TCB	γ-PCCH1 -> 1,2,3-TCB	γ-PCCH1 -> 1,3,5-TCB	γ-PCCH2 -> 1,2,4-TCB	γ-PCCH2 -> 1,2,3-TCB	γ-PCCH2 -> 1,3,5-TCB
$LinA1_{B90A}$	6.60E-02	5.80E-03		<1.0E-04	<1.0E-04	
$LinA2_{B90A}$	5.00E+02	3.10E+01		8.00E-01	5.20E-03	
$LinA_{LL02}$	1.20E-02	1.60E-03	7.10E-03	1.00E-04	3.10E-03	<1.0E-04

	δ-PCCH1 → 1,2,4-TCB	δ-PCCH1 → 1,2,3-TCB	δ-PCCH2 → 1,2,4-TCB	δ-PCCH2 → 1,2,3-TCB
$LinA1_{B90A}$	4.50E-04		<1.0E-04	
$LinA2_{B90A}$	3.10E+04	3.40E+04	1.50E-03	2.40E-04
$LinA_{LL02}$				

Given that there may well be ongoing divergent selection on LinA, it then follows to ask what additional variation may have arisen among LinA sequences since the analysis of Pearce (2015).

To address this, Figure 42 presents an alignment of all known LinA variants that have been deposited in the NCBI database. The figure shows there are now at least six additional LinA amino acid sequences in this database, together involving five additional amino acid substitutions. Four of those substitutions lie in regions contributing to the active site. Of particular interest are the three variants (BAI82452.1, ABG77566.1 and CAI43917.1) which are all very similar to LinA-type1 but have T110 and C111 instead of A110 and A111 in the active site. A previous mutagenesis study of these residues had shown that they are involved in isomer preferences among α- and γ-HCHs (Sharma et al., 2011). These three sequences, which were lodged in the NCBI database in 2016, 2008 and 2006, respectively, show no synonymous site variation and would seem to be prime candidates for encoding emerging new LinA functionality.

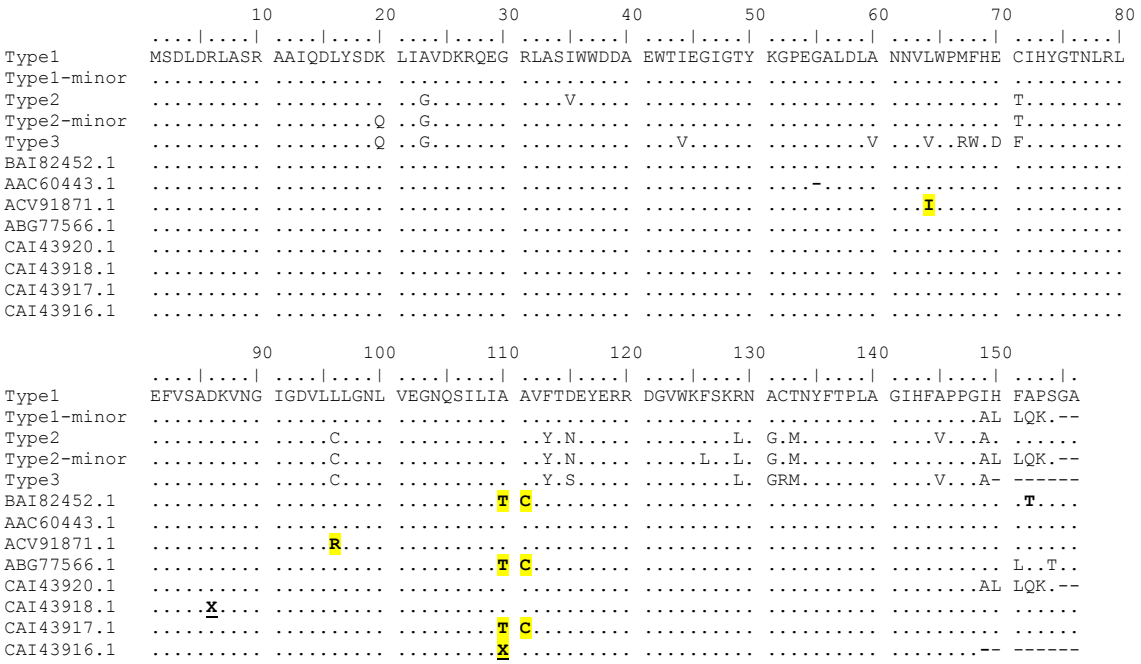

Figure 42 *Alignments of known LinA variants deposited into NCBI database. Variants included in LinA-type1, LinA-type2 and LinA-type3 are not shown. Variants with mutations outside of the known sequences for the three LinA types are listed using their GenBank accession numbers as identifiers. X denotes an unknown residue. Mutations in the vicinity of the active site for the variants outside of the known three LinA types are highlighted in yellow.*

7.3 Priorities for future research

While this work has managed to provide several new insights into LinA biochemistry and evolution, it was also beset by some key empirical and modelling issues. My assays were limited by substrate solubility issues and my inability to prepare β-PCCH standards. The latter problem

should have tractable solutions as others have apparently succeeded using the same protocol in the past (Buser and Müeller, 1995; Shrivastava et al., 2015). Some of the solubility issues might be addressable by using some proportion of a water-miscible organic solvent (e.g., DMSO, acetonitrile, MeOH, EtOH) in the assays. However, it is quite likely that it will remain unfeasible to solubilise sufficient HCH and possibly PCCH to obtain separate K_m and k_{cat} estimates without adversely affecting the enzymes using this approach.

My MD trajectories only investigated the distance between H73 and the hydrogen in *trans*-diaxial H-Cl pairs on the substrate, and this proved to be insufficient to predict the occurrence of reactions. Longer and multiple MD trajectories along with deeper analyses (i.e., using MMPBSA for free energy calculations and distance metrics to other active site residues) might uncover further details of not only which other specific active site interactions might be primary contributors to catalytic activity (e.g., W42), but also the larger-scale enzymatic dynamics that provide the energy required for the deprotonation step. Further, MD studies with multiple external-to-the-enzyme (i.e., non-docked) substrates could reveal additional residues removed from (i.e. surface), and/or proximate to, the active sites that are important in channelling substrates to the appropriate positions for catalysis from bulk solvent (Wilding et al., 2018). This could provide vital clues for further engineering of enzymes for bioremediation applications.

Technical and modelling issues aside, my data also reveal several tantalising new aspects of LinA biology that warrant further research. In terms of fundamental research, the biophysical basis for the *syn*-1,4-elimination and in particular the proposed new *anti*-1,4-elimination reactions deserve attention, as does the apparent enzyme dependence of the previously assumed spontaneous TCDN to TCB transformations. Further computational efforts would also seem worthwhile in attempting to resolve these issues. Further biochemical work would also seem worthwhile to investigate the kinetics of the new LinA variants lodged in GenBank, while *in vitro* mutagenesis and *in vitro* evolution could be useful to explore the possibility of still further enhancements of LinA activities, particularly in relation to the α-HCH enantiomers. Finally, there

would be great value in more work studying the population genetics of the system, both in dump and other contaminated sites in the field and in synthetic 'microcosms' with various mixtures of HCHs. Such work could provide important new information on the respective ecological niches which the different LinA variants enable their hosts to occupy. My work, and some of the extensions of it outlined above, could provide some clear and testable predictions of just how the biochemical differences translate into ecological and evolutionary benefits.

My findings also bear on ongoing efforts to use LinA-based strategies for bioremediating HCH dump sites and contaminated soils and water bodies. To date, bioremediation of HCH-contaminated soil by bioaugmentation with innocula of naturally occurring *Sphingobium* strains expressing *lin* genes has been tested, yielding promising results (Mertens et al., 2006; Raina et al., 2008). Free-enzyme bioremediation of HCH-contaminated soil and water by LinA has also been contemplated (Lal et al., 2010) although to my knowledge, not yet tested in the field. The knowledge gained from my study could help with the selection of better strains for microbially based bioremediation strategies, and with the selection or development of improved LinA variants for free-enzyme based strategies. I would also advocate for 'assisted evolution' approaches involving, for example, co-culturing of multiple strains expressing the Lin pathway with others able to degrade TCBs under appropriate selective conditions to isolate recombinant organisms capable of higher throughput through the pathway and/or avoiding the accumulation of TCBs. I note that Sharma et al. (2014) have already developed a high throughput screening system for the identification of strains with improved HCH degrading activities. Such strains would not classify as Genetically Modified Organisms (GMOs) and would thus avoid the still problematic regulatory issues around the release of such organisms into the open environment.

7.4 Conclusions

Notwithstanding the technical challenges I faced, my results clearly extend earlier evidence that the ability of certain bacteria to utilise HCHs as recent new pollutants has indeed required the development of some complex new biochemical adaptations. While there are still several

important issues and uncertainties to follow up in future research, it appears that no one LinA variant is yet able to effectively initiate the degradation of all the key HCHs. Indeed the picture emerging is that a complementary set of variants variously specialised for different isomers are being selected for. As with other aspects of the pathway, for example the dispersed distribution of different *lin* genes across the genomes (Pearce et al., 2015) and the build-up of TCBs, it seems that the LinA component of the system is not yet optimised. It therefore holds great promise for ongoing study of the evolution of a new biochemical function and, as such, it also warrants further effort to resolve some of the significant technical issues in studying the system.

References

Bajaj, S., Sagar, S., Khare, S., & Singh, D. K. (2017). Biodegradation of γ-hexachlorocyclohexane (lindane) by halophilic bacterium *Chromohalobacter* sp. LD2 isolated from HCH dumpsite. *International Biodeterioration and Biodegradation*, *122*, 23–28. https://doi.org/10.1016/j.ibiod.2017.04.014

Bala, K., Geueke, B., Miska, M. E., Rentsch, D., Poiger, T., Dadhwal, M., Lal, R., Holliger, C., & Kohler, H. P. E. (2012). Enzymatic conversion of ε-hexachlorocyclohexane and a heptachlorocyclohexane isomer, two neglected components of technical hexachlorocyclohexane. *Environmental Science and Technology*, *46*(7), 4051–4058. https://doi.org/10.1021/es204143x

Bar-Even, A., Noor, E., Savir, Y., Liebermeister, W., Davidi, D., Tawfik, D. S., & Milo, R. (2011). The moderately efficient enzyme: Evolutionary and physicochemical trends shaping enzyme parameters. *Biochemistry*, *50*(21), 4402–4410. https://doi.org/10.1021/bi2002289

Bickelhaupt, F. M. (2001). Base-induced 1,4-elimination: Insights from theory and mass spectrometry. *Mass Spectrometry Reviews*, *20*, 347–361. https://doi.org/10.1002/mas.10007

Bidleman, T. F., Jantunen, L. M., Falconer, R. L., Barrie, L. A., & Fellin, P. (1995). Decline of hexachlorocyclohexane in the Arctic atmosphere and reversal of air-sea gas exchange. *Geophysical Research Letters*, *22*(3), 219–222. https://doi.org/10.1029/94GL02990

Böltner, D., Moreno-Morillas, S., & Ramos, J. L. (2005). 16S rDNA phylogeny and distribution of *lin* genes in novel hexachlorocyclohexane-degrading *Sphingomonas* strains. *Environmental Microbiology*, *7*(9), 1329–1338. https://doi.org/10.1111/j.1462-5822.2005.00820.x

Bosma, T. N. P., van der Meer, J. R., Schraa, G., Tros, M. E., & Zehnder, A. J. B. (1988). Reductive dechlorination of all trichloro- and dichlorobenzene isomers. *FEMS Microbiology Letters*, *53*(3–4), 223–229. https://doi.org/10.1016/0378-1097(88)90446-6

Bourne, L. B. (1945). Hexachlorocyclohexane as an insecticide. *Nature*, *395*, 85.

Brittain, D. R. B., Pandey, R., Kumari, K., Sharma, P., Pandey, G., Lal, R., Coote, M. L., Oakeshott, J. G., & Jackson, C. J. (2011). Competing SN2 and E2 reaction pathways for hexachlorocyclohexane degradation in the gas phase, solution and enzymes. *Chemical Communications*, *47*, 976–978. https://doi.org/10.1039/c0cc02925d

Buser, H.-R., & Müeller, M. D. (1995). Isomer and enantioselective degradation of hexachlorocyclohexane isomers in sewage sludge under anaerobic conditions. *Environmental Science & Technology*, *29*(3), 664–672. https://doi.org/10.1021/es00003a013

Campbell, R. G. (1951). *US2573676A*. United States of America: US Grant.

Case, D. A., Ben-Shalom, I. Y., Brozell, S. R., Cerutti, D. S., Cheatham, T. E., Cruzeiro, V. W. D., Darden, T. A., Duke, R. E., Ghoreishi, D., Gilson, M. K., Gohlke, H., Goetz, A. W., Greene, D., Harris, R., Homeyer, N., Izadi, S., Kovalenko, A., Kurtzman, T., Lee, T. S., LeGra, S., York, D. M., & Kollman, P. A. (2018). Amber18. San Francisco: University of California.

Cérémonie, H., Boubakri, H., Mavingui, P., Simonet, P., & Vogel, T. M. (2006). Plasmid-encoded γ-hexachlorocyclohexane degradation genes and insertion sequences in *Sphingobium francense* (ex-*Sphingomonas paucimobilis* Sp+). *FEMS Microbiology Letters*, *257*(2), 243–252. https://doi.org/10.1111/j.1574-6968.2006.00188.x

Cortes, D. R., & Hites, R. A. (2000). Detection of statistically significant trends in atmospheric concentrations of semivolatile compounds. *Environmental Science and Technology*, *34*(13), 2826–2829. https://doi.org/10.1021/es990466l

Cristol, S. J., Hause, N. L., & Meek, J. S. (1951). Mechanisms of elimination reactions. III. The kinetics of the alkaline dehydrochlorination of the benzene hexachloride isomers. II. *Journal of the American Chemical Society*, *73*(2), 674–679. https://doi.org/10.1021/ja01146a050

Darden, T., York, D., & Pedersen, L. (1993). Particle mesh Ewald: An N.log(N) method for Ewald sums in large systems. *Journal of Chemical Physics*, *98*(12), 10089–10092. https://doi.org/10.1063/1.464397

Dassault Systèmes BIOVIA. (2017). BIOVIA Materials Studio. San Diego: Dassault Systèmes. Retrieved from http://accelrys.com/products/collaborative-science/biovia-materials-studio/

De Souza, M. L., Sadowsky, M. J., & Wackett, L. P. (1996). Atrazine chlorohydrolase from *Pseudomonas* sp. strain ADP: Gene sequence, enzyme purification, and protein characterization. *Journal of Bacteriology*, *178*(16), 4894–4900.

Dogra, C., Raina, V., Pal, R., Suar, M., Lal, S., Gartemann, K., Holliger, C., & van der Meer, J. R. (2004). Organization of lin genes and IS6*100* among different strains of *Sphingomonas paucimobilis* : Evidence for horizontal gene transfer. *Journal of Bacteriology*, *186*(8), 2225–2235. https://doi.org/10.1128/JB.186.8.2225

Endo, R., Kamakura, M., Miyauchi, K., Fukuda, M., Ohtsubo, Y., Tsuda, M., & Nagata, Y. (2005). Identification and characterization of genes involved in the downstream degradation pathway of γ -hexachlorocyclohexane in *Sphingomonas paucimobilis* UT26. *Journal of Bacteriology*, *187*(3), 847–853. https://doi.org/10.1128/JB.187.3.847

Endo, R., Ohtsubo, Y., Tsuda, M., & Nagata, Y. (2007). Identification and characterization of genes encoding a putative ABC-type transporter essential for utilization of γ-hexachlorocyclohaxane in *Sphingobium japonicum* UT26. *Journal of Bacteriology*, *189*(10), 3712–3720. https://doi.org/10.1128/JB.01883-06

FAISD Handbook. (2018). Retrieved March 1, 2018, from https://apvma.gov.au/node/26586

Faraday, M. (1825). On new compounds of carbon and hydrogen, and on certain other products obtained during the decomposition of oil by heat. *Philosophical Transactions of the Royal Society of London*, *115*, 440–466. https://doi.org/10.1098/rstl.1825.0022

Geueke, B., Miska, M. E., Poiger, T., Rentsch, D., Lal, R., Holliger, C., & Kohler, H. P. E. (2013). Enantioselective dehydrochlorination of δ-hexachlorocyclohexane and δ-pentachlorocyclohexene by LinA1 and LinA2 from *Sphingobium indicum* B90A. *Applied and Environmental Microbiology*, *79*(19), 6180–6183. https://doi.org/10.1128/AEM.01770-13

Glotfelty, D. E., Taylor, A. W., Turner, B. C., & Zoller, W. H. (1984). Volatilization of surface-applied pesticides from fallow soil. *Journal of Agricultural and Food Chemistry*, *32*(3), 638–643. https://doi.org/10.1021/jf00123a053

Gregor, D. J., & Gummer, W. D. (1989). Evidence of atmospheric transport and deposition of organochlorine pesticides and polychlorinated biphenyls in Canadian Arctic snow. *Environmental Science and Technology*, *23*(5), 561–565. https://doi.org/10.1021/es00063a008

Gronert, S., & Kass, S. R. (1997). Theoretical studies of eliminations. 6. The regiochemistry and stereochemistry of the gas-phase reactions of 3-halocyclohexenes with fluoride. An *ab initio* study. *The Journal of Organic Chemistry*, *62*(23), 7991–8000. https://doi.org/10.1021/jo970626g

Hargrave, B. T., Vass, W. P., Erickson, P. E., & Fowler, B. R. (1988). Atmospheric transport of organochlorines to the Arctic Ocean. *Tellus B: Chemical and Physical Meteorology*, *40*(5), 480–493. https://doi.org/10.1111/j.1600-0889.1988.tb00118.x

Hartley, W. N. (1881). Researches on the relation between the molecular structure of carbon compounds, and their absorption spectra. *Journal of the Chemical Society, Transactions*,

39, 153–168.

Hoops, S., Sahle, S., Gauges, R., Lee, C., Pahle, J., Simus, N., Singhal, M., Xu, L., Mendes, P., & Kummer, U. (2006). COPASI - A COmplex PAthway SImulator. *Bioinformatics*, *22*(24), 3067–3074. https://doi.org/10.1093/bioinformatics/btl485

Horne, I., Sutherland, T. D., Harcourt, R. L., Russell, R. J., & Oakeshott, J. G. (2002). Identification of an *opd* (organophosphate degradation) gene in an Agrobacterium isolate. *Applied and Environmental Microbiology*, *68*(7), 3371–3376. https://doi.org/10.1128/AEM.68.7.3371

Humphrey, W., Dalke, A., & Schulten, K. (1996). VMD: Visual Molecular Dynamics. *Journal of Molecular Graphics*, *14*, 33–38. https://doi.org/10.1016/0263-7855(96)00018-5

Imai, R., Nagata, Y., Fukuda, M., Takagi, M., & Yano, K. (1991). Molecular cloning of a *Pseudomonas paucimobilis* gene encoding a 17-kilodalton polypeptide that eliminates HCl molecules from γ-hexachlorocyclohexane. *Journal of Bacteriology*, *173*(21), 6811–6819. https://doi.org/10.1128/JB.173.21.6811-6819.1991

Immig, J. (2010). A List of Australia's Most Dangerous Pesticides. *National Toxics Network*, (July), 1–17. Retrieved from http://awsassets.wwf.org.au/downloads/fs025_a_list_of_australias_most_dangerous_pesticides_1jul10.pdf

Ito, M., Prokop, Z., Klvaňa, M., Otsubo, Y., Tsuda, M., Damborský, J., & Nagata, Y. (2007). Degradation of β-hexachlorocyclohexane by haloalkane dehalogenase LinB from γ-hexachlorocyclohexane-utilizing bacterium *Sphingobium* sp. MI1205. *Archives of Microbiology*, *188*(4), 313–325. https://doi.org/10.1007/s00203-007-0251-8

Iwata, H., Tanabe, S., Sakal, N., & Tatsukawa, R. (1993). Distribution of persistent organochiorines in the oceanic air and surface seawater and the role of ocean on their global transport and fate. *Environmental Science and Technology*, *27*(6), 1080–1098.

https://doi.org/10.1021/es00043a007

Jürgens, H. J., & Roth, R. (1989). Case study and proposed decontamination steps of the soil and groundwater beneath a closed herbicide plant in Germany. *Chemosphere*, *18*(1–6), 1163–1169. https://doi.org/10.1016/0045-6535(89)90250-6

Kaur, H., Kapoor, S., & Kaur, G. (2016). Application of ligninolytic potentials of a white-rot fungus *Ganoderma lucidum* for degradation of lindane. *Environmental Monitoring and Assessment*, *188*(10). https://doi.org/10.1007/s10661-016-5606-7

Kelley, L. A., Mezulis, S., Yates, C. M., Wass, M. N., & Sternberg, M. J. E. (2015). The Phyre2 web portal for protein modeling, prediction and analysis. *Nature Protocols*, *10*(6), 845–858. https://doi.org/10.1038/nprot.2015-053

Kidd, H., James, D. R., & Royal Society of Chemistry (Great Britain). Information Services (1991). *The Agrochemicals Handbook* (3rd ed.). Royal Society of Chemistry, Information Services, Cambridge, England.

Kohli, P., Dua, A., Sangwan, N., Oldach, P., Khurana, J. P., & Lal, R. (2013). Draft genome sequence of a hexachlorocyclohexane-degrading bacterium. *Genome Announcements*, *1*(6), e00956-13. https://doi.org/10.1128/genomeA.00715-13.Kumar

Kumar, M., Chaudhary, P., Dwivedi, M., Kumar, R., Paul, D., Jain, R. K., Garg, S. K., & Kumar, A. (2005). Enhanced biodegradation of β- and δ-hexachlorocyclohexane in the presence of α- and γ-isomers in contaminated soils. *Environmental Science and Technology*, *39*(11), 4005–4011. https://doi.org/10.1021/es048497q

Kumari, R., Subudhi, S., Suar, M., Dhingra, G., Raina, V., Dogra, C., Lal, S., van der Meer, J. R., Holliger, C., & Lal, R. (2002). Cloning and characterization of *lin* genes responsible for the degradation of hexachlorocyclohexane isomers by *Sphingomonas paucimobilis* strain B90. *Applied and Environmental Microbiology*, *68*(12), 6021–6028. https://doi.org/10.1128/AEM.68.12.6021-6028.2002

Lal, R., Dogra, C., Malhotra, S., Sharma, P., & Pal, R. (2006). Diversity, distribution and divergence of *lin* genes in hexachlorocyclohexane-degrading *Sphingomonads*. *Trends in Biotechnology*, *24*(3), 121–130. https://doi.org/10.1016/j.tibtech.2006.01.005

Lal, R., Pandey, G., Sharma, P., Kumari, K., Malhotra, S., Pandey, R., Raina, V., Kohler, H. P. E., Holliger, C., Jackson, C., & Oakeshott, J. G. (2010). Biochemistry of microbial degradation of hexachlorocyclohexane and prospects for bioremediation. *Microbiology and Molecular Biology Reviews*, *74*(1), 58–80. https://doi.org/10.1128/MMBR.00029-09

Li, Y. F. (1999). Global technical hexachlorocyclohexane usage and its contamination consequences in the environment: From 1948 to 1997. *Science of the Total Environment*, *232*(3), 121–158. https://doi.org/10.1016/S0048-9697(99)00114-X

Liu, S., & Suflita, J. M. (1993). Ecology and evolution of microbial populations for bioremediation. *Trends in Biotechnology*, *11*(8), 344–352.

Luek, J. L., Dickhut, R. M., Cochran, M. A., Falconer, R. L., & Kylin, H. (2017). Persistent organic pollutants in the Atlantic and southern oceans and oceanic atmosphere. *Science of the Total Environment*, *583*, 64–71. https://doi.org/10.1016/j.scitotenv.2016.12.189

MacRae, I. C., Raghu, K., & Bautista, E. M. (1969). Anaerobic degradation of the insecticide lindane by *Clostridium* sp. *Nature*, *221*, 859–860. https://doi.org/10.1038/224488a0

Macwan, A. S., Javed, S., & Kumar, A. (2011). Isolation of a novel thermostable dehydrochlorinase (LinA) from a soil metagenome. *3 Biotech*, *1*(4), 193–198. https://doi.org/10.1007/s13205-011-0012-x

Macwan, A. S., Kukshal, V., Shrivastava, N., Javed, S., Kumar, A., & Ramachandran, R. (2012). Crystal structure of the hexachlorocyclohexane dehydrochlorinase (LinA-Type2): Mutational analysis, thermostability and enantioselectivity. *PLoS ONE*, *7*(11). https://doi.org/10.1371/journal.pone.0050373

Mahillon, J., & Chandler, M. (1998). Insertion sequences. *Microbioliology and Molecular Biology Review*, *62*(3), 725–74. https://doi.org/10.1016/B978-0-12-374984-0.00799-3

Mandelbaum, R. T., Sadowsky, M. J., & Wackett, L. P. (2008). Microbial degradation of s-triazine herbicides. In H. M. LeBaron, J. E. MacFarland, & O. C. Burnside (Eds.), *The triazine herbicides* (1st ed., pp. 301–328). Elsevier B.V.

Manickam, N., Reddy, M. K., Saini, H. S., & Shanker, R. (2008). Isolation of hexachlorocyclohexane-degrading *Sphingomonas* sp. by dehalogenase assay and characterization of genes involved in γ-HCH degradation. *Journal of Applied Microbiology*, *104*(4), 952–960. https://doi.org/10.1111/j.1365-2672.2007.03610.x

Manna, R. N., & Dybala-Defratyka, A. (2013). Insights into the elimination mechanisms employed for the degradation of different hexachlorocyclohexane isomers using kinetic isotope effects and docking studies. *Journal of Physical Organic Chemistry*, *26*(10), 797–804. https://doi.org/10.1016/j.jhydrol.2007.12.015

Manna, R. N., Zinovjev, K., Tuñón, I., & Dybala-Defratyka, A. (2015). Dehydrochlorination of hexachlorocyclohexanes catalyzed by the LinA dehydrohalogenase. A QM/MM study. *Journal of Physical Chemistry B*, *119*(49), 15100–15109. https://doi.org/10.1021/acs.jpcb.5b07538

Marco-Urrea, E., Pérez-Trujillo, M., Caminal, G., & Vicent, T. (2009). Dechlorination of 1,2,3- and 1,2,4-trichlorobenzene by the white-rot fungus *Trametes versicolor*. *Journal of Hazardous Materials*, *166*(2–3), 1141–1147. https://doi.org/10.1016/j.jhazmat.2008.12.076

Marinucci, A. C., & Bartha, R. (1979). Biodegradation of 1,2,3- and 1,2,4-trichlorobenzene in soil and in liquid enrichment culture. *Applied and Environmental Microbiology*, *38*(5), 811–817.

Mertens, B., Boon, N., & Verstraete, W. (2006). Slow-release inoculation allows sustained

biodegradation of γ-hexachlorocyclohexane. *Applied and Environmental Microbiology*, *72*(1), 622–627. https://doi.org/10.1128/AEM.72.1.622-627.2006

Miyauchi, K., Adachi, Y., Nagata, Y., & Takagi, M. (1999). Cloning and sequencing of a novel meta-cleavage dioxygenase gene whose product is involved in degradation of γ -hexachlorocyclohexane in *Sphingomonas paucimobilis*. *Journal of Bacteriology*, *181*(21), 6712–6719.

Miyauchi, K., Lee, H.-S., Fukuda, M., Takagi, M., & Nagata, Y. (2002). Cloning and characterization of *linR*, involved in regulation of the downstream pathway for γ-hexachlorocyclohexane degradation in *Sphingomonas paucimobilis* UT26. *Applied and Environmental Microbiology*, *68*(4), 1803–1807. https://doi.org/10.1128/JB.187.3.847-853.2005

Miyauchi, K., Suh, S.-K., Nagata, Y., & Takagi, M. (1998). Cloning and sequencing of a 2,5-dichlorohydroquinone reductive dehalogenase gene whose product is involved in degradation of γ-hexachlorocyclohexane by *Sphingomonas paucimobilis*. *Journal of Bacteriology*, *180*(6), 1354–1359.

Nagasawa, S., Kikuchi, R., Nagata, Y., Takagi, M., & Matsuo, M. (1993a). Aerobic mineralization of γ-HCH by *Pseudomonas paucimobilis* UT26. *Chemosphere*, *26*(9), 1719–1728. https://doi.org/10.1016/0045-6535(93)90115-L

Nagasawa, S., Kikuchi, R., Nagata, Y., Takagi, M., & Matsuo, M. (1993b). Stereochemical analysis of γ-HCH degradation by *Pseudomonas paucimobilis* UT26. *Chemosphere*, *26*(6), 1187–1201. https://doi.org/10.1016/0045-6535(93)90205-J

Nagata, Y., Endo, R., Ito, M., Ohtsubo, Y., & Tsuda, M. (2007). Aerobic degradation of lindane (γ-hexachlorocyclohexane) in bacteria and its biochemical and molecular basis. *Applied Microbiology and Biotechnology*, *76*(4), 741–752. https://doi.org/10.1007/s00253-007-1066-x

Nagata, Y., Hatta, T., Imai, R., Kimbara, K., Fukuda, M., Yano, K., & Takagi, M. (1993a). Purification and characterization of γ-hexachlorocyclohexane (γ-HCH) dehydrochlorinase (LinA) from *Pseudomonas paucimobilis*. *Bioscience, Biotechnology, and Biochemistry*, *57*(9), 1582–1583.

Nagata, Y., Imai, R., Sakai, A., Fukuda, M., Yano, K., & Takagi, M. (1993b). Isolation and characterization of Tn5-induced mutants of *Pseudomonas paucimobilis* UT26 defective in γ-hexachlorocyclohexane dehydrochlorinase (LinA). *Bioscience, Biotechnology, and Biochemistry*, *57*(5), 703–709. https://doi.org/10.1271/bbb.57.703

Nagata, Y., Miyauchi, K., & Takagi, M. (1999). Complete analysis of genes and enzymes for γ-hexachlorocyclohexane degradation in *Sphingomonas paucimobilis* UT26. *Journal of Industrial Microbiology and Biotechnology*, *23*, 380–390. https://doi.org/10.1038/sj.jim.2900736

Nagata, Y., Mori, K., Takagi, M., Murzin, A. G., & Damborský, J. (2001). Identification of protein fold and catalytic residues of γ-hexachlorocyclohexane dehydrochlorinase LinA. *Proteins*, *45*(4), 471–477. Retrieved from http://www.ncbi.nlm.nih.gov/pubmed/11746694

Nagata, Y., Nariya, T., Ohtomo, R., Fukuda, M., Yano, K., & Takagi, M. (1993c). Cloning and sequencing of a dehalogenase gene encoding an enzyme with hydrolase activity involved in the degradation of γ-hexachlorocyclohexane in *Pseudomonas paucimobilis*. *Journal of Bacteriology*, *175*(20), 6403–6410.

Nagata, Y., Natsui, S., Endo, R., Ohtsubo, Y., Ichikawa, N., Ankai, A., Oguchi, A., Fukui, S., Fujita, N., & Tsuda, M. (2011). Genomic organization and genomic structural rearrangements of *Sphingobium japonicum* UT26, an archetypal γ-hexachlorocyclohexane-degrading bacterium. *Enzyme and Microbial Technology*, *49*(6–7), 499–508. https://doi.org/10.1016/j.enzmictec.2011.10.005

Nagata, Y., Ohtomo, R., Miyauchi, K., Fukuda, M., Yano, K., & Takagi, M. (1994). Cloning and

sequencing of a 2,5-dichloro-2,5-cyclohexadiene-1,4-diol dehydrogenase gene involved in the degradation of γ-hexachlorocyclohexane in *Pseudomonas paucimobilis*. *Journal of Bacteriology*, *176*(11), 3117–3125. https://doi.org/10.1128/JB.175.20.6403-6410.1993

Nagata, Y., Ohtsubo, Y., Endo, R., Ichikawa, N., Ankai, A., Oguchi, A., Fukui, S., Fujita, N., & Tsuda, M. (2010). Complete genome sequence of the representative γ-hexachlorocyclohexane-degrading bacterium *Sphingobium japonicum* UT26. *Journal of Bacteriology*, *192*(21), 5852–5853. https://doi.org/10.1128/JB.00961-10

Nagata, Y., Prokop, Z., Sato, Y., Jerabek, P., Kumar, A., Ohtsubo, Y., Tsuda, M., & Damborský, J. (2005). Degradation of β -hexachlorocyclohexane by haloalkane dehalogenase LinB from *Sphingomonas paucimobilis* UT26. *Applied and Environmental Microbiology*, *71*(4), 2183–2185. https://doi.org/10.1128/AEM.71.4.2183

Nalin, R., Simonet, P., Vogel, T. M., & Normand, P. (1999). *Rhodanobacter lindaniclasticus* gen. nov., sp. nov., a lindane-degrading bacterium. *International Journal of Systematic Bacteriology*, (49), 19–23.

National Toxicology Program. (2016a). *Lindane, hexachlorocyclohexane (technical grade), and other hexachlorocyclohexane isomers*. *Report on carcinogens, 14th Edition*. Retrieved from https://ntp.niehs.nih.gov/ntp/roc/content/profiles/lindane.pdf

National Toxicology Program. (2016b). *Substances listed in the Fourteenth Report on Carcinogens*. *Report on carcinogens, 14th Edition*. Retrieved from http://ntp.niehs.nih.gov/go/roc14

Okai, M., Kubota, K., Fukuda, M., Nagata, Y., Nagata, K., & Tanokura, M. (2010). Crystal structure of γ-hexachlorocyclohexane dehydrochlorinase LinA from *Sphingobium japonicum* UT26. *Journal of Molecular Biology*, *403*(2), 260–269. https://doi.org/10.1016/j.jmb.2010.08.043

Okeke, B. C., Siddique, T., Arbestain, M. C., & Frankenberger, W. T. (2002). Biodegradation of γ-

hexachlorocyclohexane (Lindane) and α-hexachlorocyclohexane in water and a soil slurry by a *Pandoraea* species. *Journal of Agricultural and Food Chemistry*, *50*(9), 2548–2555. https://doi.org/10.1021/jf011422a

Olsson, M. H. M., Søndergaard, C. R., Rostkowski, M., & Jensen, J. H. (2011). PROPKA3: Consistent treatment of internal and surface residues in empirical pKa predictions. *Journal of Chemical Theory and Computation*, *7*(2), 525–537. https://doi.org/10.1021/ct100578z

Orloff, H. D., & Kolka, A. J. (1954). The mechanism of dehydrohalogenation of benzene tetrachloride and related compounds. *Journal of the American Chemical Society*, *76*(21), 5484–5490. https://doi.org/10.1021/ja01650a068

Pearce, S. L. (2015). *Acquisition and ongoing evolution of synthetic xenobiotic metabolic pathways in soil bacteria.* (PhD thesis). Australian National University.

Pearce, S. L., Oakeshott, J. G., & Pandey, G. (2015). Insights into ongoing evolution of the hexachlorocyclohexane catabolic pathway from comparative genomics of ten *Sphingomonadaceae* strains. *G3-Genes Genomes Genetics*, *5*(6), 1081–1094. https://doi.org/10.1534/g3.114.015933

Pettersen, E. F., Goddard, T. D., Huang, C. C., Couch, G. S., Greenblatt, D. M., Meng, E. C., & Ferrin, T. E. (2004). UCSF Chimera - A visualization system for exploratory research and analysis. *Journal of Computational Chemistry*, *25*(13), 1605–1612. https://doi.org/10.1002/jcc.20084

Raina, V., Hauser, A., Buser, H.-R., Rentsch, D., Sharma, P., Lal, R., Holliger, C., Poiger, T., Muller, M. D., & Kohler, H. P. E. (2007). Hydroxylated metabolites of β- and δ-hexachlorocyclohexane: Bacterial formation, stereochemical configuration, and occurrence in groundwater at a former production site. *Environmental Science and Technology*, *41*(12), 4291–4298. https://doi.org/10.1021/es062908g

Raina, V., Suar, M., Singh, A., Prakash, O., Dadhwal, M., Gupta, S. K., Dogra, C., Lawlor, K., Lal, S., van der Meer, J. R., Holliger, C., & Lal, R. (2008). Enhanced biodegradation of hexachlorocyclohexane (HCH) in contaminated soils via inoculation with *Sphingobium indicum* B90A. *Biodegradation*, *19*(1), 27–40. https://doi.org/10.1007/s10532-007-9112-z

Ramsey, L., & Patterson, W. (1946). Separation and purification of some constituents of commercial hexachlorocyclohexane. *Journal of Association of Official Agricultural Chemists*, *29*, 337.

Sahu, S. K., Patnaik, K. K., Sharmila, M., & Sethunathan, N. (1990). Degradation of α-, β-, and γ-hexachlorocyclohexane by a soil bacterium under aerobic conditions. *Applied and Environmental Microbiology*, *56*(11), 3620–3622.

Scouras, A. D., & Daggett, V. (2011). The dynameomics rotamer library: Amino acid side chain conformations and dynamics from comprehensive molecular dynamics simulations in water. *Protein Science*, *20*(2), 341–352. https://doi.org/10.1002/pro.565

Senoo, K., & Wada, H. (1989). Isolation and identification of an aerobic γ-HCH-decomposing bacterium from soil. *Soil Science and Plant Nutrition*, *35*(1), 79–87. https://doi.org/10.1080/00380768.1989.10434739

Sharma, P., Jindal, S., Bala, K., Kumari, K., Niharika, N., Kaur, J., Pander, G., Pander, R., Russell, R. J., Oakeshott, J. G., & Lal, R. (2014). Functional screening of enzymes and bacteria for the dechlorination of hexachlorocyclohexane by a high-throughput colorimetric assay. *Biodegradation*, *25*(2), 179–187. https://doi.org/10.1007/s10532-013-9650-5

Sharma, P., Pandey, R., Kumari, K., Pandey, G., Jackson, C. J., Russell, R. J., Oakeshott, J. G., & Lal, R. (2011). Kinetic and sequence-structure-function analysis of known LinA variants with different hexachlorocyclohexane isomers. *PLoS ONE*, *6*(9), 7–10. https://doi.org/10.1371/journal.pone.0025128

Sharma, P., Raina, V., Kumari, R., Malhotra, S., Dogra, C., Kumari, H., Kohler, H. P. E., Buser, H. –

R., Holliger, C., & Lal, R. (2006). Haloalkane dehalogenase LinB is responsible for β- and δ-hexachlorocyclohexane transformation in *Sphingobium indicum* B90A. *Applied and Environmental Microbiology*, *72*(9), 5720–5727. https://doi.org/10.1128/AEM.00192-06

Sharom, M. S., Miles, J. R. W., Harris, C. R., & McEwen, F. L. (1980). Persistence of 12 insecticides in water. *Water Research*, *14*(8), 1089–1093. https://doi.org/10.1016/0043-1354(80)90157-8

Shrivastava, N., Macwan, A. S., Kohler, H. P. E., & Kumar, A. (2017). Important amino acid residues of hexachlorocyclohexane dehydrochlorinases (LinA) for enantioselective transformation of hexachlorocyclohexane isomers. *Biodegradation*, *28*(2–3), 171–180. https://doi.org/10.1007/s10532-017-9786-9

Shrivastava, N., Prokop, Z., & Kumar, A. (2015). Novel LinA type 3 δ-hexachlorocyclohexane dehydrochlorinase. *Applied and Environmental Microbiology*, *81*(21), 7553–7559. https://doi.org/10.1128/aem.01683-15

Singh, A. K., Chaudhary, P., Macwan, A. S., Diwedi, U. N., & Kumar, A. (2007). Selective loss of *lin* genes from hexachlorocyclohexane-degrading *Pseudomonas aeruginosa* ITRC-5 under different growth conditions. *Applied Microbiology and Biotechnology*, *76*(4), 895–901. https://doi.org/10.1007/s00253-007-1056-z

Singh, A. K., Sangwan, N., Sharma, A., Gupta, V., Khurana, J. P., & Lal, R. (2013). Draft genome sequence of *Sphingobium quisquiliarum* strain P25T, a novel hexachlorocyclohexane (HCH)-degrading bacterium isolated from an HCH dumpsite. *Genome Announcements*, *1*(5), e00717-13. https://doi.org/10.1128/genomeA.00717-13

Singh, G., Kathpal, T. S., Spencer, W. F., & Dhankar, J. S. (1991). Dissipation of some organochlorine insecticides in cropped and uncropped soil. *Environmental Pollution*, *70*(3), 219–239. https://doi.org/10.1016/0269-7491(91)90011-K

Soltaninejad, K., & Shadnia, S. (2014). History of the use and epidemiology of

organophosphorus poisoning. In M. Balali-Mood & M. Abdollahi (Eds.), *Basic and Clinical Toxicology of Organophosphorus Compounds* (pp. 25–43). London: Springer London. https://doi.org/10.1007/978-1-4471-5625-3_2

Suar, M., Hauser, A., Poiger, T., Buser, H.-R., Müller, M. D., Dogra, C., Raina, V., Holliger, C., van der Meer, J. R., Lal, R., & Kohler, H. P. E. (2005). Enantioselective transformation of α-hexachlorocyclohexane by the dehydrochlorinases LinA1 and LinA2 from the soil bacterium *Sphingomonas paucimobilis* B90A. *Applied and Environmental Microbiology*, *71*(12), 8514–8518. https://doi.org/10.1128/AEM.71.12.8514

Szeto, S. Y., & Price, P. M. (1991). Persistence of pesticide residues in mineral and organic soils in the Fraser Valley of British Columbia. *Journal of Agricultural and Food Chemistry*, *39*(9), 1679–1684. https://doi.org/10.1021/jf00009a027

Tabata, M., Endo, R., Ito, M., Ohtsubo, Y., Kumar, A., Tsuda, M., & Nagata, Y. (2011). The *lin* genes for γ-hexachlorocyclohexane degradation in *Sphingomonas* sp. MM-1 proved to be dispersed across multiple plasmids. *Bioscience, Biotechnology, and Biochemistry*, *75*(3), 466–472. https://doi.org/10.1271/bbb.100652

Tabata, M., Ohhata, S., Kawasumi, T., Nikawadori, Y., Kishida, K., Sato, T., Ohtsubo, Y., Tsuda, M., & Nagata, Y. (2016a). Complete genome sequence of a γ-hexachlorocyclohexane degrader, *Sphingobium* sp. strain TKS, isolated from a γ-hexachlorocyclohexane-degrading microbial community. *Genome Announcements*, *4*(2). https://doi.org/10.1128/genomeA.00247-16.Copyright

Tabata, M., Ohhata, S., Nikawadori, Y., Kishida, K., Sato, T., Kawasumi, T., Kato, H., Ohtsubo, Y., Tsuda, M., & Nagata, Y. (2016b). Comparison of the complete genome sequences of four γ-hexachlorocyclohexane-degrading bacterial strains: Insights into the evolution of bacteria able to degrade a recalcitrant man-made pesticide. *DNA Research*, *23*(6), 581–599. https://doi.org/10.1093/dnares/dsw041

Tabata, M., Ohhata, S., Nikawadori, Y., Sato, T., Kishida, K., Ohtsubo, Y., Tsuda, M., & Nagata, Y. (2016c). Complete genome sequence of a γ-hexachlorocylohexane-degrading bacterium, *Sphingobium* sp. strain MI1205. *Genome Announcements*, *4*(2). https://doi.org/10.1128/genomeA.00956-15.Copyright

Tabata, M., Ohtsubo, Y., Ohhata, S., Tsuda, M., & Nagata, Y. (2013). Complete genome sequence of the γ-hexachlorocyclohexane-degrading bacterium *Sphingomonas* sp. strain MM-1. *Genome Announcements*, *1*(3), e00247-13. https://doi.org/10.1128/genomeA.00247-13.Copyright

Tanaka, K. (2015). γ-BHC: Its history and mystery – why is only γ-BHC insecticidal? *Pesticide Biochemistry and Physiology*, *120*, 91–100. https://doi.org/10.1016/j.pestbp.2015.01.010

Taylor, E. L. (1945). Acaricidal property of a new insecticide, hexachlorobenzene. *Nature*, *155*, 393–394.

The new POPs under the Stockholm Convention. (2017). Stockholm Convention. Retrieved March 1, 2018, from http://chm.pops.int/TheConvention/ThePOPs/TheNewPOPs/tabid/2511/Default.aspx

Thomas, J.-C., Berger, F., Jacquier, M., Bernillon, D., Baud-Grasset, F., Truffaut, N., Normand, P., Vogel, T. M., & Simonet, P. (1996). Isolation and characterization of a novel γ-hexachlorocyclohexane-degrading bacterium. *Journal of Bacteriology*, *178*(20), 6049–6055.

Trantírek, L., Hynková, K., Nagata, Y., Murzin, A. G., Ansorgová, A., Sklenář, V., & Damborský, J. (2001). Reaction mechanism and stereochemistry of γ-hexachlorocyclohexane dehydrochlorinase LinA. *Journal of Biological Chemistry*, *276*(11), 7734–7740. https://doi.org/10.1074/jbc.M007452200

Trott, O., & Olson, A. J. (2010). AutoDock Vina: Improving the speed and accuracy of docking with a new scoring function, efficient optimization, and multithreading. *Journal of*

Computational Chemistry, *31*(2), 455–461. https://doi.org/10.1002/jcc.21334

van der Linden, T. (1912). Uber die benzol-hexachloride und ihren zerfall in trichlor-benzole. *European Journal of Inorganic Chemistry*, *45*(1), 231–247.

van der Meer, J. R., Neerven, A. R. W. Van, Vries, E. J. De, Vos, W. M. De, & Zehnder, A. J. B. (1991). Cloning and characterization of plasmid-encoded genes for the degradation of 1,2-dichloro-, 1,4-dichloro-, and 1,2,4- trichlorobenzene of *Pseudomonas* sp. strain P51. *Journal of Bacteriology*, *173*(1), 6–15.

Vijgen, J., Abhilash, P. C., Li, Y. F., Lal, R., Forter, M., Torres, J., Singh, N., Yunus, M., Tian, C., Schaffer, A., & Weber, R. (2011). Hexachlorocyclohexane (HCH) as new Stockholm Convention POPs-a global perspective on the management of Lindane and its waste isomers. *Environmental Science and Pollution Research*, *18*(2), 152–162. https://doi.org/10.1007/s11356-010-0417-9

Vijgen, J., Yi, L. F., Forter, M., Lal, R., & Weber, R. (2006). The legacy of lindane and technical HCH production. *Organohalogen Compounds*, *68*, 899–904.

Voldner, E. C., & Li, Y. F. (1995). Global usage of selected persistent organochlorines. *Science of the Total Environment*, *160–161*, 201–210. https://doi.org/10.1016/0048-9697(95)04357-7

Weber, R., Gaus, C., Tysklind, M., Johnston, P., Forter, M., Hollert, H., Heinisch, E., Holoubek, I., Lloyd-Smith, M., Masunaga, S., Moccarelli, P., Santillo, D., Seike, N., Symons, R., Torres, J. P. M., Verta, M., Varbelow, G., Vijgen, J., Watson, A., Costner, P., Woelz, J., Wycisk, P., & Zennegg, M. (2008). Dioxin- and POP-contaminated sites - Contemporary and future relevance and challenges: Overview on background, aims and scope of the series. *Environmental Science and Pollution Research*, *15*(5), 363–393. https://doi.org/10.1007/s11356-008-0024-1

Wilding, M., Scott, C., & Warden, A. C. (2018). Computer-guided surface engineering for

enzyme improvement. *Scientific Reports*, *8*(1), 1–7. https://doi.org/10.1038/s41598-018-30434-5

Willett, K. L., Ulrich, E. M., & Hites, R. A. (1998). Differential toxicity and environmental fates of hexachlorocyclohexane isomers. *Environmental Science and Technology*, *32*(15), 2197–2207. https://doi.org/10.1021/es9708530

Wu, J., Hong, Q., Sun, Y., Hong, Y., Yan, Q., & Li, S. (2007). Analysis of the role of LinA and LinB in biodegradation of d-hexachlorocyclohexane. *Environmental Microbiology*, *9*(9), 2331–2340. https://doi.org/10.1111/j.1462-2920.2007.01350.x

Yamamoto, S., Otsuka, S., Murakami, Y., Nishiyama, M., & Senoo, K. (2009). Genetic diversity of γ-hexachlorocyclohexane-degrading *Sphingomonads* isolated from a single experimental field. *Letters in Applied Microbiology*, *49*(4), 472–477. https://doi.org/10.1111/j.1472-765X.2009.02691.x

Yule, W. N., Chiba, M., & Morley, H. V. (1967). Fate of insecticide residues. decomposition of lindane in soil. *Journal of Agricultural and Food Chemistry*, *15*(6), 1000–1004. https://doi.org/10.1021/jf60154a037

Zdravkovski, Z. (2004). Theoretical study of the stability of hexachloro- and hexafluorocyclohexane isomers. *Bulletin of the Chemists and Technologists of Macedonia*, *23*(2), 131–137.

Zoeteman, B. C. J., Harmsen, K., Linders, J. B. H. J., Morra, C. F. H., & Slooff, W. (1980). Persistent organic pollutants in river water and ground water of the Netherlands. *Chemosphere*, *9*(4), 231–249. https://doi.org/10.1016/0045-6535(80)90080-6

Bajaj, S., Sagar, S., Khare, S., & Singh, D. K. (2017). Biodegradation of γ-hexachlorocyclohexane (lindane) by halophilic bacterium Chromohalobacter sp. LD2 isolated from HCH dumpsite. *International Biodeterioration and Biodegradation*, *122*, 23–28.

https://doi.org/10.1016/j.ibiod.2017.04.014

Bala, K., Geueke, B., Miska, M. E., Rentsch, D., Poiger, T., Dadhwal, M., … Kohler, H. P. E. (2012). Enzymatic conversion of e-hexachlorocyclohexane and a heptachlorocyclohexane isomer, two neglected components of technical hexachlorocyclohexane. *Environmental Science and Technology*, *46*(7), 4051–4058. https://doi.org/10.1021/es204143x

Bar-Even, A., Noor, E., Savir, Y., Liebermeister, W., Davidi, D., Tawfik, D. S., & Milo, R. (2011). The moderately efficient enzyme: Evolutionary and physicochemical trends shaping enzyme parameters. *Biochemistry*, *50*(21), 4402–4410. https://doi.org/10.1021/bi2002289

Bickelhaupt, F. M. (2001). Base-induced 1,4-elimination: Insights from theory and mass spectrometry. *Mass Spectrometry Reviews*, *20*, 347–361. https://doi.org/10.1002/mas.10007

Bidleman, T. F., Jantunen, L. M., Falconer, R. L., Barrie, L. A., & Fellin, P. (1995). Decline of hexachlorocyclohexane in the Arctic atmosphere and reversal of air-sea gas exchange. *Geophysical Research Letters*, *22*(3), 219–222. https://doi.org/10.1029/94GL02990

Böltner, D., Moreno-Morillas, S., & Ramos, J. L. (2005). 16S rDNA phylogeny and distribution of lin genes in novel hexachlorocyclohexane-degrading Sphingomonas strains. *Environmental Microbiology*, *7*(9), 1329–1338. https://doi.org/10.1111/j.1462-5822.2005.00820.x

Bosma, T. N. P., van der Meer, J. R., Schraa, G., Tros, M. E., & Zehnder, A. J. B. (1988). Reductive dechlorination of all trichloro- and dichlorobenzene isomers. *FEMS Microbiology Letters*, *53*(3–4), 223–229. https://doi.org/10.1016/0378-1097(88)90446-6

Bourne, L. B. (1945). Hexachlorocyclohexane as an insecticide. *Nature*, *395*, 85.

Brittain, D. R. B., Pandey, R., Kumari, K., Sharma, P., Pandey, G., Lal, R., … Jackson, C. J. (2011).

Competing SN2 and E2 reaction pathways for hexachlorocyclohexane degradation in the gas phase, solution and enzymes. *Chemical Communications*, *47*, 976–978. https://doi.org/10.1039/c0cc02925d

Buser, H.-R., & Mueller, M. D. (1995). Isomer and enantioselective degradation of hexachlorocyclohexane isomers in sewage sludge under anaerobic conditions. *Environmental Science & Technology*, *29*(3), 664–672. https://doi.org/10.1021/es00003a013

Campbell, R. G. (1951). *Patent No. US2573676A*. United States of America: US Grant.

Case, D. A., Ben-Shalom, I. Y., Brozell, S. R., Cerutti, D. S., Cheatham, T. E., Cruzeiro, V. W. D., … Kollman, P. A. (2018). *Amber18*. San Francisco: University of California.

Cérémonie, H., Boubakri, H., Mavingui, P., Simonet, P., & Vogel, T. M. (2006). Plasmid-encoded γ-hexachlorocyclohexane degradation genes and insertion sequences in Sphingobium francense (ex-Sphingomonas paucimobilis Sp+). *FEMS Microbiology Letters*, *257*(2), 243–252. https://doi.org/10.1111/j.1574-6968.2006.00188.x

Cortes, D. R., & Hites, R. A. (2000). Detection of statistically significant trends in atmospheric concentrations of semivolatile compounds. *Environmental Science and Technology*, *34*(13), 2826–2829. https://doi.org/10.1021/es990466l

Cristol, S. J., Hause, N. L., & Meek, J. S. (1951). Mechanisms of elimination reactions. III. The kinetics of the alkaline dehydrochlorination of the benzene hexachloride isomers. II. *Journal of the American Chemical Society*, *73*(2), 674–679. https://doi.org/10.1021/ja01146a050

Darden, T., York, D., & Pedersen, L. (1993). Particle mesh Ewald: An N.log(N) method for Ewald sums in large systems. *Journal of Chemical Physics*, *98*(12), 10089–10092. https://doi.org/10.1063/1.464397

Dassault Systèmes BIOVIA. (2017). *BIOVIA Materials Studio*. Retrieved from http://accelrys.com/products/collaborative-science/biovia-materials-studio/

De Souza, M. L., Sadowsky, M. J., & Wackett, L. P. (1996). Atrazine chlorohydrolase from Pseudomonas sp. strain ADP: Gene sequence, enzyme purification, and protein characterization. *Journal of Bacteriology*, *178*(16), 4894–4900.

Dogra, C., Raina, V., Pal, R., Suar, M., Lal, S., Gartemann, K., … van der Meer, J. R. (2004). Organization of lin genes and IS6100 among different strains of Sphingomonas paucimobilis : Evidence for horizontal gene transfer. *Journal of Bacteriology*, *186*(8), 2225–2235. https://doi.org/10.1128/JB.186.8.2225

Endo, R., Kamakura, M., Miyauchi, K., Fukuda, M., Ohtsubo, Y., Tsuda, M., & Nagata, Y. (2005). Identification and characterization of genes involved in the downstream degradation pathway of γ -hexachlorocyclohexane in Sphingomonas paucimobilis UT26. *Journal of Bacteriology*, *187*(3), 847–853. https://doi.org/10.1128/JB.187.3.847

Endo, R., Ohtsubo, Y., Tsuda, M., & Nagata, Y. (2007). Identification and characterization of genes encoding a putative ABC-type transporter essential for utilization of γ-hexachlorocyclohaxane in Sphingobium japonicum UT26. *Journal of Bacteriology*, *189*(10), 3712–3720. https://doi.org/10.1128/JB.01883-06

FAISD Handbook. (2018). Retrieved March 1, 2018, from https://apvma.gov.au/node/26586

Faraday, M. (1825). On new compounds of carbon and hydrogen, and on certain other products obtained during the decomposition of oil by heat. *Philosophical Transactions of the Royal Society of London*, *115*, 440–466. https://doi.org/10.1098/rstl.1825.0022

Geueke, B., Miska, M. E., Poiger, T., Rentsch, D., Lal, R., Holliger, C., & Kohler, H. P. E. (2013). Enantioselective dehydrochlorination of δ-hexachlorocyclohexane and δ-pentachlorocyclohexene by LinA1 and LinA2 from Sphingobium Indicum B90A. *Applied and Environmental Microbiology*, *79*(19), 6180–6183.

https://doi.org/10.1128/AEM.01770-13

Glotfelty, D. E., Taylor, A. W., Turner, B. C., & Zoller, W. H. (1984). Volatilization of surface-applied pesticides from fallow soil. *Journal of Agricultural and Food Chemistry*, *32*(3), 638–643. https://doi.org/10.1021/jf00123a053

Gregor, D. J., & Gummer, W. D. (1989). Evidence of atmospheric transport and deposition of organochlorine pesticides and polychlorinated biphenyls in Canadian Arctic snow. *Environmental Science and Technology*, *23*(5), 561–565. https://doi.org/10.1021/es00063a008

Gronert, S., & Kass, S. R. (1997). Theoretical studies of eliminations. 6. The regiochemistry and stereochemistry of the gas-phase reactions of 3-halocyclohexenes with fluoride. An ab initio study. *The Journal of Organic Chemistry*, *62*(23), 7991–8000. https://doi.org/10.1021/jo970626g

Hargrave, B. T., Vass, W. P., Erickson, P. E., & Fowler, B. R. (1988). Atmospheric transport of organochlorines to the Arctic Ocean. *Tellus B: Chemical and Physical Meteorology*, *40*(5), 480–493. https://doi.org/10.1111/j.1600-0889.1988.tb00118.x

Hartley, W. N. (1881). Researches on the relation between the molecular structure of carbon compounds, and their absorption spectra. *Journal of the Chemical Society, Transactions*, *39*, 153–168.

Hoops, S., Sahle, S., Gauges, R., Lee, C., Pahle, J., Simus, N., … Kummer, U. (2006). COPASI - A COmplex PAthway SImulator. *Bioinformatics*, *22*(24), 3067–3074. https://doi.org/10.1093/bioinformatics/btl485

Horne, I., Sutherland, T. D., Harcourt, R. L., Russell, R. J., & Oakeshott, J. G. (2002). Identification of an opd (organophosphate degradation) gene in an Agrobacterium isolate. *Applied and Environmental Microbiology*, *68*(7), 3371–3376. https://doi.org/10.1128/AEM.68.7.3371

Humphrey, W., Dalke, A., & Schulten, K. (1996). VMD: Visual Molecular Dynamics. *Journal of Molecular Graphics*, *14*, 33–38. https://doi.org/10.1016/0263-7855(96)00018-5

Imai, R., Nagata, Y., Fukuda, M., Takagi, M., & Yano, K. (1991). Molecular cloning of a Pseudomonas paucimobilis gene encoding a 17-kilodalton polypeptide that eliminates HCl molecules from g-hexachlorocyclohexane. *Journal of Bacteriology*, *173*(21), 6811–6819. https://doi.org/10.1128/JB.173.21.6811-6819.1991

Immig, J. (2010). A List of Australia's Most Dangerous Pesticides. *National Toxics Network*, (July), 1–17. Retrieved from http://awsassets.wwf.org.au/downloads/fs025_a_list_of_australias_most_dangerous_pesticides_1jul10.pdf

Ito, M., Prokop, Z., Klvaňa, M., Otsubo, Y., Tsuda, M., Damborský, J., & Nagata, Y. (2007). Degradation of b-hexachlorocyclohexane by haloalkane dehalogenase LinB from g-hexachlorocyclohexane-utilizing bacterium Sphingobium sp. MI1205. *Archives of Microbiology*, *188*(4), 313–325. https://doi.org/10.1007/s00203-007-0251-8

Iwata, H., Tanabe, S., Sakal, N., & Tatsukawa, R. (1993). Distribution of persistent organochiorines in the oceanic air and surface seawater and the role of ocean on their global transport and fate. *Environmental Science and Technology*, *27*(6), 1080–1098. https://doi.org/10.1021/es00043a007

Jürgens, H. J., & Roth, R. (1989). Case study and proposed decontamination steps of the soil and groundwater beneath a closed herbicide plant in Germany. *Chemosphere*, *18*(1–6), 1163–1169. https://doi.org/10.1016/0045-6535(89)90250-6

Kaur, H., Kapoor, S., & Kaur, G. (2016). Application of ligninolytic potentials of a white-rot fungus Ganoderma lucidum for degradation of lindane. *Environmental Monitoring and Assessment*, *188*(10). https://doi.org/10.1007/s10661-016-5606-7

Kelley, L. A., Mezulis, S., Yates, C. M., Wass, M. N., & Sternberg, M. J. E. (2015). The Phyre2 web

portal for protein modeling, prediction and analysis. *Nature Protocols*, *10*(6), 845–858. https://doi.org/10.1038/nprot.2015-053

Kidd, H., & James, D. R. (Eds.). (1991). *The Agrochemicals Handbook* (3rd ed.). Cambridge, England: Royal Society of Chemistry, Information Services.

Kohli, P., Dua, A., Sangwan, N., Oldach, P., Khurana, J. P., & Lal, R. (2013). Draft genome sequence of a hexachlorocyclohexane-degrading bacterium. *Genome Announcements*, *1*(6), e00956-13. https://doi.org/10.1128/genomeA.00715-13.Kumar

Kumar, M., Chaudhary, P., Dwivedi, M., Kumar, R., Paul, D., Jain, R. K., … Kumar, A. (2005). Enhanced biodegradation of β- and δ-hexachlorocyclohexane in the presence of α- and g-isomers in contaminated soils. *Environmental Science and Technology*, *39*(11), 4005–4011. https://doi.org/10.1021/es048497q

Kumari, R., Subudhi, S., Suar, M., Dhingra, G., Raina, V., Dogra, C., … Lal, R. (2002). Cloning and characterization of lin genes responsible for the degradation of hexachlorocyclohexane isomers by Sphingomonas paucimobilis strain B90. *Applied and Environmental Microbiology*, *68*(12), 6021–6028. https://doi.org/10.1128/AEM.68.12.6021-6028.2002

Lal, R., Dogra, C., Malhotra, S., Sharma, P., & Pal, R. (2006). Diversity, distribution and divergence of lin genes in hexachlorocyclohexane-degrading sphingomonads. *Trends in Biotechnology*, *24*(3), 121–130. https://doi.org/10.1016/j.tibtech.2006.01.005

Lal, R., Pandey, G., Sharma, P., Kumari, K., Malhotra, S., Pandey, R., … Oakeshott, J. G. (2010). Biochemistry of microbial degradation of hexachlorocyclohexane and prospects for bioremediation. *Microbiology and Molecular Biology Reviews*, *74*(1), 58–80. https://doi.org/10.1128/MMBR.00029-09

Li, Y. F. (1999). Global technical hexachlorocyclohexane usage and its contamination consequences in the environment: From 1948 to 1997. *Science of the Total Environment*, *232*(3), 121–158. https://doi.org/10.1016/S0048-9697(99)00114-X

Liu, S., & Suflita, J. M. (1993). Ecology and evolution of microbial populations for bioremediation. *Trends in Biotechnology*, *11*(8), 344–352.

Luek, J. L., Dickhut, R. M., Cochran, M. A., Falconer, R. L., & Kylin, H. (2017). Persistent organic pollutants in the Atlantic and southern oceans and oceanic atmosphere. *Science of the Total Environment*, *583*, 64–71. https://doi.org/10.1016/j.scitotenv.2016.12.189

MacRae, I. C., Raghu, K., & Bautista, E. M. (1969). Anaerobic degradation of the insecticide lindane by Clostridium sp. *Nature*, *221*, 859–860. https://doi.org/10.1038/224488a0

Macwan, A. S., Javed, S., & Kumar, A. (2011). Isolation of a novel thermostable dehydrochlorinase (LinA) from a soil metagenome. *3 Biotech*, *1*(4), 193–198. https://doi.org/10.1007/s13205-011-0012-x

Macwan, A. S., Kukshal, V., Shrivastava, N., Javed, S., Kumar, A., & Ramachandran, R. (2012). Crystal structure of the hexachlorocyclohexane dehydrochlorinase (LinA-Type2): Mutational analysis, thermostability and enantioselectivity. *PLoS ONE*, *7*(11). https://doi.org/10.1371/journal.pone.0050373

Mahillon, J., & Chandler, M. (1998). Insertion sequences. *Microbioliology and Molecular Biology Review*, *62*(3), 725-74. https://doi.org/10.1016/B978-0-12-374984-0.00799-3

Mandelbaum, R. T., Sadowsky, M. J., & Wackett, L. P. (2008). Microbial degradation of s-triazine herbicides. In H. M. LeBaron, J. E. MacFarland, & O. C. Burnside (Eds.), *The triazine herbicides* (1st ed., pp. 301–328). Elsevier B.V.

Manickam, N., Reddy, M. K., Saini, H. S., & Shanker, R. (2008). Isolation of hexachlorocyclohexane-degrading Sphingomonas sp. by dehalogenase assay and characterization of genes involved in γ-HCH degradation. *Journal of Applied Microbiology*, *104*(4), 952–960. https://doi.org/10.1111/j.1365-2672.2007.03610.x

Manna, R. N., & Dybala-Defratyka, A. (2013). Insights into the elimination mechanisms

employed for the degradation of different hexachlorocyclohexane isomers using kinetic isotope effects and docking studies. *Journal of Physical Organic Chemistry*, *26*(10), 797–804. https://doi.org/10.1016/j.jhydrol.2007.12.015

Manna, R. N., Zinovjev, K., Tuñón, I., & Dybala-Defratyka, A. (2015). Dehydrochlorination of hexachlorocyclohexanes catalyzed by the LinA dehydrohalogenase. A QM/MM study. *Journal of Physical Chemistry B*, *119*(49), 15100–15109. https://doi.org/10.1021/acs.jpcb.5b07538

Marco-Urrea, E., Pérez-Trujillo, M., Caminal, G., & Vicent, T. (2009). Dechlorination of 1,2,3- and 1,2,4-trichlorobenzene by the white-rot fungus Trametes versicolor. *Journal of Hazardous Materials*, *166*(2–3), 1141–1147. https://doi.org/10.1016/j.jhazmat.2008.12.076

Marinucci, A. C., & Bartha, R. (1979). Biodegradation of 1,2,3- and 1,2,4-trichlorobenzene in soil and in liquid enrichment culture. *Applied and Environmental Microbiology*, *38*(5), 811–817.

Mertens, B., Boon, N., & Verstraete, W. (2006). Slow-release inoculation allows sustained biodegradation of γ-hexachlorocyclohexane. *Applied and Environmental Microbiology*, *72*(1), 622–627. https://doi.org/10.1128/AEM.72.1.622-627.2006

Miyauchi, K., Adachi, Y., Nagata, Y., & Takagi, M. (1999). Cloning and sequencing of a novel meta-cleavage dioxygenase gene whose product is involved in degradation of γ -hexachlorocyclohexane in Sphingomonas paucimobilis. *Journal of Bacteriology*, *181*(21), 6712–6719.

Miyauchi, K., Lee, H.-S., Fukuda, M., Takagi, M., & Nagata, Y. (2002). Cloning and characterization of linR, involved in regulation of the downstream pathway for g-hexachlorocyclohexane degradation in Sphingomonas paucimobilis UT26. *Applied and Environmental Microbiology*, *68*(4), 1803–1807. https://doi.org/10.1128/JB.187.3.847-

853.2005

Miyauchi, K., Suh, S.-K., Nagata, Y., & Takagi, M. (1998). Cloning and sequencing of a 2,5-dichlorohydroquinone reductive dehalogenase gene whose product is involved in degradation of g-hexachlorocyclohexane by Sphingomonas paucimobilis. *Journal of Bacteriology*, *180*(6), 1354–1359.

Nagasawa, S., Kikuchi, R., Nagata, Y., Takagi, M., & Matsuo, M. (1993a). Aerobic mineralization of γ-HCH by Pseudomonas paucimobilis UT26. *Chemosphere*, *26*(9), 1719–1728. https://doi.org/10.1016/0045-6535(93)90115-L

Nagasawa, S., Kikuchi, R., Nagata, Y., Takagi, M., & Matsuo, M. (1993b). Stereochemical analysis of g-HCH degradation by Pseudomonas paucimobilis UT26. *Chemosphere*, *26*(6), 1187–1201. https://doi.org/10.1016/0045-6535(93)90205-J

Nagata, Y., Endo, R., Ito, M., Ohtsubo, Y., & Tsuda, M. (2007). Aerobic degradation of lindane (g-hexachlorocyclohexane) in bacteria and its biochemical and molecular basis. *Applied Microbiology and Biotechnology*, *76*(4), 741–752. https://doi.org/10.1007/s00253-007-1066-x

Nagata, Y., Hatta, T., Imai, R., Kimbara, K., Fukuda, M., Yano, K., & Takagi, M. (1993). Purification and characterization of g-hexachlorocyclohexane (g-HCH) dehydrochlorinase (LinA) from Pseudomonas paucimobilis. *Bioscience, Biotechnology, and Biochemistry*, *57*(9), 1582–1583.

Nagata, Y., Imai, R., Sakai, A., Fukuda, M., Yano, K., & Takagi, M. (1993). Isolation and characterization of Tn5-induced mutants of Pseudomonas paucimobilis UT26 defective in g-hexachlorocyclohexane dehydrochlorinase (LinA). *Bioscience, Biotechnology, and Biochemistry*, *57*(5), 703–709. https://doi.org/10.1271/bbb.57.703

Nagata, Y., Miyauchi, K., & Takagi, M. (1999). Complete analysis of genes and enzymes for g-hexachlorocyclohexane degradation in Sphingomonas paucimobilis UT26. *Journal of*

Industrial Microbiology and Biotechnology, *23*, 380–390. https://doi.org/10.1038/sj.jim.2900736

Nagata, Y., Mori, K., Takagi, M., Murzin, A. G., & Damborský, J. (2001). Identification of protein fold and catalytic residues of g-hexachlorocyclohexane dehydrochlorinase LinA. *Proteins*, *45*(4), 471–477. Retrieved from http://www.ncbi.nlm.nih.gov/pubmed/11746694

Nagata, Y., Nariya, T., Ohtomo, R., Fukuda, M., Yano, K., & Takagi, M. (1993). Cloning and sequencing of a dehalogenase gene encoding an enzyme with hydrolase activity involved in the degradation of g-hexachlorocyclohexane in Pseudomonas paucimobilis. *Journal of Bacteriology*, *175*(20), 6403–6410.

Nagata, Y., Natsui, S., Endo, R., Ohtsubo, Y., Ichikawa, N., Ankai, A., … Tsuda, M. (2011). Genomic organization and genomic structural rearrangements of Sphingobium japonicum UT26, an archetypal γ-hexachlorocyclohexane-degrading bacterium. *Enzyme and Microbial Technology*, *49*(6–7), 499–508. https://doi.org/10.1016/j.enzmictec.2011.10.005

Nagata, Y., Ohtomo, R., Miyauchi, K., Fukuda, M., Yano, K., & Takagi, M. (1994). Cloning and sequencing of a 2,5-dichloro-2,5-cyclohexadiene-1,4-diol dehydrogenase gene involved in the degradation of g-hexachlorocyclohexane in Pseudomonas paucimobilis. *Journal of Bacteriology*, *176*(11), 3117–3125. https://doi.org/10.1128/JB.175.20.6403-6410.1993

Nagata, Y., Ohtsubo, Y., Endo, R., Ichikawa, N., Ankai, A., Oguchi, A., … Tsuda, M. (2010). Complete genome sequence of the representative γ- hexachlorocyclohexane-degrading bacterium Sphingobium japonicum UT26. *Journal of Bacteriology*, *192*(21), 5852–5853. https://doi.org/10.1128/JB.00961-10

Nagata, Y., Prokop, Z., Sato, Y., Jerabek, P., Kumar, A., Ohtsubo, Y., … Damborský, J. (2005). Degradation of β -hexachlorocyclohexane by haloalkane dehalogenase LinB from Sphingomonas paucimobilis UT26. *Applied and Environmental Microbiology*, *71*(4), 2183–

2185. https://doi.org/10.1128/AEM.71.4.2183

Nalin, R., Simonet, P., Vogel, T. M., & Normand, P. (1999). Rhodanobacter lindaniclasticus gen. nov., sp. nov., a lindane-degrading bacterium. *International Journal of Systematic Bacteriology*, (49), 19–23.

National Toxicology Program. (2016a). Lindane, hexachlorocyclohexane (technical grade), and other hexachlorocyclohexane isomers. In *Report on carcinogens, 14th Edition*. Retrieved from https://ntp.niehs.nih.gov/ntp/roc/content/profiles/lindane.pdf

National Toxicology Program. (2016b). Substances listed in the Fourteenth Report on Carcinogens. In *Report on carcinogens, 14th Edition*. Retrieved from http://ntp.niehs.nih.gov/go/roc14

Okai, M., Kubota, K., Fukuda, M., Nagata, Y., Nagata, K., & Tanokura, M. (2010). Crystal structure of g-hexachlorocyclohexane dehydrochlorinase LinA from Sphingobium japonicum UT26. *Journal of Molecular Biology*, *403*(2), 260–269. https://doi.org/10.1016/j.jmb.2010.08.043

Okeke, B. C., Siddique, T., Arbestain, M. C., & Frankenberger, W. T. (2002). Biodegradation of g-hexachlorocyclohexane (Lindane) and a-hexachlorocyclohexane in water and a soil slurry by a Pandoraea species. *Journal of Agricultural and Food Chemistry*, *50*(9), 2548–2555. https://doi.org/10.1021/jf011422a

Olsson, M. H. M., Søndergaard, C. R., Rostkowski, M., & Jensen, J. H. (2011). PROPKA3: Consistent treatment of internal and surface residues in empirical pKa predictions. *Journal of Chemical Theory and Computation*, *7*(2), 525–537. https://doi.org/10.1021/ct100578z

Orloff, H. D., & Kolka, A. J. (1954). The mechanism of dehydrohalogenation of benzene tetrachloride and related compounds. *Journal of the American Chemical Society*, *76*(21), 5484–5490. https://doi.org/10.1021/ja01650a068

Pearce, S. L. (2015). *Acquisition and ongoing evolution of synthetic xenobiotic metabolic pathways in soil bacteria*. Australian National University.

Pearce, S. L., Oakeshott, J. G., & Pandey, G. (2015). Insights into ongoing evolution of the hexachlorocyclohexane catabolic pathway from comparative genomics of ten Sphingomonadaceae strains. *G3-Genes Genomes Genetics*, *5*(6), 1081–1094. https://doi.org/10.1534/g3.114.015933

Pettersen, E. F., Goddard, T. D., Huang, C. C., Couch, G. S., Greenblatt, D. M., Meng, E. C., & Ferrin, T. E. (2004). UCSF Chimera - A visualization system for exploratory research and analysis. *Journal of Computational Chemistry*, *25*(13), 1605–1612. https://doi.org/10.1002/jcc.20084

Raina, V., Hauser, A., Buser, H.-R., Rentsch, D., Sharma, P., Lal, R., … Kohler, H. P. E. (2007). Hydroxylated metabolites of b- and d-hexachlorocyclohexane: Bacterial formation, stereochemical configuration, and occurrence in groundwater at a former production site. *Environmental Science and Technology*, *41*(12), 4291–4298. https://doi.org/10.1021/es062908g

Raina, V., Suar, M., Singh, A., Prakash, O., Dadhwal, M., Gupta, S. K., … Lal, R. (2008). Enhanced biodegradation of hexachlorocyclohexane (HCH) in contaminated soils via inoculation with Sphingobium indicum B90A. *Biodegradation*, *19*(1), 27–40. https://doi.org/10.1007/s10532-007-9112-z

Ramsey, L., & Patterson, W. (1946). Separation and purification of some constituents of commercial hexachlorocyclohexane. *Journal of Association of Official Agricultural Chemists*, *29*, 337.

Sahu, S. K., Patnaik, K. K., Sharmila, M., & Sethunathan, N. (1990). Degradation of a-, b-, and g-hexachlorocyclohexane by a soil bacterium under aerobic conditions. *Applied and Environmental Microbiology*, *56*(11), 3620–3622.

Scouras, A. D., & Daggett, V. (2011). The dynameomics rotamer library: Amino acid side chain conformations and dynamics from comprehensive molecular dynamics simulations in water. *Protein Science*, *20*(2), 341–352. https://doi.org/10.1002/pro.565

Senoo, K., & Wada, H. (1989). Isolation and identification of an aerobic γ-HCH-decomposing bacterium from soil. *Soil Science and Plant Nutrition*, *35*(1), 79–87. https://doi.org/10.1080/00380768.1989.10434739

Sharma, Pooja, Jindal, S., Bala, K., Kumari, K., Niharika, N., Kaur, J., … Lal, R. (2014). Functional screening of enzymes and bacteria for the dechlorination of hexachlorocyclohexane by a high-throughput colorimetric assay. *Biodegradation*, *25*(2), 179–187. https://doi.org/10.1007/s10532-013-9650-5

Sharma, Pooja, Pandey, R., Kumari, K., Pandey, G., Jackson, C. J., Russell, R. J., … Lal, R. (2011). Kinetic and sequence-structure-function analysis of known LinA variants with different hexachlorocyclohexane isomers. *PLoS ONE*, *6*(9), 7–10. https://doi.org/10.1371/journal.pone.0025128

Sharma, Poonam, Raina, V., Kumari, R., Malhotra, S., Dogra, C., Kumari, H., … Lal, R. (2006). Haloalkane dehalogenase LinB is responsible for β- and δ-hexachlorocyclohexane transformation in Sphingobium indicum B90A. *Applied and Environmental Microbiology*, *72*(9), 5720–5727. https://doi.org/10.1128/AEM.00192-06

Sharom, M. S., Miles, J. R. W., Harris, C. R., & McEwen, F. L. (1980). Persistence of 12 insecticides in water. *Water Research*, *14*(8), 1089–1093. https://doi.org/10.1016/0043-1354(80)90157-8

Shrivastava, N., Macwan, A. S., Kohler, H. P. E., & Kumar, A. (2017). Important amino acid residues of hexachlorocyclohexane dehydrochlorinases (LinA) for enantioselective transformation of hexachlorocyclohexane isomers. *Biodegradation*, *28*(2–3), 171–180. https://doi.org/10.1007/s10532-017-9786-9

Shrivastava, N., Prokop, Z., & Kumar, A. (2015). Novel LinA type 3 delta-hexachlorocyclohexane dehydrochlorinase. *Applied and Environmental Microbiology*, *81*(21), 7553–7559. https://doi.org/10.1128/aem.01683-15

Singh, Amit Kumar, Sangwan, N., Sharma, A., Gupta, V., Khurana, J. P., & Lal, R. (2013). Draft genome sequence of Sphingobium quisquiliarum strain P25T, a novel hexachlorocyclohexane (HCH)-degrading bacterium isolated from an HCH dumpsite. *Genome Announcements*, *1*(5), e00717-13. https://doi.org/10.1128/genomeA.00717-13

Singh, Atul K, Chaudhary, P., Macwan, A. S., Diwedi, U. N., & Kumar, A. (2007). Selective loss of lin genes from hexachlorocyclohexane-degrading Pseudomonas aeruginosa ITRC-5 under different growth conditions. *Applied Microbiology and Biotechnology*, *76*(4), 895–901. https://doi.org/10.1007/s00253-007-1056-z

Singh, G., Kathpal, T. S., Spencer, W. F., & Dhankar, J. S. (1991). Dissipation of some organochlorine insecticides in cropped and uncropped soil. *Environmental Pollution*, *70*(3), 219–239. https://doi.org/10.1016/0269-7491(91)90011-K

Soltaninejad, K., & Shadnia, S. (2014). History of the use and epidemiology of organophosphorus poisoning. In M. Balali-Mood & M. Abdollahi (Eds.), *Basic and Clinical Toxicology of Organophosphorus Compounds* (pp. 25–43). https://doi.org/10.1007/978-1-4471-5625-3_2

Suar, M., Hauser, A., Poiger, T., Buser, H.-R., Müller, M. D., Dogra, C., … Kohler, H. P. E. (2005). Enantioselective transformation of a-hexachlorocyclohexane by the dehydrochlorinases LinA1 and LinA2 from the soil bacterium Sphingomonas paucimobilis B90A. *Applied and Environmental Microbiology*, *71*(12), 8514–8518. https://doi.org/10.1128/AEM.71.12.8514

Szeto, S. Y., & Price, P. M. (1991). Persistence of pesticide residues in mineral and organic soils in the Fraser Valley of British Columbia. *Journal of Agricultural and Food Chemistry*, *39*(9),

1679–1684. https://doi.org/10.1021/jf00009a027

Tabata, M., Endo, R., Ito, M., Ohtsubo, Y., Kumar, A., Tsuda, M., & Nagata, Y. (2011). The lin genes for g-hexachlorocyclohexane degradation in Sphingomonas sp. MM-1 proved to be dispersed across multiple plasmids. *Bioscience, Biotechnology, and Biochemistry*, *75*(3), 466–472. https://doi.org/10.1271/bbb.100652

Tabata, M., Ohhata, S., Kawasumi, T., Nikawadori, Y., Kishida, K., Sato, T., … Nagata, Y. (2016). Complete genome sequence of a g-hexachlorocyclohexane degrader, Sphingobium sp. strain TKS, isolated from a g-hexachlorocyclohexane-degrading microbial community. *Genome Announcements*, *4*(2). https://doi.org/10.1128/genomeA.00247-16.Copyright

Tabata, M., Ohhata, S., Nikawadori, Y., Kishida, K., Sato, T., Kawasumi, T., … Nagata, Y. (2016). Comparison of the complete genome sequences of four γ-hexachlorocyclohexane-degrading bacterial strains: Insights into the evolution of bacteria able to degrade a recalcitrant man-made pesticide. *DNA Research*, *23*(6), 581–599. https://doi.org/10.1093/dnares/dsw041

Tabata, M., Ohhata, S., Nikawadori, Y., Sato, T., Kishida, K., Ohtsubo, Y., … Nagata, Y. (2016). Complete genome sequence of a g-hexachlorocylohexane-degrading bacterium, Sphingobium sp. strain MI1205. *Genome Announcements*, *4*(2). https://doi.org/10.1128/genomeA.00956-15.Copyright

Tabata, M., Ohtsubo, Y., Ohhata, S., Tsuda, M., & Nagata, Y. (2013). Complete genome sequence of the g-hexachlorocyclohexane-degrading bacterium Sphingomonas sp. strain MM-1. *Genome Announcements*, *1*(3), e00247-13. https://doi.org/10.1128/genomeA.00247-13.Copyright

Tanaka, K. (2015). γ-BHC: Its history and mystery – why is only γ-BHC insecticidal? *Pesticide Biochemistry and Physiology*, *120*, 91–100. https://doi.org/10.1016/j.pestbp.2015.01.010

Taylor, E. L. (1945). Acaricidal property of a new insecticide, hexachlorobenzene. *Nature*, *155*,

393–394.

The new POPs under the Stockholm Convention. (2017). Retrieved March 1, 2018, from http://chm.pops.int/TheConvention/ThePOPs/TheNewPOPs/tabid/2511/Default.aspx

Thomas, J.-C., Berger, F., Jacquier, M., Bernillon, D., Baud-Grasset, F., Truffaut, N., … Simonet, P. (1996). Isolation and characterization of a novel g-hexachlorocyclohexane-degrading bacterium. *Journal of Bacteriology*, *178*(20), 6049–6055.

Trantírek, L., Hynková, K., Nagata, Y., Murzin, A. G., Ansorgová, A., Sklenář, V., & Damborský, J. (2001). Reaction mechanism and stereochemistry of g-hexachlorocyclohexane dehydrochlorinase LinA. *Journal of Biological Chemistry*, *276*(11), 7734–7740. https://doi.org/10.1074/jbc.M007452200

Trott, O., & Olson, A. J. (2010). AutoDock Vina: Improving the speed and accuracy of docking with a new scoring function, efficient optimization, and multithreading. *Journal of Computational Chemistry*, *31*(2), 455–461. https://doi.org/10.1002/jcc.21334

van der Linden, T. (1912). Uber die benzol-hexachloride und ihren zerfall in trichlor-benzole. *European Journal of Inorganic Chemistry*, *45*(1), 231–247.

van der Meer, J. R., Neerven, A. R. W. Van, Vries, E. J. De, Vos, W. M. De, & Zehnder, A. J. B. (1991). Cloning and characterization of plasmid-encoded Genes for the degradation of 1,2-dichloro-, 1,4-dichloro-, and 1,2,4- trichlorobenzene of Pseudomonas sp. strain P51. *Journal of Bacteriology*, *173*(1), 6–15.

Vijgen, J., Abhilash, P. C., Li, Y. F., Lal, R., Forter, M., Torres, J., … Weber, R. (2011). Hexachlorocyclohexane (HCH) as new Stockholm Convention POPs-a global perspective on the management of Lindane and its waste isomers. *Environmental Science and Pollution Research*, *18*(2), 152–162. https://doi.org/10.1007/s11356-010-0417-9

Vijgen, J., Yi, L. F., Forter, M., Lal, R., & Weber, R. (2006). The legacy of lindane and technical

HCH production. *Organohalogen Compounds*, *68*, 899–904.

Voldner, E. C., & Li, Y. F. (1995). Global usage of selected persistent organochlorines. *Science of the Total Environment*, *160–161*, 201–210. https://doi.org/10.1016/0048-9697(95)04357-7

Weber, R., Gaus, C., Tysklind, M., Johnston, P., Forter, M., Hollert, H., … Zennegg, M. (2008). Dioxin- and POP-contaminated sites - Contemporary and future relevance and challenges: Overview on background, aims and scope of the series. *Environmental Science and Pollution Research*, *15*(5), 363–393. https://doi.org/10.1007/s11356-008-0024-1

Wilding, M., Scott, C., & Warden, A. C. (2018). Computer-guided surface engineering for enzyme improvement. *Scientific Reports*, *8*(1), 1–7. https://doi.org/10.1038/s41598-018-30434-5

Willett, K. L., Ulrich, E. M., & Hites, R. A. (1998). Differential toxicity and environmental fates of hexachlorocyclohexane isomers. *Environmental Science and Technology*, *32*(15), 2197–2207. https://doi.org/10.1021/es9708530

Wu, J., Hong, Q., Sun, Y., Hong, Y., Yan, Q., & Li, S. (2007). Analysis of the role of LinA and LinB in biodegradation of d-hexachlorocyclohexane. *Environmental Microbiology*, *9*(9), 2331–2340. https://doi.org/10.1111/j.1462-2920.2007.01350.x

Yamamoto, S., Otsuka, S., Murakami, Y., Nishiyama, M., & Senoo, K. (2009). Genetic diversity of g-hexachlorocyclohexane-degrading sphingomonads isolated from a single experimental field. *Letters in Applied Microbiology*, *49*(4), 472–477. https://doi.org/10.1111/j.1472-765X.2009.02691.x

Yule, W. N., Chiba, M., & Morley, H. V. (1967). Fate of insecticide residues. decomposition of lindane in soil. *Journal of Agricultural and Food Chemistry*, *15*(6), 1000–1004. https://doi.org/10.1021/jf60154a037

Zdravkovski, Z. (2004). Theoretical study of the stability of hexachloro- and hexafluorocyclohexane isomers. *Bulletin of the Chemists and Technologists of Macedonia*, *23*(2), 131–137.

Zoeteman, B. C. J., Harmsen, K., Linders, J. B. H. J., Morra, C. F. H., & Slooff, W. (1980). Persistent organic pollutants in river water and ground water of the Netherlands. *Chemosphere*, *9*(4), 231–249. https://doi.org/10.1016/0045-6535(80)90080-6

Appendices

Appendix A.

Chromatograms showing the retention times for 1,2,4-, 1,2,3- and 1,3,5-TCB on GC-ECD with a Chiraldex D-BP column as per Section 2.2. The TCBs were sourced from Sigma-Aldrich.

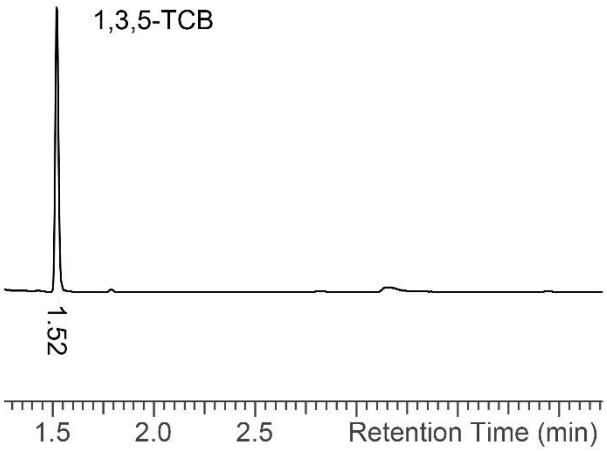

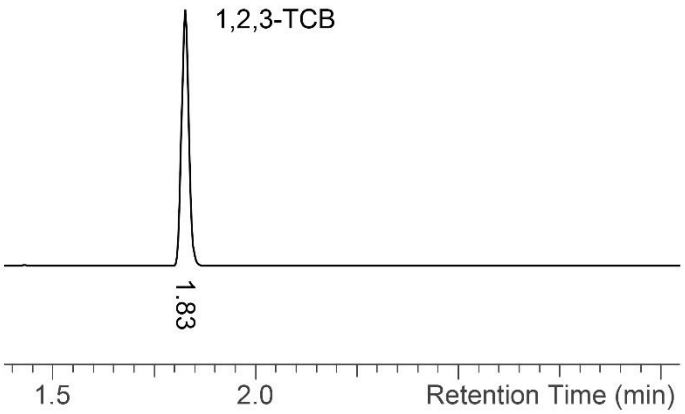

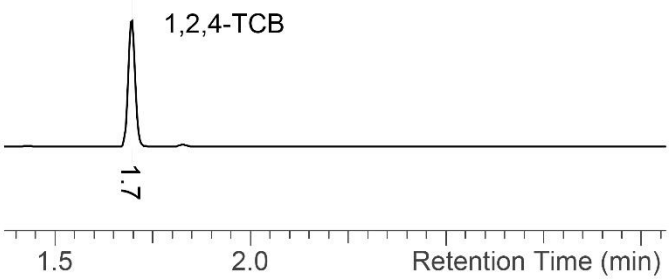

Appendix B.

Chromatograph of a failed attempt at synthesising β-PCCH from α-HCH using the protocol developed by Trantírek et al. (2001). The same protocol was used with success for the synthesis of γ- and δ-PCCH by Shrivastava et al. (2015) and myself; however, it seems to be incompatible for the synthesis of β-PCCH. Shrivastava et al. (2015) applied the protocol of Buser and Müeller (1995) for the synthesis of β-PCCH with success; however, my attempt to use the same protocol for β-PCCH synthesis was unsuccessful as the dichloromethane used for the extraction process was lost during the procedure (data unavailable). The two protocols are provided below.

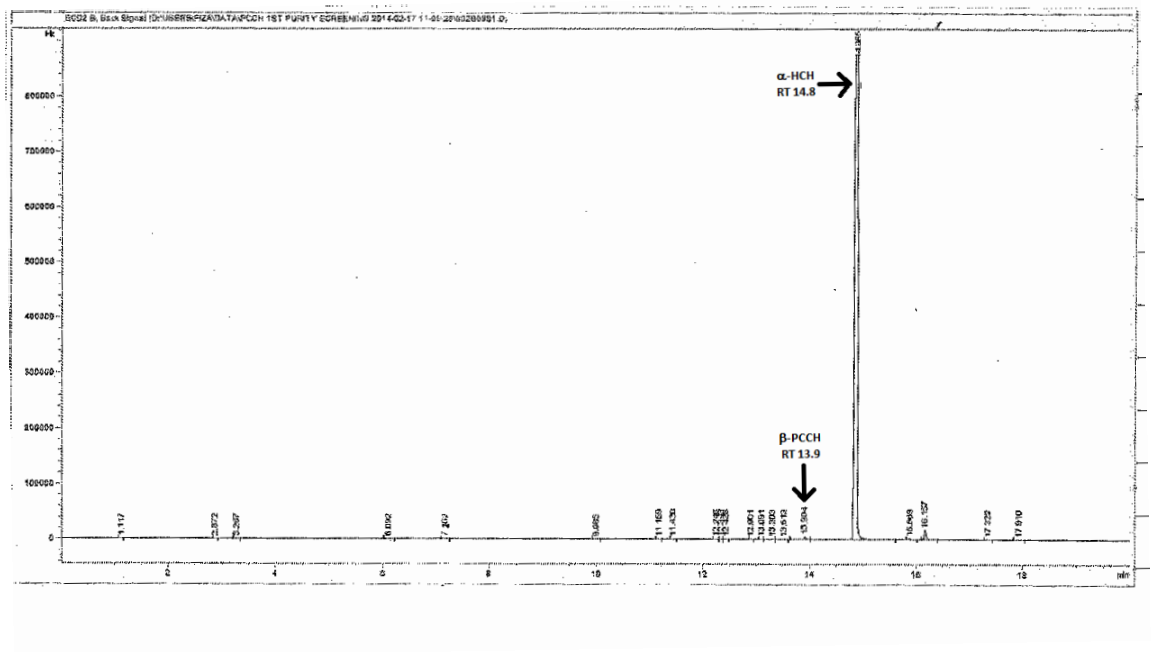

Method by Trantírek et al. (2001)	Method by Buser and Müeller (1995)
1. Dissolve 50 mg of HCH in 5 ml acitonitrile. 2. Add 2.5 ml of 0.1 M NaOH to the mixture 3. Heat for 20 min at 40 °C 4. Extract with hexane 5. Purify by preparative liquid chromatography with steel column (8 x 250 mm) packed with silica gel (7 µm). (Mobile phase: 20% dichloromethane in hexane)	1. Dissolve approximately 20 mg α-HCH in ~1 ml of dry pyridine 2. Heat in glass ampules for 14 h at 65 °C 3. Dilute the mixture with ~5% HCl 4. Partition with 2-3 ml of dichloromethane 5. Wash the extract with dilute HCl, 5% $NaHCO_3$ solution and water 6. Dry over anhydrous Na_2SO_4 7. Concentrate the solution 8. Redissolve residue in *n*-hexane 9. Analyse in GC-ECD/MS

Appendix C.

Progress curves for α-HCH degradation assays using purified LinA1$_{B90A}$ without cell lysate and three different estimations of β-PCCH1 and β-PCCH2 concentrations. The three estimations were obtained using the slopes from the γ-PCCH and δ-PCCH standard curves, and averages of the two. All progress curves give similar mass-balance results. a-HCH1 and a-HCH2 are α-HCH1 and α-HCH2, respectively, and b-PCCH1 and b-PCCH2 are β-PCCH1 and β-PCCH2, respectively.

With average slopes

(0.0534 for β-PCCH1 and 0.0531 for β-PCCH2)

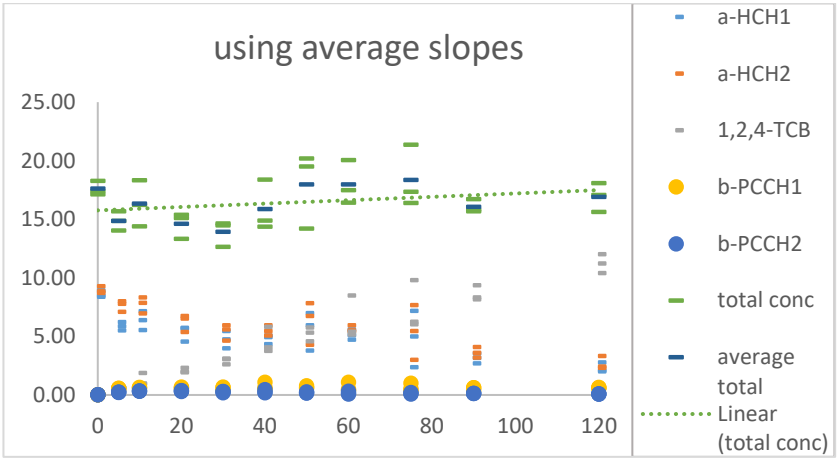

With γ-PCCH slopes

(0.0484 for γ-PCCH1 and 0.0477 for γ-PCCH2)

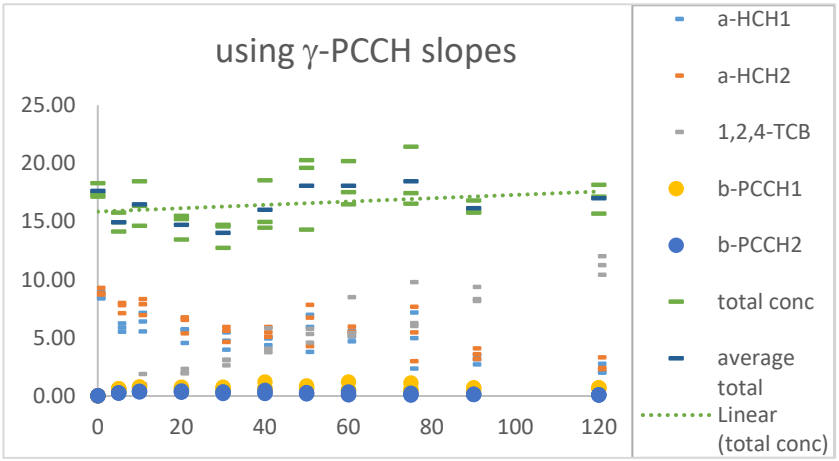

With δ-PCCH slopes

(0.0596 for δ-PCCH1 and 0.0600 for δ-PCCH2)

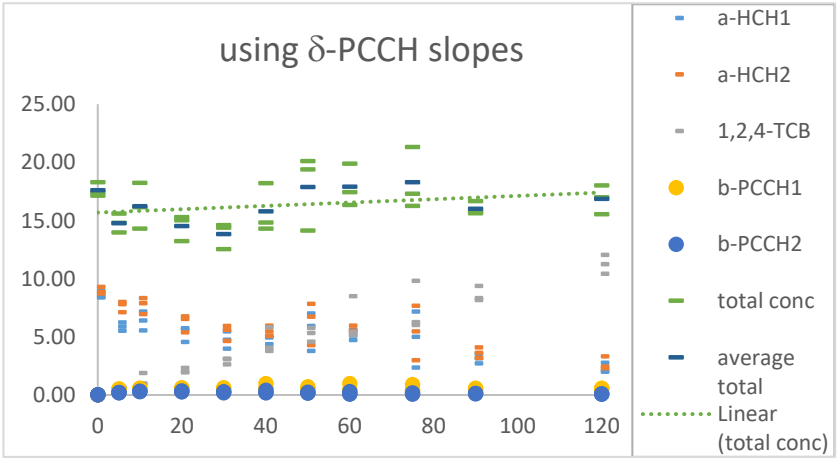

Appendix D.

Values from Copasi calculations for α-HCH degradation by LinA1$_{B90A}$ using slopes for γ-PCCH and δ-PCCH standard curves, and averages of both. The 'Value' in the tables refer to the *k* value of the reaction. The *k* values provided by Copasi were used to calculate k_{cat}/K_m of the reaction. Note that the *k* values for the three estimates for each reaction are similar to one another. Specifically, the values obtained from the other two slopes are always within 10% of those obtained from the average slopes for the HCH to PCCH transformations, and within 20% of them for the PCCH to TCB transformations.

Values from Copasi for reactions from α-HCH degradation assays by LinA1$_{B90A}$ using average of γ- and δ-PCCH slopes for estimating β-PCCH concentrations

Parameter	Value	Standard Deviation
α-HCH1 → β-PCCH1	0.009074	0.000449
α-HCH2 → β-PCCH2	0.009664	0.000495
β-PCCH1 → 1,2,4-TCB	0.075384	0.00364
β-PCCH2 → 1,2,4-TCB	0.242557	0.011738

Values from Copasi for reactions from α-HCH degradation assays by LinA1$_{B90A}$ using γ-PCCH slopes for estimating β-PCCH concentrations

Parameter	Value	Standard Deviation
α-HCH1 → β-PCCH1	0.009415	0.000462
α-HCH2 → β-PCCH2	0.009705	0.000494
β-PCCH1 → 1,2,4-TCB	0.070057	0.003385
β-PCCH2 → 1,2,4-TCB	0.217048	0.010445

Values from Copasi for reactions from α-HCH degradation assays by LinA1$_{B90A}$ using δ-PCCH slopes for estimating β-PCCH concentrations

Parameter	Value	Standard Deviation
α-HCH1 → β-PCCH1	0.009933	0.00048
α-HCH2 → β-PCCH2	0.008923	0.000475
β-PCCH1 → 1,2,4-TCB	0.090163	0.004174
β-PCCH2 → 1,2,4-TCB	0.255335	0.01276

Appendix E.

Nucleotide sequence alignment for LinA-type1 enzyme $LinA2_{B90A}$, LinA-type2 enzyme $LinA1_{B90A}$ and LinA-type3 enzyme $LinA_{LL02}$. LinA-type1 sequence was used as reference. Yellow highlights single point mutations that have resulted in amino acid changes. Green highlights mutations of more than one nucleotide that have resulted in amino acid changes. Turquoise highlights one synonymous site mutation that I found in LinA-type2 at residue 148, which is part of the IS6*100*-associated C-terminal. The affected codons are highlighted with black boxes. The numbers for the affected residues are written in red.

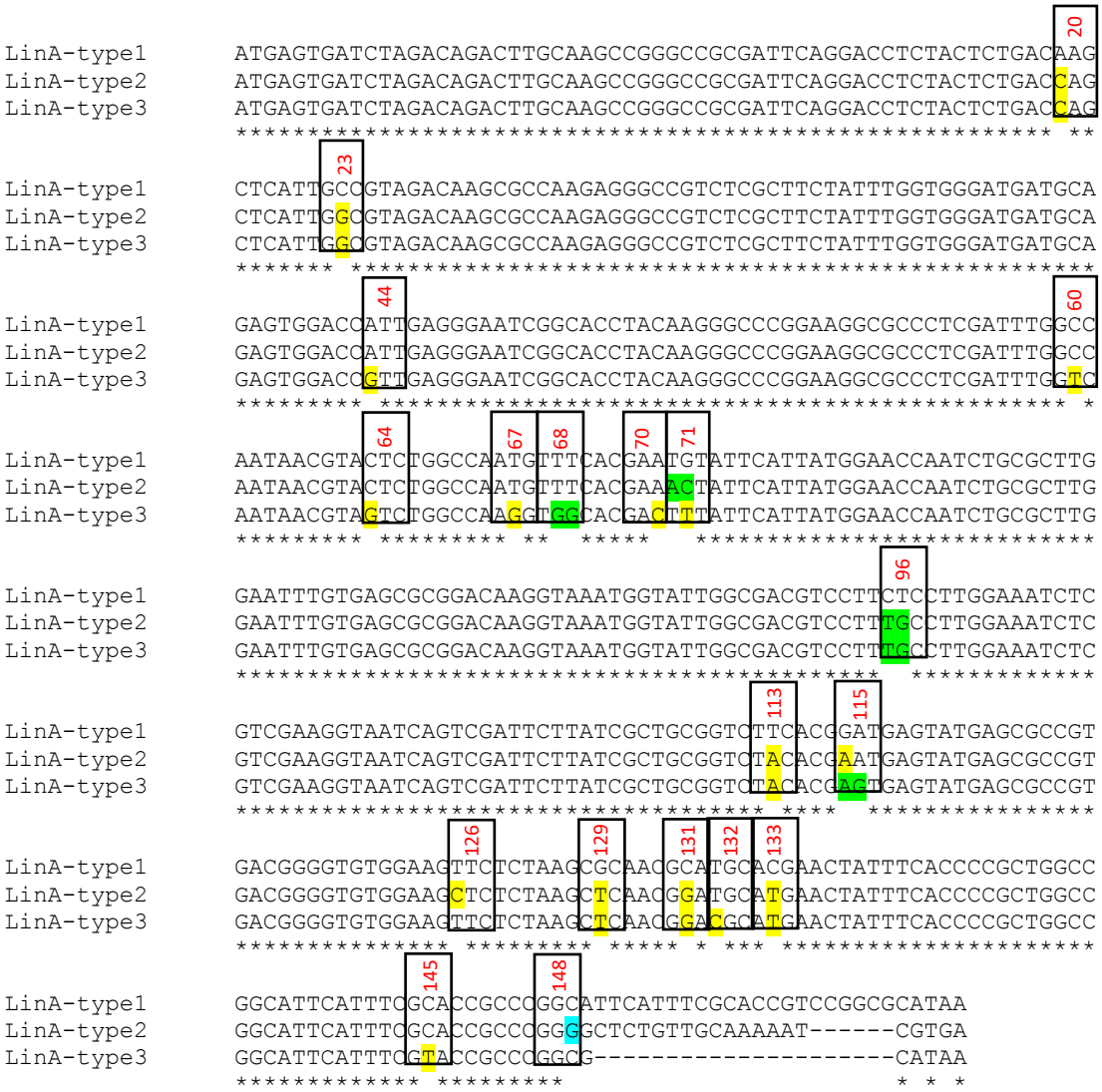

The table below lists the affected residues. Residues highlighted in blue are the different residues between LinA-type1 and LinA-type2, and are a result of twelve nucleotide differences. Residues highlighted in orange are unique to LinA-type3 and resulted from single point

mutations. A residue highlighted in purple is unique to LinA-type3 and results of a double mutation.

LinA	20	23	44	60	64	67	68	70	71	96	113	115	126	129	131	132	133	145	148
Type1	K	A	I	A	L	M	F	E	C	L	F	D	F	R	A	C	T	A	G
Type2	Q	G	I	A	L	M	F	E	T	C	Y	N	L	L	G	C	M	A	G
Type3	Q	G	V	V	V	R	W	D	F	C	Y	S	F	L	G	R	M	V	G

Appendix F.

SDS-PAGE of the purified mutant enzymes. Arrows highlight the purified enzymes. The lanes between the ladder (first lane) and the purified enzymes (last lanes) are the crude extracts and dialysis solution obtained during the purification process.

<table>
<tr>
<td>LinA1B90A I44V
Purity: ~90%
 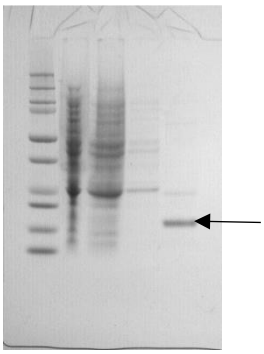 </td>
<td>LinALL02 V44I
Purity: ~99%
 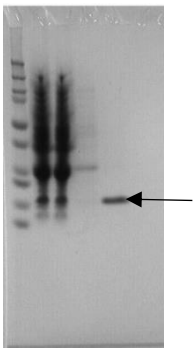 </td>
</tr>
<tr>
<td>LinA1B90A L64V
Purity: ~40%
 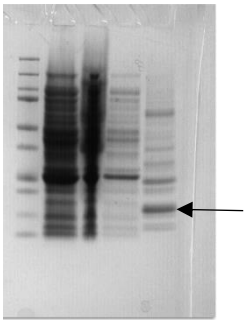 </td>
<td>LinALL02 V64L
Purity: ~90%
 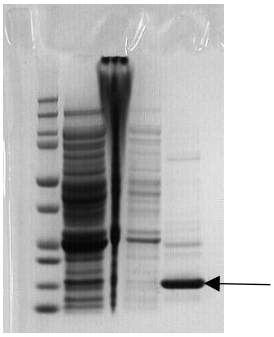 </td>
</tr>
</table>